

**ELICITATION, DETECTION AND BIOPROFILING OF
SECONDARY METABOLITES IN *MUSA* SPECIES USING
PLANT TISSUE CULTURE TECHNIQUES AND HIGH
PERFORMANCE THIN LAYER CHROMATOGRAPHY**

BY

ORESANYA, Ibukun Oluwabukola

B. Sc. (Hons) Botany, OAU, Ile-Ife, Nigeria (2010), M.Sc. Pharmacognosy,
University of Ibadan (2014)

MATRIC. NO: 168454

A Project in the Department of Pharmacognosy

Submitted to

The Faculty of Pharmacy

In partial fulfilment of the requirements for the award of

Doctor of Philosophy (Ph.D.) Degree

of the

University of Ibadan

JANUARY, 2020

ABSTRACT

The search for new bioactive compounds from the wild often leads to conservation issues. Plant tissue culture, a less destructive source of plant materials is a priority technique. There is paucity of studies on potentials of plant tissue culture for the accumulation of secondary metabolites in wild and cultivated *Musa* species, with wide medicinal applications. This study was, therefore, designed to improve the phytoconstituents and profile the biological activities of selected *Musa* species.

Fifteen taxonomic reference *Musa* species accessions (A-O) were micropropagated. Genomic DNA obtained from each accession was used to generate Single Nucleotide Polymorphic (SNP) markers using Diversity Array Sequencing (DArTseq) approach to analyse genetic fidelity. Antioxidant and anticholinesterase activities of field and micropropagated accessions were evaluated using spectrophotometric methods and High Performance Thin Layer Chromatography (HPTLC) hyphenated with High Resolution Mass Spectrometry (HRMS) for compounds identification. The Effect-Directed Analysis (EDA) of the *Musa* species was done on HPTLC plates with antioxidant, anticholinesterase, antidiabetic, and genotoxicity assays for bioprofiling. Gallic acid, eserine, acarbose, 4-nitroquinoline-1-oxide, were used as standards. Compounds were characterised with HRMS. Six of the accessions were subjected to elicitation experiments using different doses of sugar (30-50 g/L), temperature (15, 20 and 25 °C) and Jasmonic Acid (JA, 0–200 µM) as elicitors. The Total Phenolic Content (TPC), antioxidant profile and biological activities of the resulting elicited samples (71) were analysed with HPTLC. Data were analysed using one-way ANOVA followed by Dunnett's multiple comparison at $\alpha_{0.05}$.

The micropropagated accessions were shown to be true-to-type with the field samples. Micropropagated plants gave significantly higher TPC (2.43±0.30 to 124.52±12.72 mgGAE/g), DPPH antioxidant (10.68±0.27 to 154.42±6.44 µg/mL), ferric reducing antioxidant power (10.58±0.52 to 152.16±2.80 mgTE/g) and acetylcholinesterase (11.53±0.12 to 1181.00±91.25 µg/mL) activities than the field plants.

Acetylcholinesterase (AChE) activity of micropropagated accession F (11.53 ± 6.52 $\mu\text{g/mL}$) was significantly higher than that of eserine (31.23 ± 7.33 $\mu\text{g/mL}$). Results of the HPTLC-EDA were similar to those of the spectrophotometric assays; accession F also had the highest AChE inhibition. Three multipotent compounds characterised by their base peaks (m/z) and molecular formula were identified as asparagine (1), aniracetam (2) and linolenic acid (3). All the compounds had AChE and butyrylcholinesterase (BuChE) inhibitory activities. Compounds 1 and 2 had antioxidant activity, while compound 1 exhibited α and β -glucosidase inhibition. None of the samples were genotoxic at the concentrations tested. The elicitation experiments increased the TPC and antioxidant activity of *Musa* species. In accession B, the TPC increased from 39.43 to 138.64 ngGAE/g (4.89 folds) when 30 and 50 g/L of sugar were used, respectively. Plants grown at 20 °C gave a higher TPC than other treatments. Addition of JA (200 μM) increased the TPC of accessions L and N by 2.24 and 1.68 folds, respectively.

The plant tissue culture technique was validated as a suitable method for the production of genetically uniform *Musa* species and for sustainable supply of more bioactive metabolites. The identified compounds had antioxidant, anticholinesterase and antidiabetic activities. The diversity and titre of the phytoconstituents were also improved in the elicited accessions.

Keywords: *Musa* species, Plant tissue culture, Effect-directed analysis, Bioactive metabolites

Word count: 497

DEDICATION

This work is dedicated to God my father, my source and the source of all wisdom and knowledge. He alone created and searched out what we research and to my Treasure; Adedamola Omolade, Oresanya.

ACKNOWLEDGEMENTS

I give thanks to God Almighty for his faithfulness and sustenance all through the course of this work. I give glory to God, the source of all wisdom for ideas and flow of thoughts during this research and write up.

My sincere appreciation goes to my supervisor, Prof. Mubo A. Sonibare for her awesome contributions, motherly advice, thorough supervision and mentorship roles since I met her. I am privileged to have studied under your tutelage. I learnt hard work, orderliness, punctuality and being detailed among many others. God bless you and all yours.

Also to Dr. Badara Gueye, my very detailed IITA supervisor, I am grateful for your coaching. I have learnt a lot under your supervision. You taught me scientific writings and many more. Now I can make beautiful power-point presentations. Special thanks to Prof. Michael Abberton (Head, Genetic Resource Centre, GRC-IITA) and Dr. Rajneesh Paliwal for the privilege of working under their scientific orientation and funding from IITA. I appreciate all the scientific exposures and sponsorship to attend international conferences, from the All Africa Horticultural Congress (IHC) at IITA, to the Genomics of Plant Genetic Resources (GPGR4) in Germany and to the International Horticultural Congress (IHC) in Istanbul. Those moments were wonderful, thank you sirs.

Special thanks to Prof. J.O. Moody, the Head of the Department of Pharmacognosy: and to all my other lecturers; Prof. A. A. Elujoba, Prof. Edith O. Ajaiyeoba, Dr. Taiwo O. Elufioye, Dr. Omonike O. Ogbole, Mr J. O. Olayemi, Mr. A.A. Adeyemi thank you for impacting my life. Members of staff of the Department of Pharmacognosy (Miss Rita Etim-Okon, Mr. A. R. Waheed, Mr. Oyewale Oyediran, Mrs. Abosede Akinleye, Aunty Joyce and Mrs Oyewusi), I say thank you all and may you all obtain favour from God.

I also want to appreciate all the members of staff, Corp members and students of the Plant tissue culture unit, GRC, IITA; Mrs. Adeyemi the laboratory manager, Mrs. Bimpe Obisesan, Mrs. Wunmi Thabit (Mummy James), Mrs. Motunrayo Olagunju (Mummy Israel), Sis. Bose Adebayo, Grace Abodunrin, Titilope Olabisi, Owuala Faith, Rashidat

Akinsanya, Sis Busola Bankole, Aunty Yemi Salawu, Mr. Solomon Adeyemo, Mr. Adeleke, and others, thanks to you all for the training.

I am grateful to IITA for the graduate research fellowship given to me. I also appreciate the Post-graduate College, University of Ibadan for the post-graduate scholar award given to me; I must say that it opened the door for other fellowships. Many thanks to the Association of African Universities (AAU), for the small grant for theses and dissertations given to me. I say a big thank you to the African-German Network of Excellence in Science for the grant given to me to do a part of this research in South Africa. I must not forget my host, Dr. Tom Ashafa, thank you for hosting me in your laboratory at the Department of Plant Sciences, University of the Free State, Qwaqwa campus, Free State, South Africa. Lastly, special thanks to the German Academic Exchange Service (DAAD) for the 5 months short-term research grant (57378443) given to me and to my German host, Prof. Gertrud Morlock, the Head of the Institute of Food Sciences, Justus Liebig University, Giessen where I learned HPTLC. Thank you for your kind-heartedness. This work would not have been completed without the use of your high-throughput HPTLC technique.

I am grateful to Dr. Balogun of the Yam Improvement for Incomes and Food Security in West Africa (YIIFSWA)-IITA for allowing me use their growth chamber for some of my *in vitro* plant tissue culture experiments. Special thanks to my colleagues at IARSAF, members of the Biodiversity Conservation and Medicinal Plant Research group, colleagues and senior colleagues (Dr. Dapo Adeniran and Dr. Peter Segun), Joe, the graphics designer and Damilola, you are the best! I want to thank all my friends for their love and care during this programme. To mention a few names: Adeola, Julius, Mr. Chuks (YIIFSWA people), Akinyele Akinbimpe, Mr. and Mrs. Bisi-Adelere, Faith Bankole (Statistician), Mr. Emmanuel (structure elucidation expert). God bless you all. Special thanks to my data analyst and teacher, Mr. Lekan Jolayemi, who taught me data analysis all the way from Sweden, you are the best!

I must not fail to mention my wonderful family of God for spiritual and moral backing during this Ph.D. The Adeyeyes, Adegboyegas and my wonderful Pastor and his wife,

(Pastor and Dr. (Mrs) Owoade) who will never fail to ask me; “bawo ni o, nibo le ko de”. God bless you all (Amen).

My profound gratitude goes to my loving and caring parents, Mr. and Mrs. B.O Ayoola who contributed immeasurably financially, morally and spiritually towards the success of this programme. Special thanks to my other parents, Mr. and Mrs. A. O. Oresanya. I pray God keep you in good health to eat the fruit of your labour. Also, I deeply appreciate my siblings for their support: Oladayo, Olawale and my cousins Ayodeji, Christie, Busayo, Bro Jide, Bro Wole, Auntie Ike, the Fagbenros, Ayodeles, Okes, and my brothers and sister-in-law: Bro Seun, Mrs Akinnuoye, Oluwole, Boluwatife and Ayooluwa Oresanya. I love you all. To Daddy and Mummy Abodunrin thanks for being there for me. I also want to thank all my loved ones; The Banjos, Fayeuns, Ogunyas, Adedejis, the Temples and others time and space will not permit me to mention.

My deep appreciation goes to my knight in shining armour, my Treasure. Thank you for always standing by my side, no one is as supportive as you are. You were the brain behind all the scholarships and fellowships. I cannot imagine how someone surfs the internet like you do. Your doggedness and aspirations marvels me. I am so inspired by you. You are simply the best! I am grateful to God for bringing us together. God bless the day you were born, Adedamola Omolade Oresanya.

CERTIFICATION

This is to certify that this research work was carried out by Ibukun Oluwabukola ORESANYA in the Department of Pharmacognosy, Faculty of Pharmacy, University of Ibadan, under our supervision.

.....

(Supervisor)

Prof. Mubo A. Sonibare

Department of Pharmacognosy

Faculty of Pharmacy

University of Ibadan

Ibadan

.....

(Host Supervisor)

Dr Badara Gueye

In vitro Propagation and Conservation Specialist

International Institute of Tropical Agriculture (IITA)

Ibadan

TABLE OF CONTENTS

Contents	Page	
Title page	i	
Abstract	ii	
Dedication	iv	
Acknowledgement	v	
Certification	viii	
Table of Contents	ix	
List of Tables	xvi	
List of Figures	xviii	
List of Plates	xxii	
List of Appendices	xxiii	
List of Abbreviations	xxvi	
1.0	CHAPTER ONE INTRODUCTION	1
1.1	Plants as Sources of Secondary Metabolites	1
1.2	Secondary Metabolites Production via <i>in vitro</i> Plant Tissue Culture Techniques	2
1.3	Elicitation	4
1.4	High-Performance Thin Layer Chromatography	4
1.5	<i>Musa</i> spp.	6
1.6	Justification for the Study	6
1.7	Research Hypothesis	7
1.8	Research Questions	8

1.9	Aim and Objectives of the Study	8
2.0	CHAPTER TWO LITERATURE REVIEW	10
2.1	Usefulness of Secondary Metabolites as Leads in Drug Discovery	10
2.2	Biotechnology Application for Secondary Metabolites Production	13
2.3	<i>In Vitro</i> Plant Tissue Culture Techniques	14
2.3.1	Explant source	15
2.3.2	Sterilisation	15
2.3.3	Plant tissue culture media	15
2.3.4	Plant growth hormones	16
2.3.5	Types of tissue culture techniques	18
2.3.6	Hardening and acclimatisation of tissue culture plantlets	19
2.4	Production of Secondary Metabolites via Plant Cell and Tissue Culture Systems	20
2.5	Approaches to Increase the Production of Secondary Metabolites via <i>In Vitro</i> Plant Tissue Culture Techniques	23
2.5.1	Selection of efficient plant material for growth	23
2.5.2	Production in differentiated tissues	23
2.5.3	Screening of high-growth cell line to produce metabolites of interest	23
2.5.4	Optimisation of culture conditions	24
2.5.5	Addition of precursors	28
2.5.6	Use of elicitors	28
2.6	Isolation and purification of bioactive compounds	30
2.6.1	Effect directed analysis (EDA) and hyphenations coupled with high-performance thin layer chromatography (HPTLC)	31

2.6.2	Structural elucidation of bioactive compounds	32
2.7	Assessment of Genetic Fidelity of <i>In Vitro</i> -grown Plants Using Molecular Markers	33
2.8	Botanical Description of Research Plant	33
2.8.1	Taxonomy of <i>Musa</i>	33
2.8.2	Taxonomical classification	35
2.8.3	Ecology and distribution	38
2.8.4	Propagation of <i>Musa</i> species	38
2.8.5	Economic uses and nutritional values of <i>Musa</i>	39
2.8.6	Traditional and medicinal uses of <i>Musa</i>	39
2.8.7	Pharmacological activities of <i>Musa</i>	40
2.8.8	Some of the chemical constituents and compounds isolated from <i>Musa</i> species	42
2.9	Antioxidants and Cholinesterase Inhibition	48
2.10	Anti-inflammation and Antidiabetes	48
3.0	CHAPTER THREE MATERIALS AND METHODS	50
3.1	Chemicals and Reagents Used	50
3.1.1	The chemicals used for <i>in vitro</i> plant tissue culture experiment	50
3.1.2	Chemicals and reagents used for DNA extraction	50
3.1.3	Chemicals and reagents used for biological assays and isolation	51
3.2	Materials and Apparatuses	51
3.3	Plant Materials	52
3.4	Micropropagation, Multiplication and Acclimatisation	54
3.4.1	Preparation of growth media (regeneration and proliferation media)	54

3.4.2	Source of explant and sterilisation	56
3.4.3	Meristem excision and subculturing	56
3.4.4	Acclimatisation	59
3.5	DNA Extraction and DArTseq SNP Analysis for Genetic Fidelity Study	61
3.5.1	DNA extraction	61
3.5.2	Measurement of concentration and purity of DNA sample	61
3.6	Plant Crude Extraction	62
3.7	UV Spectrophotometric Assays	63
3.8	HPTLC Methods	64
3.8.1	Sample preparation and HPTLC separation	64
3.8.2	HPTLC derivatisations	64
3.8.3	Neutralisation of chromatograms	65
3.8.4	HPTLC-Effect Directed Analysis (EDA)	65
3.8.5	HPTLC-Electron spray ionisation (ESI)-high-resolution mass spectrometry (HRMS)	67
3.9	<i>In Vitro</i> Plant Tissue Culture Elicitation Experiment	67
3.9.1	Increase in sugar level experiment	68
3.9.2	Reduced temperature experiments	68
3.9.3	Addition of jasmonic acid experiment	68
3.10	Analysis of Elicited Samples Using HPTLC	70
3.10.1	Sample preparation and extraction	70
3.10.2	HPTLC derivatisation	70
3.10.3	HPTLC-EDA of elicited samples and HPTLC-HRMS of antioxidant compounds	71
3.11	Large Scale Extraction of the Best Field Accession	74

3.12	Solvent-solvent Partition Extraction	74
3.13	TLC of Partitioned Fractions	76
3.14	Bioassay of Partitioned Fractions	76
3.14.1	Antioxidant assays	76
3.14.2	Antidiabetic assay	77
3.14.3	Anti-inflammatory assay	79
3.14.4	Anticholinesterase assay	79
3.15	Statistical Analysis	79
3.16	Column Chromatography of the Leaf EAF	80
3.17	Isolation and Characterisation of Bioactive Compound Using MS, NMR and HPTLC	80
4.0	CHAPTER FOUR RESULTS	82
4.1	Micropropagation of the <i>Musa</i> species Accessions	82
4.2	Genetic Fidelity and Relationship Among the Accessions	84
4.3	Crude Extraction Yield	94
4.4	UV Spectrophotometric Biological Activities	94
4.4.1	DPPH• antioxidant activity	94
4.4.2	Ferric reducing antioxidant power	94
4.4.3	Total phenolic and total flavonoid content	94
4.4.4	Correlation among the antioxidant assays	95
4.4.5	Acetylcholinesterase (AChE) inhibitory activity	95
4.5	Characterisation of Metabolites and Bioprofiling using HPTLC Methods	103
4.5.1	Mobile phase development	103

4.5.2	HPTLC Derivatisation	103
4.5.3	Effect directed analysis (EDA) with HPTLC	103
4.5.3.1	Detection of cholinesterase inhibitors	104
4.5.3.2	Identification of glucosidase and amylase inhibitors	104
4.5.3.3	Detection of antimicrobials in <i>Musa</i> spp.	104
4.5.3.4	Absence of toxins as determined by the mutagenotoxicity assay	105
4.5.4	Characterisation of active zones via HPTLC-High resolution mass spectrometry (HRMS)	105
4.6	Tissue Culture Elicitation Experiments	117
4.6.1	The effect of increase in sugar on the growth parameters and antioxidant activity of the selected accessions	117
4.6.2	The effect of reduced temperature on the growth parameters and antioxidant activity of the selected accessions	117
4.6.3	The effect of the addition of jasmonic acid in the culture media on the growth parameters and antioxidant activity of the selected accessions	118
4.6.4	Glucosidase and cholinesterase inhibitors and no toxic compounds in elicited samples	118
4.6.5	Characterisation of elicited antioxidant compounds from HPTLC-HRMS	118
4.7	Bioassay Guided Isolation of Compounds from the Most Bioactive Field Accession	146
4.7.1	Yield of the large scale crude extraction and partitioned fractions	146
4.7.2	Thin layer chromatography of the crude and partitioned fractions	146
4.7.3	Biological activities of the crude methanol extracts and the partitioned fractions	146
4.7.4	Column chromatography of the ethyl acetate fraction of the leaf of <i>Musa acuminata</i> (Simili radjah)	164
4.7.5	Identification of isolates HD ₁ (compounds 12 and 13) using High performance thin layer chromatography (HPTLC), HPTLC-high resolution	164

mass spectrometry (HRMS) and Nuclear magnetic resonance (NMR)

5.0	CHAPTER FIVE DISCUSSION, CONCLUSION AND RECOMMENDATION	181
5.1	Discussion	181
5.1.1	Micropropagation and genetic fidelity assessment of the <i>Musa</i> spp. accessions	181
5.1.2	Extraction yield and biological assays of field and <i>in vitro</i> -grown accessions	183
5.1.3	Chemical profile of field, <i>in vitro</i> and acclimatised samples using high-performance thin layer chromatography	185
5.1.4	Effect directed analysis (EDA) with HPTLC	186
5.1.5	Absence of toxins as determined by the mutagenotoxicity assay	188
5.1.6	Characterisation of active zones via HPTLC-High resolution mass spectrometry (HRMS)	189
5.1.7	Elicitation experiments and their effect on increasing the total phenolic content and antioxidant compounds	191
5.1.8	Biological activities of the crude and partitioned fraction of the fruit and leaf of <i>Musa acuminata</i>	195
5.1.9	Characterisation of HD ₁ isolates (compounds 12 and 13) using HPTLC-HRMS and NMR	197
5.2	Contributions to Knowledge	200
5.3	Conclusions	201
5.4	Recommendations	203
	References	204
	Appendices	223

LIST OF TABLES

Table no	Table title	Page
Table 2.1	Important Plant-derived Pharmaceuticals	11
Table 2.2	Yield of Secondary Metabolites from Cell Cultures Compared with the Parent Plants	21
Table 2.3	Different Types of Elicitors Utilised to Induce Secondary Metabolite Production	29
Table 3.1	Passport Data of the Taxonomic Reference Accessions	53
Table 3.2	Meristem and Proliferation Media Composition	55
Table 3.3	Media Composition for Increase in Sugar Experiment	69
Table 4.1.1	<i>In vitro</i> plant tissue culture growth parameters	83
Table 4.2.1	Distribution of 114285 SNP of 56 banana samples of <i>Musa</i> spp. on banana genome both nuclear and mitochondrial genome	86
Table 4.3.1	Extraction yield of field and micropropagated accessions	96
Table 4.4.1.1	DPPH• antioxidant activity as shown by the IC ₅₀ Values (µg/mL)	97
Table 4.4.2.1	FRAP of field (F) and tissue culture (TC) accessions	98
Table 4.4.3.1	TPC and TFC of field (F) and tissue culture (TC) accessions	99
Table 4.4.4.1	Spearman's correlation coefficients (r) among the antioxidant assays	100
Table 4.4.5.1	AChE inhibitory activity of field (F) and tissue culture (TC) samples	101
Table 4.5.1.1	List of mobile phases investigated for separation of the leaf sample no. 2 of <i>Musa acuminata</i> (Foconah)	106
Table 4.5.4.1	HPTLC-HRMS data of multipotent compounds in selected samples F ₂ and F ₃	116
Table 4.6.1.1	Peak area and total phenolic content from the densitometric measurement and gallic acid calibration curve of the sugar increase experiment	124
Table 4.6.2.1	Peak area and total phenolic content from the densitometric	129

	measurement and gallic acid calibration curve of the temperature experiment	
Table 4.6.3.1	Peak area and total phenolic content from the densitometric measurement and gallic acid calibration curve of the jasmonic acid experiment	134
Table 4.6.5.1	HPTLC-HRMS data of bioactive compounds in the selected elicited sample	145
Table 4.7.1.1	Yield of CME and partitioned fractions of the leaf and fruit of <i>Musa acuminata</i> (Simili radjah)	149
Table 4.7.3.1.1	Total phenolic content and DPPH• antioxidant activity of the leaf and fruit crude extract and fractions	152
Table 4.7.3.4.1	Anti-inflammatory activity of <i>Musa acuminata</i> (Simili radjah) leaf and fruit fractions	161
Table 4.7.3.5.1	Anticholinesterase activity of <i>Musa acuminata</i> (Simili radjah) leaf and fruit fractions	162
Table 4.7.4.1	Ethyl acetate sub-fractions obtained by silica gel column chromatography: colour, yield and means of TPC and DPPH• antioxidant activity	166
Table 4.7.4.2	Yield of sub-fractions from H loaded on sephadex column	168
Table 4.7.4.3	Biological activities of compounds in the sub-fraction H	170
Table 4.7.5.1	HPTLC-HRMS data of HD ₁ compounds	174
Table 4.7.5.2	¹ H, ¹³ C NMR and DEPT of Kaempferol-3- <i>O</i> -rutinoside (12)	175
Table 4.7.5.3	¹ H, ¹³ C NMR and DEPT of Quercetin-3- <i>O</i> -rutinoside (13)	176
Table 4.7.5.4	Antioxidant and antidiabetic activities of HD ₁ compounds	179

LIST OF FIGURES

Figure no	Figure title	Page
Fig. 2.1	Structures of some plant-derived products	12
Fig. 2.2	Structures of compounds with better yield via plant cell culture	22
Fig. 2.3	Different strategies to enhance secondary metabolites production in <i>in vitro</i> plant tissue culture	27
Fig. 2.4	Crossing relationships of most cultivated edible <i>Musa</i>	34
Fig. 2.6	Structures of some compounds isolated from <i>Musa</i> species	45
Fig. 3.1	<i>In vitro</i> plant tissue culture techniques	58
Fig. 3.2	Procedures for acclimatisation	60
Fig. 3.3	Sample preparation for HPTLC	72
Fig. 3.4	HPTLC methods	73
Fig. 3.5	Flow chart of the partitioning of the crude methanol extract	75
Fig. 4.2.1	Distribution of minor allele frequency based on SNP summary of 56 banana samples	87
Fig. 4.2.2	Distribution of heterozygosity proportion in 56 banana samples	88
Fig. 4.2.3	Frequency distribution of IBS pairwise genetic distance matrix of 56 banana samples	89
Fig. 4.2.4	Neighbour joining tree showing trueness-to-type in tissue culture <i>Musa</i> spp. accessions using 114k SNP markers	90
Fig. 4.2.5	Heatmap distribution of IBS pairwise genetic distance matrix of 56 banana samples	91
Fig. 4.2.6	Principal Component analysis of PC1vsPC2	92
Fig. 4.2.7	Principal Component analysis of PC1vsPC3	93
Fig. 4.4.5.1	AChE percentage inhibition of field and tissue culture accessions at 1 mg/mL	102
Fig. 4.5.1.1	Mobile phase development	107

Fig. 4.5.2.1	HPTLC fingerprints of field, <i>in vitro</i> -grown and acclimatised <i>Musa</i> spp.	108
Fig. 4.5.3.1	HPTLC-EDA fingerprints of field, <i>in vitro</i> -grown and acclimatised <i>Musa</i> spp. accessions developed in ethyl acetate: toluene: formic acid: water (3.4: 0.5: 0.7: 0.5)	109
Fig. 4.5.3.2	HPTLC-EDA fingerprints of field, <i>in vitro</i> -grown and acclimatised <i>Musa</i> spp. accessions developed in toluene: ethyl acetate: methanol (6: 3: 1)	110
Fig. 4.5.3.3	HPTLC chromatogram of genotoxicity assay of selected samples	111
Fig. 4.5.3.4	HPTLC chromatograms (A–N) of bioactive components in the <i>Musa</i> spp. leaf extract developed in ethyl acetate: toluene: formic acid: water; 3.4: 0.5: 0.7: 0.5	112
Fig. 4.5.3.5	HPTLC chromatograms (A–P) of bioactive components in the <i>Musa</i> spp. leaf extract developed in medium polar mobile phase	113
Fig. 4.5.4.1	HPTLC-HRMS spectra of compounds developed in the polar mobile phase	114
Fig. 4.5.4.2	HPTLC-HRMS spectra of compounds 4 developed in the medium polar mobile phase and recorded in the ESI ⁺ (A) and ESI ⁻ (B) mode	115
Fig. 4.6.1	Shoot culture of <i>Musa</i> species	119
Fig. 4.6.1.1	Average shoot length of all the <i>Musa</i> spp. accessions grown under different sugar concentrations	120
Fig. 4.6.1.2	Average number of leaves of all the <i>Musa</i> spp. accessions grown under different sugar concentration	121
Fig. 4.6.1.3	Average number of shoots of all the <i>Musa</i> spp. accessions grown under different sugar concentrations	122
Fig. 4.6.1.4	HPTLC chromatogram of sugar elicited samples developed in ethyl acetate: toluene: formic acid: H ₂ O; 3.4: 0.5: 0.7: 0.5 and the 3D densitogram at 546 nm of all tracks	123
Fig. 4.6.2.1	Average shoot length of all the <i>Musa</i> spp. accessions grown under different temperature conditions	125
Fig. 4.6.2.2	Average number of leaves of all the <i>Musa</i> spp. accessions grown under different temperature conditions	126

Fig. 4.6.2.3	Average number of shoots of all the <i>Musa</i> spp. accessions grown under different temperature conditions	127
Fig. 4.6.2.4	HPTLC chromatogram of temperature elicited samples developed in ethyl acetate: toluene: formic acid: H ₂ O; 3.4: 0.5: 0.7: 0.5 and 3D densitogram at 546 nm of all the tracks	128
Fig. 4.6.3.1	Average shoot length of all the <i>Musa</i> spp. accessions grown on proliferation media with the addition of jasmonic acid and the control	130
Fig. 4.6.3.2	Average number of leaves of all the <i>Musa</i> spp. accessions grown on proliferation media with the addition of jasmonic acid (JA) and the control	131
Fig. 4.6.3.3	Average number of shoots of all the <i>Musa</i> spp. accessions grown on proliferation media with the addition of jasmonic acid and the control	132
Fig. 4.6.3.4	HPTLC chromatogram of jasmonic acid elicited samples developed in ethyl acetate: toluene: formic acid: H ₂ O; 3.4: 0.5: 0.7: 0.5 and 3D densitogram at 546 nm of all the tracks	133
Fig. 4.6.4.1	HPTLC-effect directed analysis fingerprint of selected elicited <i>Musa</i> spp. samples	135
Fig. 4.6.4.2	HPTLC chromatogram of genotoxicity assay of selected elicited samples	136
Fig. 4.6.5.1	Elicited sample developed in ethyl acetate – toluene - formic acid - water 6.8: 1 : 1.4: 1, and derivatised in neu's reagent and DPPH• revealing antioxidant compounds	137
Fig. 4.6.5.2	HPTLC-HRMS spectra of compound 5 recorded in the electron spray ionisation (A) positive and (B) negative mode	138
Fig. 4.6.5.3	HPTLC-HRMS spectra of compound 6 recorded in the electron spray ionisation (A) positive and (B) negative mode	139
Fig. 4.6.5.4	HPTLC-HRMS spectra of compound 7 recorded in the electron spray ionisation (A) positive and (B) negative mode	140
Fig. 4.6.5.5	HPTLC-HRMS spectra of compound 8 recorded in the electron spray ionisation (A) positive and (B) negative mode	141
Fig. 4.6.5.6	HPTLC-HRMS spectra of compound 9 recorded in the electron spray ionisation (A) positive and (B) negative mode	142

Fig. 4.6.5.7	HPTLC-HRMS spectra of compound 10 recorded in the electron spray ionisation (A) positive and (B) negative mode	143
Fig. 4.6.5.8	HPTLC-HRMS spectra of compound 11 recorded in the electron spray ionisation (A) positive and (B) negative mode	144
Fig. 4.7.2.1	TLC of <i>Musa acuminata</i> (Simili radjah, ABB) leaf fractions	150
Fig. 4.7.2.2	TLC of <i>Musa acuminata</i> (Simili radjah, ABB) fruit fractions	151
Fig. 4.7.3.1.1	Total phenolic content of leaf and fruit fractions	153
Fig. 4.7.3.1.2	DPPH• antioxidant activity of leaf and fruit fractions	154
Fig. 4.7.3.2.1	Hydroxyl radical inhibition by leaf and fruit fractions	155
Fig. 4.7.3.2.2	ABTS radical inhibition by leaf and fruit fractions	156
Fig. 4.7.3.3.1	α -amylase inhibitory activity of leaf and fruit fractions	157
Fig. 4.7.3.3.2	Alpha-glucosidase inhibitory activity of leaf and fruit fractions	158
Fig. 4.7.3.3.3	Lineweaver-Burk plot for the mode of inhibition of <i>Musa acuminata</i> (Simili radjah, ABB) fruit fractions	159
Fig. 4.7.3.3.4	Lineweaver-Burk plot for the mode of inhibition of <i>Musa acuminata</i> (Simili radjah, ABB) leaf fractions	160
Fig. 4.7.3.5.1	Acetylcholinesterase percentage inhibition of simili radjah leaf and fruit fractions at 1 mg/mL	163
Fig. 4.7.4.2	Preparative thin layer chromatography of HB, HC and HD	169
Fig. 4.7.5.1	HD ₁ on HPTLC fluorescence plate (Silica gel 60 F ₂₅₄) developed in ethyl acetate: toluene: formic acid: H ₂ O (3.4: 0.5: 0.7: 0.5)	171
Fig. 4.7.5.2	HPTLC-HRMS spectra of compound 12 recorded in the electron spray ionisation (A) negative mode (B) positive mode	172
Fig. 4.7.5.3	HPTLC-HRMS spectra of compound 13 recorded in the electron spray ionisation (A) negative mode (B) positive mode	173
Fig. 4.7.5.4	Confirmation of the two compounds in the subfraction HD ₁ to be kaempferol-3- <i>O</i> -rutinoside (12) and rutin (13),	177

Fig. 4.7.5.5	Biological activities of compounds 12 and 13	178
Fig. 4.7.5.6	Molecular structures of compounds 12 and 13	180

LIST OF PLATES

Plate no	Plate title	Page
Plate 2.5.1	Young <i>Musa</i> spp. on the field	36
Plate 2.5.2	<i>Musa acuminata</i> plant with fruits	37
Plate 4.7.4.1	DPPH• antioxidant activity of pooled column sub-fractions A – K	167

LIST OF APPENDICES

Appendix	Title	Page
Table 1	Imputation report of missing data with six different algorithms of 150.5K SNP in 56 banana samples	223
Table 2	Peak area of HPTLC-Effect directed analysis	224
Table 3	Means of ABTS and hydroxyl radical scavenging activities (IC ₅₀) of <i>Musa acuminata</i> leaf and fruit crude extract and fractions	226
Table 4	Antidiabetic activity of <i>Musa acuminata</i> leaf and fruit crude extract and fractions	227
Figure 1	Average Shoot length (cm) of the different tissue culture-grown accessions	228
Figure 2	Average number of leaves of the different tissue culture-grown accessions	229
Figure 3	Average number of roots of the different tissue culture-grown accessions	230
Figure 4	Average number of shoots of the different tissue culture-grown accession	231
Figure 5	DPPH• IC ₅₀ values of field and tissue culture accessions	232
Figure 6	Ferric reducing antioxidant power of field and tissue culture-grown accessions	233
Figure 7	Gallic acid calibration curve for TPC	234
Figure 8	Quercetin calibration curve for TFC	235
Figure 9	Total phenolic contents of field and tissue culture-grown accessions	236
Figure 10	Extraction with different solvents for the selection of best extraction solvent	237
Figure 11	HPTLC Chromatogram showing α -glucosidase and α -amylase inhibition	238
Figure 12	<i>Musa</i> spp. accession grown on media with different doses of sugar used as elicitor	239
Figure 13	<i>Musa</i> spp. accession grown on proliferation media incubated at different temperature	240

Figure 14	<i>Musa</i> spp. accession grown on media with different doses of jasmonic acid used as elicitor	241
Figure 15	<i>Musa</i> spp. accession grown on media with reduction in the nitrate source component of the media	242
Figure 16	Sugar (1 – 15) calibration curve Sample	243
Figure 17	Sugar (16 – 30) calibration curve	244
Figure 18	Temperature GA calibration curves	245
Figure 19	Jasmonic acid calibration curve	246
Figure 20	HPTLC chromatograms of elicited accessions (1-15) using different doses of sugar	247
Figure 21	HPTLC chromatograms of elicited accessions (16-30) using different doses of sugar	248
Figure 22	HPTLC chromatograms of elicited accessions grown under different temperature conditions	249
Figure 23	HPTLC chromatograms of elicited accessions grown in media with reduced nitrate components	250
Figure 24	HPTLC Chromatograms of elicited accessions using different doses of jasmonic acid	251
Figure 25	Column chromatography of ethyl acetate fraction	252
Figure 26	Picture of collected sub-fractions	253
Figure 27	TLC of pooled sub-fractions A-K from silica gel column	254
Figure 28	TLC of pooled sub-fractions A-K from sephadex column	255
Figure 29	¹ H NMR full spectral of compounds HD ₁	256
Figure 30	Expanded ¹ H NMR spectral of compounds HD ₁ showing peaks found between 0.7 and 2.1 ppm chemical shifts	257
Figure 31	Expanded ¹ H NMR spectral of compounds HD ₁ showing peaks found	258

between 3.25 and 3.85 ppm chemical shifts

Figure 32	Expanded ^1H NMR spectral of compounds HD ₁ showing peaks found between chemical shifts 4.2 and 5.3 ppm	259
Figure 33	Expanded ^1H NMR spectral of compounds HD ₁ showing peaks found between chemical shifts 6.3 and 8.1 ppm	260
Figure 34	^{13}C NMR full spectral of compounds HD ₁	261
Figure 35	Expanded ^{13}C NMR spectral of compounds HD ₁ showing peaks found between chemical shifts 66 and 78 ppm	262
Figure 36	Expanded ^{13}C NMR spectral of compounds HD ₁ showing peaks found between chemical shifts 95 and 135 ppm	263
Figure 37	Expanded ^{13}C NMR spectral of compounds HD ₁ showing peaks found between chemical shifts 158 and 182 ppm	264
Figure 38	Distortionless Enhancement by Polarisation Transfer (DEPT) spectral of compounds HD ₁	265
Figure 39	Correlation spectroscopy (COSY) spectral of compounds HD ₁	266
Figure 40	Expanded correlation spectroscopy (COSY) spectral of compounds HD ₁	267
Figure 41	HMBC spectral of Compounds HD ₁	268
Figure 42	HSQC spectral of compounds HD ₁	269
Figure 43	Expanded HSQC spectral of compounds HD ₁	270

LIST OF ABBREVIATIONS

ABTS	2,2-azinobis-3-ethylbenzothiazoline-6-sulfonic acid
AChE	Acetylcholinesterase
α -AML	Alpha-amylase
α -GCD	Alpha-glucosidase
AD	Alzheimer's disease
ATCI	Acetylcholine iodide
BAP	6-Benzylaminopurine
CC	Column chromatography
CTAB	Cetyl trimethyl ammonium bromide
CME	Crude methanol extract
NHF	<i>n</i> -Hexane fraction
DCMF	Dichloromethane fraction
EAF	Ethyl acetate fraction
NBF	<i>n</i> -Butanol fraction
AMF	Aqueous methanol fraction
DArTSeq	Diversity Array Technology Sequencing
DMSO	Deuterated dimethyl sulphoxide
DNA	Deoxyribonucleic acid
DPPH•	2,2-diphenyl-1-picrylhydrazyl
DTNB	5,5'-dithio-bis-2-nitrobenzoic acid
EA	Ethyl acetate
EDTA	Ethylenediaminetetraacetic acid
ESI	Electron spray ionisation
EDA	Effect-directed analysis
FA	Formic acid
FRAP	Ferric Reducing Antioxidant Power
GC	Gas chromatography
hR_F	Homologous retention factor ($R_f \times 100$)
HPLC	High performance liquid chromatography

HPTLC	High-performance thin layer chromatography
HRMS	High-resolution mass spectrometry
IAA	Indole-3-acetic acid
IBS genetic distance matrix	Identity-by-state genetic distance matrix
IC ₅₀	50% Inhibitory concentration
JA	Jasmonic acid
15-LOX	15-lipoxygenase
MAF	Minor allele frequency
MS media	Murashige and Skoog media
MS	Mass spectrometry
MTT	3-(4,5-Dimethylthiazol-2-yl)-2,5-diphenyltetrazolium bromide
NAA	α -Naphthalene acetic acid
NaCl	Sodium chloride
NaOCl	Sodium hypochlorite
NMR	Nuclear magnetic resonance
PBS	Phosphate buffered saline
PCA	Principal component analysis
PEG	Polyethyleneglycol
PGRs	Plant growth regulators
pNPG	<i>p</i> -Nitrophenyl glucopyranoside
PTC	Plant tissue culture
R _f	Retardation factor
SRF	Simili radjah fruit
SRL	Simili radjah leaf
TFC	Total flavonoid content
TPC	Total phenolic content
TLC	Thin layer chromatography
SNP markers	Single nucleotide polymorphic markers

UPLC-qTOF-MS	Ultra-performance liquid chromatography quadrupole time of flight electron ionization-Mass Spectrometry
UV	Ultraviolet

CHAPTER ONE

1.0 INTRODUCTION

1.1 Plants as Sources of Secondary Metabolites

Plants produce a lot of chemicals classified as primary metabolites and secondary metabolites. The class of chemicals that are necessary for the survival and growth of the plants are named primary metabolites. They are; proteins, carbohydrates and lipids. Before now, secondary metabolites were believed to be waste products without obvious functions. They are not particularly essential for plant survival but without secondary metabolites, the plant suffers. The importance and the roles of secondary metabolites in plants were recently discovered to be crucial for many plant processes. They defend the plants from pathogens and herbivores attacks, some of the secondary metabolites attract insect pollinators and other fruit dispersers; they help in the competition with neighbouring plants and organisms; they provide mechanical support for the plants and help to absorb harmful ultraviolet radiation. Secondary metabolites also give plants some specific colour, odours and tastes (Pagare *et al.*, 2015).

Several billion years of evolution has resulted into a great diversity of plant species. Christenhusz and Byng (2016) estimated recently that, there are at least 374,000 different plant species and they comprise a wide array of secondary metabolites. Thangaraj (2016) reported that there should be more than a hundred thousand known secondary metabolites from the relatively few studied plant species. Moreso, most species have been studied for only a certain type of compound, for example alkaloids. The information from the already studied species gives us a notion that a lot of compounds could be isolated from different plant species. It is therefore clear that nature provides a huge prospect for unearthing of bioactive secondary products.

Secondary metabolites are important resources for flavors, fragrances, dyes, pesticides and pharmaceuticals apart from their benefits to the plant itself (Guerriero *et al.*, 2018). Since ancient times quite a lot of drugs used in the pharmaceutical industry are secondary metabolites detected from plants whose characteristics have been explored. Till date, several of these important drugs are in use. Synthetic substitutes have been elaborated but do not always have similar effectiveness, pharmacological specificity or viability compared to the ones derived from plants. Currently, 80% of drug substances in the market contain compounds that were either directly or indirectly or even through semi-synthesis derived from plants (Maridass and De Britto, 2008). More so, 11% of the 252 medications considered as fundamental and basic by WHO are obtained from flowering plants (Rates, 2001). Popular examples are the anti-cancer drugs ‘Taxol’, podophyllotoxin and camptothecin from *Catharanthus roseus*. Another example is the anagelsic morphine extracted from Opium plant.

The search for new plant-derived bioactive secondary metabolites and a continuous supply of plant material ought to remain a need in present and prospective endeavours toward continuous and sustainable preservation and rational usage of biodiversity (Karuppusamy, 2009). The importance and advancing commercial use of secondary metabolites in these modern days has led to a great increase in the interest especially in the area of advanced biotechnology with the likelihood of producing bioactive plant metabolites using tools such as *in vitro* plant tissue culture systems.

1.2 Secondary Metabolites Production via *in vitro* Plant Tissue Culture Techniques

The interest in therapeutic plants is developing at an exceptionally fast pace, leading to the necessity to set up a standardised, uniform, continuously available and controllable plant production system. Moreso, the extensive use of plant materials resulted progressively in a threat on the biodiversity and its habitats. It is clear that the conventional (wild) supply of plant materials for herbal medicine can no longer meet the demand (Nalawade and Tsay, 2004). Therefore, plant culture technologies were emphasised in the search for alternatives for the production of needed plant-derived therapeutic phytochemicals. Regeneration of plants via *in vitro* propagation has a remarkable potential for the production of high-quality and uniform medicinal compounds from plants and it can be used as a means for

large-scale production of medicinal compounds. Hence, it is essential to understand the cultivation, conservation, and sustainable utilisation of vital medicinal plant species for present use and for future generations.

In vitro plant tissue culture techniques (PTC), which are biotechnological techniques, are useful when it comes to the search for substitutes to the production of interesting bioactive phytochemicals. Ramachandra and Ravishankar (2002) reported that *in vitro* PTC tool is a reliable supplemental method to conventional agriculture in commercial production of therapeutic agents. Plant cells, tissues and organ cultures are routinely established from explants, like; meristem, roots, leaves and stems under sterile conditions, to produce and culture plantlets in artificial conditions. This can be used for large-scale multiplication of plant materials in view to extract secondary metabolites. Secondary metabolites are obtainable from large-scale cell suspension culture with the benefit of eventually providing a steady, uninterrupted and dependable source of medicinal compounds (Hussain *et al.*, 2012).

Cell cultures capable of producing particular secondary metabolites have been discovered. Nowadays, phytochemicals can be produced using *in vitro* plant tissue culture at a similar or better rate than from conventional field material. New and interesting bioactive phytochemicals have been found through biological assays. Urbanska *et al.* (2014) obtained saponins from *Platycodon grandiflorum* using hairy root culture in shake flask and mist bioreactor. Bioactive phytochemicals have been produced in undifferentiated cell cultures as well as in specific organised cultures. For example, Fett-Neto *et al.* (1994) was able to produce taxol, an anticancer agent, using cell suspension culture. The possibility of the utilisation of *in vitro* PTC techniques for biotransformation of specific secondary metabolites has been demonstrated by a number of researchers (Krings and Berger, 1998; Ravishankar and Ramachandra, 2000). The purposeful elicitation of defined chemical products using *in vitro* cultures makes possible the study of biochemical and metabolic pathways without interference from external sources, thanks to the possibility to control micro-environmental culture conditions.

The major advantages of *in vitro* plant cell and tissue culture for secondary metabolites production rather than from the conventional field plants are: (i) controlled culture conditions avoiding environment (soil, climate, pathogens) influences, (ii) simpler and

predictable production, (iii) high productivity, (iv) traceability (labeled or probed molecules), (v) possibility for boosting the production of a specific component by elicitation, (vi) programmable, uniform and synchronal production.

Strategies to boost secondary metabolites production using tissue culture techniques include; hairy root culture, elicitation, plant cell immobilization and metabolic engineering among others.

1.3 Elicitation

Elicitation is an effective and a notable method for the enhancement and generation of numerous commercially useful medicinal compounds from plants. Elicitors are signals or molecules triggering the formation of secondary metabolites. Use of elicitors for producing numerous secondary metabolites has been reported in the literature (Wang and Zhong, 2002). Elicitors can be classified as biotic or abiotic. Biotic elicitors are of biological origin and they include organisms, whole cells and cell components such as chitosan, arachidonic acid, yeast extract, and cell walls of pathogens (Sanchez-Sampedro *et al.*, 2005a). Abiotic elicitors are not of biological origin. They are physical stimuli like ultrasound, UV light or chemicals such as jasmonic acid and salicylic acid (Namdeo, 2007). Temperature condition, intensity of light and its duration can also trigger the production of enzymes necessary for the production of secondary compounds. It was reported that abiotic elicitors are of better alternative to biotic elicitors because with time, biotic elicitors lose their potentials to enhance the synthesis of secondary metabolites and may even affect the physiological behaviour of the cells or tissue cultures negatively (Kaimoyo *et al.*, 2008).

When secondary metabolites are triggered or enhanced through elicitation and *in vitro* PTC techniques, then it is important to identify and characterise these important secondary metabolites using chromatographic techniques.

1.4 High-Performance Thin Layer Chromatography (HPTLC)

The HPTLC is a powerful, simple, quick, and effective tool in quantitative analysis of compounds. The HPTLC is an analytical technique which utilises the separation principles

of thin layer chromatography (TLC), yet with enhancements anticipated to improve the resolution of the compounds to be separated and to permit the quantitative analysis of the compounds. It is an exceedingly sensitive and high throughput screening method for the quick examination of large numbers of compounds (Choma and Jesionek, 2015). It is generally utilised for quality control of food and botanicals as well as characterisation of metabolites.

The HPTLC is an advanced form of thin layer chromatography (TLC) allowing a highly efficient chromatographic separation. It is an automated technique that involves steps such as sample application, development and visualisation which gives standard and a reproducible chromatogram. Quantitative evaluation is also possible using the CAMAG TLC scanner and WINCAT software. High-performance thin-layer chromatography (HPTLC) meets all quality requirements needed in recent analytical labs, even in a fully regulated environment (Morlock and Schwack, 2010). The HPTLC ensures the simultaneous analysis of up to twenty samples per plate, making it cost-effective and reliable. With HPTLC, it is possible to link bioassays with chromatography; this is called Effect Directed Analysis (EDA). Actual bioassays with cuvette, petri dish and microtiter plates, gives a sum parameter which might be derived from antagonistic or synergistic effects and the compounds responsible for the bioactivity are unknown. But with HPTLC, bioassay can be combined with chromatography, which reveals the bioactivity of single compounds. Effect Directed Analysis (EDA), in combination with chromatography, leads to targeted answers in a comprehensive context and range of potentially relevant compounds. Thus, important bioactive compounds are identified among many compounds present in plant sample. Another advantage of HPTLC is its amenability to hyphenations. Hyphenation involves combination of spectrometers with chromatographic systems for further characterisation of samples. High performance liquid chromatography-based or gas chromatography-based hypernations (super-hyphenation) are more expensive and results in large data set which is a major setback. The instrumentation in high performance liquid chromatography-based or gas chromatography-based hypernations is more complex and this makes their routine use difficult (Morlock and Schwack, 2010). The problem of hyphenation is less challenging with HPTLC because of its open system. It is highly adaptive to different sensitivities and is cost-effective (Brosseau *et al.*, 2009). It generates

less data because only zones of interest are evaluated. The HPTLC have been combined with spectrometers such as Ultraviolet- Visible (UV-Vis) spectroscopy, Fluorescence Detection (FLD) and Fourier-transform Infrared Spectroscopy (FTIR) followed by Surface-enhanced Raman Spectroscopy (SERS), Mass spectrometry (MS) or high-resolution MS (HRMS) (Brosseau *et al.*, 2009). HPTLC technique is an effective tool for the detection, characterisation, and bioprofiing of bioactive compounds in many plant species.

1.5 *Musa* spp.

Musa species are among the popular and highly consumed crops for its nutritional values and have been reported as a reliable source of medicinal compounds. They are grown majorly in the tropics and belong to Musaceae family, including the popular edible banana and plantain. Edible bananas are diploids, triploids or tetraploids hybrids from the wild types *Musa acuminata* and *Musa balbisiana*, and are widely grown. The fruits of *Musa* spp. as well as the other parts (pseudo stem, leaves, sap, root, flowers) are known to be used for treating many ailments in traditional medicine. Dried banana fruits, roots and flowers are used for diabetes in India (Ingale *et al.*, 2009). Different parts of different *Musa* species have been studied for antiulcer, hypoglycemic (Ojewole and Adewunmi, 2003), antihypertensive, anticholinesterase (Ayoola *et al.*, 2017), wound healing (Apriasari *et al.*, 2015) and anti-inflammatory activities (Abad *et al.*, 2000), among others. Banana and plantain fruits have been identified to be rich in bioactive compounds like Carotenoids, Catecholamines e.g. Dopamine (Kanazawa and Sakakibara, 2000). Alkaloids, flavonoids, tannins, anthocyanin and its derivatives have been identified in different parts of *Musa* spp. Different amino acids such as threonine, tryptamine and tryptophan are present in *Musa* spp. (Ivan, 2005).

1.6 Justification for the Study

Musa species were chosen based on a previous ethnobotanical survey where they were reported to be used traditionally to treat neurodegenerative disorders especially Alzheimer's disease (Sonibare and Ayoola, 2015). Different parts of *Musa* spp. are used for the treatment of many diseases including ulcer and diabetes. Moreso, many studies

have focused on the characterisation and isolation of bioactive metabolites from the fruit, pulp and peel but minimal attention was given to the leaves. From literature, different parts of *Musa* plant contain several antioxidant compounds some of which have been isolated especially from the fruits.

From preliminary work on the comparison of presence and activity of phytochemical compounds in field and micropropagated *Musa* spp. leaves, it was reported that the micropropagated plants have higher DPPH• antioxidant activity and total phenolic contents than the field plants (Ayoola *et al.*, 2017). Finding out the reasons why *in vitro* *Musa* spp. material produced more phytochemical compounds with higher activity and if this difference would be the same after acclimatisation would be an interesting study. Also, understanding the difference between the two originated materials (*in vitro* plant tissue culture and field) will allow further development such as boosting secondary metabolites production through elicitation process and *in vitro* plant tissue culture conditions. Moreso, the role of elicitors on secondary metabolites accumulation in *Musa* spp. had not been studied. However, before using PTC techniques for large scale secondary metabolites production, the genetic fidelity (trueness-to-type) of the *in vitro*-grown plantlets should be confirmed. This is a vital pre-requisite in *in vitro* PTC techniques due to the presence of somaclonal variations and genetic defects from *in vitro*-grown plants which can limit the commercial use of *in vitro* plant tissue culture technique (Salvi *et al.*, 2001).

The current interest is to boost the phenolics and antioxidant compounds production using biotechnology techniques. Given the fact that *Musa* spp. have many medicinal uses, it will be necessary to have an accurate identification of the compounds responsible for the different activities in the different accessions using a metabolomic approach, e.g. High performance thin layer chromatography (HPTLC).

1.7 Research Hypothesis

In vitro plant tissue culture technique, nutrient stress and abiotic elicitors can increase the secondary metabolites composition in *Musa* spp. leaves and these metabolites can

scavenge free radicals and inhibit cholinesterase which could serve as a means of treating neurodegenerative diseases.

The verification of this hypothesis entails many questions.

1.8 Research Questions

1. Do the selected *Musa* accessions possess bioactive compounds in support of traditional claims on their application for treating Alzheimer's and other diseases?
2. What are these bioactive compounds and can they be identified using HPTLC?
3. If the micropropagated plants are true-to-type with the field materials, can *in vitro* plant tissue culture provide an alternate source of plant materials for secondary metabolites production in *Musa* spp.?
4. Can abiotic elicitors and nutrient stress increase secondary metabolites production via *in vitro* plant tissue culture technique?

1.9 Aim and Objectives of the study

The general aim of this study is to improve the secondary metabolites in *Musa* species using *in vitro* plant tissue culture techniques and isolate compounds with antioxidant, antidiabetic and cholinesterase inhibitory activity.

The specific objectives of this study are:

1. To assess the genetic fidelity of micropropagated *Musa* accessions.
2. To identify the *Musa* spp. accessions with total phenolic content and high anticholinesterase and antioxidant activity.
3. To test the anticholinesterase and antioxidant activity of *in vitro*-derived plants, in comparison to field plants.
4. To determine the chemical and biological profile of the field, *in vitro*-grown and acclimatised *Musa* accessions using HPTLC.
5. To carry out effect directed analysis of the field, *in vitro*-grown and acclimatised accessions using HPTLC.

6. To determine the influence of different abiotic elicitors and nutrient stress on the production of secondary metabolites in *Musa* species and their potential elicitation role.
7. To carry out bioassay guided fractionation and isolation of active metabolites in *Musa* spp.

CHAPTER TWO

2.0 LITERATURE REVIEW

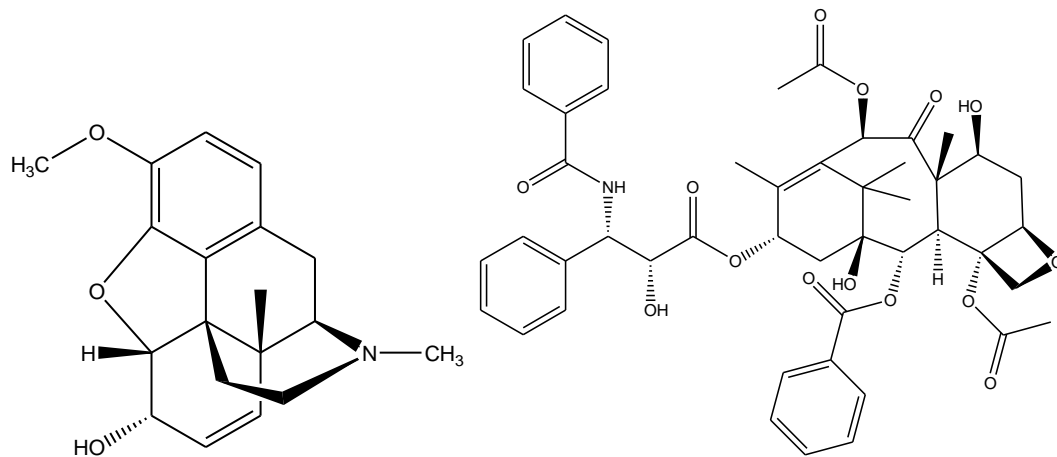
2.1 Usefulness of Secondary Metabolites as Leads in Drug Discovery

Flowering plants provide an outstanding bioactive metabolites source used in the pharmaceutical industry. Many available drugs in the pharmaceutical industry were derived from plants examples include cocaine derived from *Erythroxylum coca* Lam. and quinine from *Cinchona officinalis* L. There are also anti-cancer *Catharanthus roseus* alkaloids (vincristine and vinblastine), *Atropa belladonna* alkaloids (atropines, hyoscyamine and scopolamine), reserpine, physostigminine, and steroids, like digoxin, digitoxin and diosgenin (Namdeo, 2007). Globally, 121 clinically beneficial prescribed drugs are derived from plants (Rao and Ravishankar, 2002). From surveys, the usage of medicinal plants in the United States of America increased from about 3% to 37% from 1991 to 1998 (Rao and Ravishankar, 1999). Raskin *et al.* (2002) reported that prescribed medications containing phytochemicals were estimated to be above thirty billion USD in the US. Seventy-five percent of the world's populace depends on plants for remedy. Examples of pharmaceuticals obtained from plants are recorded in Table 2.1.

Table 2.1: Important Plant-derived Pharmaceuticals

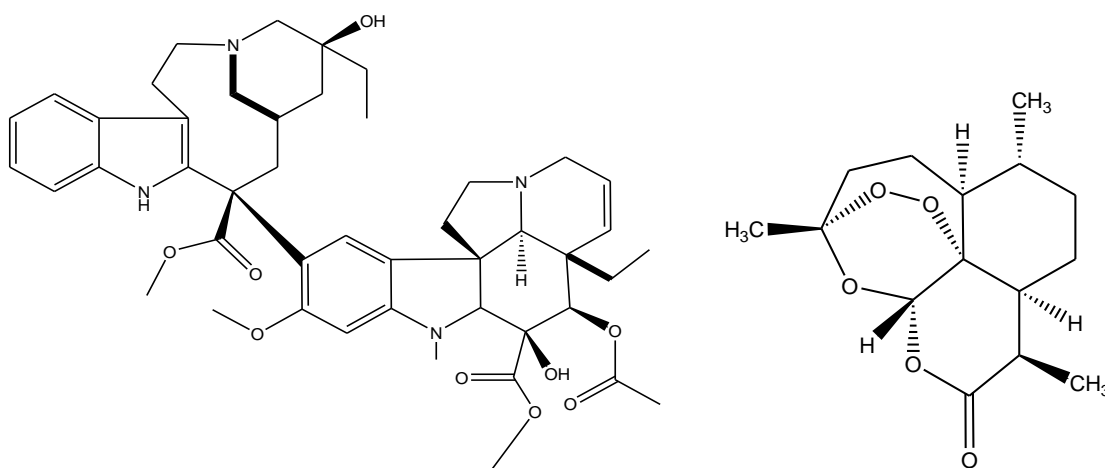
Product	Use	Plants	Cost USD /Kg
Ajmalicine	Antihypertensive	<i>Catharanthus roseus</i> (L.) G. Don	37 000
Codeine (1)	Sedative	<i>Papaver somniferum</i> L.	17 000
Vincristine	Antileukemic	<i>Catharanthus roseus</i>	2 000 000
Taxol (2)	Anticancer	<i>Taxus brevifolia</i> Nutt.	600 000
Camptothecin	Antitumour	<i>Camptotheca acuminata</i> Decne.	432 000
Colchicine	Antitumour	<i>Colchium autumnale</i> L.	35 000
Vinblastine (3)	Antileukemic	<i>Catharanthus roseus</i>	1 000 000
Shikonin	Antibacterial	<i>Lithospermum erythrorhizon</i> Siebold and Zucc.	4500
Ajmaline	Antimalarial	<i>Rauwolfia serpentina</i> (L.) Benth. ex Kurz	75 000
Morphine	Sedative	<i>Papaver somniferum</i>	340 000
Artemisinin (4)	Antimalarial	<i>Artemisia annua</i> L.	400
Digoxin (5)	Heart stimulant	<i>Digitalis lanata</i> Ehrh.	3000
Quinine	Antimalarial	<i>Cinchona ledgeriana</i> Wedd.	500
Capsaisin (6)	Counter-irritant	<i>Capsicum frutescens</i> L.	750
Berberine	Intestinal ailment	<i>Coptis japonica</i> Makino	3250

Adapted from Ravishankar and Ramachandra Rao (2000); *Structures of plant-derived products (1) to (6) are shown in Figure 2.1



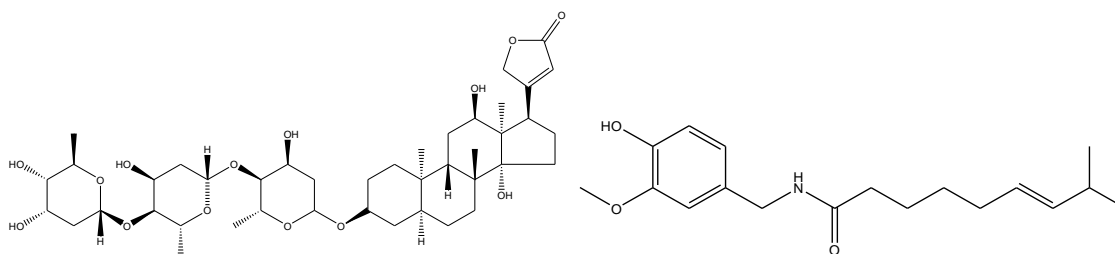
Codeine (1)

Taxol (2)



Vinblastine (3)

Artemisinin (4)



Digoxin (5)

Capsaicin (6)

Figure 2.1 Structures of some plant-derived products

2.2 Biotechnology Application for Secondary Metabolites Production

The world population is greatly increasing so there may be huge demand for the utilisation of available land for the production of food, shelter and other basic needs. The available land should therefore be used effectively for other uses such as production of phytochemicals. Hence, it is appropriate to ensure the development of modern technologies that would improve plants and better utilise the available land and natural resources. Moreover, this would reduce the ruthless exploitation of the available germplasm and help to conserve them while using them in a sustainable manner. In the past twenty years, *in vitro* plant tissue culture has provided a promising and new field in plant biotechnology, with focus on secondary metabolites production. Different aspects of biotechnological methods can be envisaged such as transgenic plants or organisms, metabolic engineering and micropropagation of medicinal and endangered plants among others. Recent advances and new improvement in molecular biology (metabolic engineering) and biotechnology research has resulted in the production of multiple and novel secondary products. For example, D, L-tetrahydropalmatine and D-corydaline were produced from the tubers of *Corydalis yanhusuo*, which was derived by somatic embryogenesis (Lee *et al.*, 2001). Guerriero *et al.* (2018) also highlighted the production of artemisinin and caffeine in heterologous hosts and plant species (*Artemisia* spp., *Coffea arabica* L., *Urtica dioica* L.) using different biotechnological strategies. Another important factor that has brought biotechnological methods to lime light is the need for safer drugs with mild side effects. Scientists are always searching for efficacious drugs from plants and other natural sources with little or devoid of side effects. This factor in particular has emphasised the utilisation of biotechnological techniques to enhance quality and amount of drugs and food flavorings production (Ramanchandra and Ravishankar, 2002). Tissue culture especially, provides a reliable substitute for secondary metabolite production. It provides several advantages over conventional cultivation which is faced with challenges such as political instability, infestation of the field by pests and diseases, drought, long period of cultivation and many more. All of these are ruled out with cultivation of plants via *in vitro* plant tissue culture techniques. It further gives other advantages like high productivity and reproducibility coupled with simpler and predictable results. The advantages of *in vitro* plant tissue culture (PTC) techniques for cultivation of

medicinal plant over conventional method of plant cultivation and production are as follows:

1. The secondary metabolites production is done in a controlled environment which is autonomous of geographical and seasonal variations and environmental factors. The negative influence of insect and pest attack is eliminated.
2. With *in vitro* plant tissue culture system, a constant source of product with even quality and high yield is ensured because the production system is well-defined.
3. Selection of cell lines with higher secondary metabolites production is possible.
4. Novel phytochemicals that are not present in the mother plant can be generated in plant tissue culture grown plants.
5. Biotransformation using precursors for novel secondary metabolites is possible.
6. The production cost can be reduced and productivity increased with the automatisation of cell growth and regulation of metabolic processes (Vanisree *et al.*, 2004).

2.3 *In Vitro* Plant tissue Culture (PTC) Techniques

The PTC has been utilised in the field of plant breeding for crop improvement and has a lot of potentials. The PTC is defined as the ability to regenerate and propagate plants from single cells, tissues and organs under sterile and controlled conditions. Plant tissue culture works with the principle of plant totipotency which is the characteristic of any plant part or single cell to divide and be regenerated into an intact adult plant. *In vitro* plant tissue culture techniques were mainly used for large-scale production or micropropagation of elite planting material with desirable characteristics. The PTC is also generally used for producing biologically active compounds for pharmaceutical industries. For a successful *in vitro* culture, several parameters such as explant source, culture medium and growth regulators among others should be considered (Rao and Ravishankar, 2002).

2.3.1 Explant source

Explant is initial material used for PTC experiment. As plant cells do not express totipotency in the same manner, the success of *in vitro* culture is largely dependent on the age, type and position of explants (Sasikumar *et al.*, 2009). The explants frequently utilised are shoot tips, nodal buds and root tips. Meristems are preferred as explants to other large explants (nodal cutting) because they can be free of endogenous pathogens which are high in large explants. However, the limitation with meristem explant is the slow growth rate (Gueye *et al.*, 2012).

2.3.2 Sterilisation

Maintaining an aseptic environment is key in *in vitro* plant tissue culture. The culture container, medium, explant and any other instrument must be properly sterilised before use. A common challenge of *in vitro* plant tissue culture is microbial contamination (Rout *et al.*, 2000). Common bacterial contaminants are *Lactobacillus*, *Bacillus* and *Staphylococcus*. Micro-organisms inhibit plant growth and can alter the medium or culture pH in *in vitro* culture. They also compete with explants for nutrients which might lead to the death of the explants. It is therefore imperative to use sterile techniques for *in vitro* plant tissue culture. Laboratory instruments are sterilised by autoclaving, alcohol washing, flaming. Fumigation of the culture rooms is also important. Culture media, distilled water and other stable mixtures are sterilised by autoclaving in sealed glass containers sealed with cotton plugs, aluminum foil or plastic lids. Generally, for liquid media, autoclaving is done at 121 °C and 15 psi for fifteen to thirty minutes.

2.3.3 Plant Tissue culture (PTC) media

The PTC medium comprises vital nutrients and elements for plant growth *in vitro*. Choosing the right media composition is one of the pre-requisites and is important for effective *in vitro* plant propagation. Different types of media composition are available for PTC, but Murashige and Skoog (1962), revised by Linsmaier and Skoog (1965) medium is commonly used and can be regarded as the standard medium. Other media used are Schenk and Hilderbrandt (SH) (1972), Gamborg, B5 (Gamborg *et al.*, 1968) and Woody plant medium (WPM) (Lloyd and McCrown, 1980). Generally, all culture media consists

of: inorganic nutrients (macro and micro elements), vitamins, growth regulators, and a carbon source (sucrose).

Inorganic nutrients: These are mineral elements that are important in plant physiological development. They are macro and micro elements. Macro elements are necessary for plant growth they include; nitrogen, potassium, phosphorus, sulphur, carbon, magnesium, hydrogen, calcium and oxygen. Deficiency in nitrogen which is an essential part of plant protein, in many cases leads to stunted growth. Carbon is the backbone of many plants bio-molecules such as starches and cellulose. It stores energy in the plant. Potassium helps to reduce the loss of water from the leaves and it can increase drought tolerances. Potassium deficiency may cause necrosis or interveinal chlorosis. Microelements are also essential as catalysts for many biochemical reactions. Microelements include; Iron (Fe), Molybdenum (Mo), Manganese (Mn), Zinc (Zn), Copper (Cu), cobalt (Co) and Boron (B). Microelements (Fe, Zn, and Mn) deficiency symptoms include leaf chlorosis and shoot tip necrosis for B, Co, Ni deficiency.

Organic nutrients:

Vitamins: Although plants can produce the required vitamins, culture medium needs to be supplemented with vitamins like thiamine (vitamin B1), Pyridoxine (vitamin B6), Myo-inositol (part of the vitamin B complex) and Niacin (vitamin B3). Thiamine is directly involved in the biosynthesis of some amino acids and essential co-factor of carbohydrates metabolism. Vitamin C helps to prevent blacking during explant isolation.

Amino Acids: An example is glycine which may be directly utilised by plants or serve as a nitrogen source.

Carbon Sources: This includes sucrose, which is the most commonly used, glucose and fructose. They support the growth of the plant and are usually used at a concentration of 3%. Sucrose is necessary for various metabolic activities.

2.3.4 Plant growth hormones

Plant growth hormones are also called plant growth regulators (PGRs) or phytohormones. They regulate the physiological and morphological processes in plants. Plants synthesise

phytohormones for their use but exogenous hormones are needed for plant growth *in vitro* (Sasikumar *et al.*, 2009). These external plant growth hormones must be used in adequate and appropriate amount because the addition of high quantity of growth hormones can affect the plants physiologically and morphologically. The five main groups of naturally occurring PGRs are; cytokinins, auxins, gibberellins, ethylene and abscisic acid. Cytokinins and auxins are the most important plant growth regulators; however, their levels in plant cell and tissue cultures should be balanced and regulated. A higher cytokinin to auxin ratio favours shoot formation, while a higher auxin to cytokinin ratio favours root formation. When the ratio of cytokinin and auxin is almost equal, it results in callus formation (Su *et al.*, 2011).

Auxins: Auxins aid in cell growth and elongation, cell division initiation, organisation of meristems leading to callus formation or defined organs (generally roots) and promote vascular differentiation. In organised tissues, auxin appears to be involved in maintaining apical dominance, affecting abscission, promoting root formation, and tropistic curvatures, delaying leaf senescence, and fruiting (Gaspar *et al.*, 1996).

Indole-3-acetic acid (IAA) is a frequently identified natural auxin. Other natural auxins are indole-3-butyric acid (IBA) and indole-3-acrylic acid. Examples of common synthetic auxins are 2,4-dichlorophenoxyacetic acid (2,4-D); used for callus induction and suspension cultures, and 1-naphthaleneacetic acid (NAA); used for organogenesis. Others are dicamba and picloram. They are often used to induce the embryogenesis and in suspension cultures.

Cytokinin: Examples of cytokinins are; 6-benzylaminopurine (BAP), kinetin, 2-isopentenyladenine (2-iP) thidiazuron (TDZ), and zeatin. BAP is the most effective cytokinins for promoting the formation of shoot. Cytokinins help with cell division and modification of apical dominance.

Gibberellins: Gibberellic acid, GA₃ is the most commonly used. It enhances shoot formation in meristems and shoots culture.

2.3.5 Types of tissue culture techniques

The different types of *in vitro* plant tissue culture techniques are explained below:

2.3.5.1 Callus cultures

A mass of unspecialised or undifferentiated cells is known as callus. When suitable hormones are used, explants give rise to this mass of actively dividing cells. Callus can be induced from explants grown on medium containing the auxin, 2,4-D, (2, 4-dichlorophenoxy acetic acid) and often a cytokinin like BAP (Benzyl aminopurine). The medium containing the hormones excites cell division in explant; and within 2-3 weeks, callus is formed. Organs and new plantlets can then be regenerated from callus via organogenesis.

2.3.5.2 Suspension culture

Suspension cultures involve plant regeneration using liquid media. In suspension culture, agar and gelrite, which are the gelling agents, are omitted from the medium. In suspension culture calli are grown in a suitable container (conical flask) and are constantly agitated to provide large surface area to help gaseous exchange and also to make the suspension free of cells. Two types of suspension culture exists; batch and continuous. Batch cultures involve sub-culturing onto new media at regular intervals while in continuous culture; new medium is regularly added to the existing culture. Suspension cultures are used extensively in large scale secondary metabolites production.

2.3.5.3 Somatic embryogenesis

This is the development of plant from a single somatic cell. It can be done in two ways; direct or indirect embryogenesis. When embryos are regenerated from explants giving rise to an identical clone it is known as direct embryogenesis; while indirect embryogenesis involves two steps, first callus is induced from the explant and secondly the explants are transferred to other media types to differentiate the callus into leaf, shoot or root. Indirect somatic embryogenesis was reported for strawberry using 2, 4- dichlorophenoxy acetic acid, BAP and gibberellic acid (Waghmare *et al.*, 2017).

2.3.5.4 Protoplast cultures

Protoplast is a naked cell surrounded by the plasma membrane and can also be used to reproduce a whole plant. In protoplast culture, the cell protoplast is first removed either by mechanical or enzymatic method and then cultured on appropriate medium. The protoplasts form a new cell wall, divides within two to seven days of culture and then form callus. New plants are then regenerated via organogenesis.

2.3.5.5 Organogenesis

Organogenesis involves the regeneration of organs such as roots, stems, leaves or flowers in plant tissue culture. This also occurs in two stages, first the generation of callus and then generation of the desired organ from the callus. Root formation is called rhizogenesis and the initiation of shoot is called caulogenesis. Cytokinins are majorly used for shoot formation and sometimes auxins. For example, shoot organogenesis was achieved in *Lysionotus serratus* D. Don., a Chinese medicinal plant using high cytokinin. The best shoot proliferation was obtained when the MS medium was fortified with 0.5 mgL⁻¹ BAP alone or combined with 0.1 mgL⁻¹ NAA (Li *et al.*, 2013). For root formation, auxins are mainly used.

2.3.6 Hardening, acclimatisation of tissue culture plantlets

Acclimatisation is the final stage of plant tissue culture experiment and it requires careful handling of plants. It is a major step that links plant conservation to utilisation of plants. It involves transplantation of a well-developed *in vitro* growth plantlet from completely controlled *in vitro* growth conditions to the field. It should be done gradually because the plants have to adjust to new environmental changes and need to be able to photosynthesise (i.e. manufacture its own food). The plants produced in tissue culture do not prepare sufficient food for their own survival although they are green in colour. Also, the humidity of the tissue culture vessel is high therefore plant cuticle (the natural protective covering) is not fully developed. Therefore, immediately after transfer of plants they should be maintained under high humidity and plants should be kept at optimum conditions in green house.

2.4 Production of Secondary Metabolites via Plant Cell and Tissue Culture Systems

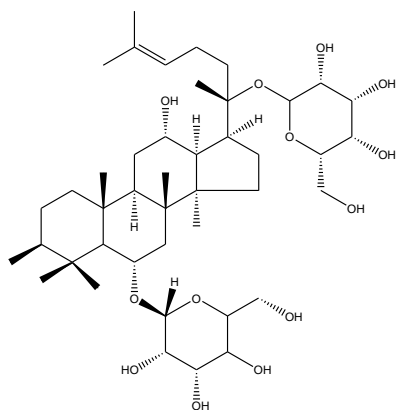
Clearly, the development of an alternate and complementary method for the production of pharmaceuticals is of economic importance. Since the inception of *in vitro* technology, the potency of plant, cell, tissue and organ culture to produce important pharmaceuticals just like conventional plant cultivation has been identified (Anand, 2010). The intentional elicitation of important phytochemicals inside carefully controlled *in vitro* culture environment affords an outstanding means of secondary metabolites production. Secondary metabolites production commercially using PTC has evolved during the last forty years especially in Japan, Germany, and the USA (Mulabagal and Tsay, 2004). For example, sanguinarine was produced from *Papaver somniferum*. Researchers have developed high-yielding tissue culture systems such as the cultivation of specific organ and cell culture as seen in Table 2.2.

Table 2.2: Yield of Secondary Metabolites from Cell Cultures Compared with the Parent Plants

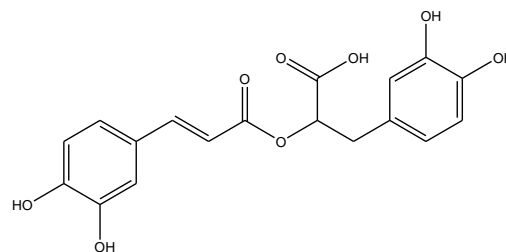
Compound	Plant species	Yield from cell culture (%)	Yield from whole plant (%)
Ginsenoside (7)	<i>Panax ginseng</i> C.A. Mey.	27	4.5
Anthraquinone	<i>Morinda citrifolia</i> L.	18	2.2
Rosmarinic acid (8)	<i>Coleus blumeii</i> Benth.	15	3.0
Berberine (9)	<i>Thalictrum minus</i> L.	10	0.01
Nicotine (10)	<i>Nicotiana tabacum</i> L.	3.4	2.0
Shikonin (11)	<i>Lithospermum erythrorhizon</i> Siebold and Zucc.	20	1.5
Ajmalicine (12)	<i>Catharanthus roseus</i> (L.) G. Don	1.0	0.3

Adapted from Smetanska (2008); *Structures of compounds (7) to (12) are shown in

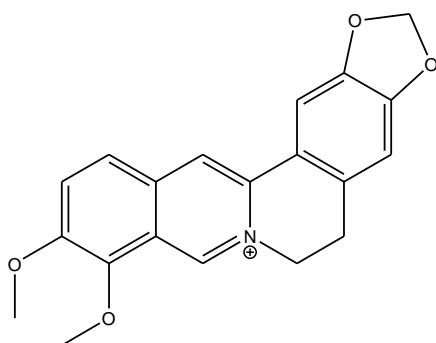
Figure 2.2



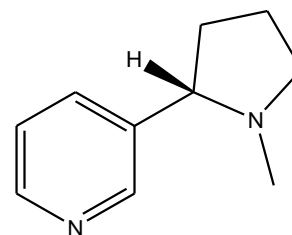
Ginsenoside (7)



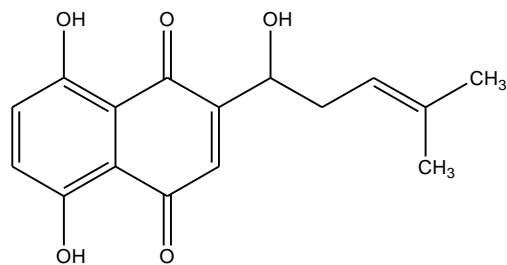
Rosmarinic acid (8)



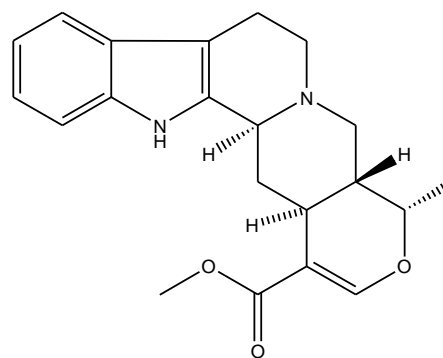
Berberine (9)



Nicotine (10)



Shikonin (11)



Ajmalicine (12)

Figure 2.2: Structures of compounds with better yield via plant cell culture

2.5 Approaches to Increase Secondary Metabolites Production using *In Vitro* Plant Tissue Culture (PTC) Techniques

Research in the pharmaceutical and food industries has focused on developing new techniques which will allow secondary metabolites production from the PTC. It is less expensive than extraction of the whole plant and at the same time cheaper than the synthesis of the product. Some of the methods to increase secondary metabolites in plant cell cultures are explained below.

2.5.1 Selection of efficient plant material for growth

The first step in enhancing secondary metabolites synthesis using PTC techniques is the selection of parent plant according to its molecular and biochemical characteristics. Plants with high contents of the desired metabolites should be selected. Next to it is the determination of the plant part to be used as explant. Young and fresh explants are preferable (Gonçalves and Romano, 2018).

2.5.2 Production in differentiated tissues

From different studies, secondary metabolites production in organ cultures was better than in undifferentiated cells. Studies have shown the production of secondary metabolites like alkaloids and antioxidant compounds in differentiated tissues. *In vitro* plantlets of *Ocimum basilicum* L. gave higher content of rosmarinic acid than cell cultures. Shoot culture of *Salvia officinalis* L. had antioxidant compounds (carnosol and carnosic acid) while they were absent in callus, suspension or hairy root cultures (Grzegorzczuk *et al.*, 2007). However, some reports have shown that undifferentiated cell suspensions are capable of accumulating high quantity of phenolics and alkaloids (Vanisree *et al.*, 2004; Lee *et al.*, 2011).

2.5.3 Screening of high-growth cell line to produce metabolites of interest

This involves a screening of the heterogeneous population for variant cell lines containing the highest levels of desired product because the accumulation of secondary metabolites can be genotype dependent (Murthy *et al.*, 2014). For example, accumulation of camptothecin in *Nothapodytes nimmoniana* varied in the different organs (root bark,

leaves and stem bark) of this plant species (Ramesha *et al.*, 2008). For high-yielding cell line selection, chemical methods like the use of phenylalanine analogues to monitor the metabolic flux in the targeted pathway can be used (Georgiev *et al.*, 2006).

The limitation of appropriate cell line selection for secondary metabolites production is that with time, the cell lines may lose their ability to generate the anticipated secondary metabolite. Genetic instability of long-term sub-culture might also reduce the biosynthesis of secondary metabolites from specific cell lines (Ochoa-Villarreal *et al.*, 2016).

2.5.4 Optimisation of culture conditions

Plant tissue culture conditions affect the metabolic pathways of secondary metabolites production. This can be explained in two different ways; optimisation of the medium composition and optimisation of the culture environment.

2.5.4.1 Optimisation of medium composition

Medium composition is an essential and basic factor influencing the cell metabolism and physiology. The culture medium type, salt strength, phosphate, sugar, nitrate and plant growth hormone levels can affect the accumulation of important metabolites.

Nutrient medium and salt strength: Maintenance and optimisation of culture medium is necessary to enhance high secondary metabolites production. Several types of standard PTC media are available for plant cell growth but the most regularly used is MS medium. The salt strength and medium can be manipulated to achieve the increase in secondary metabolites in *in vitro* culture. For example, cell suspension cultures of *Withania somnifera* (L.) Dunal using full strength (1.0) MS medium accumulated more withanolide A than 0.25, 0.5, 0.75, 1.5 and 2.0 strength MS (Praveen and Murthy, 2010).

Sugar levels: Sucrose level is known to influence secondary metabolites production in *in vitro* cultures. In *Ginkgo biloba* L. cell cultures, higher levels of sucrose (5%, 7%) enhanced the accumulation of ginkgolides and bilobalides whereas three percent sucrose was good for biomass accumulation. The accumulation of these metabolites could have resulted from osmotic pressure provided by the increased sugar concentration (Park *et al.*, 2004).

Nitrate levels: Nitrogen source in the culture medium can be manipulated and can affect secondary metabolites production. The nitrogen sources in the PTC medium are the nitrates and ammonium. When nitrogen levels were reduced, the production of capsaicin was improved in *Capsicum frutescens* L. Also, reduced level of nitrate and ammonium ratio in the root culture of *Morus alba* L. gave rise to a higher rutin content than medium with high nitrate and ammonium ratio (Lee *et al.*, 2011).

Phosphate levels: A higher level of phosphate in culture medium is known to promote plant growth, whereas it reduces the accumulation of secondary metabolites. The reduction in the level of phosphate triggered ajmalicine and phenolics production in *Catarathus roseus*, caffeoyl putrescines in *Nicotiana tabacum* and of Harman alkaloids in *Peganum harmala* (Ramachandra Rao and Ravishankar 2002).

2.5.4.2 Optimisation of the culture environment

Conditions of culture environment such as light, temperature, medium pH, and gases can be manipulated and tested for their effects on secondary metabolites accumulation.

Temperature: For the maintenance of plant cells cultures, temperature range of 17 to 25 °C is routinely utilised. Manipulation of culture temperature can affect the physiology of the plant culture and secondary metabolite production. In suspension culture of *Taxus chinensis* (Rehder and E.H. Wilson) Rehder, compound paclitaxel was increased to 137.5 mgL⁻¹ when a temperature range of 24 to 29 °C was used (Choi *et al.*, 2000). In strawberry cell culture, lower temperature favoured the accumulation of anthocyanin. Culture grown at 15 °C gave anthocyanin content which was 13 times higher when 35 °C was used.

Light: The different light condition in plant tissue culture are; darkness, 12 h photoperiod, 16 h photoperiod and continuous light. Plant cells can adapt to different types of light conditions and ultraviolet (UV) and red light have been used to increase secondary metabolite production. Tassoni *et al.* (2012) reported that treatment of cell suspension culture of *Vitis vinifera* L. with red light increased stilbene and anthocyanins production.

Medium pH: In plant tissue culture, extreme pH values (acidic and alkaline) are avoided. Therefore, the pH of culture medium is commonly regulated to between 5 and 6 before autoclaving. In *Withania somnifera* hairy root cultures, medium pH of 5.8 favored

biomass accumulation while pH of 6.0 favoured withanolide A accumulation (Praveen and Murthy, 2012).

The figure 2.3 below summarises the different approaches that can be used to increase the production of secondary metabolites using plant tissue culture techniques.

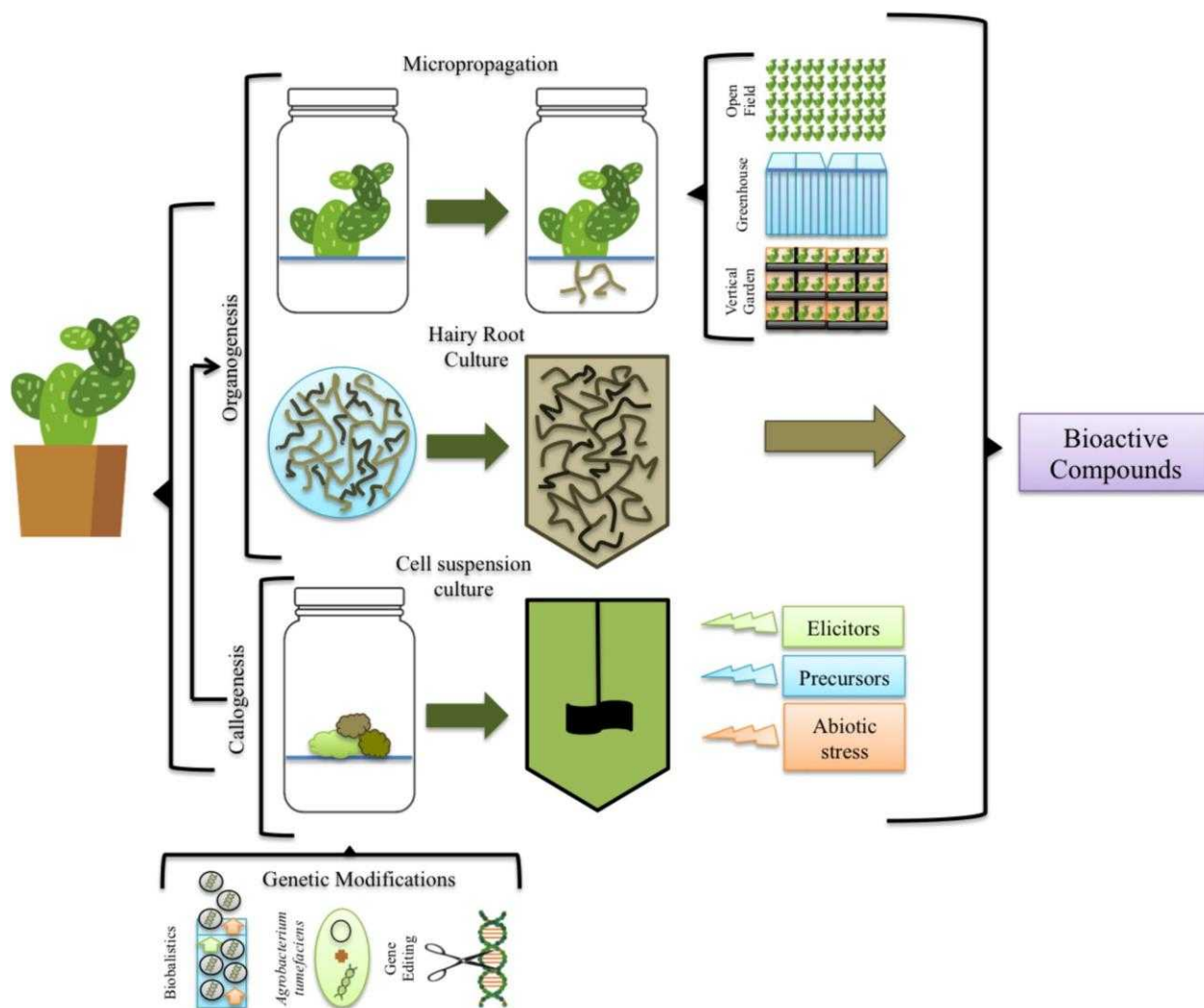


Figure 2.3: Different strategies to enhance secondary metabolites production in *in vitro* plant tissue culture (Espinosa-Leal *et al.*, 2018)

2.5.5 Addition of precursors

The comprehensive knowledge of related biosynthetic pathways can help enhance the synthesis of targeted secondary metabolites. Feeding precursors into cell cultures media can boost the yield of the final and targeted product (Hussain *et al.*, 2012). Precursor feeding was used to produce withanolides, triterpenoids, and phenolic compounds (Palacio *et al.*, 2011). Addition of 0.5 mM of L-phenylalanine into plant cell cultures of *Larrea divaricata* Cav. led to an increase in nordihydroguaiaretic acid (NDGA) by 2.2-times higher than in the control (Palacio *et al.*, 2011). Precursors such as cholesterol, isopentenyl pyrophosphate, sodium acetate, squalene, were used to boost azadirachtin production (Srivastava and Srivastava, 2014). It should be noted that precursors should be cheap, non-toxic and be able to give the desired compound of interest. The challenge with the addition of precursors to *in vitro* plant tissue culture media is that some precursors doses are toxic to plant cells and is able to prevent plants cells development instead of supporting it. Therefore, it is important to screen for non-toxic precursors and determine the dose that is safe for use (Espinosa-Leal *et al.*, 2018).

2.5.6 Use of elicitors

Elicitors are molecules that trigger the production of secondary metabolites which serve as plant defense compounds. There are different classes of elicitors depending on their source. There are the biotic and abiotic elicitors (Zhang *et al.*, 2007). Biotic elicitors include live bacteria, yeast, fungal polysaccharides, lipid, chitin, glucan (from microorganisms) and glycoproteins. They have been shown to be used to enhance the accumulation of desired secondary metabolites. Abiotic elicitors also include osmotic stress, temperature shift, light and UV, salicylic acid and jasmonic acid. They have been applied extensively (Namdeo, 2007; Ochoa-Villarreal *et al.*, 2016). Examples of abiotic and biotic elicitors that have been used to elicit secondary metabolites are presented in Table 2.3.

Table 2.3 Different Types of Elicitors Utilised to Induce Secondary Metabolite Production in Medicinal Plants

Product	Plant species	Elicitors	Yield of control	Yield after elicitation	Fold of increase	References
Biotic elicitors						
Ursolic acid	<i>Perilla frutescens</i>	Yeast elicitor	22 mg/L	27 mg/L	1.24	Wang <i>et al.</i> (2004)
Oleanolic acid	<i>Calendula officinalis</i>	Chitosan	0.074 mg/g DW	0.37 mg/g DW	5.00	Wiktorowska <i>et al.</i> (2010)
Paclitaxel	<i>Taxus cuspidata</i>	Paclitaxel-producing fungal endophyte	3.14 mg/L	5.84 mg/L	1.8	Li and Tao (2009)
Sanguinarine	<i>Papaver somniferum</i>	<i>Botrytis cinerea</i> homogenate	15.6 mg/g DW	288.0 mg/g DW	18.4	Holkova' <i>et al.</i> (2010)
Abiotic elicitors						
Anthraquinone	<i>Rubia tinctorum</i>	Methyl jasmonate	3.81 mg/g DW	6.65 mg/g DW	1.75	Komaraiah <i>et al.</i> (2005)
Oleanolic acid	<i>Calendula officinalis</i>	Jasmonic acid	0.089 mg/g DW	0.84 mg/g DW	9.4	Wiktorowska <i>et al.</i> (2010)
Catharanthine	<i>Catharanthus roseus</i>	Nitric oxide	8.3 mg/L	24.2 mg/L	2.9	Xu and Dong (2005a)
Sanguinarine	<i>Papaver somniferum</i>	Methyl jasmonate	15.6 mg/g DW	169.5 mg/g DW	10.8	Holkova' <i>et al.</i> , (2010)

Adapted from Yue *et al.* (2016)

2.6 Isolation and purification of bioactive compounds

The principal steps to isolate and characterise bioactive compounds are plant selection and collection. This usually involves recovery of ethnobotanical information so as to recognise possible bioactive phytochemicals. Plant selection is followed by extraction with different solvents in order to isolate bioactive compounds. Usually, when probing for bioactive secondary metabolites, the objective is to look for a suitable methodology which is simple, specific and rapid that is able to screen the plant materials for biological activities like cytotoxicity, antioxidant or antibacterial. *In vitro* bioassays are often times more desired than *in vivo* methods due to the fact that animal experiments are time consuming, costly, and are prone to ethical controversies (Altemimi *et al.*, 2017). However, *in vivo* experiments are sometimes necessary. Following the bioassays, the bioactive molecules can be isolated and purified by using chromatographic methods. Thin-layer (TLC) and column chromatography are still regularly utilised because of their accessibility, ease to use, low cost and the fact that different stationary phases are available. The commonly used stationary phases are silica, alumina, cellulose, and polyamide. The TLC is a simple, fast, and cheap method that gives the researcher an idea of the number and kinds of compounds in a mixture. Separation of compounds by TLC is based on the relative affinity of compounds towards the stationary and mobile phase. Spraying of phytochemical screening or derivatisation reagents and viewing under daylight or UV lamps can give additional information about the identified compounds. This is also used for confirmation of purity and identification of isolated compounds. The set back of TLC analysis is its low sensitivity, low resolution and difficulty in detecting trace constituents (Zhang *et al.*, 2011). The fractions obtained from column chromatography are monitored and pooled together based on their TLC profile.

Column chromatography (CC) is basically used to purify and isolate desired compounds from a mixture. It is also based on the affinity of the solute to the mobile phase just like TLC. In CC the stationary phase (a solid adsorbent, usually silica gel or alumina) is placed in a vertical glass column, the extract to be purified is applied and the mobile phase is added to the top and flows down through the column (by either gravity or external pressure). Sephadex are also used in columns but this does not work by the affinity or ion-exchange principle. It separates molecules based on sizes in a method called gel filtration

or size exclusion chromatography. With size exclusion, separation is based on molecular size. In many cases, sephadex column is used for further purification of fractions from silica gel column. The advantage is that the condition can be varied to suit the type of sample. It is commonly utilised for the separation of very polar compounds.

Developed instruments such as high performance liquid chromatography (HPLC) and high-performance thin layer chromatography (HPTLC) speed up the process of isolation and purification of bioactive compounds.

2.6.1 Effect Directed Analysis (EDA) and hyphenations coupled with High Performance Thin Layer Chromatography (HPTLC)

The HPTLC is a sophisticated instrumental technique based on thin layer chromatography. It has the advantages of automation, scanning, full optimisation, better resolution, selective detection principle, minimum sample preparation and hyphenation among others. All these make it a powerful analytical tool for qualitative, quantitative and characterisation of complex mixtures of inorganic, organic and biomolecules (Srivastava, 2011).

Effect Directed Analysis (EDA): HPTLC combined with biological and chemical assays to screen samples for bioactive components is called effect-directed analysis, EDA. The EDA makes it simpler to target bioactive molecules especially in bioassay-guided analysis of plant samples leaving out the inactive compounds. It is simple, fast and cost effective. Bioautographic methods and enzyme inhibition assays such as cholinesterase, glucosidase, antimicrobial, antifungal, anti-tumour, have been developed on HPTLC in laboratories. This effect directed analysis would help to identify and characterise bioactive compounds in different samples (Jamshidi-Aidji and Morlock, 2016).

HPTLC-hyphenations: Hyphenation consists of different means of coupling spectrometers with chromatographic systems. It helps to further characterise bioactive molecules. Hyphenations have increased the use of HPTLC because of its amenability to different spectrometers. To a large extent, HPTLC has been able to overcome the challenges faced by HPLC or GC-based hyphenations. The HPTLC is amenable to multiple spectrometers like UV, Fourier-transform infrared spectroscopy, MS, among others. With HPTLC-HRMS, only the zones of interest are eluted to the mass

spectrometer and are recorded. The scrapping of contaminants and other compounds like we do with prep-TLC is greatly avoided (Morlock and Schwack, 2010).

2.6.2 Structural elucidation of bioactive compounds

For the determination of the structures of molecules, data from many spectroscopic techniques such as UV-visible, Infrared (IR), Nuclear Magnetic Resonance (NMR), and mass spectroscopy are needed.

2.6.2.1 Mass spectrometry

Mass spectrometry (MS) measures the mass-to-charge ratio of ions. The procedure involves the bombardment of organic molecules with electrons or lasers which will convert some of the molecules to charged fragments or convert it to charged ion without fragmentation. These ions are then separated according to their mass-to-charge ratio. A mass spectrum is a plot of the signal intensity or relative abundance of fragmented ions as a function of the mass-to-charge ratio. Mass spectrometry helps to identify unknown compounds by giving the molecular weight and determining the isotopic composition of a molecule. It also helps to determine the structure of a compound by looking at the fragmentation pattern (Christophoridou *et al.*, 2005). The major setback of MS is that it fails to distinguish between optical and geometric isomers in an aromatic ring. It can not also distinguish between ortho, meta and para couplings in an aromatic ring. A nuclear magnetic resonance spectroscopy is needed for this.

2.6.2.2 Nuclear Magnetic Resonance Spectroscopy (NMR)

NMR is a technique that helps to determine the structure of compounds. This technique observes the magnetic properties of certain atomic nuclei; the hydrogen atom (the proton) and the ^{13}C -nucleus. NMR spectroscopy gives a clear picture of the positions and the chemical environment of these nuclei in a molecule. It also demonstrates the atoms that are found in neighboring groups. The disadvantage is that it requires a relatively large amount of sample (2-50 mg), the analysis is expensive and takes long.

2.7 Assessment of Genetic Fidelity of *In Vitro*-grown Plants Using Molecular Markers

In vitro PTC technique is a reliable supplemental method for the production of bioactive plant metabolites. However, an important pre-requisite for plant micropropagation is the genetic fidelity of the plant species. Somaclonal variation in micropropagated plants often limits the use of PTC (Salvi *et al.*, 2001). Some researchers have reported genetic differences between micropropagated plants and the mother plants. The presence of somaclonal variations in micropropagation and especially for the industrial production of phytochemicals often presents a challenge (Bhattacharyya *et al.*, 2017a). It is therefore necessary to establish genetic uniformity of micropropagated plants with the mother plants before their commercial utility.

The genetic changes in *in vitro*-grown plants occur due to: changes in chromosome number, activation of transposable elements, DNA methylation, amplification or polyploidy (Govindaraju and Arulselvi, 2018). Espinosa-Leal *et al.* (2018) in their review mentioned that regeneration of plantlets via axillary buds or direct somatic embryos often gives genetically uniform plantlets and more reliable than regeneration protocols involving a callus phase.

Different PCR-based molecular markers are used to assess the genetic fidelity of *in vitro*-grown plants. Examples are; random fragmented length polymorphism (RFLP), random amplified polymorphic DNA (RAPD) and microsatellite markers among others (Bose *et al.*, 2016). In recent times, next generation sequencing and diversity array technology sequencing (DArTseq) methods, which are high throughput sequencing techniques are used to generate single nucleotide polymorphic (SNP) markers for molecular analysis.

2.8 Botanical Description of Research Plant

2.8.1 Taxonomy of *Musa*

Bananas and plantains belong to the *Musa* genus of the Musaceae family. The family Musaceae comprises two genera *Ensete* and *Musa*. The genus *Ensete* is composed of monocarpic herbs, none of which produce edible fruits. The genus *Musa* comprises the

edible bananas. More than 60 wild species of *Musa* are known. The genus *Musa* has been divided into 5 sections based on their diploid number of chromosomes and phenotypic characteristics; they are: *Eumusa*, *Rhodochlamys*, *Callimusa* and *Australimusa*, and *Ingentimusa* (De Langhe, 2009). *Eumusa* and *Rhodochlamys* have eleven chromosomes ($2n = 22$) while *Callimusa* and *Australimusa* have ten chromosomes ($2n = 20$). *Rhodochlamys* and *Callimusa* are only used as ornamentals because they do not produce edible fruits. *Eumusa* section *Musa* as commonly described is the largest section and widely distributed geographically. They include the *Musa acuminata* Colla (AA) and *Musa balbisiana* Colla (BB), which are the wild species that served as the centre of domestication of all the edible bananas. Bananas (*Musa* spp.) are classified as dessert or cooking banana. The dessert bananas are the sweet, ready to eat bananas while the cooking banana is also known as plantain (Padam *et al.*, 2014). Edible bananas are recently classified based on their genome group (A or B) as diploids, triploid and tetraploids. The A genome is from *Musa acuminata* while the B is from *Musa balbisiana*. The hybrids were derived from intraspecific and interspecific crosses (Fig. 2.4). The domesticated dessert and cooking bananas are the hybrids belonging to AA, AB, AAA, AAB, ABB or BBB genome groups. *Musa sapientum* (banana) and *Musa paradisiaca* (plantain) are the two common hybrids of the wild species other species are; *Musa ornate*, *Musa laterita*, *Musa aurantiaca*, etc.

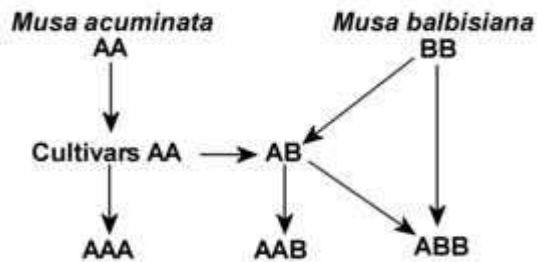


Fig. 2.4: Crossing relationships of most cultivated edible *Musa*

2.8.2 Taxonomical classification

Kingdom: Plantae

Division: Magnoliophyta

Class: Liliopsida

Order: Zingiberales

Family: Musaceae

Genus: *Musa*

Species: *M. acuminata*, *M. balbisiana*



Plate 2.5.1: Young *Musa* spp. on IITA field bank



Plate 2.5.2: *Musa acuminata* plant with fruits

2.8.3 Ecology and distribution

Banana is a familiar tropical fruit. It is a perennial herb with underground stem called corm and aerial shoots called pseudostems. The corms form suckers. The Malaysia region including Peninsula, Indonesia, the Philippines and New Guinea is believed to be the primary center of *Musa* diversity, while India was the secondary center (Simmonds and Shepherd, 1955). It is believed that the species were dispersed out of Asia due to human movement. Bananas grow in the humid tropics of Africa. Bananas thrive well in rich and fertile soils and well sheltered location. Banana plant growth requires warm or hot temperature as well as enough water; however, they are not flood tolerant.

2.8.4 Propagation of *Musa* species

2.8.4.1 *Vegetative propagation of Musa*

Most edible bananas are seedless; therefore, they are vegetatively propagated. The corms and suckers are conventionally used for banana propagation (Haq and Dahot, 2007). Banana cultivation is economical and can produce fruits under different ecological conditions. The major problem of the conventional cultivation is insect and pest attack and this can be mitigated by micropropagation.

2.8.4.2 *Micropropagation of Musa*

For breeding and crop improvement purposes, conventional cultivation is difficult because *Musa* species are parthenocarpic, more so, cultivars are found to be polyploidy and available information on genetic and genomics are still limited (De Capdeville *et al.*, 2009). Other challenges with the conventional propagation of banana include; pests and diseases attack, low reproductive fertility and slow propagation rate. These problems had been mitigated by micropropagation because *Musa* species have been found to be amenable to micropropagation. With micropropagation, multiplication rate goes up to 2 to 10 or more shoot in a month which can give rise to thousands of plants in a year. These rates are not achievable with conventional propagation. *Musa* meristem culture provides an effective method for rapid propagation, production of virus free materials and germplasm conservation (Helloit *et al.*, 2002). Plant growth regulators are generally used for *in vitro* regeneration of crops and the concentrations needed for each plant variety

must be determined. For large or commercial scale micropropagation repeatable and comprehensive method that can be applied for a wide range of genotypes should be developed.

2.8.5 Economic uses and nutritional values of *Musa*

The nutrient composition of plantain and banana is dependent on the variety, degree of ripeness and growth conditions e.g. the type of soil used. The green plant contains 61% water which increases to 68% on ripening. Green plantain contains about 21% to 26% starch, which is mainly amylose and amylopectin but, in ripe plantains, the starch are replaced with sucrose, fructose and glucose due to hydrolysis (Zakpaa *et al.*, 2010). Plantains are rich in carbohydrate and low in fat. They are also rich in vitamins and minerals such as iron, calcium, ascorbic acid, riboflavin, potassium, thiamin and niacin (Adeniji *et al.*, 2006).

Bananas contain important amino acids such as alanine, glutamine, histidine, aminobutyric acid, leucine, asparagine, serine and arginine.

Bananas can be peeled and eaten raw, fried, baked, roasted, made into a puree suitable for infants and used in many other ways. Banana leaves are used for wrapping food and as a shade protection from rain. The pseudostem can be utilised for its fiber and can also be used to enrich the soil because of its organic matter content.

2.8.6 Traditional and medicinal uses of *Musa*

Every part of *Musa* spp. plant has been found to be useful. The peel, pulp, stem, root, sap, leaf, bract and flowers have been long used traditionally to treat one ailment or the other. The fruit juice is utilised to treat gastro-intestinal disorders such as constipation and ulcers. Banana fruit is safe for ulcer patients. It is used to treat burns and wounds. Banana fruit is believed to alleviate problems associated with worms in children. Banana fruit also has a mild laxative property. Again, the fruit is known to prevent or cure scurvy, it is used as an aphrodisiac and a diuretic (Onyenekwe *et al.*, 2013). The fruit of wild banana (*Musa acuminata*) is used to lower blood pressure in Kenya and used to treat diabetes in Mauritius while its root is used for treating HIV-related infections in South Africa among other uses. The consumption of banana alongside other fruits helps to reduce the risk of renal cell carcinoma (Rashidkhani *et al.*, 2005) and breast cancer in women (Malin *et al.*,

2003). Banana leaf can also be used as an abortifacient. The extract from the core of the stem is believed to be used to treat stomach upset and diabetes. It is also useful in removing kidney stone, reducing weight and high blood pressure (Kumar *et al.*, 2012). The sap is used for treating diarrhoea, dysentery, epilepsy, and hysteria.

2.8.7 Pharmacological activities of *Musa*

Antiulcer activity: Lewis *et al.* (1999) reported that bananas are usually recommended for patients suffering from digestive disorders especially ulcers as dietary supplements. The anti-ulcer property of *Musa* spp. was reported and confirmed by many authors. Banana pulp powder was able to increase the mucosal thickness, significantly increased thymidine incorporation into mucosal DNA and also promoted healing by inducing cellular proliferation in aspirin, prednisolone, indomethacin, and phenyl butazone induced ulcer in rats (Kumar *et al.*, 2012). Antiulcer activity of *Musa acuminata* pulp and peel was reported by Abdullah *et al.* (2014) with the peel having better activity than the pulp. The flavonoid leucocyanidin was extracted from unripe plantain banana and discovered as an active anti-ulcerogenic agent (Lewis *et al.*, 1999). This compound was also found in *Musa sapientum* (Prabha *et al.* 2011). *Musa sapientum* peel methanol extract was reported to possess anti-ulcer and ulcer healing potentials (Onasanwo *et al.*, 2013).

Wound healing activity: Amutha and Selvakumari (2016) demonstrated the wound healing property of *Musa paradisiaca* stem methanol extract in wistar albino rats. The study concluded that the wound healing activity of stem extract was better than the control. The wound healing property of extracts from the peel of *Musa acuminata* was reported by Rosida *et al.* (2014); the extract was able to induce the synthesis of collagen and the production of epithelial tissues.

Hair Growth promoting activity: The unripe fruit of *Musa* spp. has been used traditionally for the treatment of hair loss. Savali *et al.* (2011) reported that unripe fruit extract of *Musa paradisiaca* was able to promote hair growth when tested on skin shaved mice. The assay was monitored for 30 days; the hair length and follicles were studied in the animals treated with the extracts, 2% minoxidil and control. The findings suggested that the extract can be used as a hair growth promoter.

Antidiarrhoeal activity: *Musa* spp. has been used traditionally to treat diarrhea which is an alteration in the normal bowel movement characterised by an increase in the volume,

fluidity, frequency, and passage of loose or watery stool for at least three times a day (WHO, 2009). Yakubu *et al.* (2015) reported the antidiarrhoeal ability of the sap of *Musa paradisiaca* using 3 models in wistar rats, which were; castor oil-induced diarrhoeal, castor oil-induced enteropooling, and gastrointestinal motility models. *Musa* sap was able to prolong the onset of diarrhoea, decrease the number, fresh weight, and water content of faeces, and inhibited defecation in the castor oil-induced model. In the enteropooling model, there was a decrease in the masses and volumes of intestinal fluid by the sap. Hossain *et al.* (2011) also reported that *Musa sapientum* seed extract reduced the diarrhoea frequency and severity in experimental rats.

Antioxidant property: Several researchers have reported the antioxidant property of different parts of banana using different antioxidant assays. Antioxidant activity of the seed extract using DPPH• and Nitric oxide scavenging method was reported by Hossain *et al.* (2011). Ayoola *et al.* (2017) and Sonibare *et al.* (2018) reported the good antioxidant activity of the fruit and leaf of different accessions of *Musa acuminata* and *Musa sapientum*. The leaves had higher phenolic content and antioxidant activity than fruits. The antioxidant activity and gallic acid, an antioxidant compound was found to be more abundant in peel than in pulp (Someya *et al.*, 2002).

Hepatoprotective activity: *Musa* species were shown to prevent liver damage using *in vivo* animal models. The hepatoprotective activity of the ethanol and aqueous extracts of the stem of *Musa paradisiaca* was reported by Nirmala *et al.* (2012). In experimental rats, paracetamol and CCl₄ (hepatotoxins) was used to induce hepatotoxicity. Administration of the hepatotoxins caused significant deteriorations in the liver of the animals. The ethanol and aqueous extracts significantly reversed the hepatic damage.

Hypoglycemic/ antidiabetic activity: Different researchers have used many animal and *in vitro* models to evaluate the antidiabetic property of different parts of *Musa* species. These models include; hypoglycaemic effects, oral glucose tolerance, inhibitory activities in carbohydrate metabolism and digestive enzymes (alpha and beta-glucosidase, alpha-amylase) and enhanced glucose uptake activity. Vilhena *et al.* (2018) did a review on the antidiabetic property of the inflorescence (flowers) of *Musa* spp. He found 16 studies reporting the antidiabetic property of the inflorescence (flowers and bract), which all supported the ethnomedicinal claim that cooked flowers are able to treat diabetes mellitus.

Uhegbu *et al.* (2016) among many others reported the hypoglycaemic effect of the unripe fruit of *M. paradisiaca* in diabetic experimental rats induced with alloxan. The result revealed that the serum glucose in the treated rat was significantly reduced.

Antimicrobial activity: Different extracts of the different parts of *Musa* spp. (leaf, fruit, and inflorescence) have been investigated for their antimicrobial potential. The leaf of *Musa paradisiaca*, *Musa acuminata* and *Musa sapientum* were reported by Karuppiah and Mustafa (2013) to possess antibacterial activity against multidrug resistant clinical pathogens. The study reported that the ethyl acetate fraction of *Musa paradisiaca* leaf gave the highest inhibitory activity against *E. coli*, *P. aeruginosa* and *Citrobacter* spp. The bract of *Musa acuminata* was investigated by Umamaheswari *et al.* (2017) for its antimicrobial property and the methanolic extract was shown to have antibacterial activity against *E. coli* and *Staphylococcus aureus*.

Antihypertensive Activity: The potential of banana to lower blood pressure was reported by Dayanand *et al.* (2015). They reported a cross-sectional study that showed consumption of banana significantly reduced the systolic and diastolic blood pressure in humans especially females.

2.8.8 Some of the chemical constituents and compounds isolated from *Musa* species

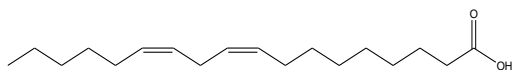
Fruit consists of carbohydrates, amino acids, sugar and starch. The primary starch components are amylose and amylopectin, present in a ratio of around 1:5. In unripe plantains about 1.3% of sugars are present but this rises to around 17% in the ripe. The peel of the fruit is rich in cellulose (10%), hemicelluloses (7%) and polyunsaturated fatty acid such as linoleic acid (13) and linolenic acid (Emaga *et al.*, 2007). The pulp is rich in pectin and proteins such as arginine (14), aspartic acid, L-tryptophan (15), leucine (16), valine, phenylalanine, glutamic acid. *Musa* species are as well known to be an important source of amine compounds such as Catecholamines, e.g. dopamine (17), norepinephrine (noradrenaline), and epinephrine (adrenaline), which are neurotransmitters (Kanazawa and Sakakibara, 2000). Other common amines found in banana are tryptamine, melatonin, putrescine, methylamine, isobutylamine, ethylamine, isoamylamine, spermidine, ethanolamine, dimethylamine, propanolamine, histamine, 2-phenyl-ethylamine, and serotonin (18) (Pereira and Maraschin, 2015).

Work done by Onyenekwe *et al.* (2013) showed that *Musa paradisiaca* stem extract contains tannins and glycosides in abundance while flavonoids, alkaloids, polyphenols, saponins and reducing sugars were moderately present. Saponins, sterols, tannins, triterpenes, reducing and non-reducing sugars were present in the flowers.

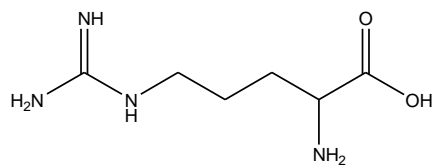
Bananas are rich in antioxidants such as vitamins, β -carotene (19) and phenolic compounds such as catechin (20), epicatechin, lignin, tannins and anthocyanins. They contain flavan-3,4-diols also known as leucoanthocyanidins (Davey *et al.*, 2009b). The anti-ulcer flavonoid, leucocyanidin (21) was also isolated from banana fruit (Prabha *et al.*, 2011). Quercetin (22) and its 3-*O*-galactoside and 3-*O*-glucoside were isolated from plantain (Lewis and Shaw, 2001). Tsamo *et al.* (2015) reported the phenolic profile of the pulp and peel of different cultivars of Banana. They found by HPLC–ESI–HR–MS and HPLC–DAD that the plantain pulp contain majorly hydroxycinnamic acids, particularly ferulic acid (23) and its hexoside. Flavonol glycosides, rutin (24) was predominant in the peels. Other phenolic compounds such as; quercetin-deoxyhexose hexoside-hexoside, myricetin-deoxyhexose hexoside-hexoside and kaempferol-3-*O*-rutinoside were identified in the pulp and peel. Phenolic compounds were identified in the leaves of *Musa acuminata* using UPLC–qToF–MS. They include; quercetin, kaempferol-7-*O*-glucoside, kaempferol-3-*O*-rutinoside, phloretin, catechin, kaempferol-3-sophortrioside, among others (Sonibare *et al.*, 2018).

Sheng *et al.* (2017) isolated phytosterols from the flowers of *Musa* spp. They include β -sitosterol (25) and 31-norcyclolaudenone. Several triterpenes have been isolated from *Musa sapientum*; they are lanosterol (26), cyclomusalenol, 24-methylenecycloartanol, β -amyrin (27), stigmast-7-methylenecycloartanol, cyclomusalenone, and stigmast-7-en-3-ol (Ragasa *et al.* 2007). More than 350 aldehydes and esters which are compounds giving banana fruit its characteristic aroma have been identified. The main aroma compounds were esters such as isoamyl acetate, 2-pentanol acetate and isoamyl butanoate (Selli *et al.*, 2012). The lipophilic components of the pulp of banana fruit (*Musa acuminata* and *Musa balbisiana*) were identified by Vilela *et al.* (2014). They include; α -tocopherol (28), stigmasterol (29), β -sitosterol and saturated fatty acids (Dodecanoic acid, Tricosanoic acid, etc.) and unsaturated fatty acids (Octadeca-9,12-dienoic acid, Octadeca-9,12,15-

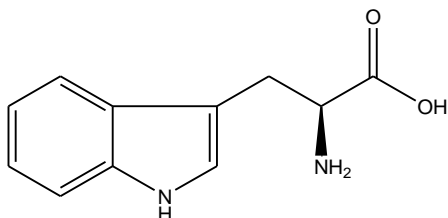
trienoic acid (30), etc.). Structures of some of these compounds are presented in Figure 2.6.



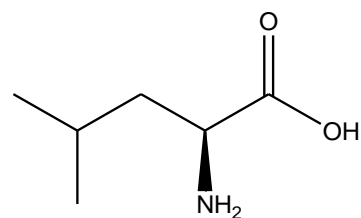
Linoleic acid (13)



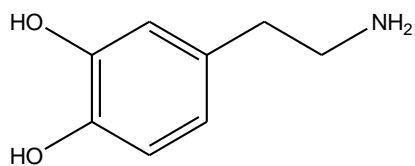
Arginine (14)



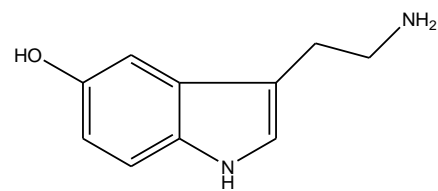
L-Tryptophan (15)



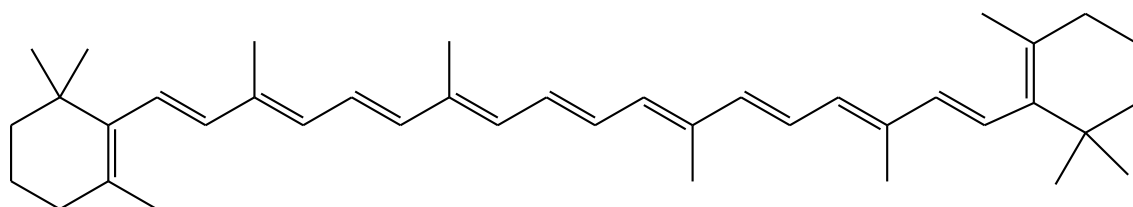
L-Leucine (16)



Dopamine (17)

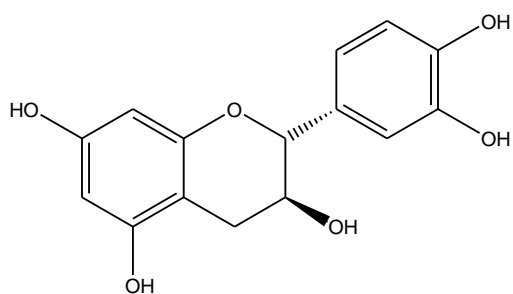


Serotonin (18)

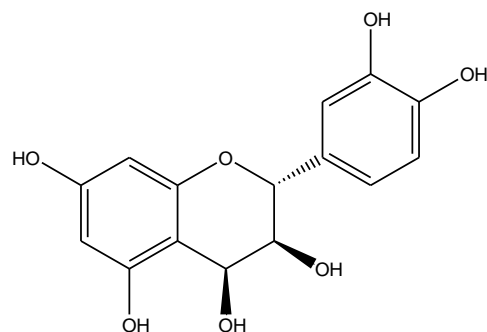


β -Carotene (19)

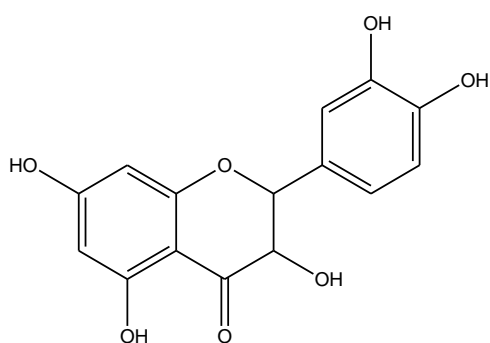
Fig. 2.6.1: Structures of some compounds isolated from *Musa* species



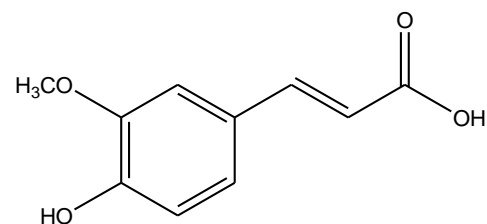
Catechin (20)



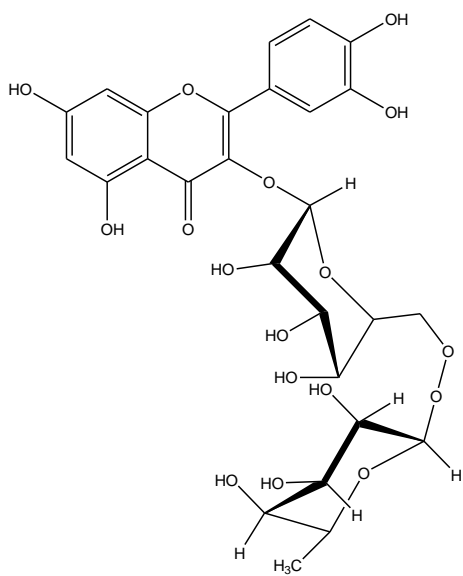
Leucocyanidin (21)



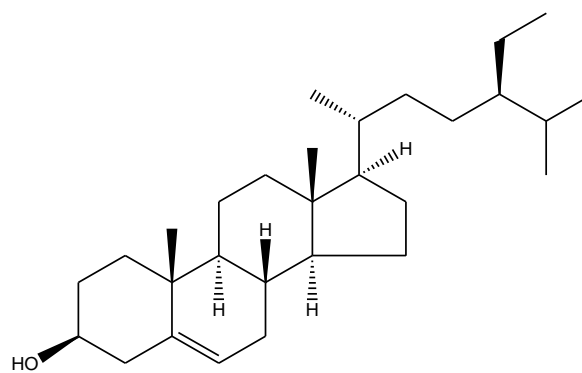
Quercetin (22)



Ferulic acid (23)

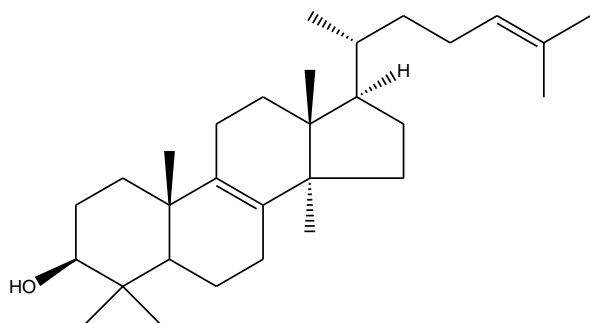


Rutin (24)

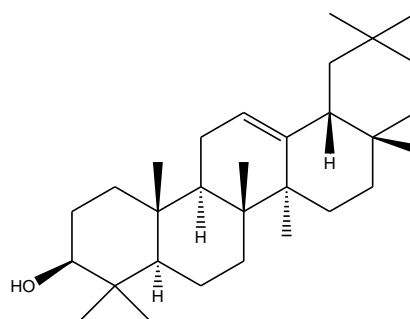


β -Sitosterol (25)

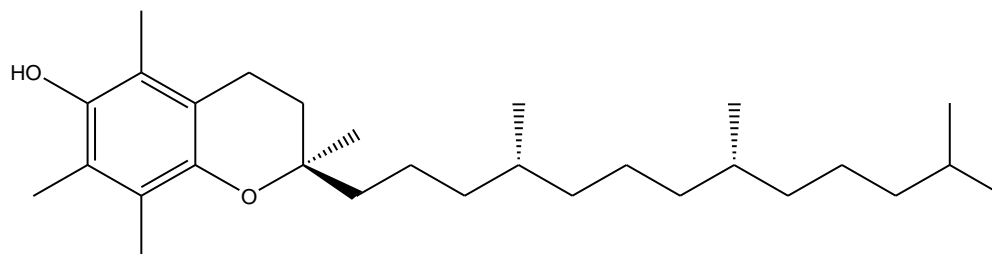
Fig. 2.6.2: Structures of some compounds isolated from *Musa* species



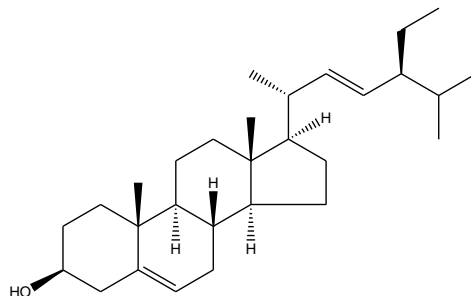
Lanosterol (26)



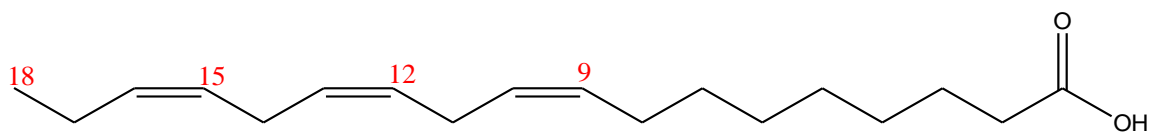
β -amyrin (27)



α -Tocopherol (28)



Stigmasterol (29)



Octadeca-9,12,15-trienoic acid (30)

Fig. 2.6.3: Structures of some compounds isolated from *Musa* species

2.9 Antioxidants and Cholinesterase Inhibition

Antioxidants are molecules that inhibit the oxidation of other molecules. They are known to prevent oxidative damage on other molecules caused by free radicals by inhibiting the oxidation process. They act by scavenging free radicals, catalytic metals and chelating agents (Buyukokuroglu *et al.*, 2001). Free radicals and ROS are reported to be the underlying factor for various diseases such as arthritis, asthma, cancer, atherosclerosis and neurodegenerative disorders (e.g. Alzheimer's and Parkinson's diseases) (Conforti *et al.*, 2008). They are also known to be able to damage cellular biomolecules like nucleic acids and proteins leading to several diseases including neurodegenerative diseases. Therefore, the use of antioxidants is a promising approach for reducing the progression of many diseases especially Alzheimer's disease (AD). The brain of an AD patient is said to be under oxidative stress; research has found a link between antioxidant intake and reduced incidence of dementia (Houghton *et al.*, 2007).

The combination of antioxidants and cholinesterase inhibitors are two therapies for the treatment of neurodegenerative disorders. The inhibition of acetylcholinesterase (AChE), the enzyme responsible for the hydrolysis of acetylcholine serves as a strategy for the treatment of Alzheimer's disease (AD) and other dementia (Atta-ur-Rahman and Choudhary, 2001). Acetylcholine (ACh) on the other hand is an important neurotransmitter which is critical for an adequately functioning memory. They are key elements in the communication between neurons, which is the essential mechanism of the nervous system functioning. Ensuring an increased and a balanced level of acetylcholine by inhibiting cholinesterase is an important strategy for the management of AD.

2.10 Anti-inflammation and Antidiabetes

Inflammation is an underlying element in the onset of several disease conditions like diabetes, cancer, infections, obesity, cardiovascular disorders etc. (Crowson *et al.*, 2013). Lipid-peroxidizing enzymes (lipoxygenase) required in the bio-formation (from arachidonic acid) of leukotriene serve as intermediary for inflammation and allergic responses. They are also involved in induction of many diseases associated with inflammation. Lipoxygenases trigger introduction of molecular oxygen to unsaturated

fatty acids (UFAs), such as linoleic and arachidonic acids, which are their common substrates (Porta and Rocha-Sosa, 2002). Interestingly, there are four major iso-enzymes of lipoxygenases including 5, 8, 12 and 15 already described, each isoform differ from each other based on the position of oxidation in the UFAs. Despite the major involvement of this enzyme in inflammation, their action is also witnessed in the formation of inflammatory lipid mediators, such as leukotrienes and prostaglandins. Interestingly, the inhibition of these enzymes is attributed as the hallmark measures for diseases prevention particularly those linked to oxidative stress and inflammation, which might also be the case in diabetes mellitus (Radmark and Samuelsson, 2007).

Diabetes mellitus (DM) is a chronic derangement attributed to partial or complete insulin deficiency arising from elevated glucose level in the blood (hyperglycemia) (Yadav *et al.*, 2008) and many other complications. The ability to salvage postprandial blood sugar levels (BGL) is very important in early diabetes mellitus therapy and reduction in chronic vascular problems (complications) (Kwon *et al.*, 2008). Persistent hydrolysis of starch by α -amylase (α -AL) of the pancreas and the subsequent glucose absorption of glucose by α -glucosidases (α -GSDs) found in the intestine lead to a continuous increase in BGL, termed hyperglycemia in non-insulin dependent diabetes (NIDD) individuals. A useful approach for NIDD management is a strong α -GSD and mild α -AL inhibitions (Krentz and Bailey, 2005). Prevention of the absorption of carbohydrates (CHO) after food uptake is a potent schedule or plan for alleviating postprandial hyperglycemia in patients with DM. Intriguingly, substances (inhibitors) that can hinder the activities of these enzymes by delaying carbohydrate digestion, would bring about a reduction in the extent to which glucose is absorbed thereby preventing the post-prandial elevation of plasma glucose. Common examples of such inhibitors of α -AML and α -GSDs available in the pharmaceutical industry are acarbose, miglitol and voglibose (Bailey, 2003). Miglitol and acarbose are α -glucosidase inhibitors known to lower the post-prandial blood glucose after a starch load. They exert their action by inhibiting the final process in CHO digestion [disaccharide to monosaccharide (glucose)] resulting in the reduction in the amount of glucose going into the blood circulation (Rabasa-Lhoret and Chiasson, 2004). However, these drugs are not without their side effects such as bloating, abdominal distension, flatulence, etc. Hence, the need for the search for alternative medicines from plants.

CHAPTER THREE

3.0 MATERIALS AND METHODS

3.1 Chemicals and Reagents Used

The chemicals and reagents used in this study were of analytical grade and MS grade as the case may be.

3.1.1 The chemicals used for *in vitro* plant tissue culture experiment

Murashige and Skoog basal medium, myo-inositol, sugar, ascorbic acid, naphthalene acetic acid (NAA), 6-benzylamino purine (BAP), indole acetic acid (IAA), gelrite, salicylic acid, jasmonic acid, sodium hydroxide (NaOH), hydrochloric acid (HCl), tween 20, sodium hypochlorite (NaOCl), ethanol, nicotinic acid and glycine were purchased from Sigma Aldrich, Germany. Thiamine, pyridoxine, ammonium nitrate (NH_4NO_3), cobalt (II) chloride hexahydrate ($\text{CoCl}_2 \cdot 6\text{H}_2\text{O}$), calcium chloride dihydrate ($\text{CaCl}_2 \cdot 2\text{H}_2\text{O}$), potassium nitrate (KNO_3), potassium dihydrogen phosphate (KH_2PO_4), magnesium sulphate heptahydrate ($\text{MgSO}_4 \cdot 7\text{H}_2\text{O}$), boric acid (H_3BO_3), manganese sulphate tetrahydrate ($\text{MnSO}_4 \cdot 4\text{H}_2\text{O}$), potassium iodide (KI) were bought from Duchefa Biochemie, Netherlands while zinc sulphate heptahydrate ($\text{ZnSO}_4 \cdot 7\text{H}_2\text{O}$), copper sulphate pentahydrate ($\text{CuSO}_4 \cdot 5\text{H}_2\text{O}$), Iron (II) sulphate heptahydrate ($\text{FeSO}_4 \cdot 7\text{H}_2\text{O}$), sodium ethylenediaminetetraacetic acid dehydrate ($\text{Na} \cdot \text{EDTA} \cdot 2\text{H}_2\text{O}$) were from VWR BDH®, UK

3.1.2 Chemicals and reagents used for DNA extraction

Cetyl trimethylammonium bromide (CTAB buffer), polyvinyl pyrrolidone (PVP), Ethylenediamine tetraacetic acid (EDTA), RNase enzyme, proteinase K, Tris-HCl, isopropanol, ethanol, chloroform, isoamyl alcohol, sodium chloride, mercaptoethanol, Trisma base, ficoll, bromophenol blue, 100 bp DNA ladder (New England biolab).

3.1.3 Chemicals and reagents used for biological assays and isolation

Gallic acid, anhydrous sodium carbonate, 2,2-diphenyl-1-picrylhydrazyl (DPPH[•]), folin-ciocalteu reagent, aluminium chloride, potassium acetate, potassium pyrosulphate (K₂S₂O₈), Iron (II) sulphate (FeSO₄), deoxyribose, hydrogen peroxide (H₂O₂), phosphate buffer, trichloroacetic acid (TCA), thiobarbituric acid (TBA), acarbose, alpha-amylase (α -AML), alpha-glucosidase (α -GCD), starch, dinitro salicylic acid (DNS), p-nitrophenyl glucopyranoside (pNPG), quercetin, silica gel (230-400 mesh size), Sephadex (LH-20) and 15-lipoxygenase from *Glycine max* were purchased from Sigma-Aldrich (South Africa). Acetylthiocholine iodide (ATCI), eserine, acetyl-cholinesterase (AChE) lyophilisate, butyrylcholinesterase (BChE) from horse serum, bovine serum albumin (BSA), 5, 5-dithiobis-(2-nitrobenzoic acid) (DTNB), sodium acetate trihydrate, glacial acetic acid, magnesium chloride hexahydrate, ferric chloride hexahydrate (FeCl₃ · 6H₂O), 2,4,6-Tri(2-pyridyl)-s-triazine (TPTZ), trolox, fast Blue B salt, acetic acid, citric acid, α -naphthyl acetate, sodium chloride, hydrochloric acid (32%), sodium monohydrogen phosphate, tris(hydroxymethyl)aminomethane (TRIS), 2-naphtyl- α -D-glucopyranoside, 2-chloro-*p*-nitrophenyl- α -D-maltotrioxide (CNP-G3) and formic acid, were all bought from Sigma-Aldrich (Germany). Natural Products reagent (NP, diphenylboryloxyethylamine), 3-(4,5-Dimethylthiazol-2-yl)-2,5-diphenyltetrazoliumbromide (MTT, $\geq 98\%$), Methanol, ethyl acetate, ethanol (95%), *Bacillus subtilis* spores (BGA, ATCC 6633), *Salmonella thyphimorium*, *Aliivibrio fischeri* (DSM no. 5171) toluene as well as linoleic acid were bought from Merck, Germany.

3.2 Materials and Apparatuses

Weighing balance (Mettler Toledo, USA), weighing bowl, spatulas, electric grinder (Marlex Ecceler), conical flasks, funnels, measuring cylinders, maceration jars, glass rod stirrer, cotton wool, rotary evaporator (Buch Rotavapor, Germany), separating funnel, water bath (GFL), clamp and retort stand, thin layer chromatography tanks, pre-coated aluminium TLC plates (Merck, Germany), glass column, capillary tubes, ultraviolet lamp (Allen 425 LCF-750-Q), beakers, filter papers, standard volumetric flasks, pipettes, graduated syringes, test tubes, test tube rack, UV/Visible spectrophotometer (Model 752 UV grating), freeze dryer (Labconco, USA), mortar and pestle, micro-pipette, liquid

nitrogen, eppendorf tubes, micro-pipette tips, 96-well plates, centrifuge (Thermo Fischer scientific), laminar flow hood (Nuair, Plymouth USA), temperature logger (Omega, Canada), incubator/conviron (Percival, Iowa, USA), nano drop spectrophotometer (Thermo Fischer scientific), PCR tubes, gel electrophoresis tank (Biometra compact, analytic-jena, Germany), parafilm, autoclave (Astell, UK), microwave, magnetic stirrer (Boeco, Germany), magnetic flea, magnetic rod, pH meter (Mettler Toledo, USA), test-tube washer (Lancer, USA), dryer (Labec, Marrickville, Australia), dispenser (Wheaton Unispense PRO, UK), bead sterilizer (Steri 350, Swiss made), microplate reader (MICRO PLATE READ), HPTLC plates, vortex machine (Vortex Genie 2, Scientific Industries, US), sonicator (Bandelin sonorex digiplus, Germany), automatic TLC sampler (ATS4), Twin Trough 20 cm × 10 cm Chamber, TLC Visualizer Documentation System, TLC Immersion Device, TLC Plate Heater, automatic development chamber (ADC2), smartCut PlateCutter, TLC-MS Interface 2 were all purchased from (CAMAG, Muttenz, Switzerland). QExactive Plus mass spectrometer (Thermo Fisher Scientific, Dreieich, Germany) and NMR (AscendTM 500, Bruker).

3.3 Plant Materials

Musa spp. were selected for this study after a literature search and an ethnobotanical survey on the medicinal plants used for management of neurodegenerative diseases (Sonibare and Ayoola, 2015). Fifteen taxonomic reference *Musa* accessions (TRA) were selected based on their genome group and country of origin. These TRAs are representatives of the different groups in the *Musa* biodiversity. Other landraces (10) and *Musa sapientum* from the Botanical Garden, University of Ibadan (UI) were used in this study. All the accessions comprised different *Musa acuminata* and *Musa balbisiana*. They were collected from the Genetic Resource Centre, International Institute of Tropical Agriculture, Ibadan. Table 3.1 provides further information on the plant species used in this study.

Table 3.1: Passport Data of the Taxonomic Reference Accessions

S/N	Accessions	Species	Genome group	Origin	F	IV	ACC
1	Simili Radjah*	<i>Musa acuminata</i>	ABB	Cote d'Ivoire	A ₁	A ₂	A ₃
2	Foconah	<i>Musa acuminata</i>	AAB	Unknown	B ₁	B ₂	B ₃
3	P. Mas	<i>Musa acuminata</i>	AA	Unknown	C ₁	C ₂	C ₃
4	P. Jaribuaya	<i>Musa acuminata</i>	AA	Homduras	D ₁	D ₂	D ₃
5	Zebrina	<i>Musa acuminata</i>	AAwild	Costa Rica	E ₁	E ₂	E ₃
6	Calcutta 4	<i>Musa acuminata</i>	AAwild	France	F ₁	F ₂	F ₃
7	Gros Michel	<i>Musa acuminata</i>	AAA	Nigeria	G ₁	G ₂	G ₃
8	Red Dacca	<i>Musa acuminata</i>	AAA	Unknown	H ₁	H ₂	H ₃
9	P. Ceylan	<i>Musa acuminata</i>	AAB	Unknown	I ₁	I ₂	I ₃
10	Pelipita	<i>Musa acuminata</i>	ABB	Austria	J ₁	J ₂	J ₃
11	<i>M. balbisiana</i> Tani	<i>Musa balbisiana</i>	BBwild	Unknown	K ₁	K ₂	K ₃
12	Dole	<i>Musa acuminata</i>	ABB	Unknown	L ₁	L ₂	L ₃
13	Safet Velchi*	<i>Musa acuminata</i>	AABcv	Unknown	M ₁	M ₂	M ₃
14	<i>M. balbisiana</i> HND	<i>Musa balbisiana</i>	BBwild	Honduras	N ₁	N ₂	-
15	Igitsiri	<i>Musa acuminata</i>	AAA	Burundi	O ₁	O ₂	-
Other landraces							
16	Ihitisim	<i>Musa acuminata</i>	AAB	Unknown			
17	Orishele*	<i>Musa acuminata</i>	AAB	Nigeria			
18	Borneo	<i>Musa acuminata</i>	AA	France			
19	Muga	<i>Musa acuminata</i>	AAA	Brazil			
20	Ouro mel	<i>Musa acuminata</i>	AAA	France			
21	P. awak	<i>Musa acuminata</i>	ABB	Sri Lanka			
22	Trumay	<i>Musa acuminata</i>	AA	Unknown			
23	P. raja	<i>Musa acuminata</i>	AAB	France			
24	Muracho	<i>Musa acuminata</i>	AAB	Philippines			
25	Egjoga	<i>Musa acuminata</i>	AAB	Nigeria			
26	<i>Musa</i> spp	<i>Musa sapientum</i>	ND	Nigeria			

F-Field-grown samples, IV-*in vitro*-grown, ACC-7 months after acclimatisation

*Accessions that were replicated and used as control in the genetic fidelity study

3.4 Micropropagation, Multiplication and Acclimatisation

3.4.1 Preparation of growth media (regeneration and proliferation media)

In vitro plant tissue culture experiment usually starts with medium preparation, which is suitable for the intended use. Two types of media were prepared; regeneration media for the introduction of accessions from the field into the lab through meristem excision from the suckers uprooted from the field and proliferation media for the rapid multiplication of the accessions. Murashige and Skoog's (MS) medium (1962) fortified with growth hormones as listed in Table 3.2, was used as culture media. The MS media fortified with 2.3 mgL^{-1} 6-Benzyl amino purine (BAP) and 0.18 mgL^{-1} Naphthelene acetic acid (NAA) was used to regenerate excised meristem, while the shoot proliferation of all the accessions was done on MS media fortified with 0.18 mgL^{-1} Indole acetic acid (IAA) and 4.5 mgL^{-1} BAP.

In a clean beaker was put one-third the volume of distilled water, a magnetic flea was put inside and placed on a magnetic stirrer. The components of the media were then weighed appropriately and added to the water in the beaker. After all the components were added apart from gelrite, the solidifying agent, it was made up to 9/10 of the desired volume and pH was taken and adjusted to 5.7 ± 0.01 . The magnetic flea was removed, distilled water added to reach the desired volume, gelrite was added and the medium was placed in a microwave for about 30 minutes so as to dissolve the gelling agent. The medium was placed back on a magnetic stirrer and then dispensed into test tubes and were covered firmly. Sterilisation of the media was done by autoclaving for 15 minutes at $121 \text{ }^{\circ}\text{C}$ and 108 KPa . The media were removed from the autoclave, allowed to cool and then placed in the refrigerator till needed. Paper towels forceps and scalpel were also autoclaved at $121 \text{ }^{\circ}\text{C}$ and 108 KPa for 30 minutes for aseptic handling of plant material.

Table 3.2: Meristem and Proliferation Media Composition

Components	<i>Musa</i> meristem Media per litre (g)	<i>Musa</i> proliferation media per litre (g)
MS basal medium	4.43	4.43
Myo-inositol	0.10	0.10
Sugar	0.03	0.03
IAA	–	0.00018
BAP	0.0023	0.0045
NAA	0.00018	–
Ascorbic acid	0.01	0.01
Gelrite	2.50	2.50

The MS medium comprises salts, micro elements, macro elements and vitamins

3.4.2 Source of explant and sterilisation

Some of the *Musa* species accessions were newly introduced (*Musa balbisiana* Tani, *Musa balbisiana* HND, Igitsiri, Zebrina, Ihitism, Orishele) and suckers were collected from the field bank of the Genetic Resources Centre, IITA. *Musa sapientum* suckers from the Botanical Garden, University of Ibadan. Three to five suckers were uprooted depending on the sucker availability. *In vitro*-grown plantlets served as explants for the remaining accessions (2 to 5 tubes per accession). They were collected from IITA tissue culture bank and multiplied. The suckers were transferred to the laboratory for surface sterilisation. All the external leaves were detached from the uprooted suckers and trimmed to obtain the internal part, which was about 2 to 3 cm long. This was put inside a clean container containing distilled water.

The following disinfection solutions were prepared: sterile distilled water, 70% ethanol solution, 5 and 10 percent sodium hypochlorite (2.6% NaOCl) solution each were containing Tween-20 droplets. Trimmed suckers were cleaned with tap water twice and soaked in the disinfection solutions successively under the laminar flow as follows:

- Five minutes in 70% ethanol solution
- 20 minutes in 5% NaOCl
- 3 times in sterile water for rinsing
- 10 minutes in 10% NaOCl
- 3 times in sterile water for rinsing

The explants which are the suckers were kept in distilled water after the disinfection steps.

3.4.3 Meristem excision and subculturing

The laminar flow and the bead sterilizer were switched on about 30 min before the start of the inoculation experiment and cleaned with paper towel soaked in 70% alcohol to keep the inside under an aseptic condition. The laminar flow bench (workstation) and operator's hands were frequently sprayed with alcohol.

Alcohol lamp and media in test tube racks were sprayed with 70% alcohol before they were placed in convenient positions within the micro flow. The scalpel and forceps were placed in the bead sterilizer (Steri 350-Swiss) to keep the sharp edges used for cutting and

picking the explants sterile. All these apparatus were left standing in the laminar flow for about 30 min.

Meristem excision was done under a stereomicroscope. The white leaf sheets was gently cut with the scalpel (blade no. 11) and removed one after the other from the outside until the meristematic dome became visible. The meristem was cut at the base after the removal of the first and second internal primordial leaves. The excised meristems were then transferred to meristem regeneration culture medium in test tubes and then sealed with parafilm. Each culture vessel (test tube) was properly labeled with a permanent marker and cultured meristems were kept in the growth chamber ($T = 25 \pm 1 \text{ } ^\circ\text{C}$, 12h light/12h dark light: $38 \text{ } \mu\text{mol/m}^2/\text{s}$).

For the multiplication of the accessions, the roots of the explants were cut off with a scalpel (blade no. 10), the older leaves were removed and the shoots were separated and trimmed. The micro-cutting was transferred into the medium in test tube, its mouth was flamed briefly and the cutting was inserted in it using long forceps. The mouth of the tube was exposed briefly to the flame before covering it with a plastic cap and sealed with parafilm. Each culture vessel was labeled with the accession number, date of subculture, and line number. The Figure 3.1 shows the micropropagation procedure from field suckers.

The sub cultured plants were then transferred to the growth chamber where the growth rate was monitored. The number of shoots, leaves, and shoot length were measured every week (twenty measurements per accession) for duration of six weeks. The mean number of; shoots, leaves, root and shoot length were calculated using SAS statistical package.



Musa plants surrounded by suckers



Trimmed sucker



Further trimmed suckers ready for meristem excision



Excised meristem



Meristem with bud now on proliferation media



6 weeks old plantlets



Musa spp. in the growth room



Plants multiplied on liquid media in a RITA vessel

Figure 3.1: *In vitro* plant tissue culture techniques

3.4.4 Acclimatisation

Well-developed *in vitro* plantlets were transferred to rooting medium, which was made up of MS media fortified with 0.18 mgL⁻¹ NAA and 2.3 mgL⁻¹ BAP. They were left to grow for about two months to have a good root system. For banana, top soil was used. The top soil was autoclaved at 120 °C for 150 minutes at the nematology laboratory, IITA, following standard procedures and dispensed into small pots three-quarter full. Plantlets with well-developed roots were cautiously cleaned to get rid of the agar, transferred to a prepared pot with sterile top soil and covered with a wet plastic bag for humidity (Fig. 3.2). Each plantlet in the pots was carefully labelled with a plastic peg. The label contained the accession number, line number, and date of acclimatisation. Pots were maintained in an insect-proof room with a warm and bright environment. The plastic bags were removed gradually (they were first punctured before final removal) after 10 weeks to allow further growth and plantlets were left to grow for up to 7 months. Water was continually added to dry soil in the pot within this period.

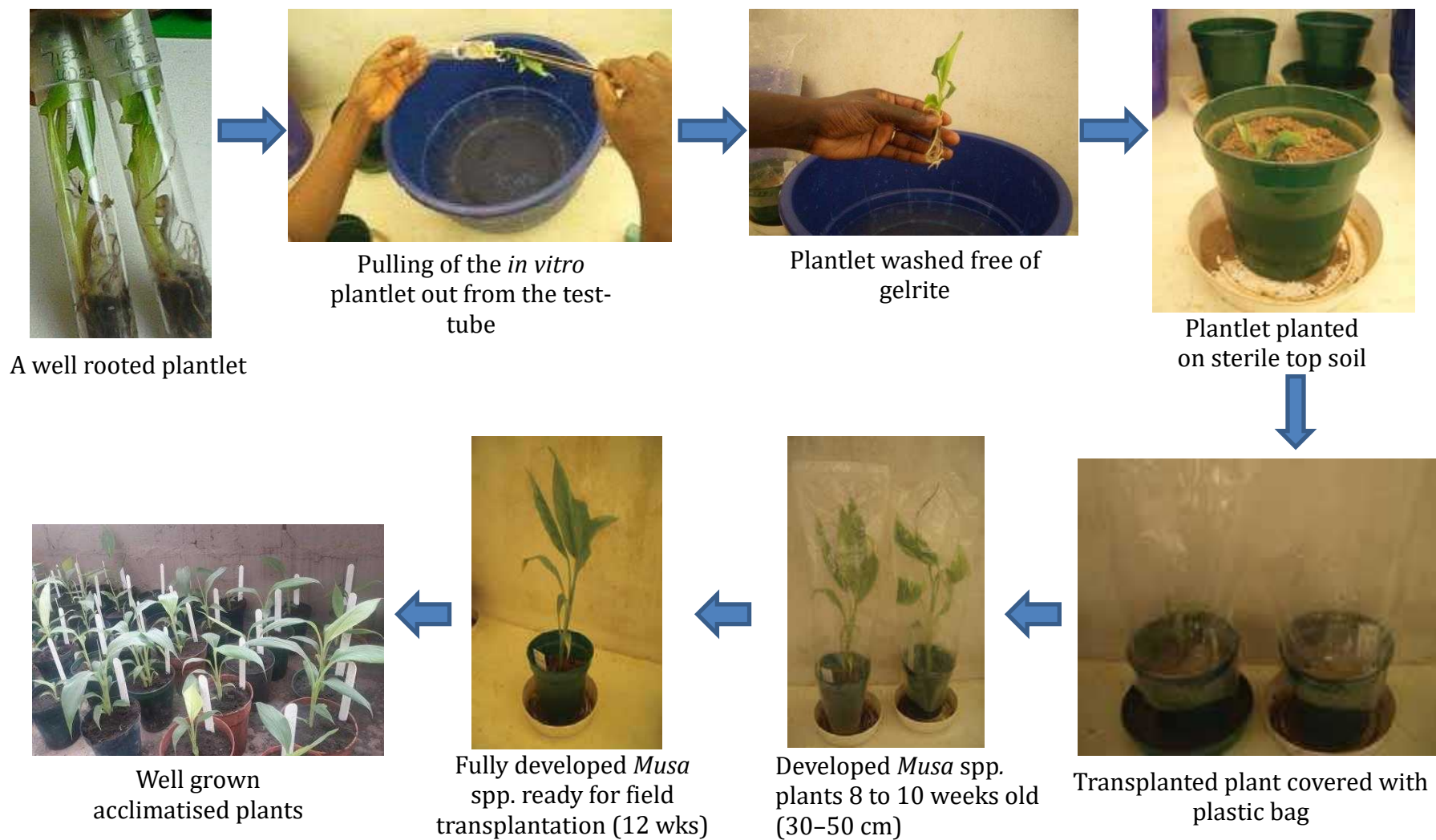


Figure 3.2: Procedures for acclimatisation of *in vitro* grown plantlets

3.5 DNA Extraction and DArTseq SNP Analysis for Genetic Fidelity Study

3.5.1 DNA extraction

Genomic DNA was obtained from each accession (field and micropropagated) using 150 mg of young leaves from both field and *in vitro* samples using CTAB protocol (Doyle, 1990) with some modifications as described by Shankar *et al.* (2011). Briefly, fresh leaves were collected in aluminum foil and dipped immediately in liquid nitrogen. Fresh leaf tissue (150 mg) was ground with liquid nitrogen in a prechilled mortar and a pestle to have a powder. The ground tissue was put in a 2 mL eppendorf tube and 10 microlitre of proteinase K was added and mixed by inverting the tube. Samples were kept in the incubator at 37 °C for 10 minutes and in the water bath at 63 °C for 30 min with frequent swirling. The tubes were cooled at room temperature and centrifuged at 8,000 rpm for 10 minutes. Supernatant were put into new eppendorf tubes. The same volume of chloroform: isoamyl alcohol (24:1) was included and the content was mixed by gently inverting the tubes 30-40 times and then centrifuged at 8,000 rpm for 10 minutes. The supernatant was transferred to a clean centrifuge tube and 200 µL of 2 M NaCl containing 4% PEG was added. Samples were incubated at 4 °C to increase the yield of DNA. All these extra steps were necessary because of the *in vitro*-grown materials. The DNA was precipitated by adding cold isopropanol (500 µL) and the content were homogenised by inverting the tubes gently. Samples were kept at -20 °C for 30 minutes and then centrifuged at 3,000 rpm for 10 minutes. The supernatant was decanted and pellet was washed twice with 70% ethanol (500 µL) and then centrifuged at three thousand rpm for fifteen minutes (4 °C). The ethanol was decanted and the DNA pellets were allowed to dry and dissolved in 100 µL of TE buffer containing 10 µL RNase. The isolated genomic DNA was kept in the refrigerator (2-8 °C) until use.

3.5.2 Measurement of concentration and purity of DNA sample

The concentration and purity of isolated DNA samples were measured using NanoDrop 2000 UV-Vis spectrophotometer (Thermo Scientific, Massachusetts, USA) and agarose gel electrophoresis. Sample purity ratio was determined by Absorbance 260/Absorbance 280 (A260/A280) and Absorbance 260/Absorbance 230 (A260/A230). The blank absorbance was measured using 1x TE (1 µL).

A total of 56 high quality DNA samples (50 µl of 100 ng µl⁻¹) including four technical replicates as control for sequencing error from three accessions Orishele (field), Simili radjah (both field and *in vitro*) and Safet velchi (*in vitro*) (Table S1) were sent to Diversity Array Technology (<http://www.diversityarrays.com/>), Canberra, Australia to generate SNP markers. The SNP markers were generated using next generation high-throughput DArTseq approach, which represents a combination of both complexity reduction using restriction enzymes method (Wenzl *et al.*, 2004). Sequence generated in FASTQ files were further processed using proprietary DArT analytical pipelines. The discovered SNP were run against the phytozome database ‘*Musa acuminata* DH Pahang v2’, which was used as the reference genome. Six different imputation methods were tested for imputation on the data set (see Appendix Table 1 for more details). A total of 150556 SNP were derived from DArTseq approach and further filtered based only on minor allele frequency (MAF) >0.01 as there was no missing data after imputation. Data filter, MAF, heterozygosity analysis, pairwise IBS (Identity-by-state) genetic distance matrix and genetic relationship cladogram analysis based on IBS matrix using neighbor-joining (NJ) method were completed using Tassel 5.2.25 software (Bradbury *et al.*, 2007). Heterozygosity results were taken into Excel to generate MAF and heterozygosity distribution plot. Similarly, IBS genetic distance matrix was used in R-program (Team, 2013) with ggplot and gplots packages.

3.6 Plant Crude Extraction

For the field samples collection, fresh and young leaves (first, second and third leaves) were collected from about a year old field plants, while leaves of about 2 months old *in vitro*-grown accessions were collected and put in freeze drying bags. Field leaves were cut into pieces before putting them in freeze drying bags and kept at -80 °C to prepare them for lyophilizing. They were freeze dried and then grinded into powder using an electric blender. Fifty grams of field samples were macerated in methanol while 3 g of *in vitro*-grown accessions were macerated. The powdered sample ratio to the methanol volume used was about 1 to 50. After 3 days, the filtrate was decanted using a buchner’s funnel which was connected to a vacuum pump. The resulting filtrates were concentrated *in vacuo* and stored at 4 °C until needed. Extraction yield was calculated for each sample.

3.7 UV Spectrophotometric Assays

3.7.1 2,2-diphenyl-1-picryl hydrazyl (DPPH•) antioxidant activity and Ferric Reducing Antioxidant Power (FRAP) assay

The DPPH• antioxidant activity of the samples and standard measured by their ability to scavenge the DPPH• was evaluated using the method described by Susanti *et al.* (2007) and as described by Ayoola *et al.* (2017).

The ferric reducing antioxidant power of the samples was determined using the method of Musa *et al.* (2011) and as described by Sonibare *et al.* (2018).

3.7.2 Estimation of Total Phenolic Content (TPC) and Total Flavonoid Content (TFC)

The method of Khatoon *et al.* (2013) and Ayoola *et al.* (2017) was used to evaluate the total phenolic content (TPC) of all the extracts. Blue coloured complex are formed when samples containing phenolic compounds were reduced by the folin–ciocalteu reagent. The TPC was expressed as mg gallic acid equivalent (GAE)/g of extract which was calculated from the regression equation of gallic acid calibration curve ($y = 0.0095x + 0.1325$, $r^2 = 0.9793$). Aluminum chloride colorimetric method was used to evaluate the total flavonoid contents of the plant samples (Ebrahimzadeh *et al.*, 2009; Ayoola *et al.*, 2017). The TFC was expressed as mg quercetin equivalent (QE)/g of extract, calculated from standard curves ($y = 0.0077x + 0.0884$, $r^2 = 0.9980$) prepared with 6.25–200 µg quercetin/ mL.

3.7.3 Anticholinesterase assay

The acetylcholinesterase inhibition was estimated spectrophotometrically using Ellman's colorimetric method (Ellman *et al.*, 1961) modified by Elufioye *et al.* (2010). All the samples, standard (eserine), DTNB and substrate (acetylcholine iodide, ATCI) were dissolved in phosphate buffer (pH 8.0). In a 96-well plate, the reaction mixture consisted of 40 µL phosphate buffer (pH 8.0), 20 µL of varying concentrations of the test samples (0.1 to 1 mg/mL of sample and 0.06 to 0.5 mg/mL of positive control, eserine) and 20 µL of the enzyme (0.26 U/mL). The reaction mixture was incubated for thirty minutes at 37 °C, and then 100 µL of 3 mM DTNB was added. ATCI (20 µL, 15 mM) was added to initiate the reaction. The change in the absorbance per minute ($\Delta A/\text{min}$) at was measured

at 405 nm over a period of 4 min at 30 s interval indicating the hydrolysis of the substrate. Buffer was used in place of the test sample as a negative control. The experiments were carried out in triplicate and percentage inhibition was calculated as follows: $(1 - a/b) \times 100$

Where $a = \Delta A/\text{min}$ of test sample; $b = \Delta A/\text{min}$ of control; $\Delta A =$ change in absorbance.

IC_{50} was calculated from the linear regression curve by plotting the percentage inhibition against extract concentration.

3.8 High Performance Thin Layer Chromatography (HPTLC) Methods

3.8.1 Sample preparation and HPTLC separation

Field, *in vitro* and acclimatised sample extracts (2.5 mg) was re-dissolved in 1 mL of methanol. For all the effect-directed analyses, apart from cholinesterase assay (15 or 25 $\mu\text{L}/\text{band}$), samples (10 $\mu\text{L band}^{-1}$) were sprayed as 7 mm bands onto the HPTLC plate by the automatic TLC sampler at 8 mm distance from the bottom edge with a track distance of 8.3 - 11 mm. The HPTLC separation was performed with majorly two solvent systems, which were selected after mobile phase (MP) development; a very polar and acidic MP (Ethyl acetate: Toluene: Formic acid: Water 3.4: 0.5: 0.7: 0.5) and a medium polar and non-acidic MP (Toluene: Ethylacetate: Methanol 6: 3: 1) so as to capture most of the plant components. The development was done in a 20 cm \times 10 cm Twin Trough Chamber up to a migration distance of 60 mm, which took 29 min. The chromatogram was documented by the TLC Visualizer Documentation System UV lamp at wavelengths 254 nm and 366 nm.

3.8.2 HPTLC post-chromatographic derivatisations

The polar chromatograms were immersed in a reagent sequence reagent for two seconds with a speed of 2.0 cms^{-1} using the immersion device. The same plates were first, dipped in natural products (NP) reagents, followed by ninhydrin and lastly in diphenylamine (DPA). The plates were heated on the TLC Plate Heater at 110 $^{\circ}\text{C}$ for 3 to 5 min before dipping in NP reagents and then visualised under 366 nm but for immersion in ninhydrin and DPA, the plates were heated at 110 $^{\circ}\text{C}$ for 3 to 5 min after dipping in the reagents and then viewed under white light. The medium polar chromatograms were immersed in p-

anisaldehyde sulfuric acid reagent for two seconds with 2.0 cm s^{-1} immersion speed and heated at $110 \text{ }^\circ\text{C}$ for 3 to 5 min.

3.8.3 Neutralisation of chromatograms

Chromatograms containing acidic mobile phase were neutralised using the CAMAG derivatiser after development in the acidic mobile phase according to the method developed by Azadniya and Morlock (2018). The developed plates were air dried and citrate-phosphate buffer (8%, pH: 7.5; made up of 8 g Na_2HPO_4 in 60 mL water and 1 M citric acid and made up to 100 mL) was piezoelectrically sprayed on the plates, followed by plate drying in the Automatic Development Chamber (ADC 2, CAMAG).

3.8.4 HPTLC-Effect Directed Analysis (EDA)

3.8.4.1 HPTLC-DPPH[•] radical scavenging assay

The chromatogram was immersed (speed 2.0 cm s^{-1} and time 5 s) in 0.02% methanolic DPPH[•] solution. The chromatogram was documented at white light illumination (reflection and transmission mode) after 1, 10 and 30 min. The absorbance of the chromatogram was measured at 546 nm using the mercury lamp in the fluorescence mode without optical filter.

3.8.4.2 HPTLC-Acetylcholinesterase (AChE) and butyrylcholinesterase (BChE) assay

The cholinesterase inhibition assays were performed according to the method described by Azadniya and Morlock (2018). Sample volume $25 \text{ } \mu\text{L band}^{-1}$ (for the polar and acidic mobile phase, PAMP) but $15 \text{ } \mu\text{L band}^{-1}$ (for medium polar and non-acidic mobile phase, MPNAMP) were sprayed as 7 mm bands onto the HPTLC plate, while the other HPTLC conditions remain the same as described above. Briefly, the neutralised chromatogram was pre-wetted with 1 mL TRIS buffer 0.05 M, pH 7.8; sprayed with 3 mL of the enzyme solution (6.66 AChE units/mL or 3.34 BChE units/mL in 100 mL TRIS buffer 0.05 M, pH 7.8 containing 1 mg/mL BSA) using the CAMAG derivatiser. The plate was incubated at $37 \text{ }^\circ\text{C}$ for 25 minutes and sprayed with the substrate (90 mg α -naphthyl acetate and 160 mg Fast Blue B salt in 90 mL water: ethanol, 2:1). The plate was dried at room temperature and zones of inhibition were documented under white light as white zones on a purple background.

3.8.4.3 HPTLC- α -Glucosidase, β -glucosidase and α -amylase assays

Glucosidase inhibitory assay was performed according to the method developed by Jamshidi-Aidji *et al.* (2019). Concisely, 2 mL of substrate (60 mg 2-naphtyl- α -D-glucopyranoside in 50 mL ethanol) was sprayed on the neutralised chromatogram and air dried for 2 min. The plate was pre-wetted with 1 mL sodium acetate buffer (pH: 7.2 - 7.5) after which the cabinet was opened and closed quickly. Two milliliter of the enzyme solution (500 units of α -glucosidase/1000 units of β -glucosidase in 50 mL buffer) was sprayed; plate was placed horizontally in a pre-prepared humidity box and incubated at 37 °C for 13 min. After the incubation, 0.5 mL of fast blue B salt solution was sprayed on the chromatogram; images were taken directly and after drying the plate by using the ADC2 humidity control under white light illumination (transmission and reflection modes).

For the HPTLC- α -amylase inhibition assay, plates were dipped into the ethanolic substrate solution (1.4 mg/mL CNP-G3), dried for 2 min (hair dryer) and immersed in the enzyme solution (1.2 mg/mL α -amylase in sodium acetate buffer, pH 7.5). After 15 min incubation at 37 °C in a moistened polypropylene box, the autogram was dried and documented at white light illumination. Active compounds were detectable as bright zones against a yellowish green background (Móricz *et al.*, 2019).

3.8.4.4 HPTLC-*Bacillus subtilis* bioassay

This was done as described by Jamshidi-Aidji and Morlock (2015). Briefly, the chromatogram developed in the medium polar mobile phase was immersed in *B. subtilis* suspension (Optical density at 600 nm= 0.8) for 7 s with 3 cms⁻¹ immersion speed, incubated at 37 °C for two hours and then visualised by dipping into PBS-buffered MTT solution (0.2%) for 1s with 3.5 cm/s immersion speed and incubated at 37 °C for thirty minutes. The plates were heated on the TLC Plate Heater (CAMAG) at 50 °C for ten minutes. Active microorganisms reduced MTT into purple formazan, whereas antimicrobials were observed as white zones on a purple background (Marston, 2011) and documented under white light illumination (reflection mode).

3.8.4.5 HPTLC-*Aliivibrio fischeri* bioassay

The Gram-negative antimicrobial profiling was performed according to the method reported by Kruger *et al.* (2013). Briefly, the chromatogram developed in the medium polar mobile phase was immersed for 2 s into the luminescent *A. fischeri* suspension (the

proper luminescence was visually checked by shaking the flask in a dark room, the medium was prepared according to the method developed by the European Committee for Standardization, 2009). The luminescent bioautogram was monitored for 30 minutes and documented with the BioLuminizer (CAMAG) using an exposure time of thirty seconds and one minute trigger interval. Dark zones are said to be bioactive as they indicated the inhibition of the luminescence of bacteria (Bulich, 1979).

3.8.4.6 HPTLC-SOS-Umu-C bioassay

A newly developed genotoxic assay (SOS-Umu-C bioassay) installed in the laboratory at JLU Giessen exploited the *Salmonella thyphimurium* bacteria (Meyer *et al.*, 2021). It was applied on the samples to indicate any genotoxic substances or mutagens in the samples. The standard 4-nitroquinoline-1-oxide was used as a positive control.

3.8.5 HPTLC-Electron spray ionization (ESI)-high-resolution mass spectrometry (HRMS)

The HPTLC plates were first washed twice in methanol–formic acid 10:1 (v/v) and eluted up to 9.5 cm. After that, a last washing step with acetonitrile–methanol 2:1 (v/v) and elution up to 9.5 cm) was carried out (Glavnik *et al.*, 2017). The selected extracts were applied on the washed plates in triplicate. The first plate was for bioassay; the second plate for derivatisation in natural product reagent for the polar/acidic mobile phase and anisaldehyde sulfuric acid reagent for the medium polar/non-acidic mobile phase; while the third section was for HRMS. The third plate with the marked targeted zones was placed on the HPTLC-HRMS interface and then the zones were stamped and eluted into the HRMS one after the other. HRMS recording was done as described by Jamshidi-Aidiji and Morlock (2016).

3.9 *In vitro* Plant Tissue Culture Elicitation Experiments

Six *Musa* accessions were selected from the fifteen taxonomic reference accessions for the elicitation experiment. Two accessions with high antioxidant activity (Simili radjah and Foconah), two with moderate activity (P. Mas and Red Dacca) and two with low antioxidant activity (Dole and *M. balbisiana* HND), were selected. This was done to see the elicitation role of the treatments on the antioxidant secondary metabolites especially on the accessions with initial moderate and low antioxidant activity. They were first

multiplied on the liquid proliferation media without the solidifying agent, gelrite, using the temporary immersion system and a RITA® apparatus for mass multiplication using the method of Jekayinoluwa *et al.* (2019). Three elicitation experiments were performed on the 6 accessions; the effect of temperature, increase in sugar and addition of jasmonic acid on the production of antioxidant compounds. The different media compositions were prepared based on the experiment, *in vitro* explants were sub-cultured and they were kept in the growth chamber for growth and data was collected for two months. Growth parameters which includes; the shoot length, leaf number, shoot number and number of root were measured weekly during the experiment.

3.9.1 Increase in sugar level experiment

The MS basal medium for shoot induction was supplemented with 35, 40, 45 and 50 g/L of sugar as seen in Table 3.3. Media with 30 gL⁻¹ of sugar was the control. *In vitro*-grown explants were sub-cultured on the different media and kept in the growth chamber. The experiment was done in replicates (40), the growth parameters were measured weekly for a period of 6 weeks. The leaves were harvested at the end of 6 weeks and kept at -80 °C till use.

3.9.2 Reduced temperature experiments

Plants were sub-cultured on the routine proliferation media (Table 3.2) but they were kept in different growth chambers and conviron with three different temperature conditions; 26 ± 2 °C which is the control, 20 ± 2 °C and 15 ± 2 °C. The temperature of the incubator was monitored with a temperature logger. Growth parameter was measured over a period of 8 weeks because of the slow growth of the plants where the temperature was reduced. The leaves were collected at the end of the experiment and kept at -80 °C till use.

3.9.3 Addition of jasmonic acid experiment

The abiotic elicitor, Jasmonic Acid (JA) was tested. A range of concentration of JA (50, 100 and 200 µM) was included separately to the MS proliferation medium. The MS medium without any elicitor served as control. The experiment was done in replicates (40); shoots were harvested at the end of 6 weeks and kept at -80 °C for phenolic compound quantification and antioxidant activity.

Table 3.3: Media Composition for Increase in Sugar Experiment

Components	<i>Musa</i> proliferation culture medium (/L) Control	35 g/L sugar	40 g/L sugar	45 g/L sugar	50 g/L
MS basal medium	4.43g	4.43g	4.43g	4.43g	4.43g
Myo-inositol	100 mg	100 mg	100 mg	100 mg	100 mg
Sugar	30 g	35 g	40 g	45 g	50 g
IAA	0.18 mg	0.18 mg	0.18 mg	0.18 mg	0.18 mg
BAP	4.5 mg	4.5 mg	4.5 mg	4.5 mg	4.5 mg
Ascorbic acid	10 mg	10 mg	10 mg	10 mg	10 mg
Gelrite	2.5 g	2.5 g	2.5 g	2.5 g	2.5 g

3.10 Analysis of Elicited Samples Using HPTLC

All the elicitation experiment resulted into 71 different samples with different treatments. For the temperature experiment using three different temperature conditions, there were 18 samples from 6 accessions. The increase in sugar from (30, 35, 40, 45, 50 g/L) resulted into 30 different samples. The treatment with jasmonic acid (control, 50, 100, 200 μ M) gave a total of 23 samples instead of 24 because all *M. balbisiana* accessions treated with 50 μ M jasmonic acid did not grow well and were lost. All the samples from the elicitation experiments were freeze dried and ready for HPTLC analysis.

3.10.1 Sample preparation and extraction

Freeze dried elicited samples were grinded with a coffee grinder and stored in an air free bottle. Different solvents (methanol (100%), ethanol : H₂O (70:30), ethyl acetate (100%) and *n*-hexane, 100%) were tried to determine the best extraction solvent. Ethanol : H₂O (70:30) was chosen because it gave the best result. Powdered samples (1 mg) were weighed into eppendorf tubes and 1 mL of Ethanol : H₂O 70:30 was added. The samples were vortexed, sonicated for 10 minutes and then centrifuged for 30 minutes. The supernatant which was the extract was then filtered into sample application tubes (Fig. 3.3). All the 71 samples were prepared and properly labelled.

3.10.2 HPTLC derivatisation

Elicited samples were arranged in the appropriate order into the automatic TLC sampler 4 and were sprayed onto the 20 x 10 cm HPTLC plate by an automatic TLC sampler at 8 mm distance from the bottom edge as 6.5, 7 or 8 mm bands depending on the number of tracks needed. The distance between tracks varied between 8.2, 9.7 and 10 mm. Samples from the different experiments were applied differently on the HPTLC plates. For, the temperature experiment there were 18 tracks applied as 8 mm bands and 1.5 μ L/band with a track distance of 10 mm. The sample concentration on the HPTLC plate was 600 ng per band. The addition of jasmonic acid experiment took 23 tracks applied as 6.5 mm band and 1.0 μ L per band with a track distance of 8.2 mm. Here, the sample concentration was 400 ng per band. Sugar increase experiments had 30 tracks. The samples were applied on two HPTLC plates; 15 tracks/samples per plate were applied as 8 mm band (1.0 μ L/band) and the distance between tracks was 10 mm.

The HPTLC separation was performed with the polar and acidic mobile phase (Ethyl acetate: Toluene: Formic acid: Water 3.4: 0.5: 0.7: 0.5) and developed in an unsaturated 20 cm × 10 cm Twin Trough Chamber up to a migration distance of 60 mm, which took 29 min. The chromatogram was documented by the TLC Visualizer Documentation System UV lamp at UV 254 nm and 366 nm (CAMAG).

All the chromatograms were derivatised in DPPH• to reveal the antioxidant compounds. They were dipped in DPPH• using the immersion device (immersion speed 2 cm/s, immersion time 2 s) (Fig. 3.4). The chromatograms were documented under white light transmittance and reflection modes after 1, 10 and 30 min of immersion. For densitometric measurement, scanning of the chromatogram was done to be able to quantify the active bands and determine the best treatment per experiment. The TLC scanner (CAMAG) (Fig. 3.4) was used to scan the chromatograms using the mercury lamp at a wave length of 546 nm and without optical filter.

For the total phenolic content the gallic acid equivalent of the samples were calculated from the linear regression curve generated by using varying concentrations of gallic acid (3 to 30 or 10 – 100 ng). The WINCATS software was used to plot the GA calibration curve and to calculate the gallic acid equivalent for all the 71 samples.

3.10.3 HPTLC-Effect directed analysis of elicited samples and HPTLC-HRMS of antioxidant compounds

The HPTLC-AChE and HPTLC- α -glucosidase assays were performed according to the methods of Azadniya and Morlock (2018) and Jamshidi-Aidji *et al.* (2019) and as described in the sections 3.8.4.2 and 3.8.4.3, respectively. Antioxidant compounds were also characterised via online elution into the HRMS via the HPTLC interface. Full scan mass spectra (m/z 100–800) were recorded in the positive and negative ionisation mode with the following settings: ESI voltage 3.3kV, capillary temperature 320 °C, and collision energy 35 eV. Nitrogen was produced by a SF2 compressor (Atlas Copco Kompressoren and Drucklufttechnik, Essen, Germany). Data evaluation and background subtraction were performed by Xcalibur 3.0.63 software (Thermo Fisher Scientific).



Grinder



Powdered samples



Weighing of samples



Vortexing



Sonication



Centrifuging



Extracts after Centrifuging



Samples ready for HPTLC application

Figure 3.3: Sample preparation for HPTLC



Sample application using Automatic TLC sampler 4



Development using Automatic development chamber 2



Development using Automatic multiple development chamber



Quantitative measurement TLC Scanner 4



Effect directed analysis using Derivatiser



Effect directed analysis using Automatic immersion chamber



Visualisation using TLC Visualiser

Figure 3.4: HPTLC methods

3.11 Large Scale Extraction of the Best Field Accession

Musa acuminata (accession Simili radjah) field sample was selected for isolation because it gave the best antioxidant activity among the field accessions tested. The leaf and fruit were collected from the field bank of Genetic Resources Center, IITA, Ibadan, in September, 2017. They were freeze dried and pulverised. Powdered leaves (1.06 kg) and fruit (1.96 kg) were macerated in 4 L of methanol each for 72 h. Each was filtered and soaked again in 1 L methanol for another 24 h before filtering. The filtrates were concentrated using the rotatory evaporator (Buch Rotavapor, Germany). The percentage yield was then calculated.

3.12 Solvent-solvent Partition Extraction

The methanolic extract (85 g) of Simili radjah leaf (SRL) and 33 g of Simili radjah fruit (SRF) crude methanol extract were dissolved in methanol: water (3:1) mixture and partitioned successively into *n*-hexane, dichloromethane, ethyl acetate and *n*-butanol using 250 mL aliquots of 2.5 L *n*-hexane and 200 mL aliquots of 1 L each of the other solvents as described in the flow chart (presented in Fig. 3.5). All fractions obtained were concentrated and preserved at -4 °C prior to assays.

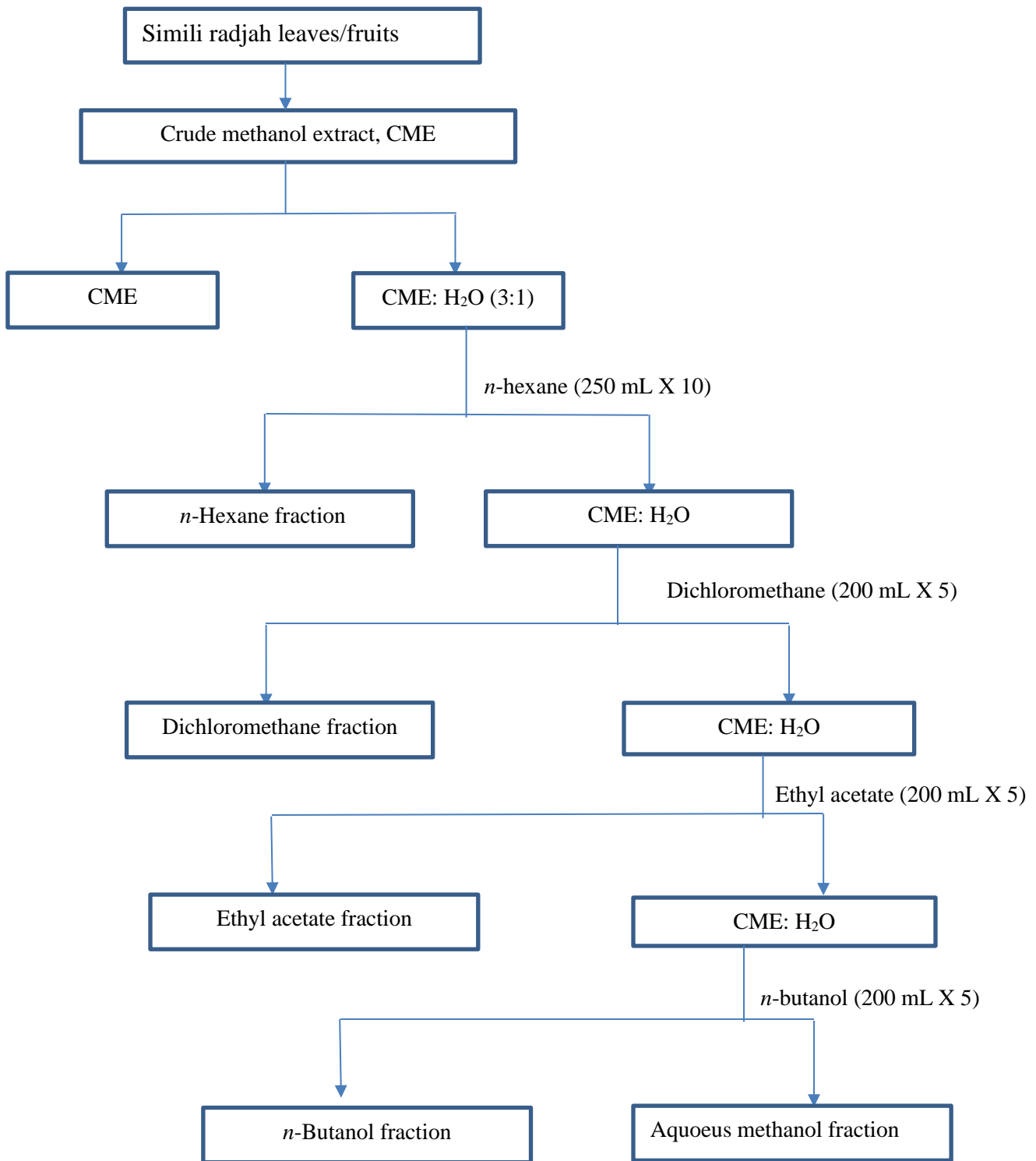


Figure 3.5: Flow chart of the partitioning of *Musa acuminata* (Simili radjah) leaf and fruit crude methanol extract

3.13 TLC of Partitioned Fractions

Thin layer chromatography was carried out on the crude methanolic extract (C) and all 5 fractions obtained i.e. the aqueous methanol (A), *n*-butanol (B), ethyl acetate (E), dichloromethane (D) and *n*-hexane (H). This was done to determine the kinds of compounds present in the different fractions. The different fractions were applied on TLC plates (Silica gel 60G F₂₅₄) and developed in various solvent systems listed below. The developed plates were viewed in daylight and under ultraviolet lamp at wavelengths of 254 nm and 365 nm.

1. Hexane : methanol (3 : 2)
2. Hexane : ethylacetate (2 : 3)
3. Toluene : ethanol (3 : 2)
4. Hexane : methanol (3.5 : 1.5)

3.14 Bioassay of Partitioned Fractions

3.14.1 Antioxidant assays

Total phenolic content and DPPH• antioxidant activity of the crude extracts and all the partitioned fractions were evaluated following the methods already described in sections 3.71 and 3.72 above so as to select the most active fraction for isolation. Other antioxidant assays (hydroxyl radical scavenging and ABTS radical scavenging assays) were carried out on the fractions as described below. *In vitro* antidiabetic and anti-inflammatory assays were also carried out on the fractions

3.14.1.1 *2,2-azinobis (3-ethylbenzothiazoline-6-sulfonic acid) ABTS radical scavenging assay*

This assay was carried out using the procedure described by Re *et al.* (1999). The ABTS⁺ was generated by reacting 7 mM ABTS aqueous solution with K₂S₂O₈ (2.45 mM, final concentration) in the dark for 16 h and adjusting the pH to 0.7 with ethanol. Exactly 0.2 mL of the various dilutions of extracts (7.81–250 µg/mL) was added to 2.0 mL ABTS⁺ solution and the absorbance was measured at 734 nm after 15 min. Gallic acid and ascorbic acid were used as standards.

3.14.1.2 Hydroxyl radical inhibitory activity

The ability of the various fractions to stop Fe²⁺/ H₂O₂ induced decomposition of deoxyribose was assayed using the modified method of Oboh and Rocha (2007). In brief, 100 µL of the freshly prepared extracts (15.63–250 µg/mL) was added to a reaction mixture containing 120 µL of 20 mM deoxyribose, 40 µL of 20 mM H₂O₂, 400 µL of 0.1 M phosphate buffer, 40 µL of 500 mM FeSO₄, and 100 µL of distilled water was added. The reaction mixture was initiated at 37 °C for 30 min, and stopped by adding 0.5 mL of 2.8% TCA (trichloroacetic acid). This was followed by the addition of 0.4 mL of 0.6% thiobarbituric acid solution. The mixture was then incubated in boiling water for 20 min and absorbance was read at 532 nm using a UV spectrophotometer. The same procedure was done for a standard antioxidant by replacing the extracts with gallic acid and ascorbic acid (15.63–250 µg/mL), and the IC₅₀ value was then calculated from the calibration curve.

3.14.2 Antidiabetic assay

3.14.2.1 Alpha (α)-Amylase inhibitory assay and mode of enzyme inhibition

The assay was carried out following the method of McCue and Shetty (2004) with a slight modification. Twenty microliter of the extract, fractions or acarbose (7.81 - 250 µg/mL) was reacted with 20 µL α-AML (0.5 mg/mL) in 0.02 M sodium phosphate buffer (pH 6.9), pre-incubated at 25 °C for 10 min, followed by addition of 20 µL of 1% starch solution (prepared in 0.02 M sodium phosphate buffer) as substrate. The second incubation was repeated as above and the reaction mixture stopped with the introduction of 10 µL of dinitro salicylic acid (DNS) reagent. At last, the mixture was incubated in boiling water for 5 min, cooled and diluted with 250 µL distilled water. The absorbance was measured at 540 nm. Distilled water was replaced with the extract to serve as the control following the same procedure. The α-AML inhibitory activity was calculated as percentage inhibition using the expression $[(A_0 - A_1)/A_0] \times 100$, where A₀ is the absorbance of the blank, and A₁ is the absorbance of the extract/control.

The enzyme kinetics and inhibition mode of α-amylase was determined according to the method described by Ali *et al.* (2006). The EAF fraction of the leaf and CME of the fruit with mild activity were used. In brief, 250 µL of the extract (2.5 mg/mL) was pre-

incubated with 250 μL of α -AML solution for 10 min at 25 $^{\circ}\text{C}$ in one set of 5 test tubes with concurrent pre-incubation of 250 μL of phosphate buffer with 250 μL of α -AML in another set of 5 test tubes. Starch (250 μL) solution of increasing concentrations (0.30-5.00 mg/mL) was added to all test tubes. This signified the beginning of the reaction which was then brought to a halt with dinitro salicylic acid following the procedure above. A maltose standard curve was used to determine the amount of reducing sugars released and converted to reaction velocities. The kinetics of inhibition of the extracts on α -AML activity was thereafter evaluated using Lineweaver and Burk equation (Kim *et al.*, 2005).

3.14.2.2 α -Glucosidase (α -GCD) inhibitory assay

The α -GCD inhibitory activity was evaluated using the method described by Kim *et al.* (2005) using α -GCD from *Saccharomyces cerevisiae*. Five millimolar of p-nitrophenyl glucopyranoside (pNPG) which is the substrate solution was prepared in 0.02 M phosphate buffer (pH 6.9). Briefly, 25 μL of the different concentrations of the extract/fractions or control (7.81 - 250 $\mu\text{g}/\text{mL}$) was pre-incubated with 50 μL of α -GCD (0.5 mg/mL) in a 96-well plate and 25 μL of pNPG was added to initiate the reaction while 200 μL of 0.1 M Na_2CO_3 terminates the process following incubation at 37 $^{\circ}\text{C}$ for 30 min. The α -GCD activity was determined by measuring the yellow coloured para-nitrophenol (pNP) released from pNPG at 405 nm. Percentage inhibition was determined by using the expression $[(A_0 - A_1)/A_0] \times 100$, where A_0 is the absorbance of the blank, and A_1 is the absorbance of the extract/control.

The modified method of Ali *et al.* (2006) was used to determine the mode of inhibition of α -GCD by the extracts. Briefly, 50 μL of the extract (2.5 mg/mL) was reacted with 100 μL of α -GCD solution for 10 min at 25 $^{\circ}\text{C}$ in one set of 5 test tubes while at the same time α -GCD was mixed with 50 μL of phosphate buffer (pH 6.9) in another set of 5 tubes. Fifty microliter of pNPG at increasing concentrations (0.25- 2.00 mg/ mL) was subsequently added to the two sets of test tubes to initiate the reaction. The resulting mixtures were allowed to stand at 25 $^{\circ}\text{C}$ and 500 μL of Na_2CO_3 was added to stop the reaction. A p-nitrophenol standard curve was used to determine spectrophotometrically the amount of reducing sugars released. A double reciprocal plot ($1/V$ versus $1/S$) where V is the reaction velocity and S is the substrate concentration was plotted. The mode of inhibition

of the extracts on α -GCD activity was determined by analysis of the double reciprocal (Lineweaver-Burk) plot using Michaelis-Menten kinetics.

3.14.3 Anti-inflammatory assay (Inhibition of 15-lipoxygenase (15-LOX) enzyme)

This was carried out according to the method described by Adebayo *et al.* (2015). The 15-LOX was made up to a working solution of 200 U/mL and kept on ice. Different sample/control concentrations (0.1 to 1 mg/mL) were dissolved in DMSO and in a 96-well plate 12.5 μ L of the sample or control was added to 487.5 μ L of 15-LOX. The mixture was incubated at room temperature for five minutes then 500 μ L substrate solutions (10 μ L linoleic acid dissolved in 30 μ L ethanol, made up to 120 mL with 2 M borate buffer at pH 9.0) was added to the solution and then incubated for 5 min at room temperature. The absorbance was measured at 234 nm with a microplate reader. Quercetin was used as a positive control, while DMSO was used as the negative control (100% enzyme activity or no enzyme inhibition). The percentage enzyme inhibition of each extract compared with negative control as 100% enzyme activity was calculated using the equation;

$$\% \text{ Enzyme Inhibition} = \frac{(OD \text{ extract} - OD \text{ blank})}{(OD \text{ negative control} - OD \text{ blank})} \times 100$$

While OD means optical density, the results were expressed as IC₅₀, i.e. concentration of the extracts/controls that gave 50% 15-LOX inhibition.

3.14.4 Anticholinesterase assay

The method (Elufioye *et al.*, 2010) described in the methodology section 3.7.3 was used to evaluate the acetylcholinesterase inhibition of the leaf and fruit fractions.

3.15 Statistical Analysis

All assays were carried out in triplicates, and the results were reported as mean of IC₅₀ which is the concentration of the sample that gave 50% activity/inhibition and the standard error of mean. One way analysis of variance and Dunnett's test for mean comparison was done using Graph Pad Prism version 5.0 for windows, Graph Pad software, San Diego, California, USA. Linear regression analysis was used to calculate the IC₅₀ values for the antioxidant, anti-inflammatory, alpha-amylase and alpha-glucosidase inhibitory activities.

3.16 Column Chromatography of the Ethyl Acetate Fraction of the Leaf and antioxidant assays of the subfractions

The leaf ethyl acetate fraction (6 g) which gave the highest antioxidant and antidiabetic activities was subjected to column chromatography on silica gel (particle/mesh size 230-400 μm , length 85 cm and diameter 3.5 cm). It was eluted with solvents of increasing polarity using *n*-hexane, ethyl acetate and methanol. The fractions were collected (50 mL portions) and spotted on TLC plates. The fractions were pooled together using the TLC profile and retention factor (hR_F) as guide. In total 220 fractions were collected and then pooled to 11 sub-fractions (A – K). The DPPH \bullet radical scavenging activity and total phenolic content of the sub-fractions were determined. The sub-fraction H was loaded on a sephadex column (LH-20, length 167 cm and diameter 2.5 cm), eluted with methanol and 10 mL portions were collected. Eighty-three (83) fractions were obtained and pooled to 11 sub-fractions (HA – HK). The sub-fraction HD with a very good yield and yellow precipitate was chosen for preparative TLC and compound isolation.

3.17 Isolation and Characterisation of Bioactive Compound Using MS, NMR and HPTLC

Sub-fraction HD was loaded on pre-coated aluminium TLC plates and gave rise to HD $_1$, HD $_2$ and HD $_3$. The isolate HD $_1$ had the best antioxidant and antidiabetic activities. It was developed in different solvent system using the aluminium TLC plates and later using HPTLC plates. The isolate HD $_1$ was characterised with nuclear magnetic resonance (NMR) (AscendTM 500, Bruker Biospin Co., Karlsruhe, Germany) and the ^1H NMR and ^{13}C NMR were recorded at 400 and 100 MHz, respectively. The isolated compound was prepared using deuterated methanol with tetramethylsilane (TMS) as internal standard in 5 mm NMR tubes. Chemical shifts were expressed in parts per million (δ) according to the TMS signal. 2D NMR spectroscopy (distortionless enhancement by polarization transfer, DEPT; homonuclear correlation spectroscopy, COSY; heteronuclear single-quantum coherence, HSQC; and heteronuclear multiple bond correlation, HMBC) was applied for assignment.

The isolate HD $_1$ was further characterised and identified with HPTLC-HRMS. The biological activities of the isolates were done on HPTLC and densitometric measurement

was used for quantitative evaluations. The chromatograms were scanned at 546 nm using mercury lamp in the fluorescence mode and no optical filter for densitometry measurement and quantification. Evaluation was assumed by area under the curve measurement. Results were obtained in μg per band of sample calculated from the gallic acid, acarbose and physostigmine calibration curve using applied volume and sample solution concentration (mg/mL).

CHAPTER FOUR

4.0 RESULTS

4.1 Micropropagation of the *Musa* spp. accessions

The selected *Musa* spp. accessions were established into *in vitro* culture via meristem excision and sub-culturing. They first formed a hard-greenish globular mass after about one month of culturing. They were then transferred to proliferation culture medium and constantly multiplied every 6 weeks. The accessions started showing signs of growth after one week of sub-culture producing 1 to 2 leaves. Many of the accessions were very responsive to the *in vitro* culture conditions, producing 6 leaves on average at the end of every 6-weeks subculture cycle; but few accessions had a slower growth rate. The number of leaves produced by each *Musa* spp. plantlet ranged from 3.14 ± 0.15 to 6.70 ± 0.38 with Calcutta-4 having the highest number of leaves followed by Zebrina and P. Mas. Foconah (5.91 ± 0.17 cm) had the highest shoot length followed by P. Mas (5.62 ± 0.25 cm) and Calcutta-4 (5.39 ± 0.44 cm). As expected, an average of one root was produced per plantlet across all the accessions due to the relatively low dose of auxin (favouring root formation) in the proliferation culture medium used for multiplication. The number of shoot initiated from each plantlet ranged from 1.08 ± 0.03 to 3.80 ± 0.18 with Calcutta-4 (3.80 ± 0.18) having the highest number of shoot followed by Zebrina (2.91 ± 0.25) and P. Mas (2.66 ± 0.19) (Table 4.1). *Musa balbisiana* HND, Pelipita and Safet Velchi had comparatively lower growth (Table 4.1).

Table 4.1.1: *In Vitro* Plant Tissue Culture Growth Parameters across Selected *Musa* spp. Accessions

Accessions	Average			
	Shoot length (SL) (cm)	Number of leaves (NL)	Number of roots (NR)	Number of shoots (NS)
Calcutta-4	5.39 ± 0.44^{ab}	6.70 ± 0.38^a	0.47 ± 0.12 ^{cd}	3.80 ± 0.18^a
Dole	3.11 ± 0.12 ^f	4.76 ± 0.23 ^{de}	0.23 ± 0.04 ^{de}	1.99 ± 0.12 ^{de}
Foconah	5.91 ± 0.17^a	4.78 ± 0.26 ^{de}	0.52 ± 0.12 ^c	1.52 ± 0.14 ^e
Gros Michel	3.30 ± 0.19 ^f	3.89 ± 0.33 ^{fg}	0.19 ± 0.06 ^e	2.22 ± 0.13^{cd}
Igitsiri	5.06 ± 0.18^{abcd}	3.14 ± 0.15^h	0.71 ± 0.13 ^{bc}	1.15 ± 0.06^f
M. balbi HND	2.71 ± 0.19^f	3.53 ± 0.17 ^{gh}	0.12 ± 0.05 ^e	1.87 ± 0.10 ^{de}
P. Ceylan	4.37 ± 0.17 ^e	4.22 ± 0.22 ^{ef}	0.83 ± 0.14^b	2.15 ± 0.14 ^d
Pelipita	2.95 ± 0.17 ^f	3.69 ± 0.20 ^{fgh}	0.23 ± 0.05 ^{de}	1.88 ± 0.15 ^{de}
P. Jaribuaya	4.62 ± 0.21 ^{de}	3.67 ± 0.19 ^{fgh}	0.81 ± 0.12^b	1.62 ± 0.09 ^e
P. Mas	5.62 ± 0.25^a	5.40 ± 0.31^c	1.56 ± 0.20^a	2.66 ± 0.19^b
Red Dacca	4.77 ± 0.17 ^{cde}	5.25 ± 0.32^{cd}	0.67 ± 0.11 ^{bc}	2.61 ± 0.15^{bc}
Safet Velchi	4.88 ± 0.21 ^{bcde}	3.52 ± 0.15 ^{gh}	0.04 ± 0.03^e	1.08 ± 0.03^f
Simili radjah	5.31 ± 0.21^{abc}	5.17 ± 0.26^{cd}	0.31 ± 0.09 ^{de}	1.79 ± 0.13 ^{de}
Zebrina	4.48 ± 0.24 ^{de}	6.02 ± 0.40^b	0.64 ± 0.10 ^{bc}	2.91 ± 0.25^b

Values are expressed as mean ± SEM (n = 20). Means with the same letter are not significantly different at (P<0.05)

4.2 Genetic Fidelity and Relationship among Selected *Musa* spp. Accessions

A total of 56 DNA, 26 *in vitro* plantlets of the selected accessions and 26 field samples of the same accessions completed with 4 duplicate lines, were extracted and used for the DArTseq analysis. From the DArTseq analysis, using imputation for missing data method, a total of 150.5K SNP markers were generated and further filtered for minor allele frequency (MAF) greater than 0.01. The retained 114,285 SNPs were used for the genetic fidelity study. Out of 114K SNP, 93,524 SNP were distributed all over the 11 chromosomes of the banana reference genome (Table 4.2.1) and 20,064 SNPs not aligned, while 697 SNPs were distributed on 12 chromosomes of mitochondrial genome. Minor allele frequency ranged from 0.018 to 0.50 (Fig. 4.2.1). The proportion of heterozygous ranged from 0.009 to 0.2436 (Fig. 4.2.2) in both field and *in vitro* samples and the average heterozygosity proportion was estimated at 0.12. The pairwise genetic distance matrix among the *Musa* spp. accessions studied ranged from 0.0199 to 0.4968 between the 56 field and *in vitro*-grown samples (Fig 4.2.3). The pairwise identity-by-state (IBS) genetic distance found 23 out of the 26 accessions *in vitro* samples to be true-to-type with the field samples. Leaf samples from Egjoga, P. raja and P. Jaribuaya accessions were not true-to-type with the field ones, as seen in the Neighbour Joining (NJ) clustering and heatmap distribution based on IBS genetic distance matrix (Fig. 4.2.4 and Fig. 4.2.5). The genetic distance based on Neighbour Joining tree (NJ-tree) mapping showed that the true-to-type field and *in vitro*-grown accessions were grouped together based on their genetic similarity. Similar result was obtained from the heterozygosity proportion distribution of the 56 banana samples.

The genetic distance based on Neighbour Joining tree (NJ-tree) mapping showed diversity among the *Musa* accessions and they were clustered into five divergent groups (Fig 4.2.4). The *Musa* plantain type, banana type, the wild accessions and the other landraces were clustered in different groups irrespective of their geographical origin. The ABB bananas accessions were clustered together, the AAB ones in another group, ABB plantain accessions in a different group, likewise the wild accessions (AAwild and BBwild) and *Musa* spp. accessions from the AA and AAA genome groups were also grouped in separate clusters. *Musa sapientum* from Botanical Garden, University of Ibadan, whose

genome group was originally unknown, was found in the AAB genome group of the NJ-tree. The principal component analysis (PCA) (Fig. 4.2.6 and 4.2.7) was also in support of the neighbour joining tree. It revealed the diversity among the accessions with PC1 and PC2 contributing about 58% of total genetic variation.

Table 4.2.1: Distribution of the 114,285 SNP of 56 samples of *Musa* spp. on banana genome both nuclear and mitochondrial genome

Chromosomes	Nuclear genome	Mitochondrial genome
Chr1	6779	75
Chr2	6649	54
Chr3	8917	161
Chr4	11249	112
Chr5	8043	44
Chr6	10706	26
Chr7	7776	36
Chr8	10041	52
Chr9	8342	31
Chr10	8003	74
Chr11	7019	9
Chr12	--	23
*Chr0	20064	--
Total	113588	697

*= non-aligned SNP on the reference genome denoted as chr0

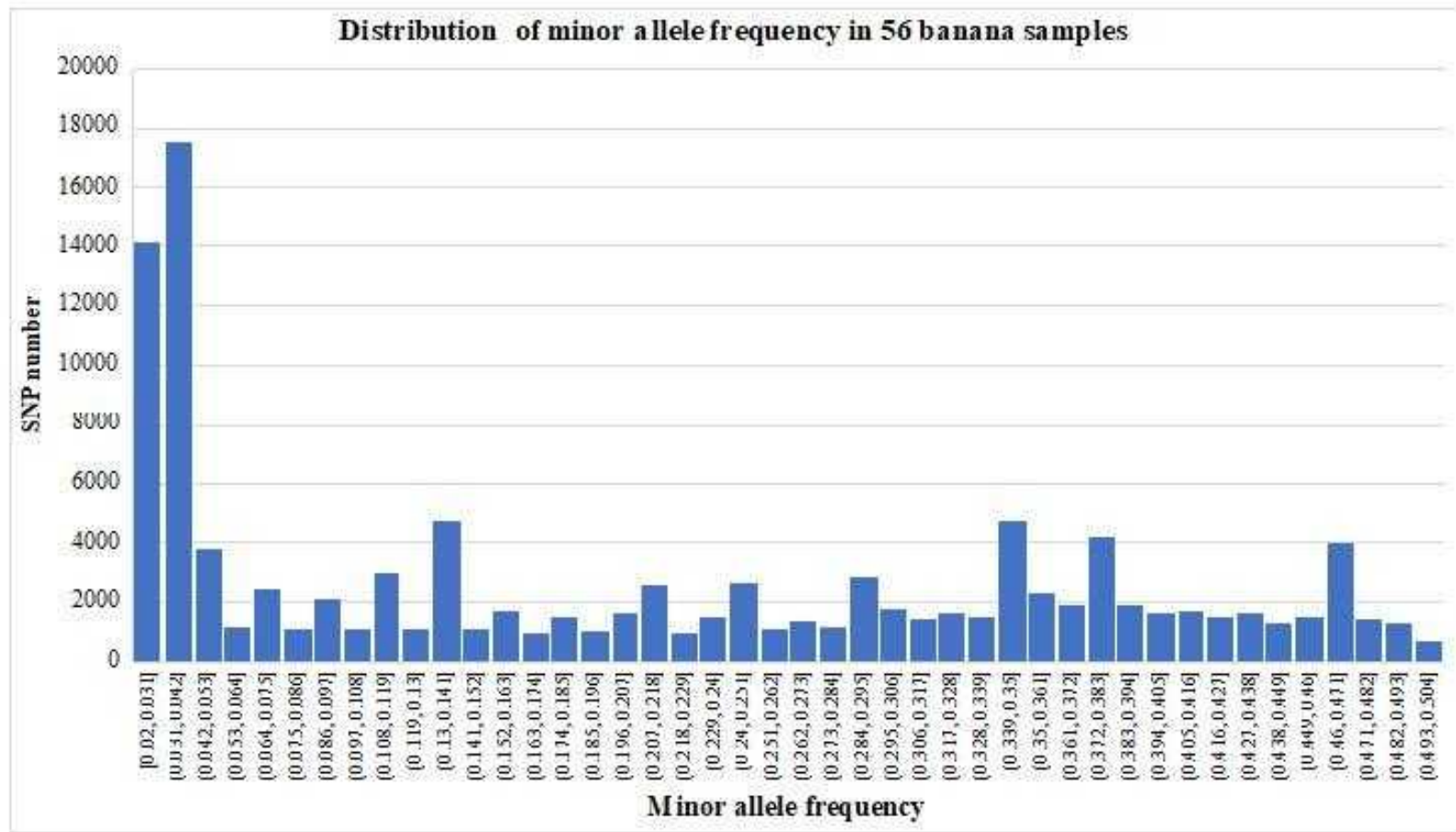


Figure 4.2.1: Distribution of minor allele frequency based on SNP summary of 56 banana samples

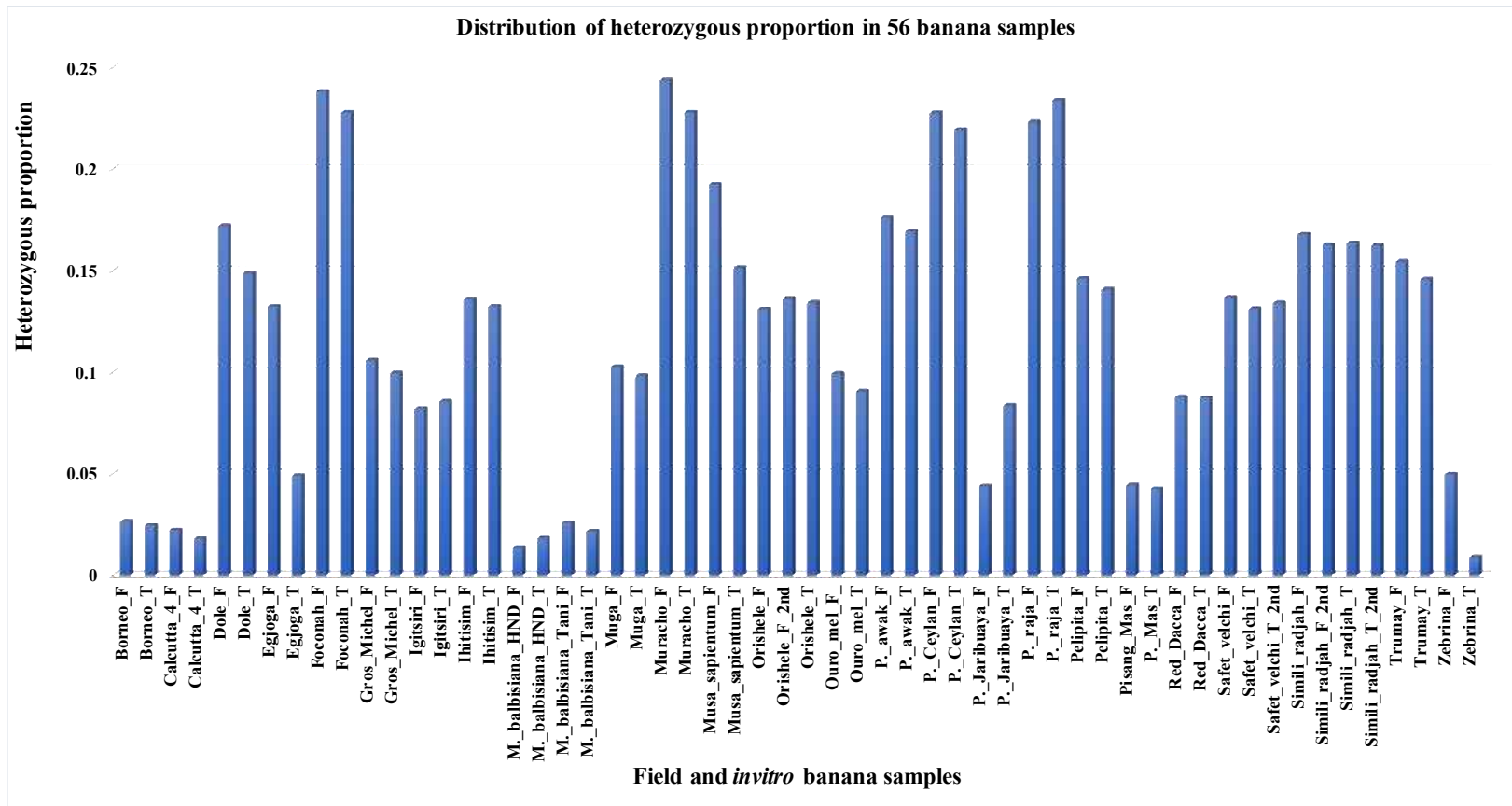


Figure 4.2.2: Distribution of heterozygosity proportion in 56 banana samples

***F:** Field samples, **T:** *in vitro* PTC samples

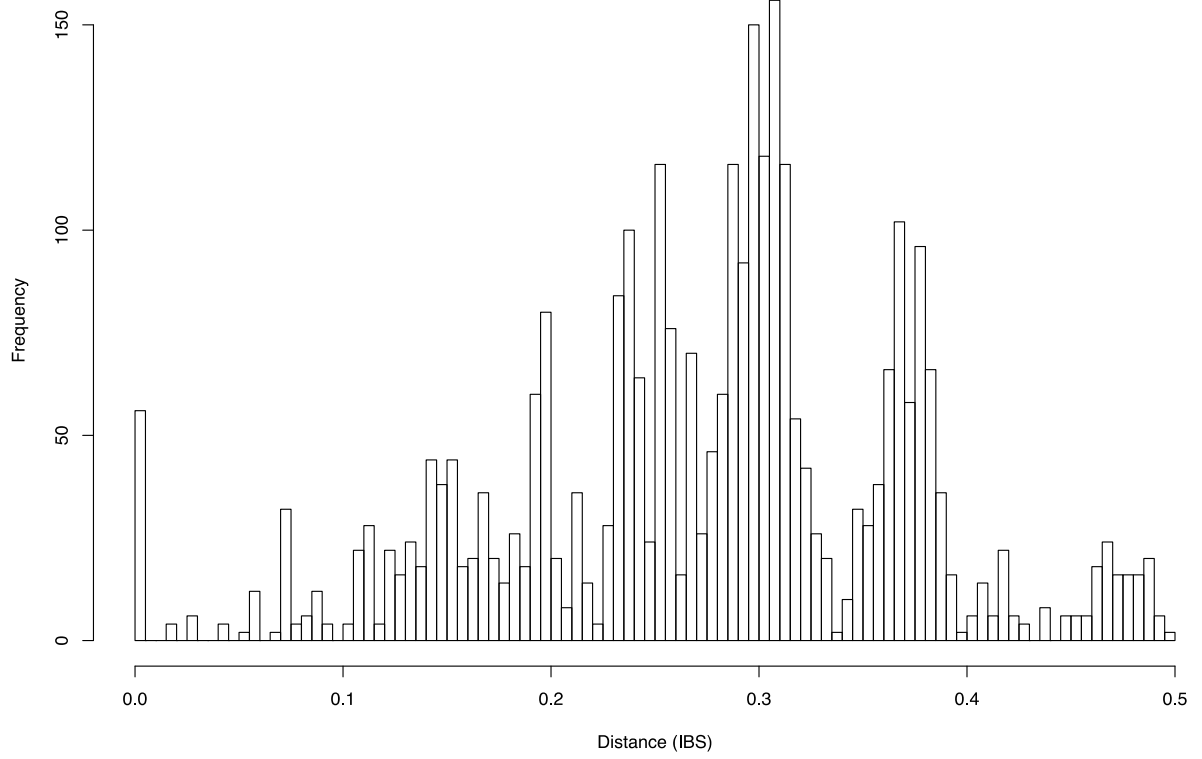


Figure 4.2.3: Frequency distribution of identity-by-state (IBS) pairwise genetic distance matrix of the 56 banana samples

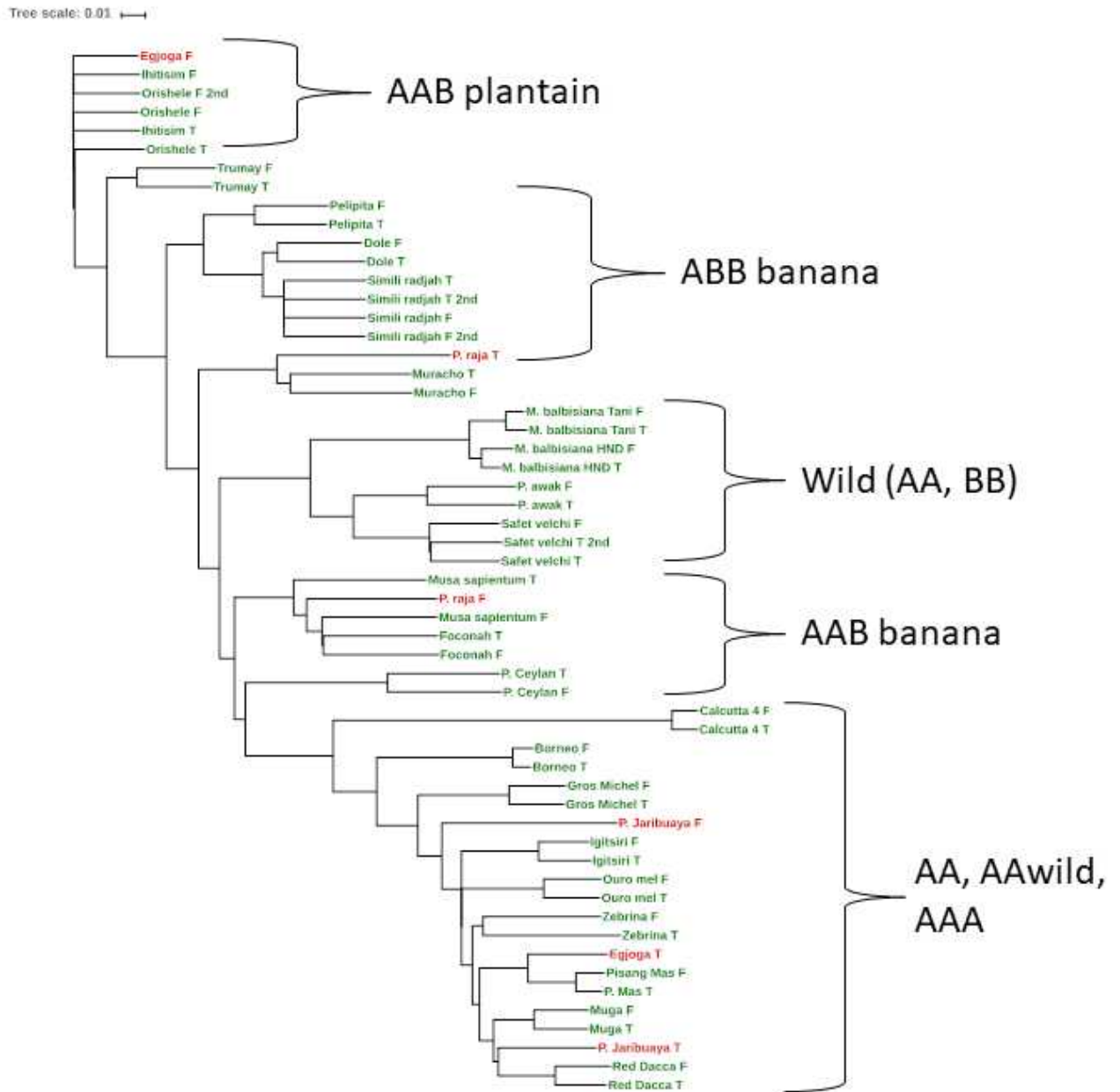


Figure 4.2.4: Neighbour joining tree of field and micropropagated *Musa* spp. accessions using 114k SNP markers.

The field accessions with F and *in vitro*-grown accessions with T are clustered together in many of the accessions apart from the accessions in red. The *Musa* spp. accessions were clustered in 5 major groups (AAB-plantain, ABB, AAB-banana, AAwild and BBwild, and AA, AAA and AAwild) based on their relatedness.

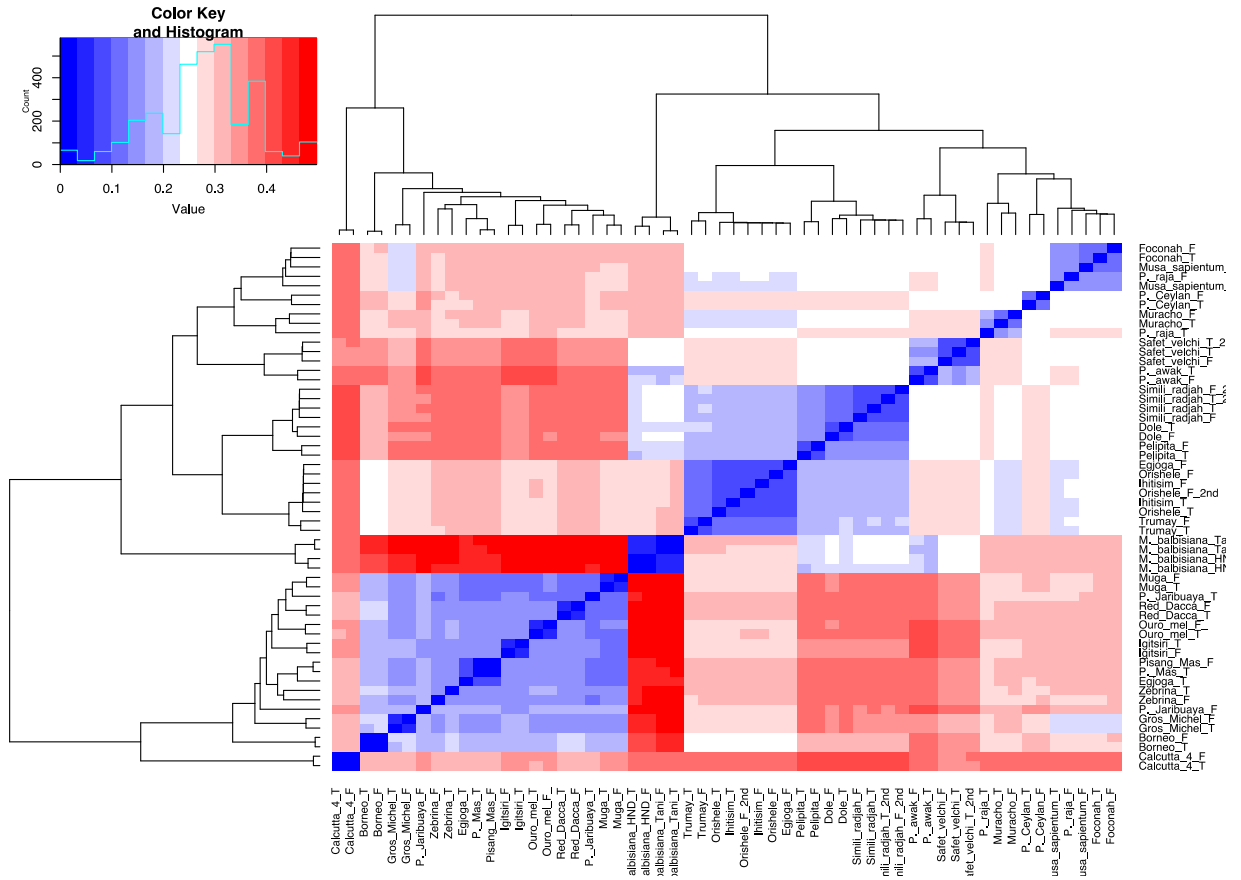


Figure 4.2.5: Heatmap distribution of IBS pairwise genetic distance matrix of the 56 banana samples.

Blocks with the same colour show they are very closely related. The degree of the colouration as shown in the colour key shows the degree of relatedness

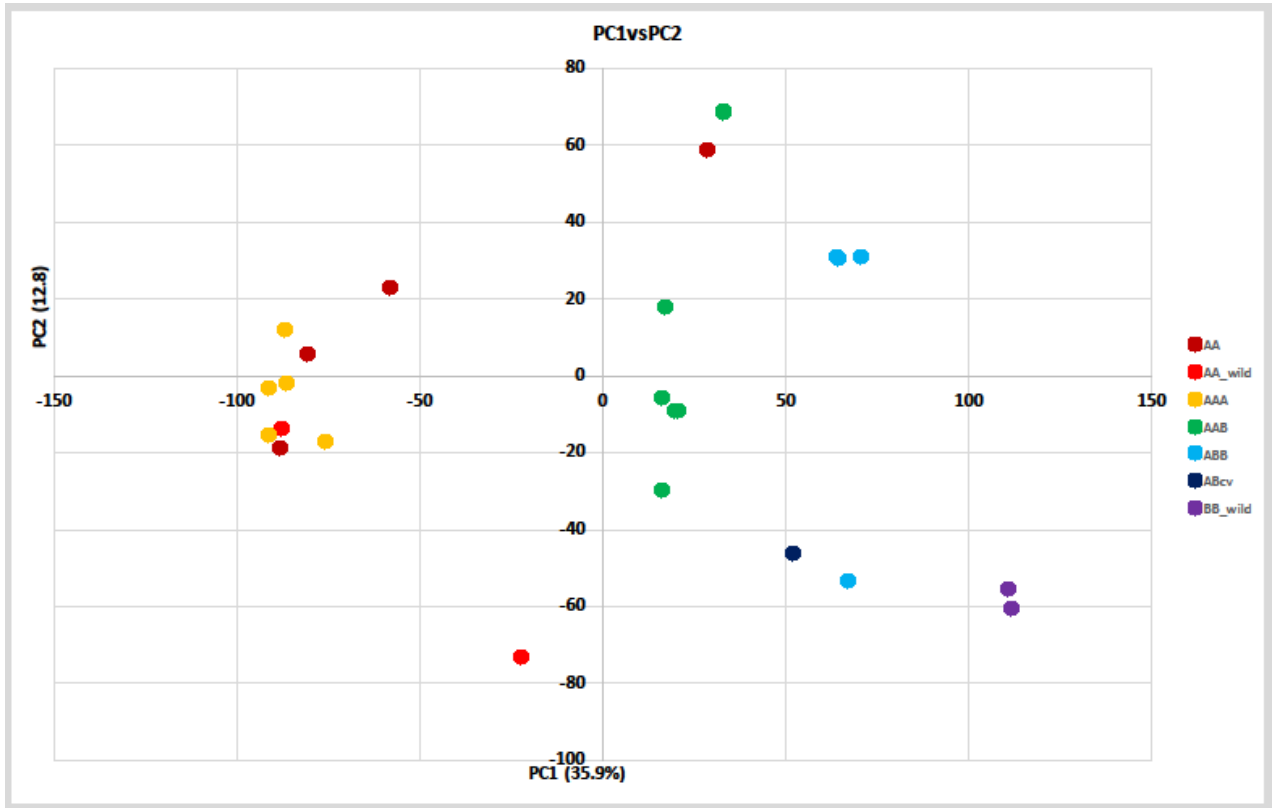


Figure 4.2.6: Principal Component Analysis of PC1 vs PC2

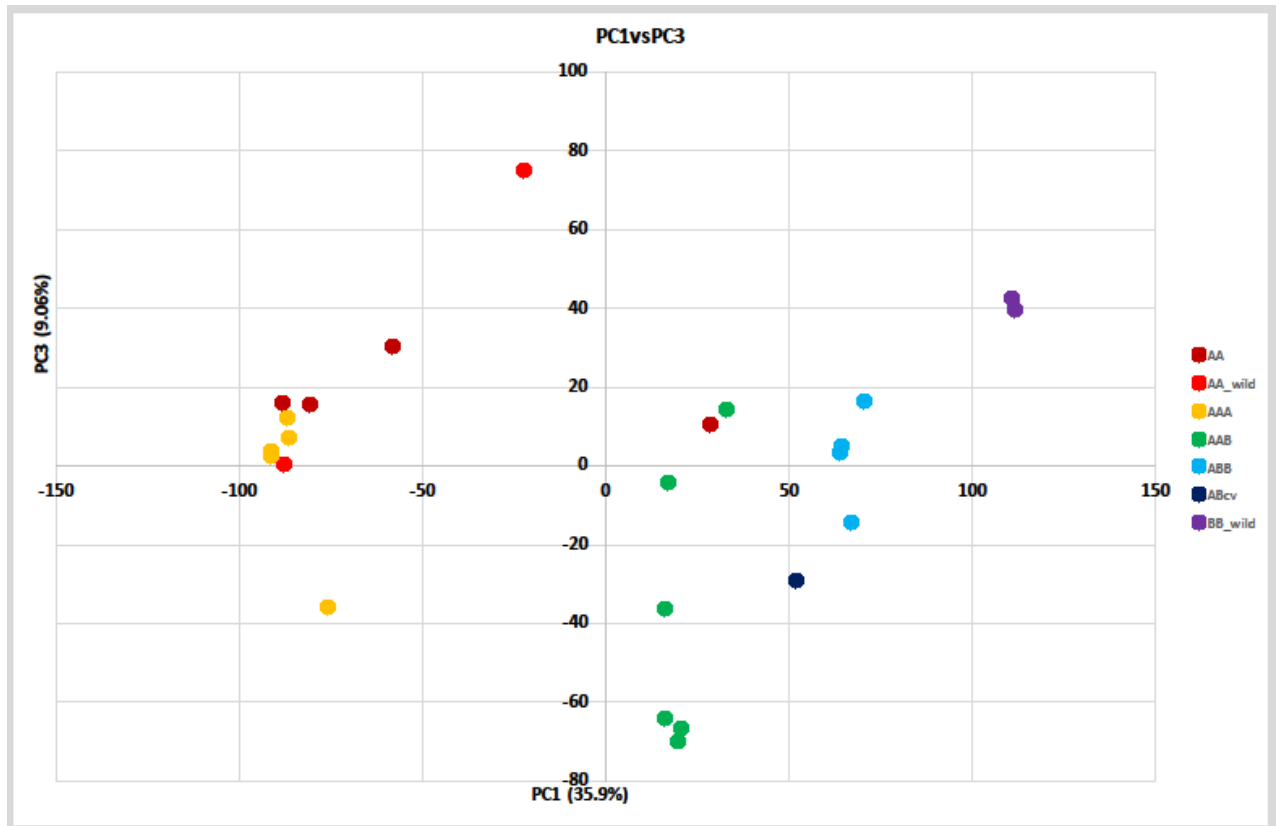


Figure 4.2.7: Principal Component Analysis of PC1 vs PC3

4.3 Crude Extraction Yield

The extraction of field and *in vitro* *Musa* accessions using methanol gave good extraction yield as seen in Table 4.3.1. However, *in vitro*-grown samples gave higher yield than the field materials.

4.4 UV Spectrophotometric Biological Activities of Field and Micropropagated *Musa* spp.

4.4.1 DPPH antioxidant activity

The antioxidant activity of the extracts expressed as IC₅₀ values ranged from 28.15 ± 1.26 to 257.92 ± 2.25 µg/mL for the field accessions, while those of the *in vitro* accessions ranged from 10.68 ± 0.27 to 154.42 ± 6.44 µg/mL (Table 4.4.1.1.). Across all the samples tested, the *in vitro*-grown accessions had lower IC₅₀ values meaning higher antioxidant activity. Accession Simili radjah showed the highest activity among the field and *in vitro*-grown accessions (Table 4.4.1.1). The field and *in vitro*-grown *M. balbisiana* Tani and *M. balbisiana* HND had low DPPH• antioxidant activity.

4.4.2 Ferric reducing antioxidant power (FRAP)

The Table 4.4.2.1 shows the FRAP activity of the *Musa* spp. samples. The micropropagated samples, also with this method, showed higher activity (higher FRAP values) than the field samples. The activity measured as trolox equivalent of the micropropagated samples ranged from 10.58 ± 0.52 to 152.16 ± 2.80 mgTE/g while those of the field samples ranged from 4.34 ± 0.12 to 23.78 ± 0.42 mgTE/g of extract. Accessions Zebrina and P. Jaribuaya had the highest FRAP activity followed by Simili radjah among the field accessions while Foconah had the highest activity followed by Simili radjah among the *in vitro*-grown accessions.

4.4.3 Total phenolic content (TPC) and total flavonoid content (TFC)

For the field samples, the TPC ranged from 3.86 ± 0.38 to 85.92 ± 1.38 mgGAE/g with Simili radjah having the highest TPC, while the TFC ranged from 3.63 ± 0.89 to 60.14 ± 6.30 mgQE/g, with Gros Michel having the highest TFC followed by Simili radjah.

Among the *in vitro*-grown accessions, Simili radjah (124.52 ± 12.72 mgGAE/g) also had the highest TPC followed by Foconah (87.5 ± 4.25 mgGAE/g) while Foconah (14.62 ± 1.35 QE/g) had the highest TFC followed by Simili radjah (11.25 ± 0.72 QE/g). *M. balbisiana* Tani, *M. balbisiana* HND, Dole and Safet velchi had comparatively low TPC and TFC. It is worthy of note that the field accessions had higher TFC than the *in vitro*-grown accessions.

4.4.4 Correlation among the antioxidant assays

The correlation among the antioxidant assays as determined by Pearson's coefficient, *r* is shown in Table 4.4.4.1. The result revealed a good and acceptable correlation between the DPPH• and FRAP assays among both the field (*r* = 0.61) and *in vitro*-grown (*r* = 0.66) accessions. For the *in vitro*-grown samples, there was a strong correlation between TPC and DPPH• (*r* = 0.74); and TPC and FRAP (*r* = 0.80) but the correlation between TFC and DPPH• (*r* = 0.43) is relatively weak.

4.4.5 Acetylcholinesterase (AChE) inhibitory activity

The result of the AChE inhibition of the field and micropropagated samples as represented by their IC₅₀ values is reported in Table 4.4.5.1. Figure 4.4.5.1 gives the percentage inhibition of the accessions at 1 mg/mL. Most of the *in vitro*-grown accessions gave better AChE inhibitory activity than the field accessions. One of the *in vitro*-grown accessions Calcutta-4, (IC₅₀: 11.53 ± 6.12) gave a better activity than even the standard, eserine (IC₅₀: 31.23 ± 7.33 µg/mL).

Table 4.3.1: Extraction yield of field and micropropagated accessions

S/N	Accessions	Extraction yield (w/w)	
		Field (%)	Tissue culture (%)
1	P. Mas	13.42	35.63
2	Simili Radjah	15.84	38.16
3	Red Dacca	6.94	52.99
4	Pelipita	10.82	49.67
5	Safet Velchi	14.95	63.56
6	Igitsiri	13.90	58.00
7	Zebrina	12.62	48.57
8	Dole	13.83	47.30
9	Foconah	12.41	21.00
10	Gros Michel	11.38	70.00
11	P. Ceylan	8.46	67.44
12	P. Jaribuaya	13.38	38.66
13	Calcutta-4	10.10	16.54
14	M. balbi HND	13.32	64.00
15	M. balbi Tani	12.67	45.71

Table 4.4.1.1: DPPH• antioxidant activity as shown by the IC₅₀ Values (µg/mL)

S/N	Accessions	Genome group	Field IC ₅₀ (µg/mL)	TC IC ₅₀ (µg/mL)
1	P. Mas	AA	95.41 ± 0.65 ^{ef}	25.42±2.14 ^d
2	Simili. Radjah	ABB	28.15 ± 1.26^a	10.68±0.27^a
3	Red Dacca	AAA	56.29 ± 1.83^b	25.07±1.21 ^d
4	Pelipita	ABB	53.90 ± 0.49^b	46.92±0.12 ^f
5	Safet Velchi	AABcv	78.81 ± 0.31 ^d	22.75±0.57^{cd}
6	Igitsiri	AAA	65.51 ± 0.96 ^c	34.08±1.02 ^f
7	Zebrina	AAwild	52.83 ± 0.13^b	17.93±0.53^{bc}
8	Dole	ABB	100.03 ± 2.22 ^{ef}	68.21±1.56^g
9	Foconah	AAB	56.18 ± 0.69^b	12.24±0.81^{ab}
10	Gros Michel	AAA	101.39 ± 0.80 ^f	49.00±0.78 ^f
11	P. Ceylan	AAB	257.92 ± 2.25ⁱ	22.81±0.48 ^{cd}
12	P. Jaribuaya	AA	92.19 ± 2.47 ^e	23.65±0.21 ^{cd}
13	Calcutta-4	AAwild	148.41 ± 2.47 ^g	20.22±0.21^{cd}
14	M. balbi HND	BBwild	190.09 ± 11.19^h	116.44±1.37^h
15	M. balbi Tani	BBwild	148.89 ± 5.53^g	154.42±6.44ⁱ

Values are expressed as mean ± SEM (n = 3). Means with the same letter along the same column are not significantly different at (P < 0.05). IC₅₀ of the standards; gallic acid = 1.72 ± 0.01 µg/mL, quercetin = 2.72 ± 0.04 µg/mL, ascorbic acid = 3.68 ± 0.09 µg/mL

Table 4.4.2.1: Ferric Reducing Antioxidant Power (FRAP) of field (F) and tissue culture (TC) samples

S/N	Accessions	Genome group	Field FRAP (mgTE/g)	TC FRAP (mgTE/g)
1	P. Mas	AA	9.79 ± 1.53 ^e	53.28 ± 0.28 ^g
2	Simili Radjah	ABB	18.75 ± 0.44 ^b	140.28 ± 2.31 ^b
3	Red Dacca	AAA	11.82 ± 0.93 ^e	102.39 ± 3.03 ^c
4	Pelipita	ABB	16.85 ± 0.50 ^c	27.65 ± 1.73 ⁱ
5	Safet Velchi	AABcv	11.31 ± 0.16 ^e	63.94 ± 0.92 ^f
6	Igitsiri	AAA	16.21 ± 2.24 ^c	78.11 ± 2.41 ^e
7	Zebrina	AAwild	22.39 ± 2.00 ^a	52.26 ± 2.95 ^g
8	Dole	ABB	8.41 ± 1.20 ^e	22.85 ± 2.60 ⁱ
9	Foconah	AAB	14.55 ± 0.56 ^d	152.16 ± 2.80 ^a
10	Gros Michel	AAA	8.64 ± 0.17 ^e	88.96 ± 0.17 ^d
11	P. Ceylan	AAB	5.73 ± 0.20 ^f	66.48 ± 0.93 ^f
12	P. Jaribuaya	AA	23.78 ± 0.42 ^a	54.48 ± 2.20 ^g
13	Calcutta-4	AAwild	4.34 ± 0.12 ^f	100.73 ± 3.45 ^c
14	M. balbi HND	BBwild	4.44 ± 0.65 ^f	32.41 ± 0.40 ^h
15	M. balbi Tani	BBwild	16.11 ± 0.48 ^c	10.58 ± 0.52 ^j

Values are expressed as mean ± SEM (n = 3). Means with the same letter along the same column are not significantly different at (P < 0.05)

Table 4.4.3.1: Total phenolic content (TPC) and flavonoid (TFC) content of field and *in vitro*-grown *Musa* spp. accessions

S/N	Accessions	Genome group	TPC (mgGAE/g)		TFC (mgQE/g)	
			Field-grown	<i>In vitro</i> -grown	Field-grown	<i>In vitro</i> -grown
1	P. Mas	AA	18.11 ± 2.67 ^e	72.06 ± 0.09^c	9.56 ± 3.07 ^f	3.40 ± 0.04 ^f
2	Simili Radjah	ABB	85.92 ± 1.38^a	124.52 ± 12.72^a	30.34 ± 2.73^b	11.25 ± 0.72^b
3	Red Dacca	AAA	19.69 ± 3.05 ^e	38.46 ± 3.48 ^e	23.97 ± 1.73 ^c	3.80 ± 0.19 ^e
4	Pelipita	ABB	14.43 ± 1.54 ^{ef}	21.71 ± 4.06 ^f	24.06 ± 1.81 ^c	2.46 ± 0.11 ^g
5	Safet Velchi	AABcv	33.55 ± 0.76 ^c	55.83 ± 3.71 ^d	3.63 ± 0.89^h	0.47 ± 0.25^g
6	Igitsiri	AAA	16.27 ± 0.84 ^e	42.98 ± 0.92 ^{cd}	9.43 ± 0.52 ^f	1.27 ± 0.07 ^g
7	Zebrina	AAwild	33.82 ± 0.09 ^c	56.27 ± 3.31^d	11.59 ± 0.28 ^e	1.64 ± 0.15 ^g
8	Dole	ABB	7.59 ± 1.50^g	9.78 ± 0.21^{fg}	4.28 ± 0.17 ^g	0.59 ± 0.20^g
9	Foconah	AAB	34.61 ± 1.78^c	87.5 ± 4.25^b	11.38 ± 0.45 ^e	14.62 ± 1.35^a
10	Gros Michel	AAA	48.38 ± 1.38^b	56.45 ± 0.66^d	60.14 ± 6.30^a	0.40 ± 0.06^g
11	P. Ceylan	AAB	27.15 ± 2.51 ^d	76.27 ± 0.31^{bc}	28.69 ± 1.97 ^c	8.56 ± 0.23^c
12	P. Jaribuaya	AA	29.17 ± 0.35 ^{cd}	66.88 ± 0.70^{cd}	11.12 ± 0.58 ^e	2.37 ± 0.56 ^g
13	Calcutta-4	AAwild	32.85 ± 0.49 ^c	75.57 ± 2.37^c	4.19 ± 0.23^g	5.53 ± 0.72 ^d
14	M. balbi HND	BBwild	16.27 ± 1.14 ^e	19.6 ± 1.97^f	18.78 ± 2.58 ^d	1.07 ± 0.26 ^g
15	M. balbi Tani	BBwild	3.86 ± 0.38^h	2.43 ± 0.30^g	30.77 ± 2.83^b	1.12 ± 0.60 ^g

Values are expressed as mean ± SEM (n = 3). Means with the same letter along the same column are not significantly different at (P < 0.05)

Table 4.4.4.1: Spearman's correlation coefficients (r) among the antioxidant assays of field (F) and *in vitro*-grown (IV) samples

	TPC_F	TFC_F	FRAP_F	DPPH•_F
TPC_F	1	0.308169	0.202885	0.600541
TFC_F	0.308169	1	-0.02086	0.027436
FRAP_F	0.202885	-0.02086	1	0.610915
DPPH•_F	0.600541	0.027436	0.610915	1

	TPC_IV	TFC_IV	FRAP_IV	DPPH•_IV
TPC_IV	1	0.729728	0.797737	0.735467
TFC_IV	0.729728	1	0.768994	0.432449
FRAP_IV	0.797737	0.768994	1	0.660483
DPPH•_IV	0.735467	0.432449	0.660483	1

Table 4.4.5.1: Acetylcholinesterase inhibitory activity of field (F) and tissue culture (TC) samples

S/N	Accessions	Genome group	Field IC ₅₀ (μg/mL)	TC IC ₅₀ (μg/mL)
1	P. Mas	AA	219.10 ± 13.81^a	137.20 ± 23.82^b
2	Simili Radjah	ABB	610.60 ± 127.10 ^c	541.30 ± 81.07 ^d
3	Red Dacca	AAA	376.30 ± 40.16 ^c	282.30 ± 59.78 ^c
4	Pelipita	ABB	282.70 ± 19.39^b	429.00 ± 53.99 ^d
5	Safet Velchi	AABcv	687.00 ± 26.12 ^c	1050.00 ± 274.10^e
6	Igitsiri	AAA	430.80 ± 45.63 ^c	791.30 ± 36.14^e
7	Zebrina	AAwild	419.00 ± 15.06 ^c	633.50 ± 71.83 ^d
8	Dole	ABB	2170.00 ± 372.90^g	771.50 ± 16.43 ^e
9	Foconah	AAB	514.30 ± 90.33 ^c	289.40 ± 9.81 ^c
10	Gros Michel	AAA	1637.00 ± 253.10^g	434.60 ± 37.49 ^d
11	P. Ceylan	AAB	555.70 ± 17.79 ^c	420.90 ± 37.22 ^d
12	P. Jaribuaya	AA	981.80 ± 62.59 ^d	494.00 ± 46.15 ^d
13	Calcutta-4	AAwild	1124.00 ± 31.30 ^e	11.53 ± 0.12^a
14	M. balbi HND	BBwild	1280.00 ± 91.88^f	1181.00 ± 91.25^e
15	M. balbi Tani	BBwild	752.30 ± 45.31 ^c	780.40 ± 21.45 ^e

Values are expressed as mean ± SEM (n = 3). Means with the same letter along the same column are not significantly different at (P < 0.05). IC₅₀ of the standard, eserine is 31.23 ± 7.33 μg/mL

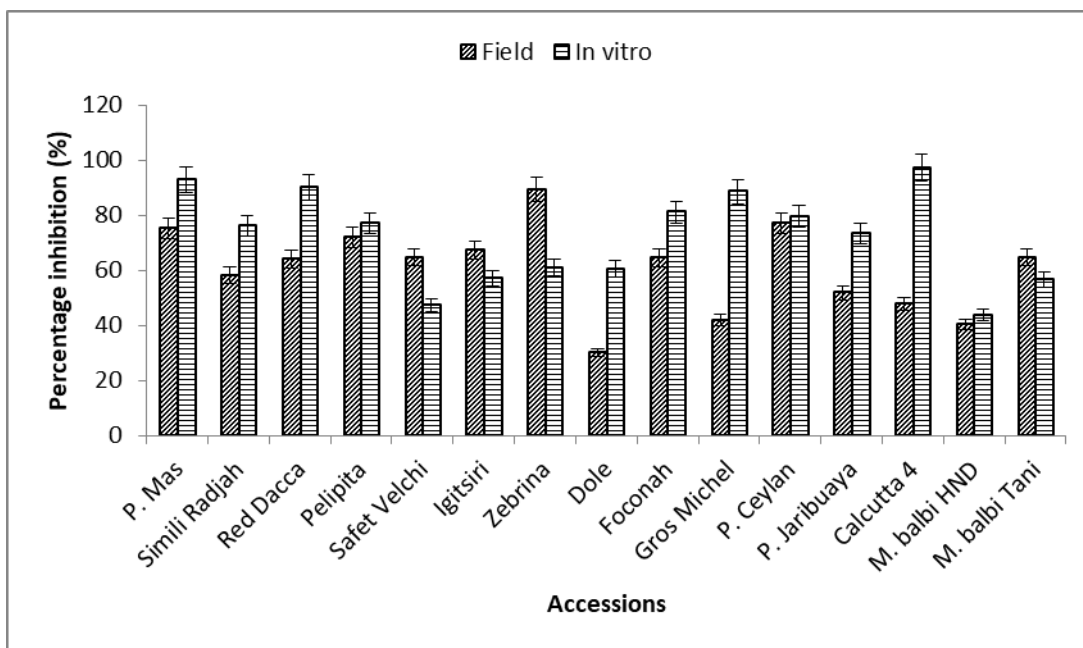


Figure 4.4.5.1: AChE percentage inhibition of field and *in vitro*-grown accessions at 1 mg/mL

4.5 Characterisation of Metabolites and Bioprofiling Using HPTLC Methods

4.5.1 Mobile phase development

Polar solvent systems were tried and modified due to prior information noted from the cuvette assay about the high phenolic content of the *Musa* spp. accessions. The different mobile phases used are reported in Table 4.5.1.1 and images in Figure 4.5.1.1. A very polar mobile phase comprising ethyl acetate: toluene: formic acid: water (3.4: 0.5: 0.7: 0.5) gave the best separation and was used. Another solvent system (toluene: ethyl acetate: methanol 6: 3: 1), a medium polar mobile phase, was later developed based on the effect directed analysis to capture other bioactive compounds which might be lost in the very polar mobile phase.

4.5.2 HPTLC derivatisation

Derivatisation in natural products (Neu's) reagents revealed the pattern of phenolics and flavonoids in the *Musa* spp. Phenolic compounds were found to be abundant from *in vitro*-grown samples (Fig. 4.5.2.1C). The pattern obtained with ninhydrin and DPA is seen in Figures 4.5.2.1D and 4.5.2.1E, respectively. Amino groups were not obvious when derivatised with ninhydrin using the reagent sequence method, while sugars were found in all the samples when derivatised with diphenylamine (DPA). Derivatisation in DPPH•, revealed the presence of antioxidant compounds in *Musa* spp. The pattern seen as white bands on a purple background is shown in (Fig. 4.5.2.1F).

4.5.3 Effect directed analysis with (EDA) HPTLC

The HPTLC-EDA was used to detect and clearly observe the constituents responsible for each biological activity. In this study, HPTLC was hyphenated with cholinesterase, glucosidase, Gram-negative (*A. fischeri*) and Gram-positive (*B. subtilis*) bacteria and genotoxicity assays. These profiles are presented in Figures 4.5.3.1-4.5.3.3. The results show for the first time the biological profiles of *Musa* spp. accessions using HPTLC hyphenated with bioassays (EDA). This work also compared the biological profiles of plants grown in different environments (field, *in vitro* and green house).

4.5.3.1 Detection of cholinesterase inhibitors

Compounds that can inhibit cholinesterase enzymes were found in the *Musa* spp. accessions tested (Fig. 4.5.3.1 A&B and 4.5.3.2 A&B). The AChE and BChE inhibitors appear as white bands on a purple background. With the polar and acidic mobile phase (Ethyl acetate: Toluene: Formic acid: Water; 3.4: 0.5: 0.7: 0.5), three major compounds (Fig. 4.5.3.4) with hR_F (retention factor * 100) 15, 44 and 83 were identified as AChE and BChE inhibitors and were observed from *in vitro*-grown accessions. With the medium polar mobile phase (Toluene: ethylacetate: methanol 6:3:1), one major compound (Fig. 4.5.3.5) with hR_F 63 was identified to inhibit AChE and BChE in almost all tested samples with increased band intensity in the acclimatised accessions. Some samples (I to O) contain no compound with BChE activity when the polar mobile phase was used.

4.5.3.2 Identification of glucosidase and amylase inhibitors

HPTLC combined with glucosidase assay revealed compounds with α -glucosidase and β -glucosidase inhibitory activity in the tested *Musa* spp. accessions. Two major compounds (hR_F 15 and 44) were identified from *in vitro*-grown accessions when the polar and acidic mobile phase (Ethyl acetate: Toluene: Formic acid: Water; 3.4: 0.5: 0.7: 0.5) was used. They appeared as white bands on purple background (Fig. 4.5.3.1C and D). Some of the accessions: Pelipita (J), *M. balbisiana* Tani (K), Dole (L), *M. balbisiana* HND (N) and Igitsiri (O) did not show any inhibition zones in both α - and β -glucosidase assays. For α -amylase, when the polar and acidic mobile phase was used, a clear inhibition zone was detected at the solvent front for sample E3 (Zebrina, Appendix Fig. 11D), whereas for other samples, the white shimmering at the solvent front was weaker. In order to reduce the elution power, the medium polar mobile phase was tested. This revealed two zones of α -amylase inhibition, at hR_F 40 and 63, which were in all samples more or less intense (Fig. 4.5.3.2C).

4.5.3.3 Detection of antimicrobials in *Musa* spp.

The effect-directed analysis of *B. subtilis* assay revealed one main inhibition zone (hR_F 74) with a very intense band in almost all the samples (Fig. 4.5.3.2D). Samples from the acclimatised *Musa* spp. plants gave more intense bands. *M. balbisiana* Tani, Dole, *M. balbisiana* HND and Igitsiri are the accessions with weak or no zones of inhibition. For

Aliivibrio fischeri bioassay, antimicrobials are detected based on their impact on the luminescence of *A. fischeri* bacteria. Antimicrobials appeared as dark (inhibiting) or bright (enhancing) zones on an instantly luminescent plate background. Many dark zones of inhibition were seen in the different *Musa* spp. accessions (Fig. 4.5.3.2E).

4.5.3.4 Absence of toxins as determined by the mutagenotoxicity assay

The results showed that the plant samples contained no toxic agents as seen in Figure 4.5.3.3. The positive control, 4-nitroquinoline-1-oxide, which is a toxic chemical appeared as blue fluorescence at 366 nm after the bioassay, while the samples even at higher concentration gave no such fluorescence using both the polar and medium polar assays (Fig 4.5.3.3A and 4.5.3.3B).

4.5.4 Characterisation of active zones via HPTLC-High resolution mass spectrometry (HRMS)

The multipotent active zones were characterised by HRMS after online elution via an elution head-based interface. Calcutta-4 extracts, F₁ (field), F₂ (*in vitro*), and F₃ (acclimatised) were considered as the representative samples based on the EDA assays results. The MS spectra of the four compounds showing their base peak and assignment are seen in Figures 4.5.4.1 and 4.5.4.2. Additionally, the mass error and the intensity are presented in Table 4.5.4.1.

Table 4.5.1.1: List of mobile phases investigated for separation of the leaf sample no. 2 of *Musa acuminata* (Foconah)

No.	Mobile phase	Ratio
1	Ethanol: toluene: water	40: 5: 5
2	Ethyl acetate: methanol: acetic acid: water	32.5: 15: 0.25: 2.5
3	Ethyl acetate: methanol: toluene: acetic acid: water	17.5: 25: 5: 0.25: 2.5
4	Ethanol: water	40: 10
5	Ethyl acetate: toluene: formic acid: water	32: 8: 6: 4
6	Ethyl acetate: toluene: formic acid: water	34: 5: 7: 5

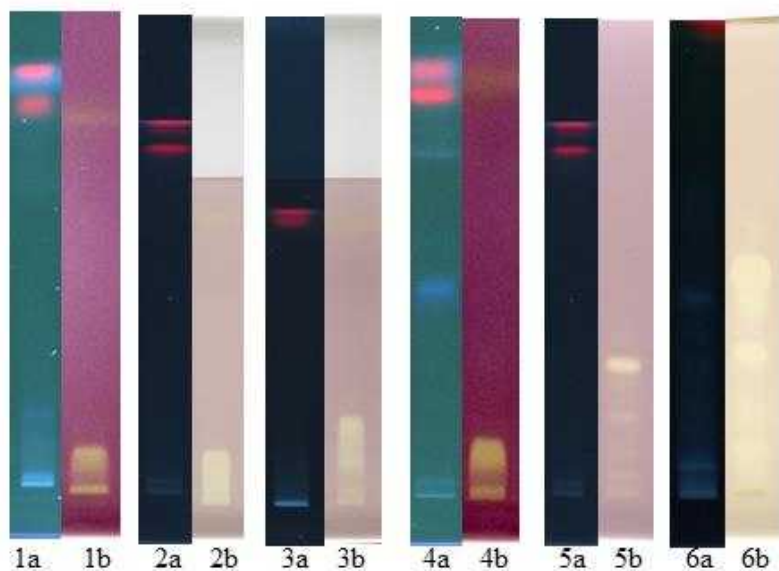


Figure 4.5.1.1: Mobile phase development for leaf sample no. 2 of *Musa acuminata* (Foconah): Chromatograms under (a) 366 nm (b) derivatised in DPPH[•] under white light illumination were developed with (1) ethanol: toluene: water 40: 5: 5 (2) ethyl acetate: methanol: acetic acid: water 32.5: 15: 0.25: 2.5 (3) ethyl acetate: methanol: toluene: acetic acid: water 17.5: 25: 5: 0.25: 2.5 (4) ethanol: water 40:10 (5) ethyl acetate: toluene: formic acid: water 32: 8: 6: 4 and (6) ethyl acetate: toluene: formic acid: water 34:5:7:5.

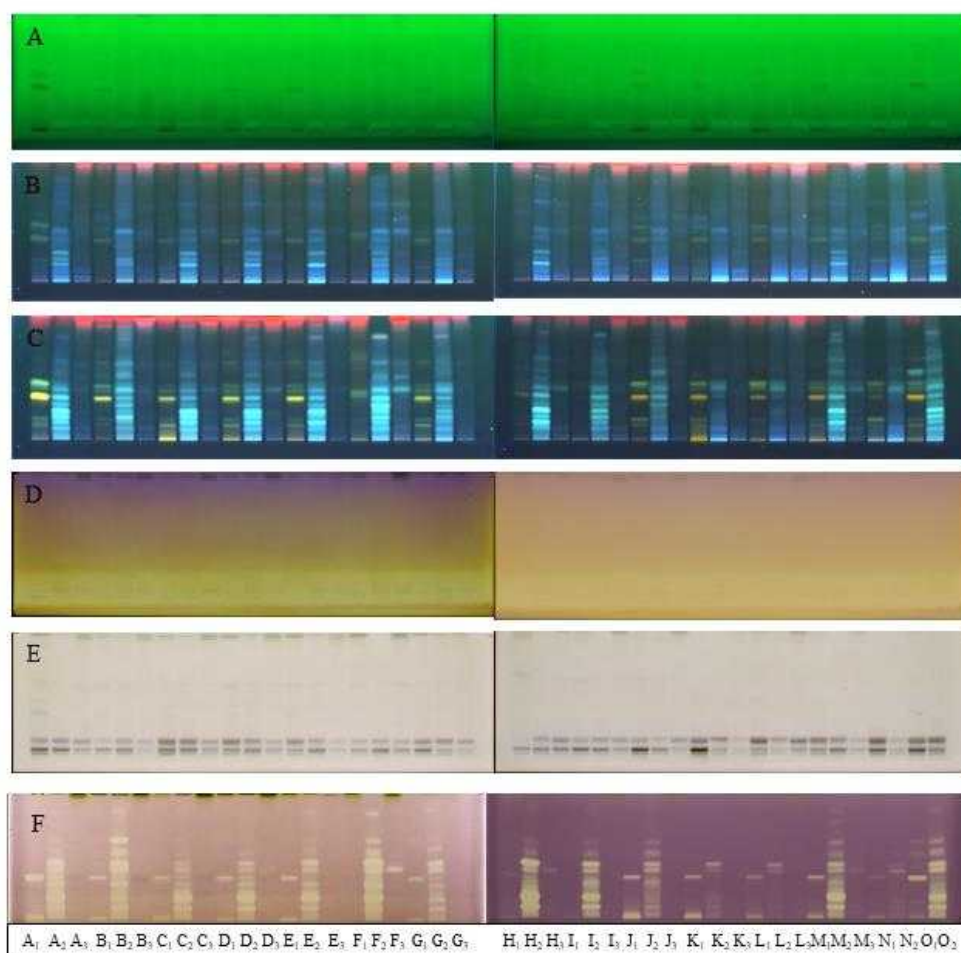


Figure 4.5.2.1: HPTLC fingerprints of field, *in vitro*-grown and acclimatised *Musa* spp. accessions (10 μ L/band) on HPTLC plates developed in ethyl acetate: toluene: formic acid: water (3.4: 0.5: 0.7: 0.5) and documented (A) at 254 nm, (B) at 366 nm, (C) after derivatisation using reagent sequence starting with natural product (neu's) reagent and visualised at 366 nm, followed by (D) ninhydrin and lastly (E) diphenylamine and (F) after derivatisation in DPPH \bullet . The identity of each track is as described in Table 3.1.

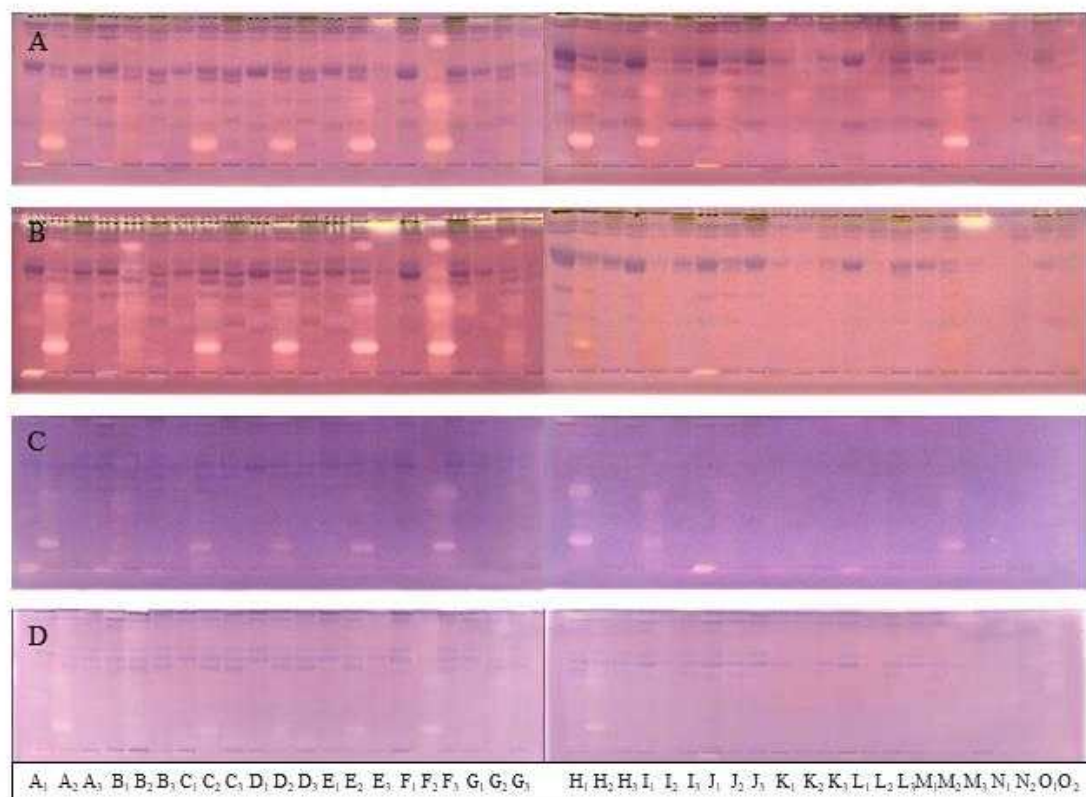


Figure 4.5.3.1: HPTLC-EDA fingerprints of field, *in vitro*-grown and acclimatised *Musa* spp. accessions developed in ethyl acetate: toluene: formic acid: water (3.4: 0.5: 0.7: 0.5) and documented under white light after (A) AChE (B) BChE (C) α -glucosidase and (D) β -glucosidase assays. 25 μ L/band and 10 μ L/band was applied for cholinesterase and glucosidase assay, respectively. The identity of each track is as described in Table 3.1.

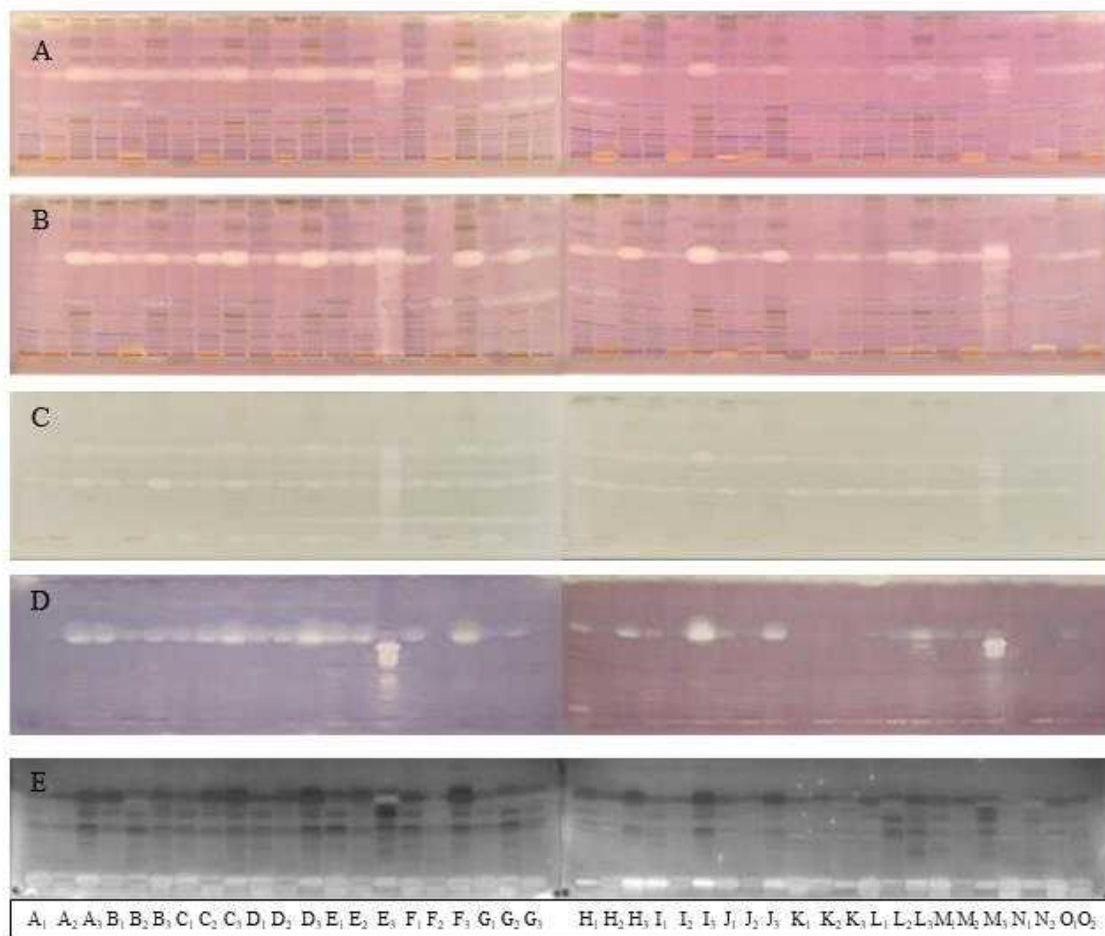


Figure 4.5.3.2: HPTLC-EDA fingerprints of field, *in vitro*-grown and acclimatised *Musa* spp. accessions developed in toluene: ethyl acetate: methanol (6: 3: 1) and documented under white light after (A) AChE (B) BChE (C) α -amylase (D) *B. subtilis* (E) *A. fischeri* assays. 10 μ L/band was applied for all the assays apart from cholinesterase where 15 μ L/band was applied. The identity of each track is as described in Table 3.1.

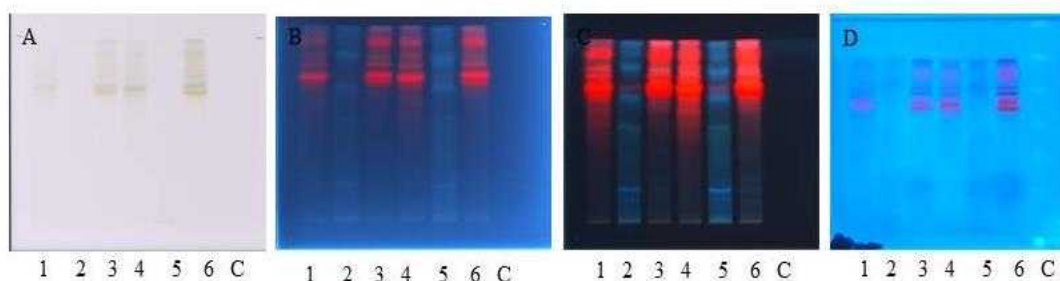


Figure 4.5.3.3A: HPTLC chromatogram of genotoxicity assay of selected samples on Rp 18 plates developed in the polar mobile phase (ethyl acetate: toluene: formic acid: water 3.4: 0.5: 0.7: 0.5) and documented (A) under white light, (B) at 254 nm, (C) at 366 nm and (D) after mutagenicity assay. 10 μL /band and 15 μL /band were applied for tracks 1-3 and tracks 4-6, respectively. Track C is the positive control with different volumes applied in the free mode.

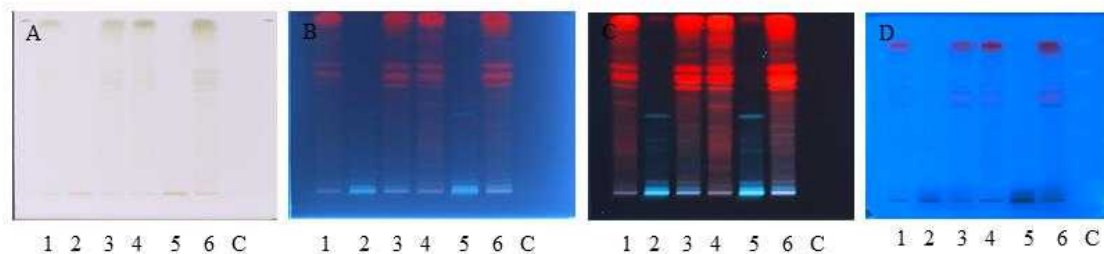


Figure 4.5.3.3B: HPTLC chromatogram of genotoxicity assay of selected samples on Rp 18 plates developed in the medium polar mobile phase (toluene: ethyl acetate: methanol 6: 3: 1) and documented (A) under white light, (B) at 254 nm, (C) at 366 nm and (D) after mutagenicity assay. 10 μL /band and 15 μL /band were applied for tracks 1-3 and tracks 4-6, respectively. Track C is the positive control with different volumes applied in the free mode

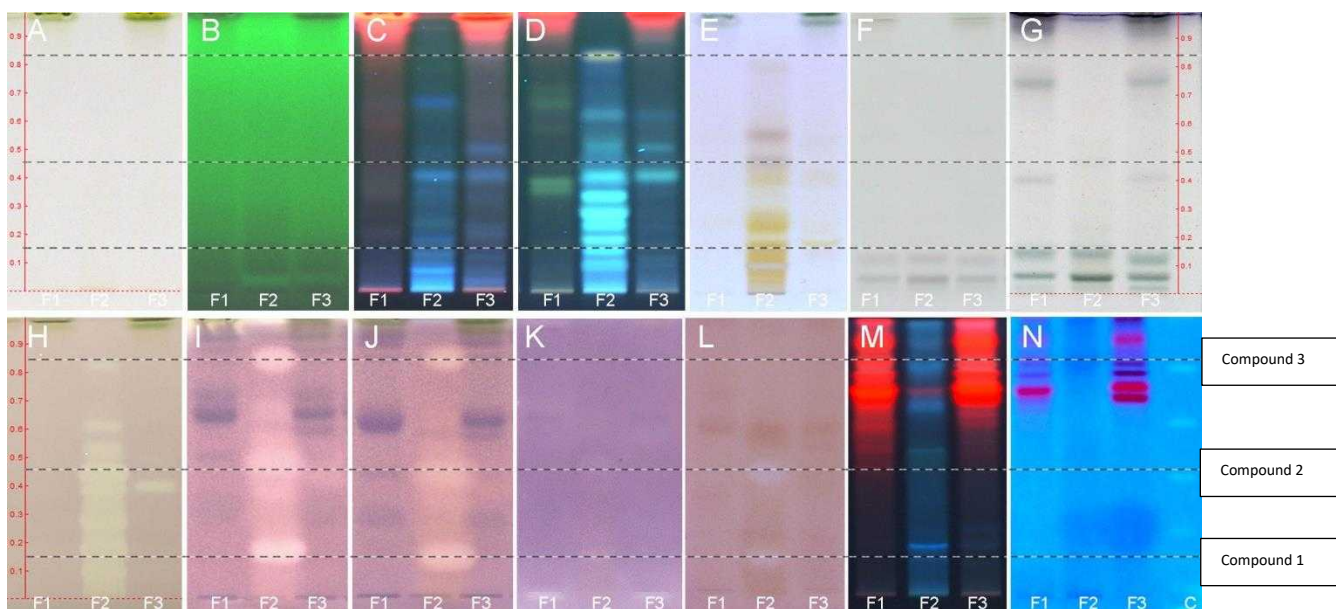


Figure 4.5.3.4 : HPTLC chromatograms (A–N) of multipotent bioactive compounds in the *Musa* spp. leaf (Calcutta-4; F1: field, F2: *in vitro*, F3: acclimatised) extract developed in EA: toluene: FA: H₂O; 3.4: 0.5: 0.7: 0.5 visualised (A) under white light (B) at UV 254 nm, (C) at UV 366 nm, (D) after derivatisation using reagent sequence starting with natural product (neu's) reagent and visualised at 366 nm, followed by (E) ninhydrin and lastly (F) diphenylamine, (G) after derivatisation in p-anisaldehyde, after (H) DPPH•, (I) AChE inhibition, (J) BChE inhibition, (K) α -glucosidase inhibition, (L) β -glucosidase inhibition, (M) 366 nm image of Rp 18 plate and (N) Genotoxicity assay. Application volume for all the bioassays is 10 μ L apart from the cholinesterase assay (25 μ L) and genotoxicity assay (15 μ L).

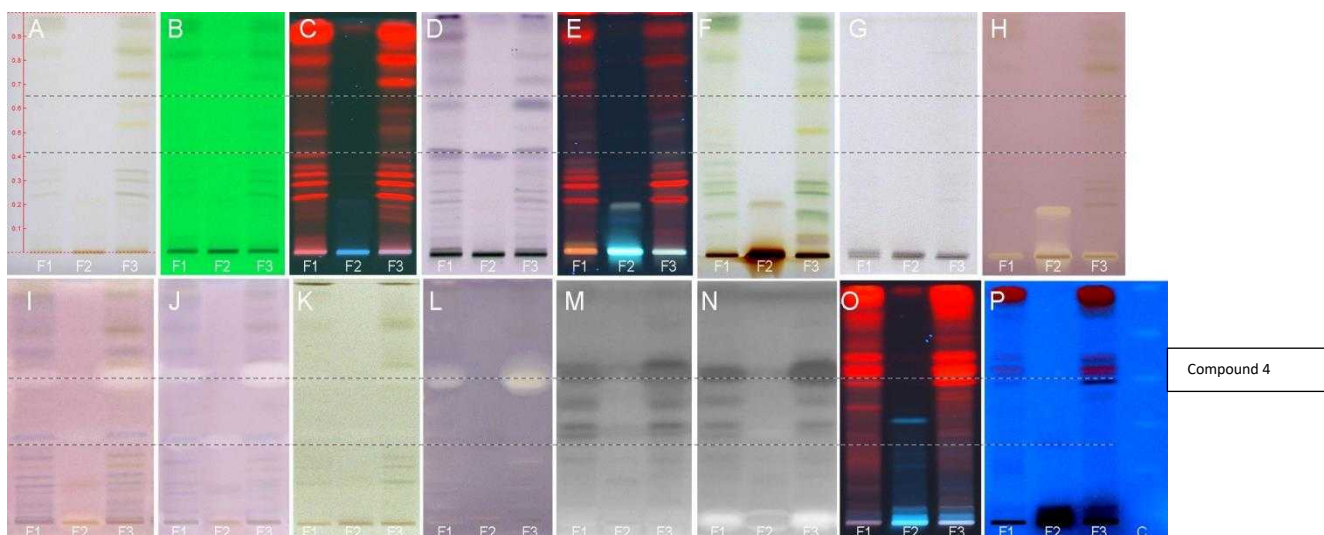


Figure 4.5.3.5: HPTLC autograms (A–P) of multipotent bioactive compounds in the *Musa* spp. leaf (Calcutta-4; F1: field, F2: *in vitro*, F3: acclimatised) extract developed in toluene: ethylacetate: methanol 6:3:1 documented (A) under white light (B) at UV 254 nm, (C) at UV 366 nm, after (D) derivatisation in p-anisaldehyde, (E) derivatisation using reagent sequence starting with natural product (neu's) reagent and visualised at 366 nm, followed by (F) ninhydrin and lastly (G) diphenylamine, (H) DPPH•, (I) AChE inhibition, (J) BChE inhibition, (K) α -amylase inhibition, (L) *B. subtilis*, (M) luminescent *A. Fischeri* after 3 min and (N) after 30 min, (O) 366 nm image of Rp 18 plate and (N) Genotoxicity assay.

Application volume for all the bioassays is 10 μ L apart from the cholinesterase assay and genotoxicity assay (15 μ L).

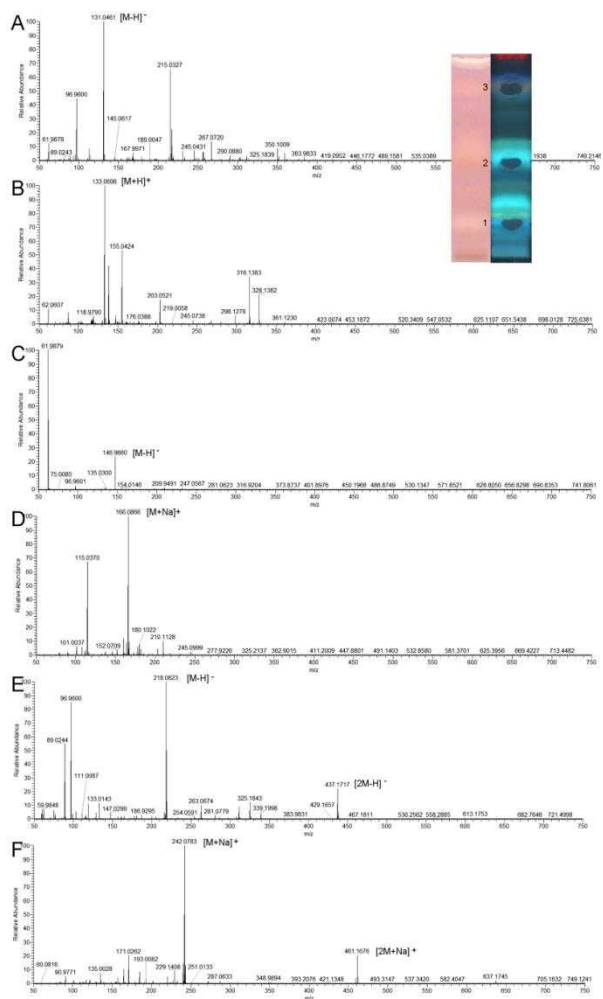


Figure 4.5.4.1: HPTLC-HRMS spectra of compounds developed in the polar mobile phase (A) compound 1 recorded in the ESI⁻ mode (B) compound 1 recorded in the ESI⁺ mode (C) compound 2 recorded in the ESI⁻ mode (D) compound 2 recorded in the ESI⁺ mode (E) compound 3 recorded in the ESI⁻ mode (F) compound 3 recorded in the ESI⁺ mode (G) compound 3 recorded in the ESI⁺ mode

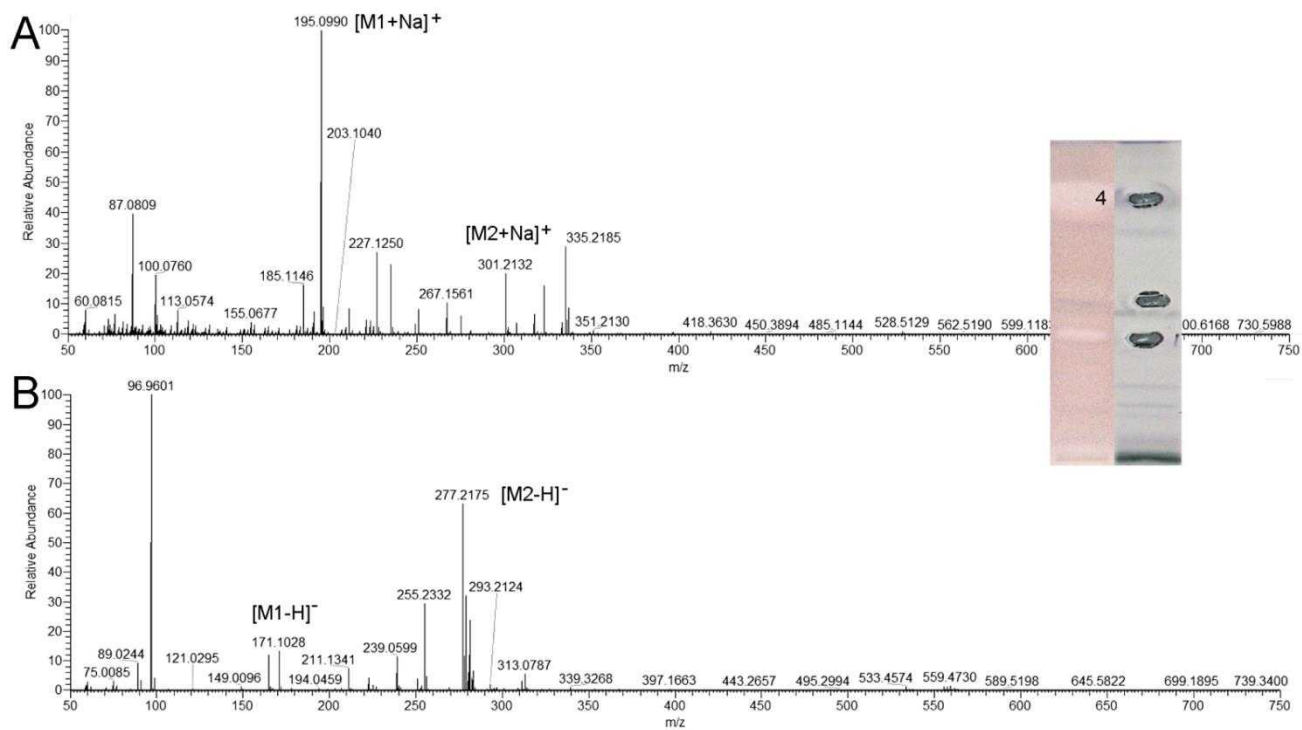


Figure 4.5.4.2: HPTLC-HRMS spectra of compounds 4 developed in the medium polar mobile phase and recorded in the ESI⁺ (A) and ESI⁻ (B) mode

Table 4.5.4.1: HPTLC-HRMS data of bioactive compounds in the selected sample, Calcutta 4 (F₂: *in vitro*, F₃: acclimatised)

Sample	Compound	<i>hR_F</i>	Observed mass (<i>m/z</i>)	assignment	Sum formular	Mass error (ppm)	Intensity	Exact Formular	Suggested substance
F ₂	1	14	131.0461	[M-H] ⁻	C ₄ H ₇ O ₃ N ₂	7.78	5.89E+07	C ₄ H ₈ O ₃ N ₂	Asparagine
			133.0606	[M+H] ⁺	C ₄ H ₉ O ₃ N ₂	1.343	9.26E+08		
	2	38	146.966	[M-H] ⁻			9.13E+07	C ₉ H ₁₁ NO ₂	4-aminohydrocinnamic acid/phenylalanine/ 2-amino-3,4-dimethylbenzoic acid/ 2-(4-methylphenoxy) acetamide
			166.0866	[M+H] ⁺	C ₉ H ₁₂ NO ₂	1.956	5.61E+08		
			218.0823	[M-H] ⁻	C ₁₂ H ₁₂ O ₃ N	4.632	1.90E+08	C ₁₂ H ₁₃ O ₃ N	
	3	71	437.1717	[2M-H] ⁻			5.62E+07		
			242.0783	[M+Na] ⁺	C ₁₂ H ₁₃ O ₃ NNa	1.754	2.95E+08		
461.1676			[2M+Na] ⁺			6.04E+07			
F ₃	4	74	277.2175	[M2-H] ⁻	C ₁₈ H ₂₉ O ₂	2.795	1.38E+08	C ₁₈ H ₃₀ O ₂	Linolenic acid (Octadeca-9, 12, 15-trienoic acid)
			301.2132	[M2+Na] ⁺			1.84E+07		
			171.1028	[M-H] ⁻	C ₉ H ₁₅ O ₃	4.154	1.21E+08	C ₉ H ₁₅ O ₃	
			195.099	[M+Na] ⁺	C ₉ H ₁₆ O ₃ Na	4.377	7.50E+07		

4.6 Tissue Culture Elicitation Experiments

Figure 4.6.1 shows the picture of the *Musa* spp. accessions growing on different elicitation experiments media.

4.6.1 Effect of sugar concentration increase in the culture media on the growth parameters and antioxidant activity of the selected accessions

The effect of increase in sugar on the length of shoot, number of leaves and shoots number is presented in Figures 4.6.1.1 to 4.6.1.3. Increase in sugar level from 30 to 45 g/L gave rise to an increased number of leaves in some of the accessions (Simili radjah and *M. balbisiana* HND). Increase in sugar level also gave an increase in the number of shoots in most of the accessions, which were better than the control in many of the accessions. The antioxidant compounds increased also along with increase in the sugar dose across all the accessions with 40 and 50 g/L giving the highest increase. This is given by the peak area and the TPC obtained from the gallic acid calibration curve $Y = 152.935X - 2464.691$, $R = 0.98615$ and $Y = 188.745X - 1446.826$, $R = 0.99820$ (Table 4.6.1.1). The 3D densitogram from the HPTLC densitometric measurement at 546 nm and the antioxidant compounds seen as white bands on a purple background are presented in Figure 4.6.1.4. The 3D densitogram gives the signal intensity of each band on all tracks for the quantitative measurement.

4.6.2 The effect of reduced temperature on the growth parameters and antioxidant activity of the selected accessions

The growth parameters varied considerably across all the accessions tested. There was a direct relationship between temperature condition and the growth of the plants; the lower the temperature, the lower the growth rate. Plants grown at 26 °C had a higher growth rate than plants grown at 15 °C. This was the case across all the tested accessions (Figure 4.6.2.1 to 4.6.2.3). In terms of TPC and antioxidant activity, plants grown at 20 °C gave a higher TPC (Figure 4.6.2.4 and Table 4.6.2.1).

4.6.3 The effect of the addition of jasmonic acid in the culture media on the growth parameters and antioxidant activity of the selected accessions

The growth parameters of the accessions treated with different doses of jasmonic acid (JA) is presented in Figures 4.6.3.1 to 4.6.3.3. Generally, the addition of JA to the proliferation media did not affect the plant growth negatively. For some accessions (Simili radjah, Foconah, Red Dacca), the highest dose of JA (200 μ M) gave shoot length which is better or same as the control (samples grown on media without JA). For the antioxidant activity, the addition of JA increased the antioxidant activity and TPC of the *Musa* spp. accessions. The addition of the highest dose of JA (200 μ M) gave the highest total phenolic content across all the tested accessions (Table 4.6.3.1).

4.6.4 Glucosidase and cholinesterase inhibitors and no toxic compounds in elicited samples

From the HPTLC-effect directed assays, alpha-glucosidase and acetylcholinesterase inhibitors were found in all the tested elicited samples. Two compounds seen as white bands on a purple background were identified to have cholinesterase inhibitory property (Figure 4.6.4.1). Two compounds were also revealed to be able to inhibit alpha-glucosidase enzyme (Figure 4.6.4.1B). The genotoxicity assay showed that there were no toxic compounds in the selected elicited *Musa* spp. accessions (Figure 4.6.4.2).

4.6.5 Characterisation of elicited antioxidant compounds from HPTLC-HRMS

The HPTLC-HRMS was used to further characterise the antioxidant compounds in one of the elicited samples. Seven compounds (5 – 11) with antioxidant activity were eluted onto the HRMS via the HPTLC interface. The mass spectra and data summary of the 7 compounds are presented in Figures 4.6.5.1 to 4.6.5.7 and Table 4.6.5.1, respectively. The compounds were suggested to be piceol, amino acids and pyrrolidinone. The HPTLC-DPPH[•] autograms of the selected elicited sample is presented in Figure 4.6.5.1.



Figure 4.6.1: Shoot culture of *Musa* species accessions (A) at 4 weeks, grown in a temporary immersion system (RITA[®] flask) for multiplication, and at 6 weeks, (B) grown on proliferation media elicited with 50 g/L sugar, (C) incubated at 20 °C and (D) elicited with 200 μ M JA (E); leaves collected at the end of the experiment for analysis.

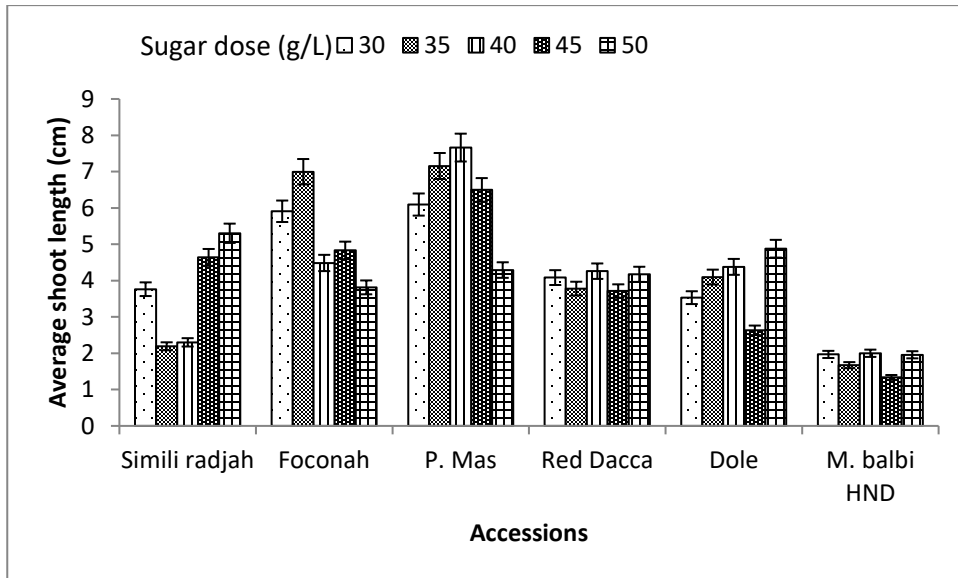


Figure 4.6.1.1: Average shoot length of all the *Musa* spp. accesions grown under different sugar concentrations.

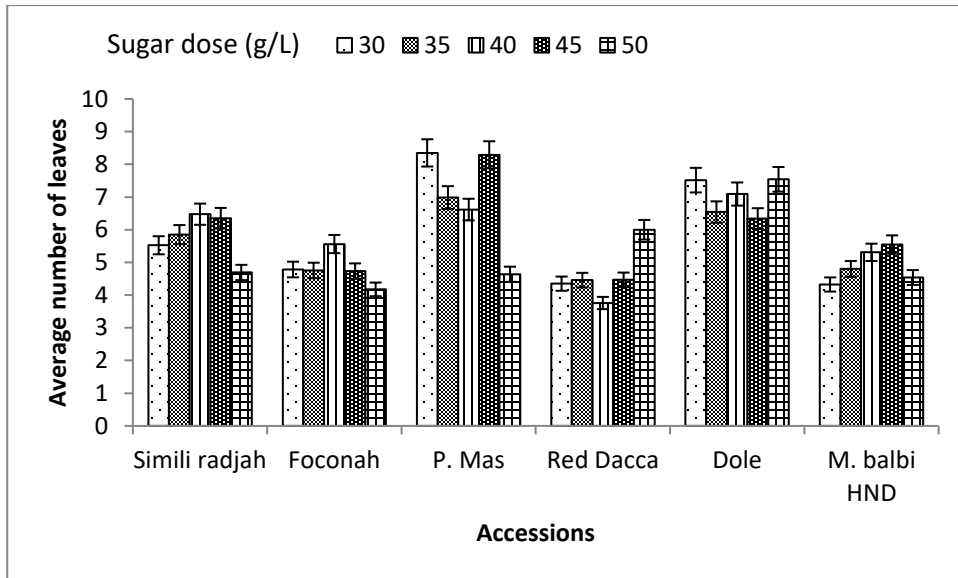


Figure 4.6.1.2: Average number of leaves of all the *Musa* spp. accessions grown under different sugar concentrations.

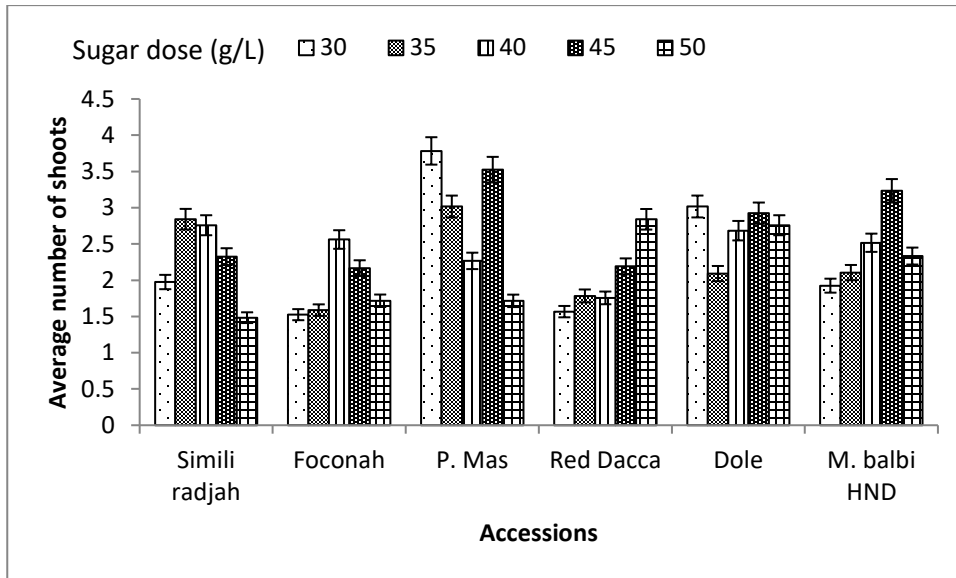


Figure 4.6.1.3: Average number of shoots of all the *Musa* spp. accessions grown under different sugar concentrations.

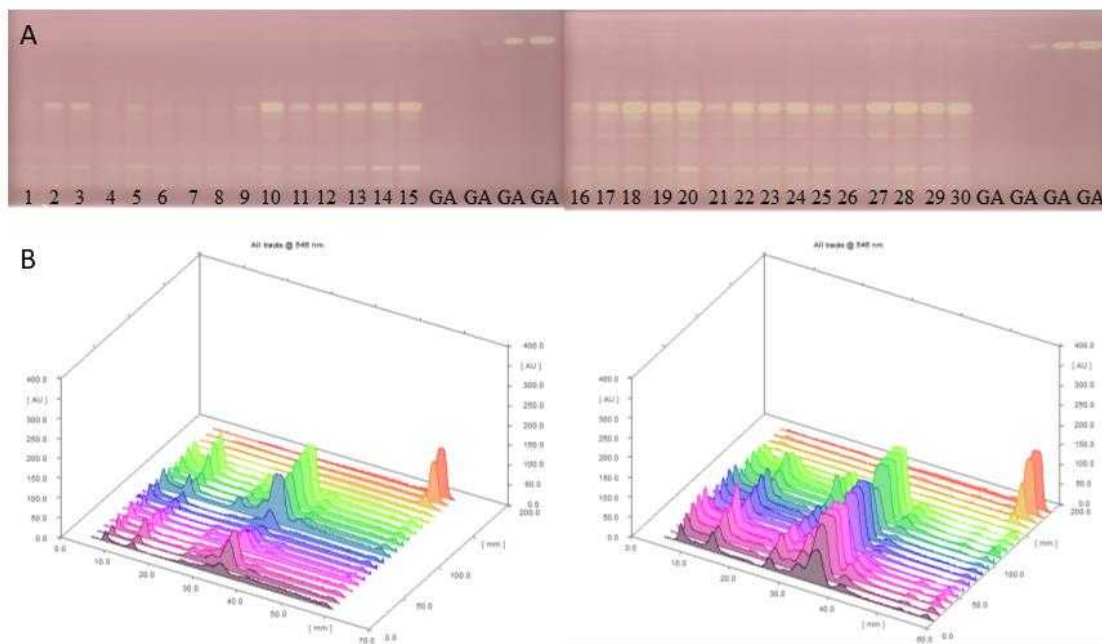


Figure 4.6.1.4: HPTLC chromatogram of sugar elicited samples developed in ethyl acetate: toluene: formic acid: H₂O; 3.4: 0.5: 0.7: 0.5 and (A) after derivatisation in DPPH showing antioxidant compounds as white bands on a purple background with varying band intensities with the different sugar concentrations B. 3D densitogram at 546 nm of all tracks (samples and standard, gallic acid) showing varying concentrations of antioxidant compounds.

Table 4.6.1.1: Peak area and total phenolic content from the densitometric measurement and gallic acid calibration curve of the increase in sugar experiment

ID Track	TRC Accession	Sugar (g/L)	Peak area	TPC (ng/g GAE)	Increase factor
1	Simili radjah	30	3167.85 ± 0.9	36.83 ± 0.0	1.0
2	Simili radjah	35	8271.29 ± 0.6	70.20 ± 0.0	1.9
3	Simili radjah	40	9942.00 ± 0.3	81.12 ± 0.1	2.2
4	Simili radjah	45	1989.98 ± 0.3	29.13 ± 0.3	0.8
5	Simili radjah	50	6341.98 ± 0.6	57.58 ± 0.3	1.6
6	Foconah	30	3565.71 ± 0.3	39.43 ± 0.6	1.0
7	Foconah	35	2562.33 ± 0.3	32.87 ± 0.6	0.8
8	Foconah	40	1874.88 ± 0.3	28.38 ± 0.6	0.7
9	Foconah	45	5397.44 ± 0.3	51.41 ± 0.6	1.3
10	Foconah	50	18737.61 ± 0.3	138.64 ± 0.6	3.5
11	P. Mas	30	9599.75 ± 0.6	78.89 ± 0.6	1.0
12	P. Mas	35	12360.41 ± 0.3	96.94 ± 0.6	1.2
13	P. Mas	40	14258.19 ± 0.3	109.35 ± 0.6	1.4
14	P. Mas	45	16399.14 ± 0.3	123.35 ± 0.3	1.6
15	P. Mas	50	17939.55 ± 0.3	133.42 ± 0.3	1.7
16	Red Dacca	30	11523.83 ± 0.3	68.72 ± 0.3	1.0
17	Red Dacca	35	18072.33 ± 0.3	103.42 ± 0.3	1.5
18	Red Dacca	40	25930.94 ± 0.3	145.05 ± 0.3	2.1
19	Red Dacca	45	23575.89 ± 0.3	132.57 ± 0.3	1.9
20	Red Dacca	50	25717.73 ± 0.3	143.93 ± 0.3	2.1
21	Dole	30	13243.66 ± 0.7	77.83 ± 0.3	1.0
22	Dole	35	22095.84 ± 0.6	124.73 ± 0.3	1.6
23	Dole	40	21438.37 ± 0.3	121.25 ± 0.3	1.6
24	Dole	45	23337.77 ± 0.3	131.31 ± 0.3	1.7
25	Dole	50	17093.48 ± 0.3	98.23 ± 0.6	1.3
26	<i>M. balbisiana</i> HND	30	12786.31 ± 0.3	75.41 ± 0.6	1.0
27	<i>M. balbisiana</i> HND	35	22985.30 ± 0.3	129.45 ± 0.6	1.7
28	<i>M. balbisiana</i> HND	40	24350.91 ± 0.0	136.68 ± 0.6	1.8
29	<i>M. balbisiana</i> HND	45	23131.05 ± 0.0	130.22 ± 0.3	1.7
30	<i>M. balbisiana</i> HND	50	23523.12 ± 0.3	132.29 ± 0.3	1.8

*Values are expressed as mean ± SEM ($n = 3$) and are significantly different from one another at $P < 0.05$

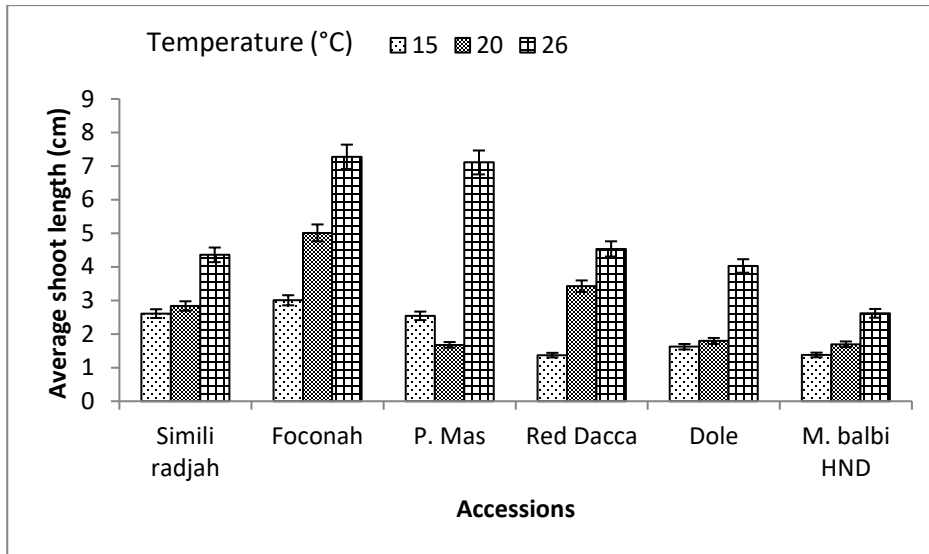


Figure 4.6.2.1: Average shoot length of all the *Musa* spp. accessions grown under different temperature conditions.

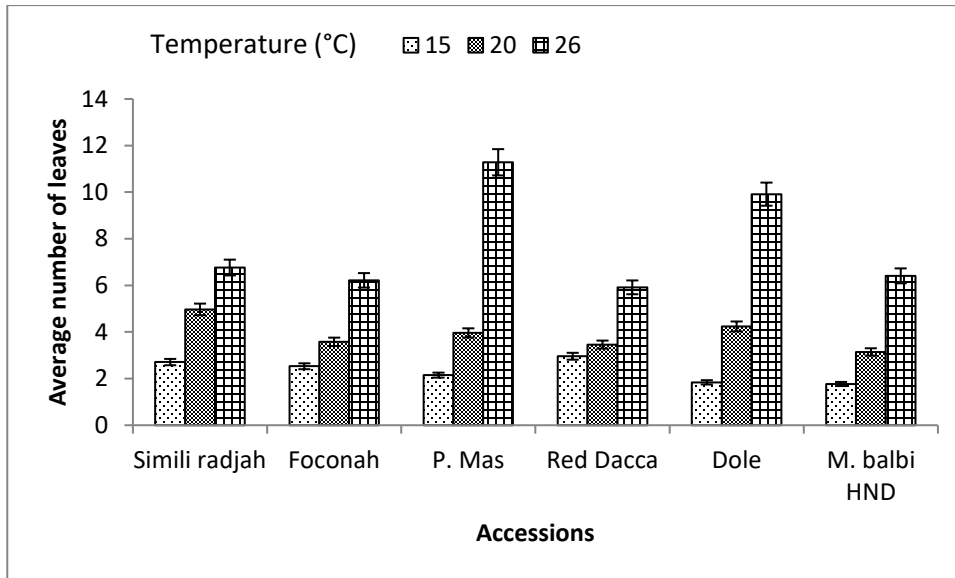


Figure 4.6.2.2: Average number of leaves of all the *Musa* spp. accessions grown under different temperature conditions.

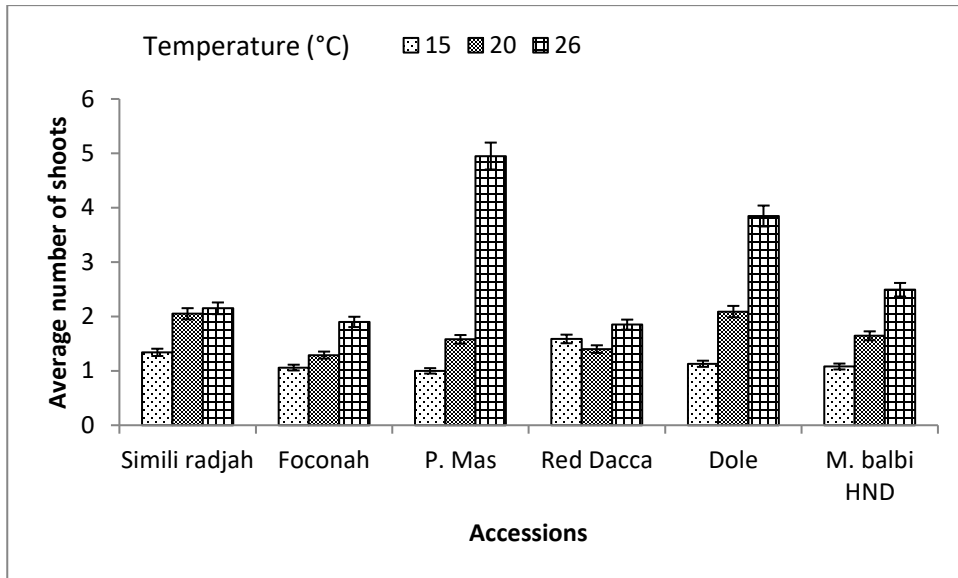


Figure 4.6.2.3: Average number of shoots of all the *Musa* spp. accessions grown under different temperature conditions.

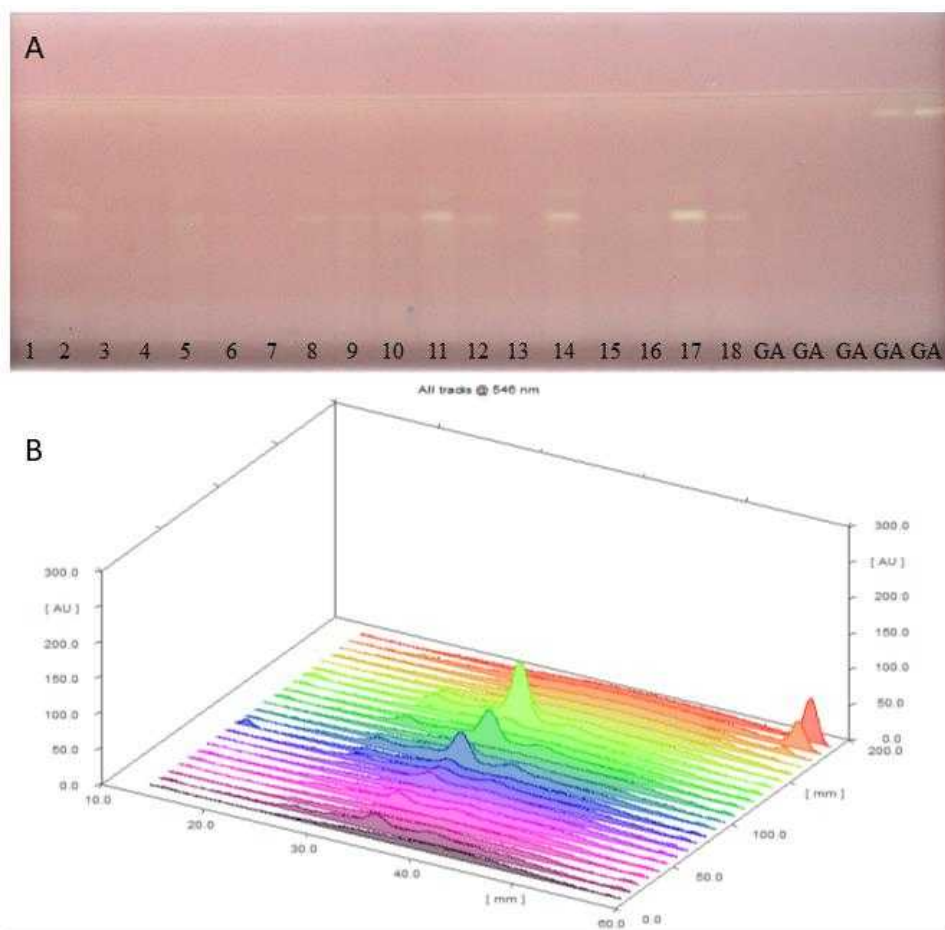


Figure 4.6.2.4: HPTLC chromatogram of temperature elicited samples developed in ethyl acetate: toluene: formic acid: H₂O; 3.4: 0.5: 0.7: 0.5 and (A) after derivatisation in DPPH showing antioxidant compounds as white bands on a purple background with higher band intensity at 20 °C B. 3D densitogram at 546 nm of all tracks (samples and standard, gallic acid) showing varying concentrations of antioxidant compounds.

Table 4.6.2.1: Peak area and total phenolic content from the densitometric measurement and gallic acid calibration curve of the temperature experiment

ID	Temperature	TPC	Increase		
Track	TRC Accession	(°C)	Peak area	(ng/g GAE)	factor
1	Simili radjah	26	458.91 ± 0.6	6.30 ± 0.6	1.0
2	Simili radjah	20	2271.95 ± 0.6	18.40 ± 0.6	2.9
3	Simili radjah	15	590.12 ± 0.6	7.19 ± 0.6	1.1
4	Foconah	26	342.58 ± 0.0	5.52 ± 0.6	1.0
5	Foconah	20	1851.96 ± 0.3	15.66 ± 0.6	2.8
6	Foconah	15	1480.50 ± 0.6	13.17 ± 0.6	2.4
7	P. Mas	26	561.61 ± 0.3	6.99 ± 0.3	1.0
8	P. Mas	20	1948.34 ± 0.6	16.31 ± 0.3	2.3
9	P. Mas	15	1783.95 ± 0.6	15.21 ± 0.3	2.2
10	Red Dacca	26	2357.17 ± 0.6	19.06 ± 0.3	1.0
11	Red Dacca	20	4835.15 ± 0.3	35.70 ± 0.3	1.9
12	Red Dacca	15	2116.89 ± 0.3	17.44 ± 0.3	0.9
13	Dole	26	798.52 ± 0.3	8.59 ± 0.3	1.0
14	Dole	20	5708.75 ± 0.3	41.57 ± 0.3	4.8
15	Dole	15	1217.34 ± 0.6	11.40 ± 0.3	1.3
16	<i>M. balbisiana</i> HND	26	2277.03 ± 0.3	18.52 ± 0.3	1.0
17	<i>M. balbisiana</i> HND	20	7256.71 ± 0.3	51.97 ± 0.3	2.8
18	<i>M. balbisiana</i> HND	15	3194.43 ± 0.3	24.68 ± 0.3	1.3

*Values are expressed as mean ± SEM ($n = 3$) and are significantly different from one another at $P < 0.05$

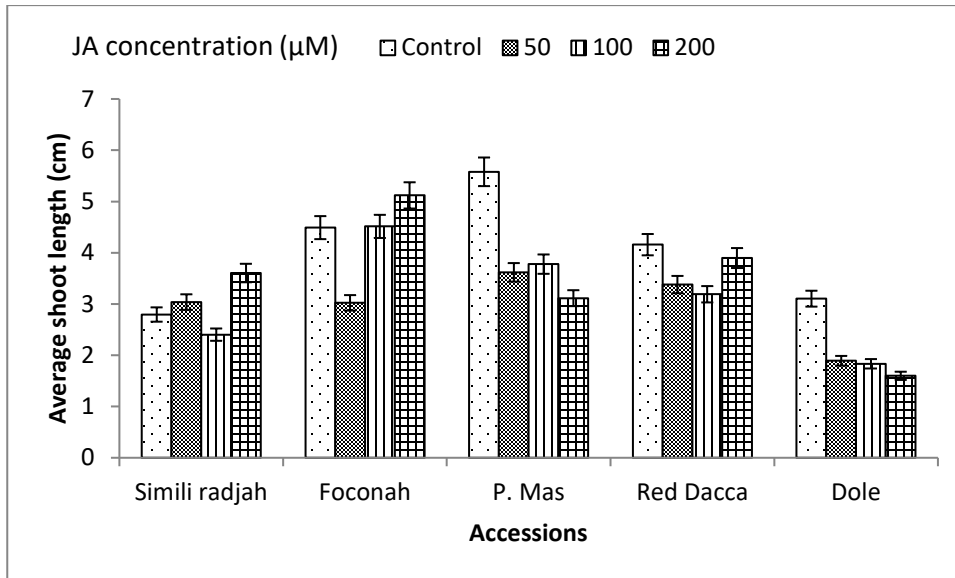


Figure 4.6.3.1: Average shoot length of all the *Musa* spp. accessions grown on proliferation media with the addition of jasmonic acid and the control.

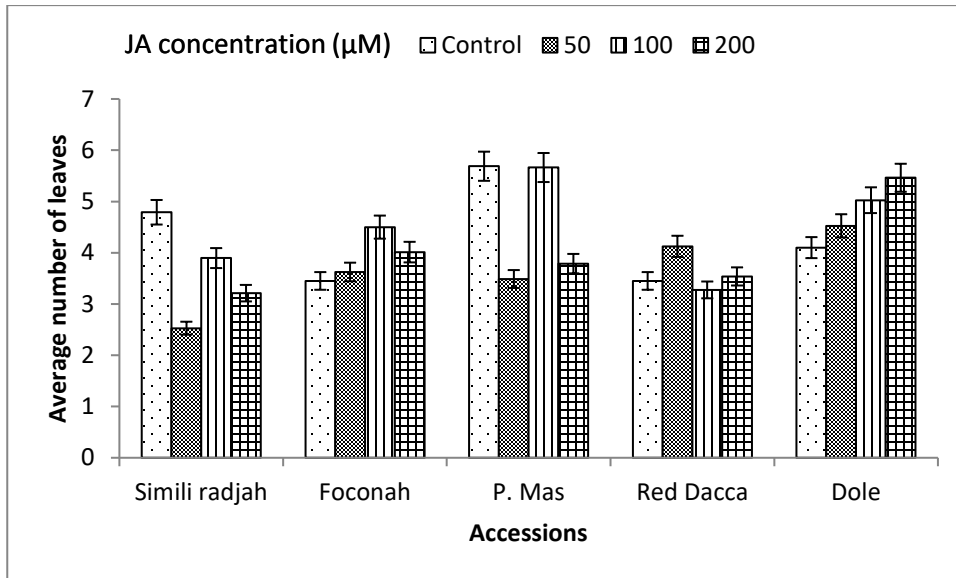


Figure 4.6.3.2: Average number of leaves of all the *Musa* spp. accessions grown on proliferation media with the addition of jasmonic acid and the control.

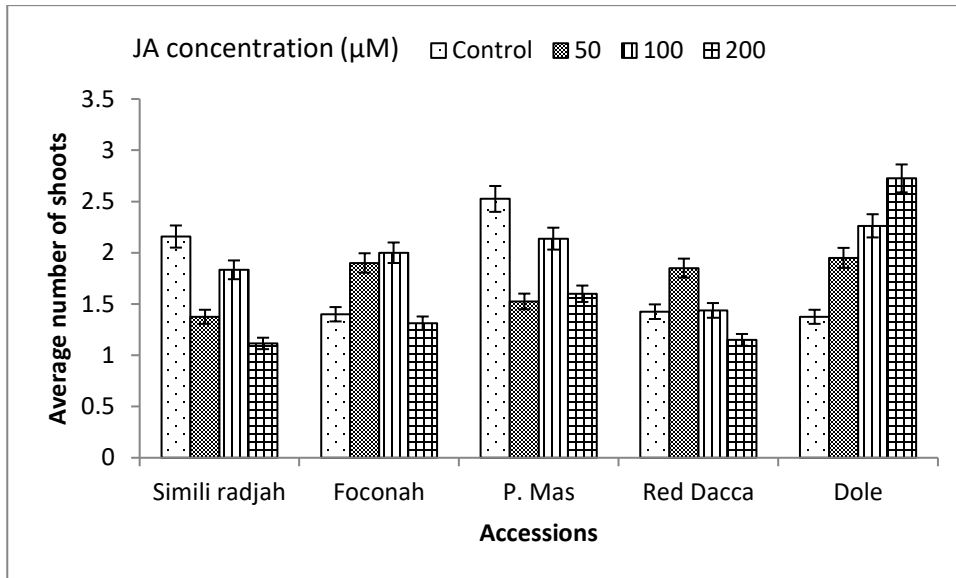


Figure 4.6.3.3: Average number of shoots of all the *Musa* spp. accessions grown on proliferation media with the addition of jasmonic acid and the control.

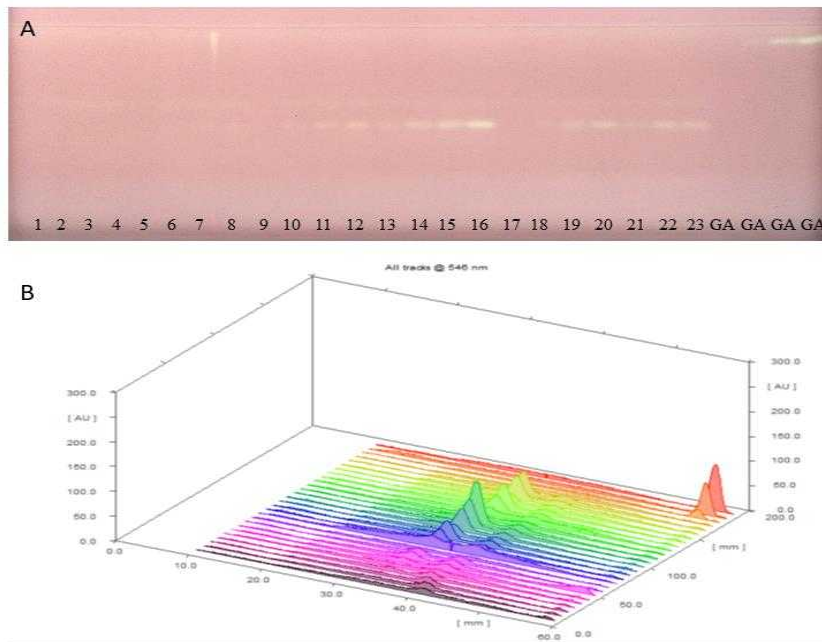


Figure 4.6.3.4: HPTLC chromatogram of jasmonic acid elicited samples developed in ethyl acetate: toluene: formic acid: H₂O; 3.4: 0.5: 0.7: 0.5 and (A) after derivatisation in DPPH showing antioxidant compounds as white bands on a purple background with addition of 200 μ M JA giving more intense bands B. 3D densitogram at 546 nm of all tracks (samples and standard, gallic acid) showing varying concentrations of antioxidant compounds.

Table 4.6.3.1: Peak area and total phenolic content from the densitometric measurement and gallic acid calibration curve of the jasmonic acid experiment

ID		JA added		TPC	Increase
Track	TRC Accession	(μM)	Peak area	(ng/g GAE)	factor
1	Simili radjah	0	508.32 \pm 0.3	7.00 \pm 0.6	1.0
2	Simili radjah	50	1138.88 \pm 0.3	9.38 \pm 0.6	1.3
3	Simili radjah	100	846.17 \pm 0.3	8.28 \pm 0.6	1.2
4	Simili radjah	200	1359.95 \pm 0.3	10.21 \pm 0.6	1.5
5	Foconah	0	1244.78 \pm 0.3	9.78 \pm 0.6	1.0
6	Foconah	50	1410.15 \pm 0.3	10.40 \pm 0.6	1.1
7	Foconah	100	2360.80 \pm 0.6	13.98 \pm 0.6	1.4
8	Foconah	200	2301.61 \pm 0.0	13.76 \pm 0.6	1.4
9	P. Mas	0	1079.36 \pm 0.3	9.16 \pm 0.6	1.0
10	P. Mas	50	1601.44 \pm 0.0	11.12 \pm 0.3	1.2
11	P. Mas	100	2878.81 \pm 0.3	15.94 \pm 0.3	1.7
12	P. Mas	200	3822.35 \pm 0.3	19.49 \pm 0.3	2.1
13	Red Dacca	0	2196.06 \pm 0.3	13.36 \pm 0.3	1.0
14	Red Dacca	50	4357.05 \pm 0.3	21.50 \pm 0.0	1.6
15	Red Dacca	100	4803.77 \pm 0.3	23.19 \pm 0.0	1.7
16	Red Dacca	200	7250.76 \pm 0.3	32.41 \pm 0.6	2.4
17	Dole	0	994.66 \pm 0.3	8.84 \pm 0.0	1.0
18	Dole	50	1722.59 \pm 0.3	11.58 \pm 0.6	1.3
19	Dole	100	2884.76 \pm 0.3	15.96 \pm 0.0	1.8
20	Dole	200	3911.28 \pm 0.3	19.82 \pm 0.0	2.2
21	<i>M. balbisiana</i> HND	0	1803.31 \pm 0.3	11.88 \pm 0.6	1.0
22	<i>M. balbisiana</i> HND	100	3730.04 \pm 0.3	19.14 \pm 0.6	1.6
23	<i>M. balbisiana</i> HND	200	3962.59 \pm 0.3	20.02 \pm 0.3	1.7

*Values are expressed as mean \pm SEM ($n = 3$) and are significantly different from one another at $P < 0.05$

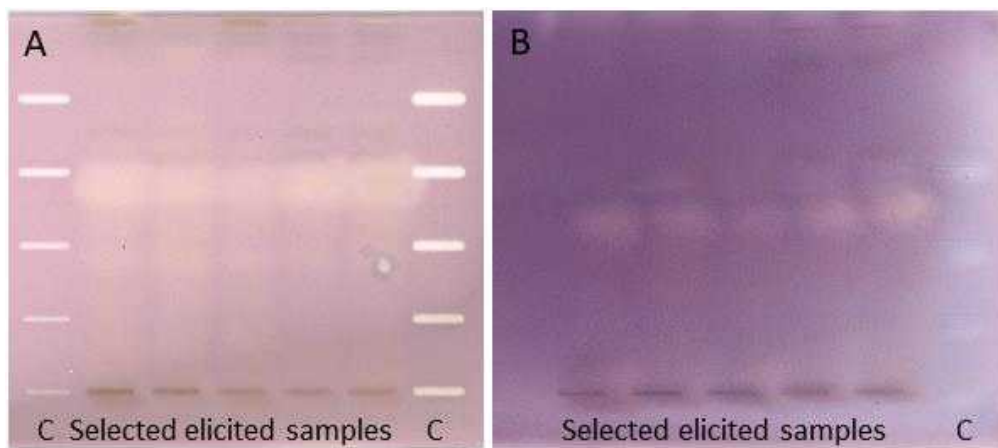


Figure 4.6.4.1: HPTLC-effect directed analysis fingerprints of selected elicited *Musa* spp. samples developed in ethyl acetate: toluene: formic acid: water (3.4: 0.5: 0.7: 0.5) and documented under white light after (A) AChE (Reflectance and transmittance, RT mode) (B) α -glucosidase assays (reflectance mode). 10 μ L/band samples were applied in both assays.

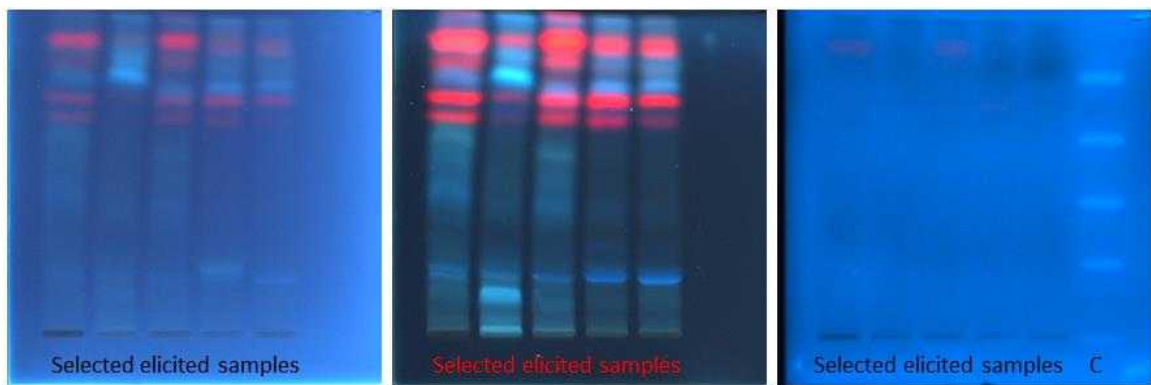


Figure 4.6.4.2: HPTLC chromatogram of genotoxicity assay of selected elicited samples on Rp 18 plates developed in ethyl acetate: toluene: formic acid: water 3.4: 0.5: 0.7: 0.5 and documented (A) at 254 nm, (B) at 366 nm and (C) after mutagenicity assay. 10 μ L/band samples were applied. Track C is the positive control with different volumes applied in the free mode.

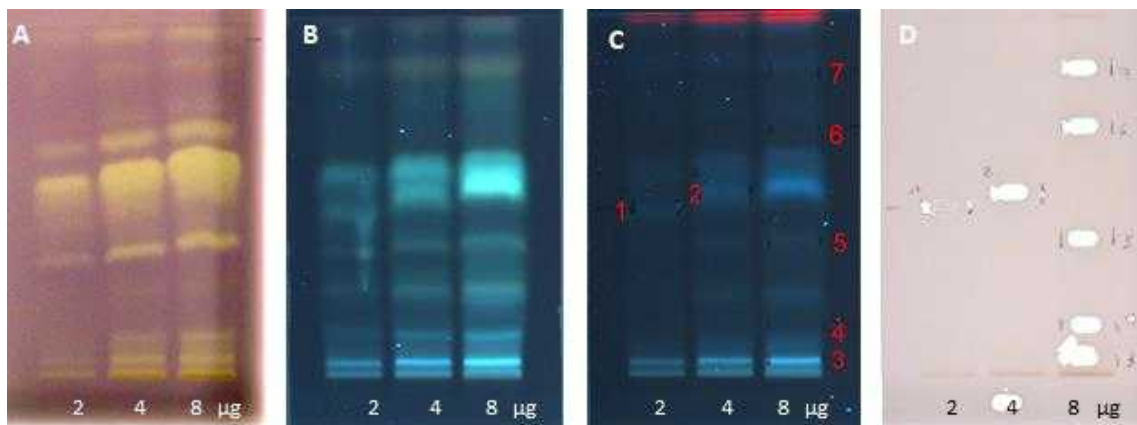


Figure 4.6.5.1: Elicited accession Red Dacca grown at 20 °C (2, 4 and 8 μg/band) after (A) DPPH• assay at white light illumination and (B) natural product reagent at UV 366 nm, both used for markings of the bands at (C) UV 366 nm for recording of the mass spectra via online elution of zones (D), respective elution head imprint)

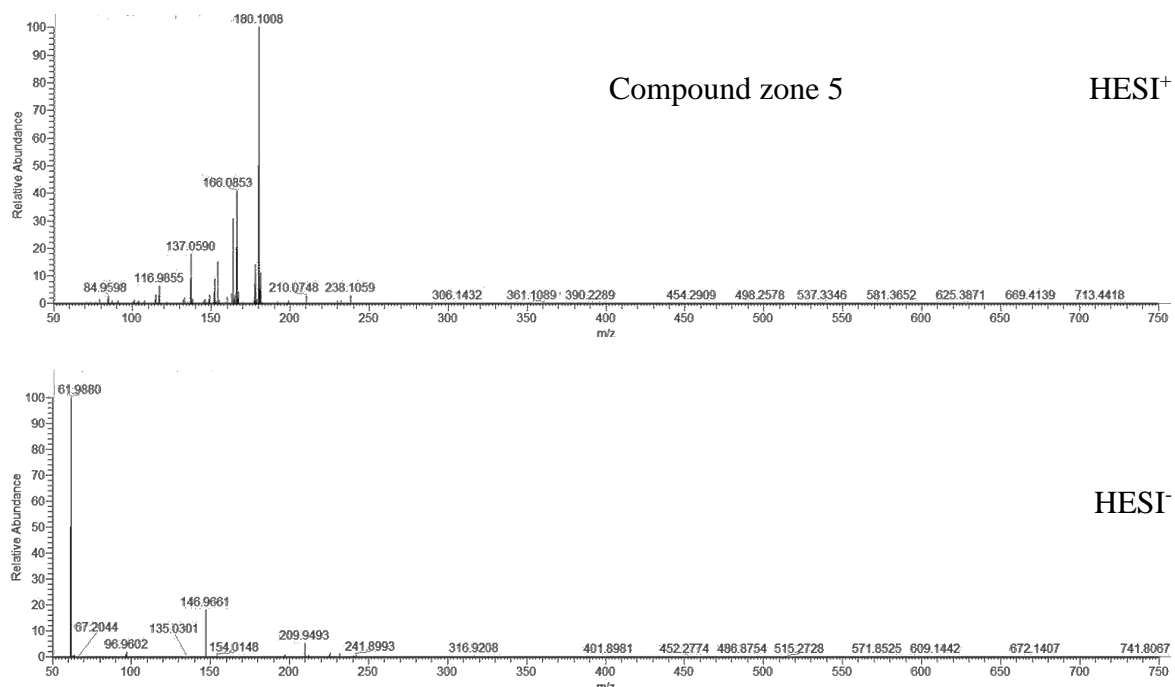


Figure 4.6.5.2: HPTLC-HRMS spectra of compound 5 recorded in the positive and negative electron spray ionisation mode

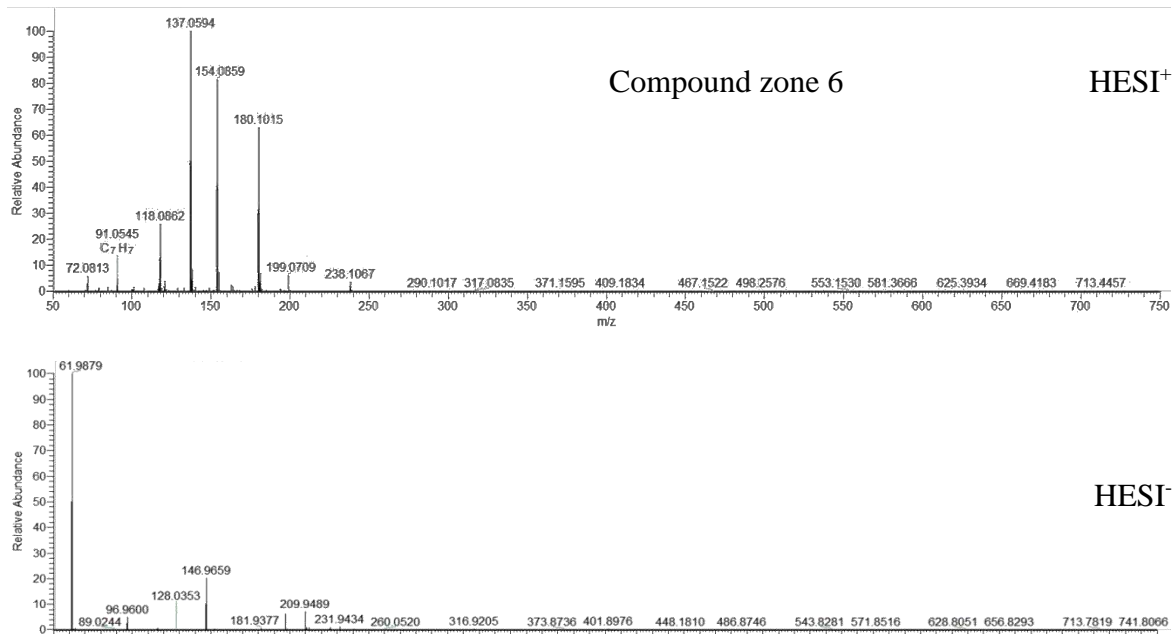


Figure 4.6.5.3: HPTLC-HRMS spectra of compound 6 recorded in the positive and negative electron spray ionisation mode

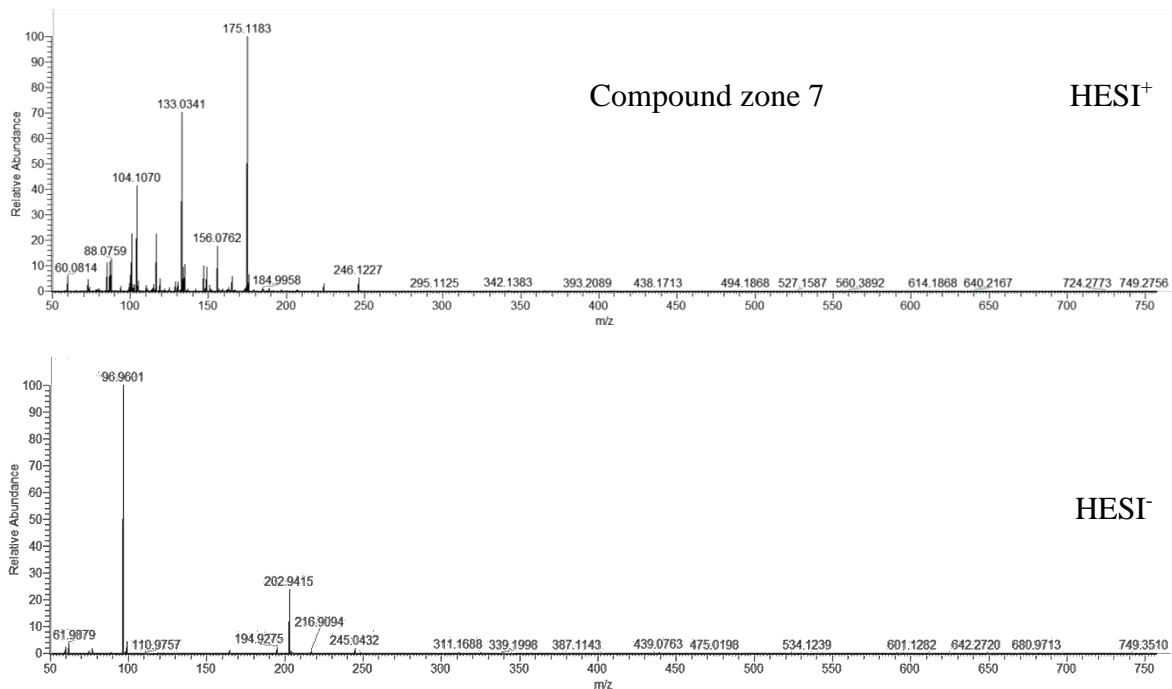


Figure 4.6.5.4: HPTLC-HRMS spectra of compound 7 recorded in the positive and negative electron spray ionisation mode

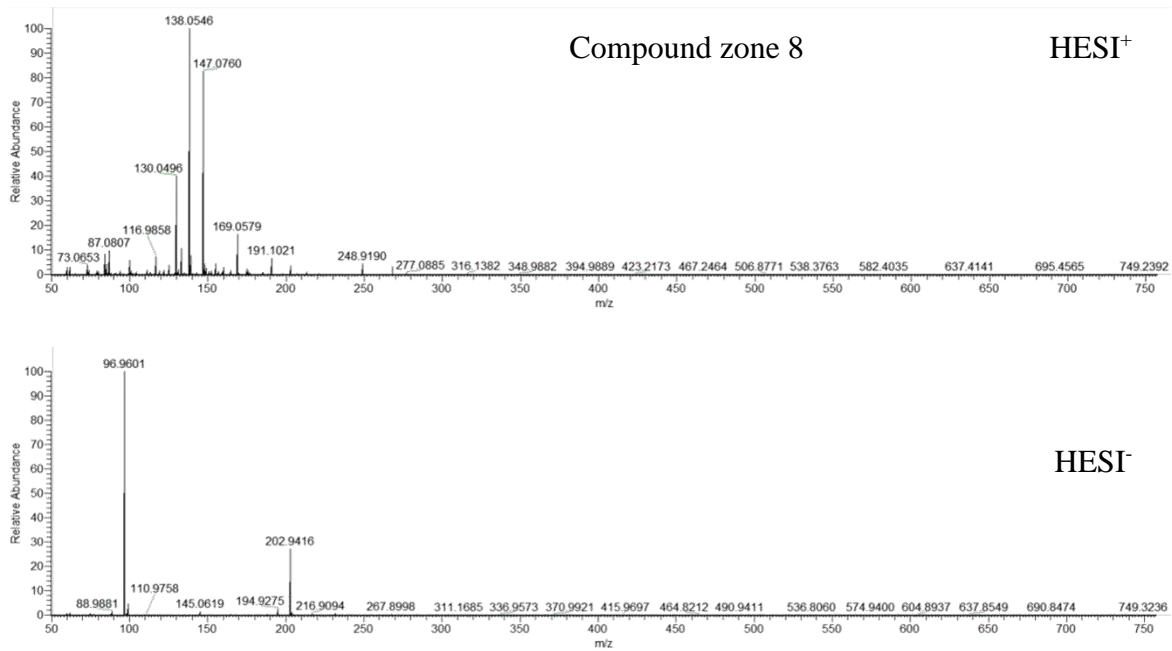


Figure 4.6.5.5: HPTLC-HRMS spectra of compound 8 recorded in the positive and negative electron spray ionisation mode

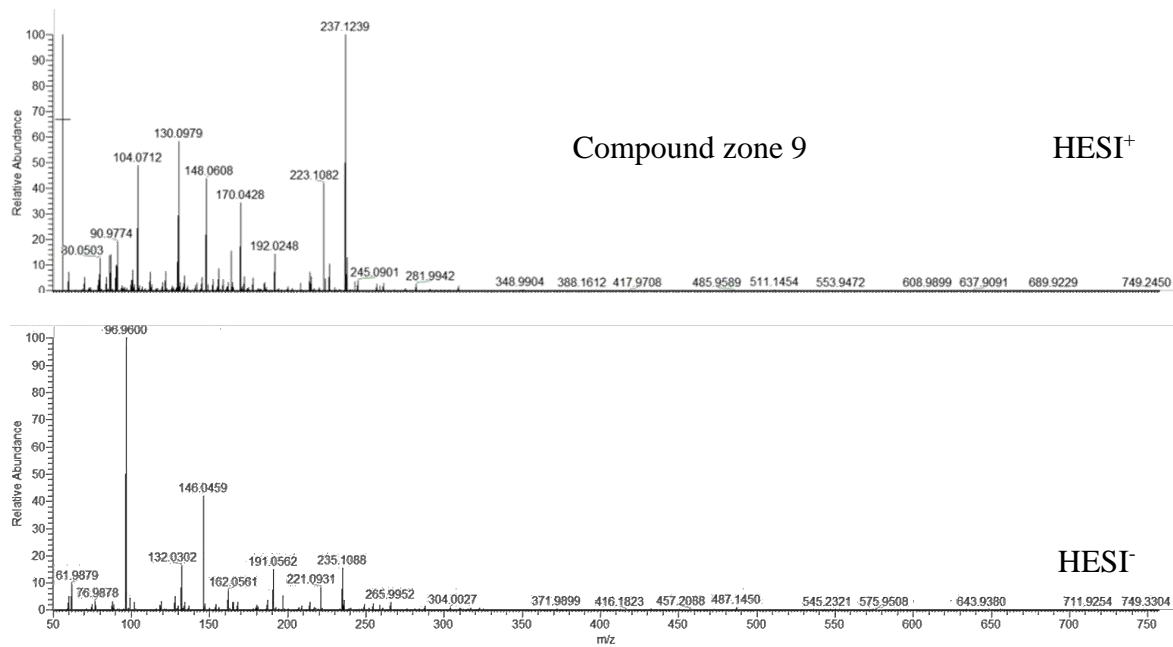


Figure 4.6.5.6: HPTLC-HRMS spectra of compound 9 recorded in the positive and negative electron spray ionisation mode

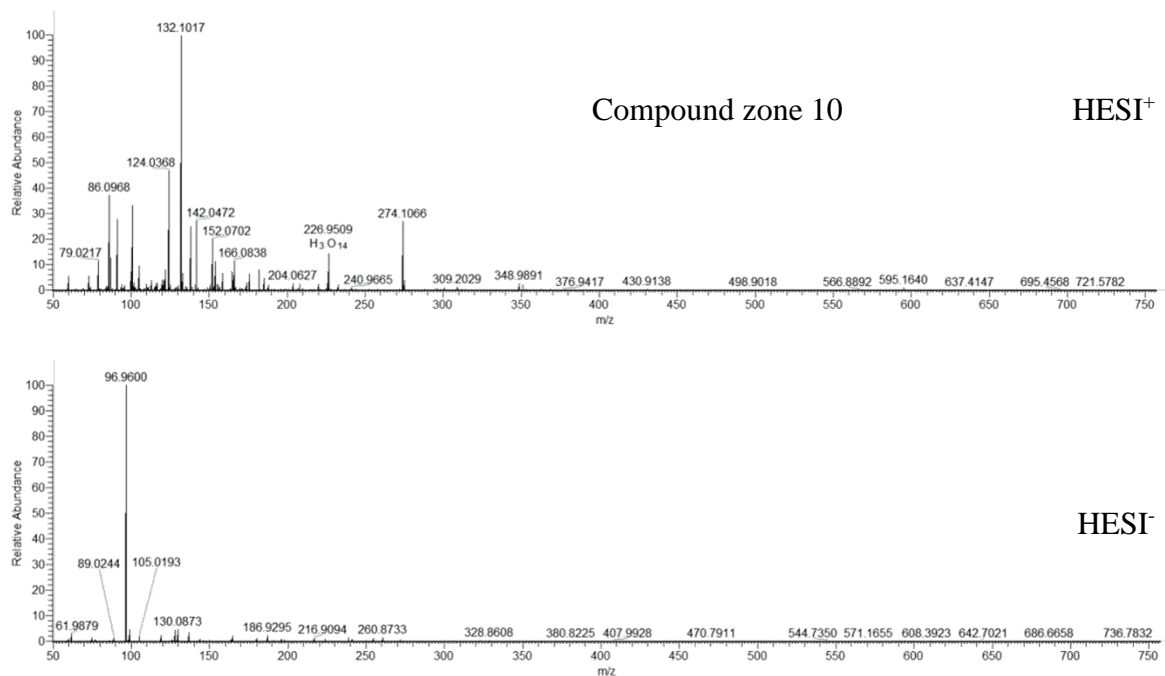


Figure 4.6.5.7: HPTLC-HRMS spectra of compound 10 recorded in the positive and negative electron spray ionisation mode

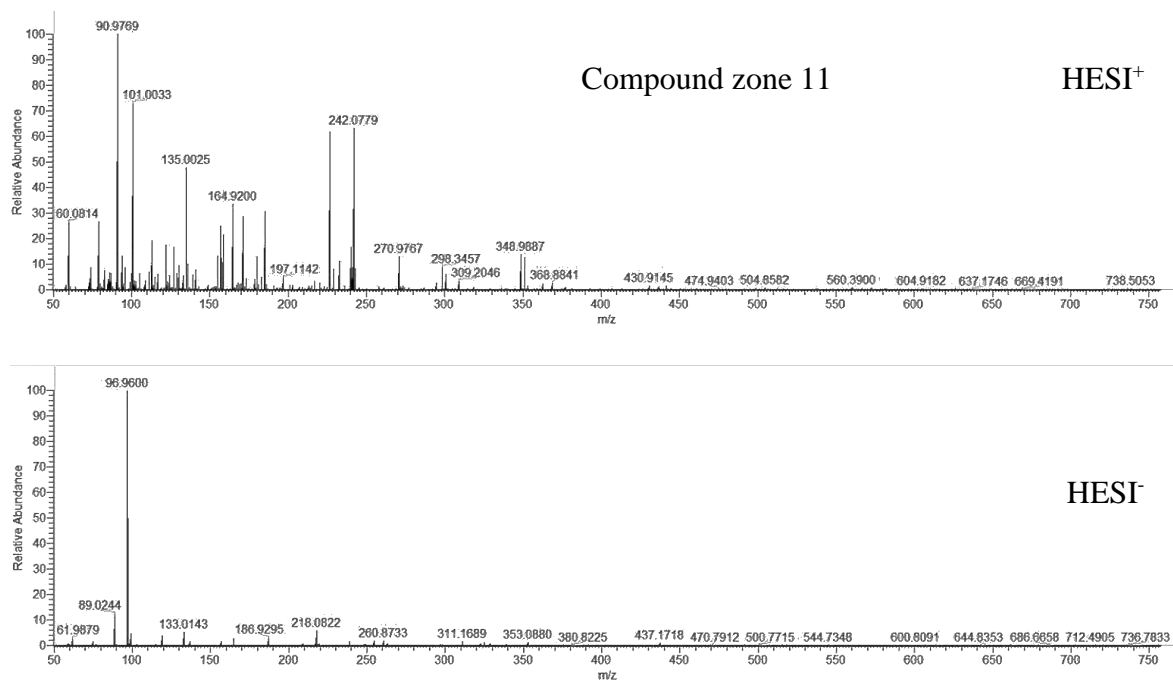


Figure 4.6.5.8: HPTLC-HRMS spectra of compound 11 recorded in the positive and negative electron spray ionisation mode

Table 4.6.5.1: HPTLC-HRMS data of antioxidant compounds in the selected elicited sample

Zone	<i>hR</i> F	Observed mass <i>m/z</i>		Molecular formula	Mass error (ppm)	Intensity (normalized level)
5	40	210.0748	[M1+H] ⁺			3.16E+07
		166.0853	[M2+H] ⁺			4.60E+08
		180.1009	[M3+H] ⁺			1.13E+09
		238.1059	[M4+H] ⁺			3.30E+07
		209.9493	[M5-H] ⁻			2.10E+07
		146.9661	[M6-H] ⁻			7.17E+07
6	42	137.0595	[M1+H] ⁺	C ₈ H ₉ O ₂ ⁺	1.9	8.04E+08
		118.0862	[M2+H] ⁺	C ₅ H ₁₂ NO ₂ ⁺	0.2	2.14E+08
		154.0859	[M3+H] ⁺	C ₈ H ₁₂ NO ₂ ⁺	2.4	7.49E+08
		180.1015	[M4+H] ⁺	C ₁₀ H ₁₄ NO ₂ ⁺	2.4	5.78E+08
		146.9659	[M5-H] ⁻			7.90E+07
		197.0567	[M6-H] ⁻			2.41E+07
7	4	175.1183	[M1+H] ⁺	C ₆ H ₁₅ N ₄ O ₂ ⁺	3.6	1.53E+08
		202.9416	[M2-H] ⁻			4.14E+07
8	12	169.0579	[M1+Na] ⁺	C ₅ H ₁₀ N ₂ O ₃ Na ⁺	3.0	2.79E+07
		147.0760	[M1+H] ⁺	C ₅ H ₁₁ N ₂ O ₃ ⁺	3.1	1.40E+08
		138.0546	[M2+H] ⁺	C ₇ H ₈ NO ₂ ⁺	2.8	1.69E+08
		202.9416	[M3*-H] ⁻			1.32E+08
9	32	237.1239	[M1+H] ⁺	C ₁₂ H ₁₇ O ₃ N ₂ ⁺	-2.0	8.08E+07
		235.1088	[M1-H] ⁻	C ₁₂ H ₁₅ O ₃ N ₂ ⁻	0.0	1.10E+07
10	59	132.1017	[M1+H] ⁺	C ₆ H ₁₄ O ₂ N ⁺	1.7	6.15E+07
		274.1066	[M2+H] ⁺			1.67E+07
		130.0873	[M3-H] ⁻			7.65E+06
11	71	218.0823	[M1-H] ⁻	C ₁₂ H ₁₂ O ₃ N ⁻	0.1	1.07E+07

*same HESI mass signal as for compound 7

4.7 Bioassay Guided Isolation of Compounds from the Most Bioactive Field Accession (*Musa acuminata*, Simili radjah)

4.7.1 Yield of the large-scale crude extraction and partitioned fractions

The percentage yield of the most bioactive field accession, Simili radjah, from fruit (SRF) and leaves (SRL) crude extract and partitioned fraction is shown in Table 4.7.1.1. The leaf sample gave a better extraction yield than the fruit. For the leaf samples, the highest extraction yield (61%) was obtained with the *n*-hexane fraction (NHF), followed by the ethyl acetate fraction (EAF) with 14%, while for the fruit, the aqueous methanol fraction (AMF) and the *n*-hexane fraction (NHF) gave the highest yield with 39% and 9%, respectively.

4.7.2 Thin layer chromatography of the crude and partitioned fractions

The TLC profile of the leaf and fruit fractions is reported in Figures 4.7.2.1 and 4.7.2.2, respectively. For the leaf fractions, the non-polar and medium polar mobile phases revealed only chlorophyll pigment. It didn't separate the EAF in these mobile phases. However, the EAF was separated with a polar mobile phase (Methanol: Toluene: Acetic acid 3: 2: 0.8) and 3 spots were observed (Fig. 4.7.2.1). The fruit fractions separated well in non-polar and medium polar mobile phases with the DCM fraction showing 2 prominent spots in Hexane: Ethyl acetate 2: 3 (Fig 4.7.2.2).

4.7.3 Biological activities of the crude methanol extracts and the partitioned fractions

4.7.3.1 Total phenolic content (TPC) and DPPH• radical scavenging activity

The leaf crude methanol extract and fractions had higher TPC and DPPH• antioxidant activity than the fruit (Table 4.7.3.1.1). Among the leaf fractions, the EAF had the highest TPC (911.88 ± 1.67 mgGAE per g) and the highest DPPH• antioxidant activity as revealed by its low IC₅₀ value (8.98 ± 0.37 μg/mL), which is close to that of the standard, gallic acid (4.07 ± 1.17 μg/mL) (Figure 4.7.3.1.1 and 4.7.3.1.2). For, the fruit fraction, the dichloromethane fraction had the highest DPPH• antioxidant activity (Figure 4.7.3.1.2B).

4.7.3.2 Hydroxyl radical and ABTS radical scavenging activities

The result of the hydroxyl and ABTS radicals scavenging activity is shown in Figures 4.7.3.2.1 and 4.7.3.2.2, respectively with the leaf fractions having better activity than the fruit. The leaf EAF also gave the highest hydroxyl and ABTS radical scavenging activities.

4.7.3.3 Alpha-amylase (α -AML) and alpha-glucosidase (α -GLD) inhibitory activities

The leaf fractions also gave a better inhibition of the two digestive enzymes than the fruit samples. Simili radjah leaf ethyl acetate fraction had a moderate α -AML inhibition and a high α -GLD inhibition (Figure 4.7.3.3.1 and 4.7.3.3.2). Different modes of α -AML and α -GLD inhibition by the EAF of the leaf and CME of the fruit *Musa acuminata* were observed (Figure 4.7.3.3.3 and 4.7.3.3.4). These two fractions were selected for the mode of inhibition study because they gave a strong α -glucosidase inhibition and a mild α -amylase inhibition. The Michaelis-Menten equation which explains the type of inhibition of a particular enzyme revealed that fruit fraction exhibited a non-competitive and an uncompetitive mode of α -amylase and α -glucosidase inhibition, respectively (Figure 4.7.3.3.3), while the leaf fractions exhibited a competitive mode of α -AML, but an uncompetitive mode of alpha-glucosidase inhibition (4.7.3.3.4). For the fruit, the mode of inhibition as depicted by the Lineweaver Burk plot revealed a constant K_m (0.054 mM) for both sample and control, while the V_{max} decreases from 0.0062 (control) to 0.0016 mM/min (sample), signifying a non-competitive α -amylase inhibition (Fig. 4.7.3.3.3A). However, for α -glucosidase the V_{max} and K_m values changes or reduces for both the sample and the control signifying an uncompetitive mode of inhibition (Fig. 4.7.3.3.3B). Moreover, for the leaf fractions, there was a constant V_{max} value (0.0019 mM/min) for both the extract and control with a decrease in K_m values from 0.028 (extract) to 0.020 mM (control, Fig. 4.7.3.3.4A), suggesting a competitive α -amylase mode of inhibition. However, the α -glucosidase mode of inhibition of the leaf fractions is uncompetitive (Fig. 4.7.3.3.4B), revealing a decrease in V_{max} values from 0.006 (control) to 0.002 mM/min (sample) and K_m values from 0.055 (control) to 0.0053 mM (sample).

4.7.3.4 Anti-inflammatory activity

The polar leaf and fruit fractions had a better 15-LOX inhibitory activity than the non-polar fractions. Overall, the *n*-butanol ($IC_{50} = 34.12 \pm 2.59 \mu\text{g/mL}$) and the ethyl acetate ($IC_{50} = 43.07 \pm 11.29 \mu\text{g/mL}$) fractions of the leaf gave a better anti-inflammatory activity than quercetin, the positive control ($IC_{50} = 54.75 \pm 17.07 \mu\text{g/mL}$) (Table 4.7.3.4.1).

4.7.3.5 Anticholinesterase activity

The IC_{50} values of the acetylcholinesterase inhibition and the percentage inhibition at 1 mg/mL are presented in Table 4.7.3.5.1 and Figure 4.7.3.5.1, respectively. The leaf fractions gave a higher inhibitory activity than the fruit. The EAF of the leaf and the NBF of the fruit gave the best inhibitory activity with their lowest IC_{50} values $404.42 \pm 8.00 \mu\text{g/mL}$ and $418.99 \pm 16.36 \mu\text{g/mL}^{-1}$, respectively. The IC_{50} value of the standard, eserine is $26.54 \pm 1.58 \mu\text{g/mL}$.

Table 4.7.1.1: Yield of crude methanol extracts and partitioned fractions of the leaf and fruit of *Musa acuminata* (Simili radjah)

Extract/fractions	Leaf		Fruit	
	Yield (g)	% Yield	Yield (g)	% Yield
Crude methanol (CME)	98.10	9.25	50.36	2.57
n-Hexane fraction (NHF)	51.85	61.00	2.91	8.82
Dichloromethane fraction (DCMF)	1.43	1.68	0.68	2.06
Ethylacetate fraction (EAF)	11.50	13.53	1.15	3.48
n-Butanol fraction (NBF)	4.20	4.94	2.10	6.36
Aqueous methanol fraction (AMF)	5.47	6.44	12.86	38.97

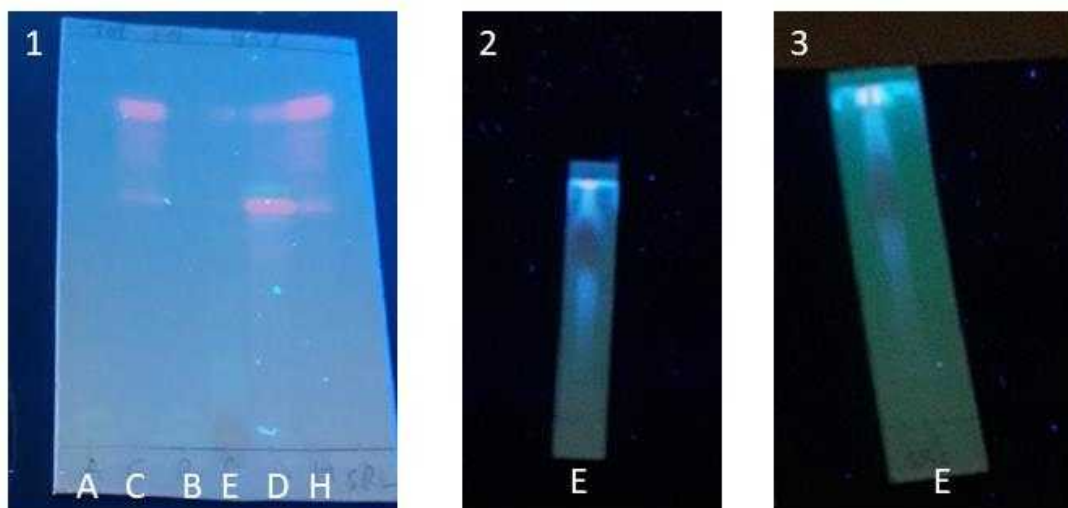


Figure 4.7.2.1: Thin layer chromatograms of *Musa acuminata* (Simili radjah, ABB) leaf fractions at wavelength 366 nm (A = Aqueous methanol fraction, C = Crude methanol extract, B = N-butanol fraction, E = Ethylacetate fraction, D = Dichloromethane fraction and H = N-hexane fraction). Plate 1: (Toluene: Ethanol; 4: 1) Plate 2: TLC of Ethyl acetate fraction using Methanol: Toluene: Acetic acid (3: 2: 0.8) Plate 3: TLC of Ethyl acetate fraction using Methanol: Toluene: Acetic acid (3: 2: 1.2)

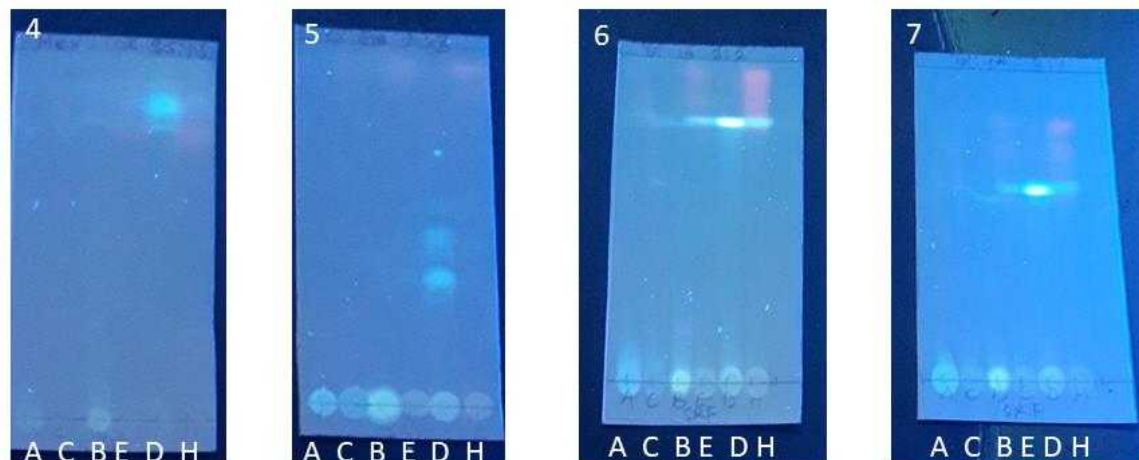


Figure 4.7.2.2: Thin layer chromatograms of *Musa acuminata* (Simili radjah, ABB) fruit fractions at wavelength 366 nm (A = Aqueous methanol fraction (AMF), C = Crude methanol extract (CME), B = *n*-butanol fraction (NBF), E = Ethylacetate fraction (EAF), D = Dichloromethane fraction (DCM) and H = *n*-hexane fraction (NHF)). Plate 4: Hex: Me 3.5: 1; Plate 5: Hex: EA 2: 3; Plate 6: Toluene: Ethanol 3: 2; Plate 7: Toluene: Ethanol 4: 1

Table 4.7.3.1.1: Total phenolic content (TPC) and DPPH• antioxidant activity of the leaf and fruit crude extract and fractions of *Musa acuminata* (Simili radjah)

S/N	Fractions	DPPH• IC ₅₀ (µg/mL)	TPC (mgGAE/g)
1	SRL CME	109.71 ± 3.04 ^c	343.08 ± 2.43 ^d
2	SRL NHF	211.82 ± 1.61 ^f	85.38 ± 3.53 ^f
3	SRL DCM	98.13 ± 1.15 ^d	187.73 ± 6.13 ^e
4	SRL EAF	8.98 ± 0.37 ^a	911.88 ± 1.67 ^a
5	SRL NBF	60.67 ± 3.18 ^c	404.83 ± 5.65 ^b
6	SRL AMF	35.09 ± 7.60 ^b	366.15 ± 7.05 ^c
7	SRF CME	323.45 ± 6.63 ⁱ	70.21 ± 6.71 ^g
8	SRF NHF	589.76 ± 7.80 ^k	12.58 ± 0.36 ^j
9	SRF DCM	226.49 ± 3.40 ^g	36.02 ± 3.33 ⁱ
10	SRF EAF	260.86 ± 6.06 ^h	55.26 ± 1.33 ^h
11	SRF NBF	319.72 ± 2.46 ⁱ	44.57 ± 2.23 ⁱ
12	SRF AMF	456.59 ± 7.26 ^j	43.08 ± 7.22 ⁱ

Values are expressed as mean ± SEM (n = 3). Means with the same letter along the same column are not significantly different at (P < 0.05). IC₅₀ of the standard, gallic acid is 4.07 ± 1.17 µg/mL.

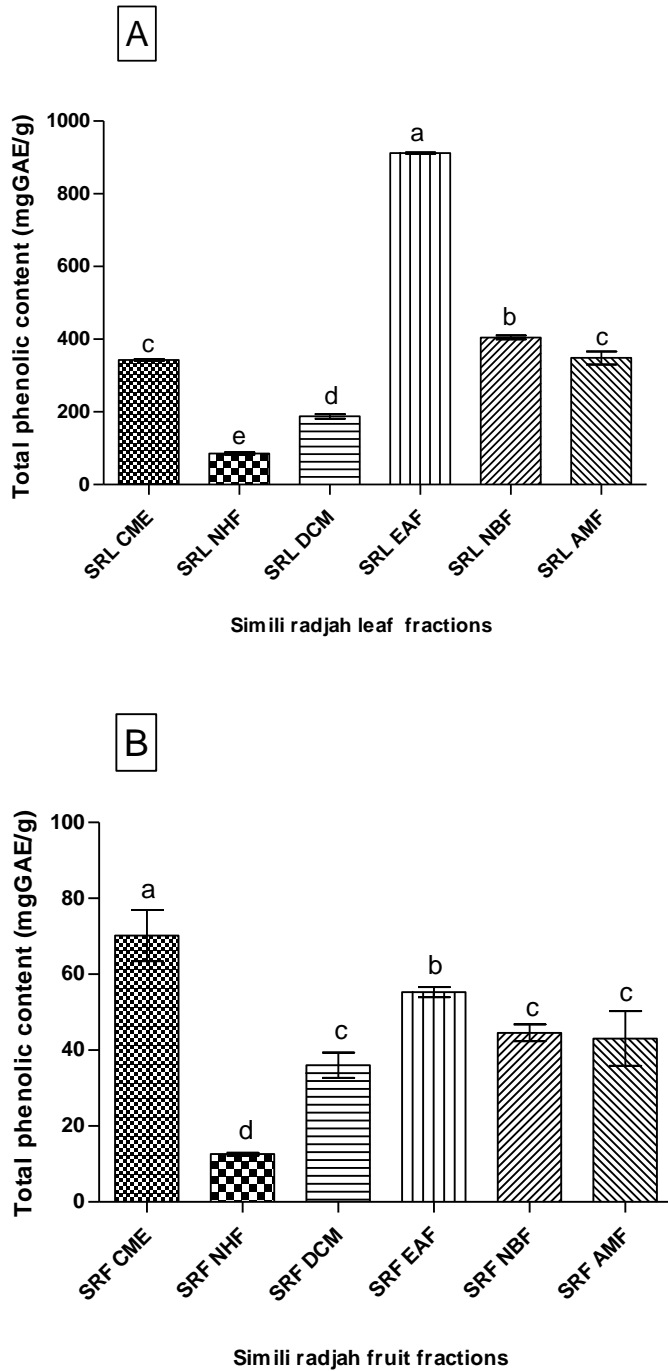


Figure 4.7.3.1.1: Total phenolic content of leaf (A) and fruit (B) fractions of *Musa acuminata* (Simili radjah). Bars with different letters are significantly different from each other ($p < 0.05$).

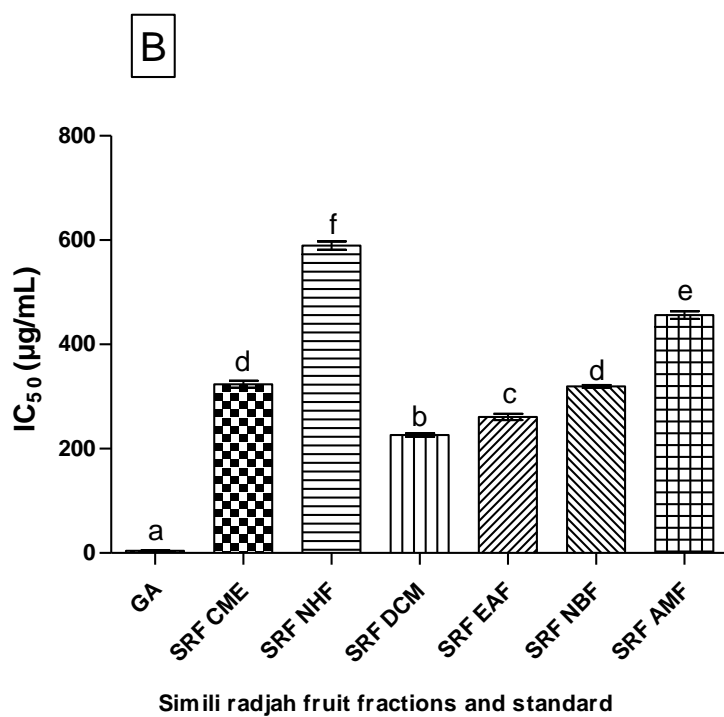
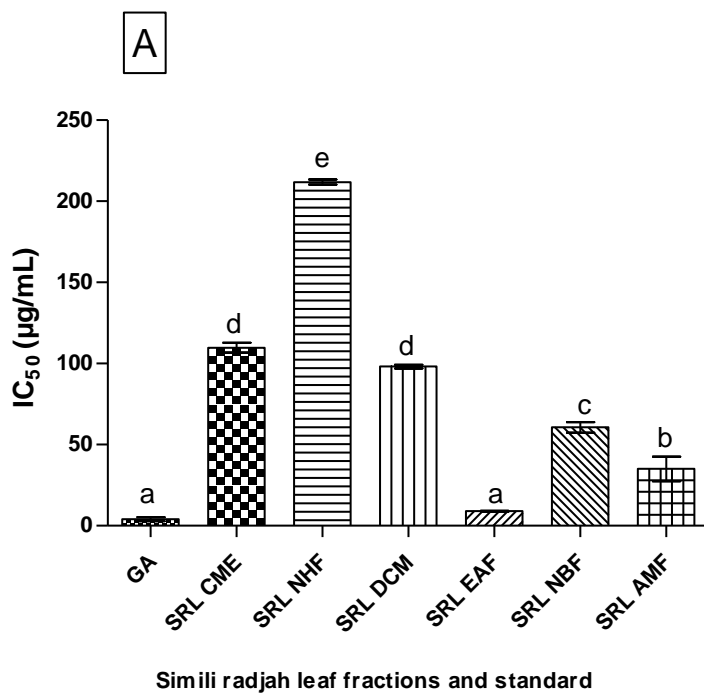


Figure 4.7.3.1.2: DPPH• radical scavenging activity of leaf (A) and fruit (B) fractions of *Musa acuminata* (Simili radjah). Bars with different letters are significantly different from each other ($p < 0.05$)

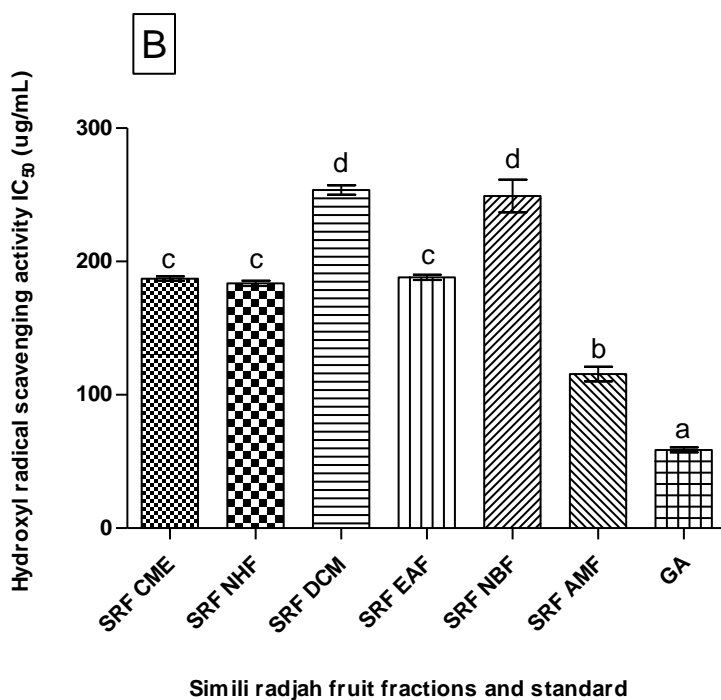
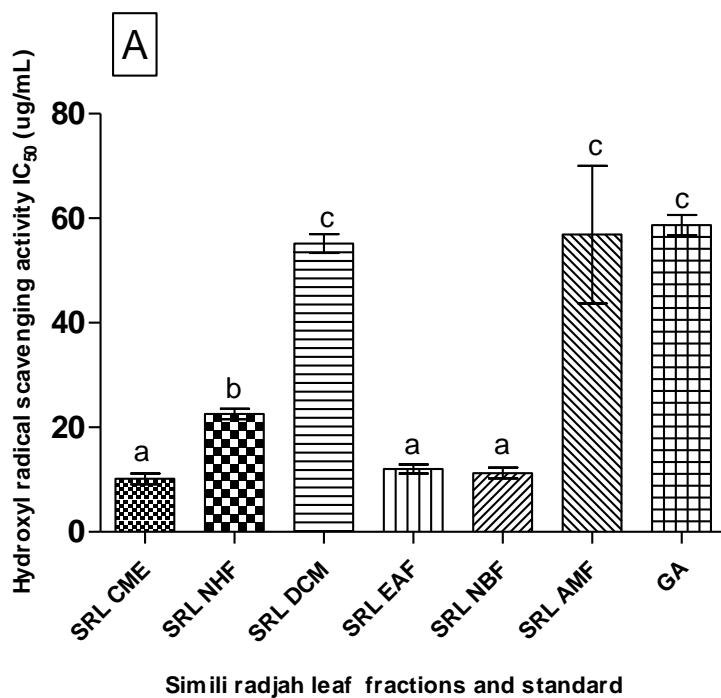


Figure 4.7.3.2.1: Hydroxyl radical scavenging activity of leaf (A) and fruit (B) fractions of *Musa acuminata* (Simili radjah). Bars with different letters are significantly different from each other ($p < 0.05$).

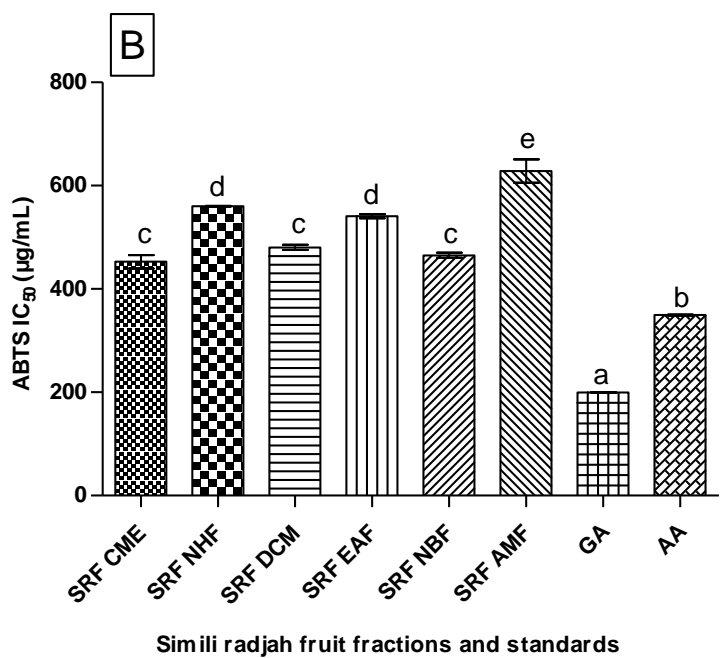
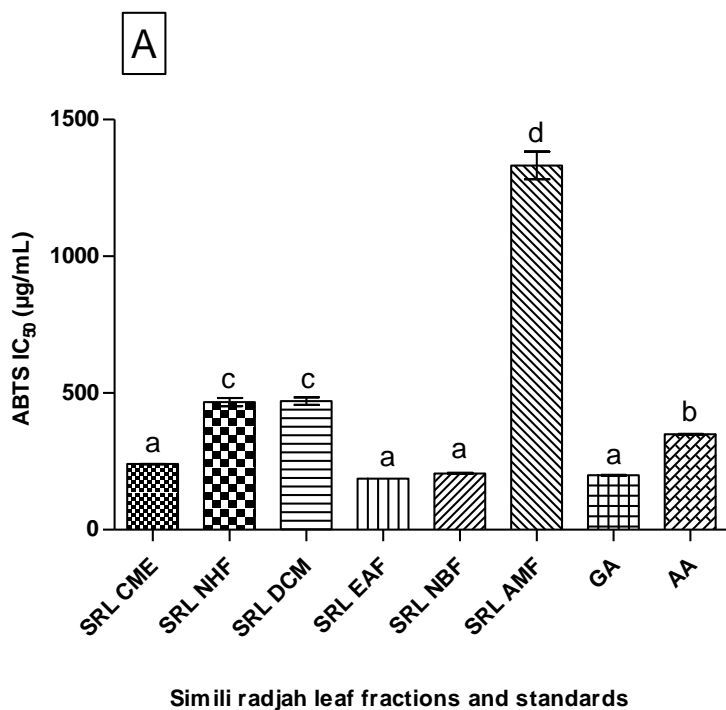


Figure 4.7.3.2.2: ABTS radical scavenging activity of leaf (A) and fruit (B) fractions of *Musa acuminata* (Simili radjah). Bars with different letters are significantly different from each other ($p < 0.05$).

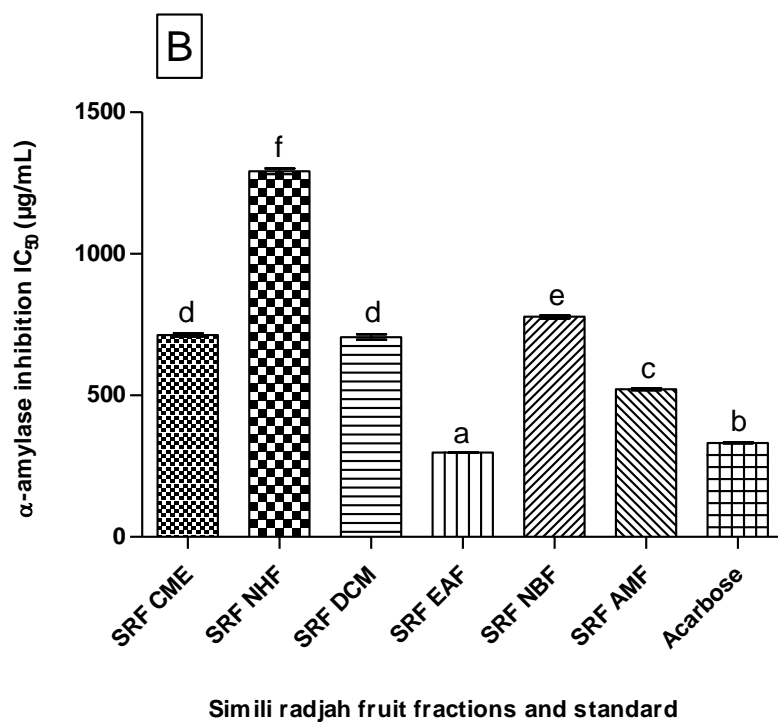
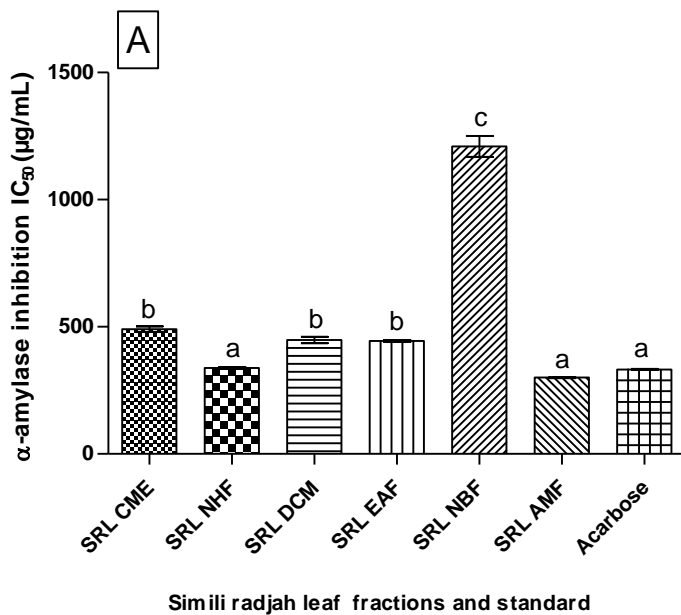


Figure 4.7.3.3.1: Alpha-amylase inhibitory activity of leaf (A) and fruit (B) fractions of *Musa acuminata* (Simili radjah). Bars with different letters are significantly different from each other ($p < 0.05$).

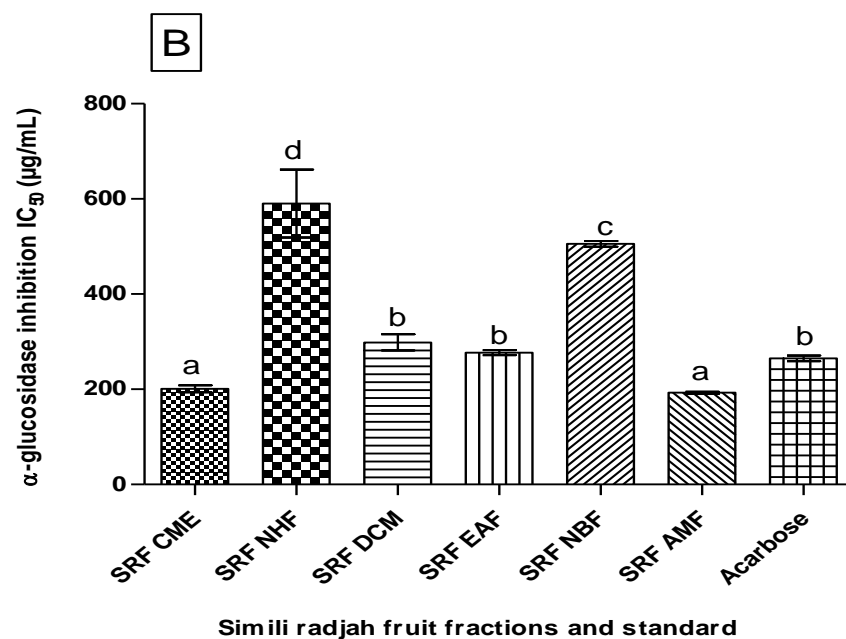
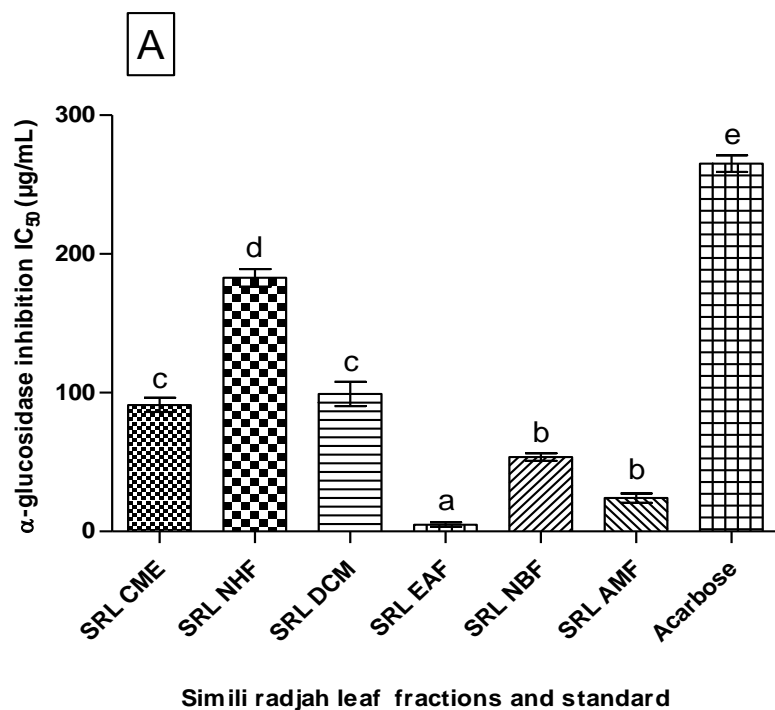


Figure 4.7.3.3.2: Alpha-glucosidase inhibitory activity of leaf (A) and fruit (B) fractions of *Musa acuminata* (Simili radjah). Bars with different letters are significantly different from each other ($p < 0.05$).

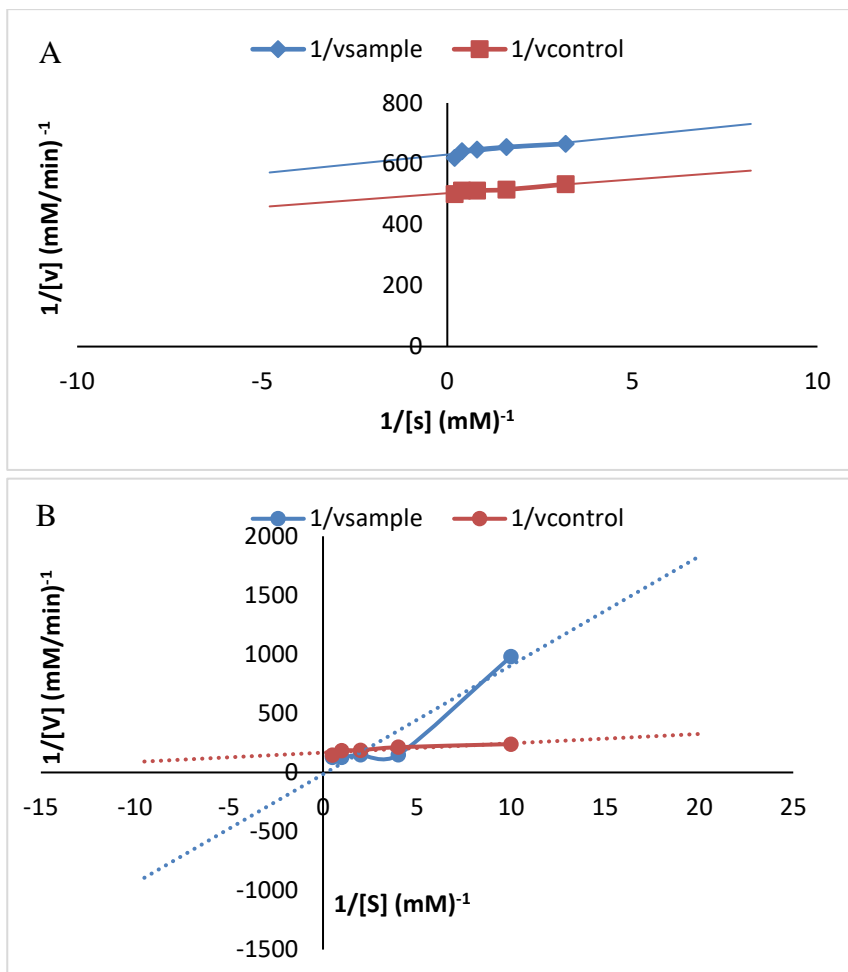


Figure 4.7.3.3.3: Lineweaver-Burk plot showing a non-competitive mode of inhibition of α -amylase (A) and uncompetitive kinetics of inhibition of α -glucosidase (B) by methanol crude extract of the fruit of *Musa acuminata* (Simili radjah).

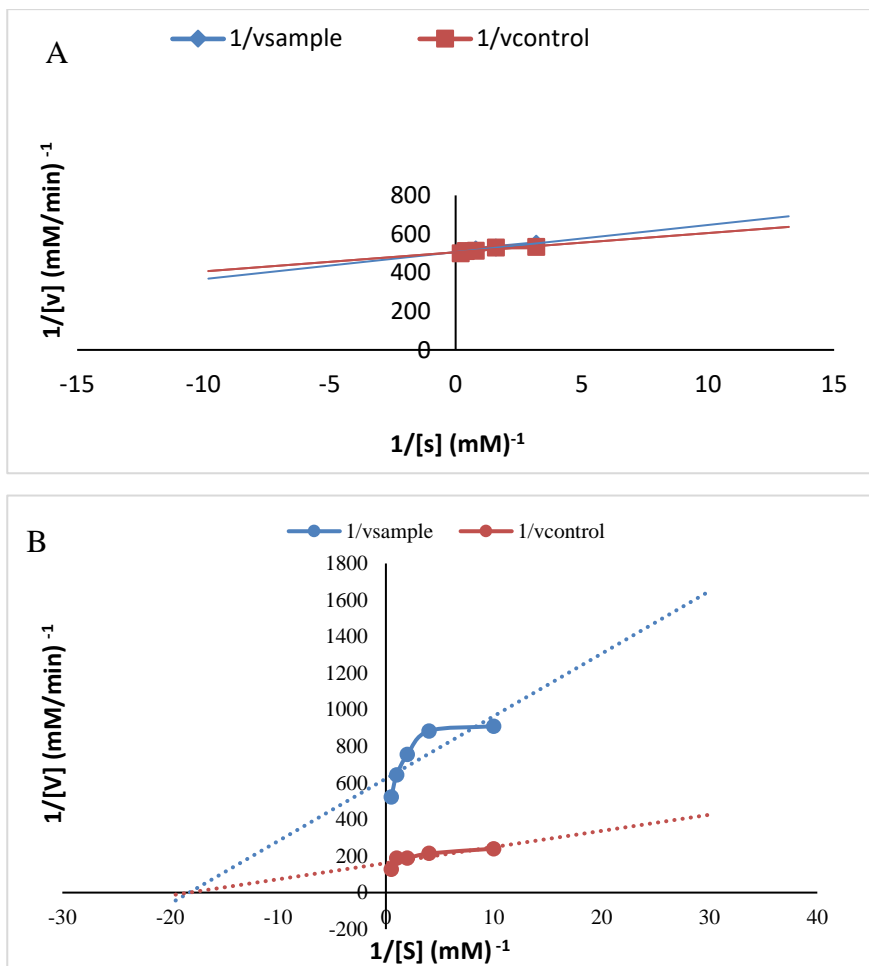


Figure 4.7.3.3.4: Lineweaver-Burk plot showing a competitive mode of inhibition of α -amylase (A) and uncompetitive kinetics of inhibition of α -glucosidase (B) by ethyl acetate fraction of the leaf of *Musa acuminata* (Simili radjah).

Table 4.7.3.4.1: Anti-inflammatory activity of *Musa acuminata* (Simili radjah) leaf and fruit fractions

S/N	Fractions	15-LOX inhibition IC ₅₀ (µg/mL)
1	SRL CME	272.36 ± 49.57 ^e
2	SRL NHF	768.08 ± 94.91 ^g
3	SRL DCM	1323.12 ± 166.29 ^h
4	SRL EAF	43.07 ± 11.29 ^a
5	SRL NBF	34.12 ± 2.59 ^a
6	SRL AMF	44.97 ± 14.34 ^{ab}
7	SRF CME	72.33 ± 3.36 ^b
8	SRF NHF	456.68 ± 37.65 ^f
9	SRF DCM	149.54 ± 12.20 ^c
10	SRF EAF	241.78 ± 43.60 ^d
11	SRF NBF	440.68 ± 56.37 ^f
12	SRF AMF	133.42 ± 30.29 ^c

Values are expressed as mean ± SEM (n = 3). Means with the same letter along the same column are not significantly different at (P < 0.05). IC₅₀ of the 15-LOX positive control, quercetin and indomethacin are 54.75 ± 17.07 µg/mL and 229.19 ± 33.24 µg/mL, respectively.

Table 4.7.3.5.1: Anticholinesterase activity of *Musa acuminata* (Simili radjah) leaf and fruit fractions

S/N	Fractions	Acetylcholinesterase inhibition IC ₅₀ (µg/mL)
1	SRL CME	530.93 ± 24.36 ^c
2	SRL NHF	1709.00 ± 5.20 ^h
3	SRL DCM	627.38 ± 11.17 ^e
4	SRL EAF	404.42 ± 8.00 ^a
5	SRL NBF	603.07 ± 5.17 ^d
6	SRL AMF	698.75 ± 29.08 ^f
7	SRF CME	565.82 ± 23.01 ^c
8	SRF NHF	1848.67 ± 5.34 ⁱ
9	SRF DCM	1359.94 ± 1.56 ^g
10	SRF EAF	478.19 ± 20.64 ^b
11	SRF NBF	418.99 ± 16.36 ^a
12	SRF AMF	698.75 ± 29.08 ^f

Values are expressed as mean ± SEM (n = 3). Means with the same letter along the same column are not significantly different at (P < 0.05). IC₅₀ value of the positive control, eserine is 26.54 ± 1.58 µg/mL.

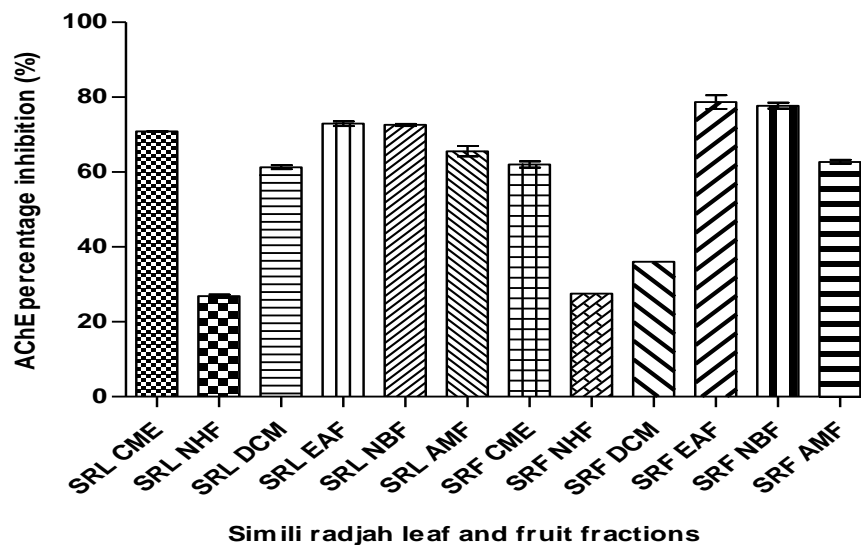


Figure 4.7.3.5.1: Acetylcholinesterase percentage inhibition of *Musa acuminata* (Simili radjah) leaf and fruit fractions at 1 mg/mL

4.7.4 Column chromatography of leaf ethyl acetate sub-fractions of *Musa acuminata* (Simili radjah) and *in vitro* antioxidant and antidiabetic evaluation

A total of 220 fractions (50 mL eluates) were collected from the column chromatography using gradient elution of *n*-hexane: ethyl acetate and ethyl acetate: methanol in increasing polarity and then pooled to 11 sub-fractions (A – K). The DPPH• antioxidant activity and TPC of the 11 sub-fractions were determined as reported in Table 4.7.4.1 and Plate 4.7.4.1. Sub-fractions H with good antioxidant activity and highest yield was loaded on sephadex (LH-20) thin column for further purification and a total of 83 fractions were collected and pooled to 11 sub-fractions (HA – HK). Sub-fractions HB, HC and HD were chosen for prep-TLC and isolation (Fig. 4.7.4.1). The TPC and TFC, DPPH• antioxidant activity, alpha-amylase and alpha-glucosidase inhibition of the H compounds are reported in Table 4.7.4.3. The isolate HD₁ with a high TFC and the highest antioxidant activity was confirmed to consist of flavonoids by spraying with AlCl₃.

4.7.5 Identification and characterisation of HD₁ (compounds **12 and **13**) using High performance thin layer chromatography (HPTLC), HPTLC-high resolution mass spectrometry (HRMS) and Nuclear magnetic resonance (NMR)**

HPTLC separation revealed that HD₁ comprises two flavonoids with close R_f values (Figure 4.7.5.1). The two flavonoid bands were characterised by HRMS after online elution via an elution head-based interface using electron spray ionisation (ESI) method. The mass spectra of the compounds are shown in Figures 4.7.5.2 and 4.7.5.3. The Table 4.7.5.1 shows the base peak, calculated mass and mass error of the two compounds. Spotting HD₁ isolates alongside the standard bought from Sigma confirmed their identity as kaempferol-3-*O*-rutinoside (**12**) and rutin (**13**) (Fig 4.7.5.4). The proton (¹H), ¹³C NMR and 2D NMR spectra of the two compounds are summarised in Tables 4.7.5.2 and 4.7.5.3 while their spectral details are presented in appendix, Figures 29-43. Compounds (**12**) and (**13**) were shown to have antioxidant activity and alpha-glucosidase inhibitory activity but no cholinesterase inhibitory activity (Fig. 4.7.5.5). The structures of the two compounds elucidated from the NMR spectroscopy are presented in Figure 4.7.5.6. Quercetin-3-*O*-

rutinoside has higher antioxidant and antidiabetic activities than kaempferol-3-*O*-rutinoside (Table 4.7.5.4).

Table 4.7.4.1: Ethyl acetate sub-fractions obtained by silica gel column chromatography: colour, yield and means of TPC and DPPH• antioxidant activity

Name of sub-fraction	Range of pooled fractions	Characteristic colour of sub-fraction	Yield (mg)	Total phenolic content (mgGAE/g)	DPPH• antioxidant activity IC ₅₀ (µg/mL)
A	1-37	Sticky and greenish	60.00	356.58 ± 3.29 ^g	1214.93 ± 86.92 ^h
B	38-40	Sticky dark green	12.40	517.21 ± 8.08 ^f	244.19 ± 7.20 ^f
C	41-42	Light green	2.78	463.49 ± 11.51 ^f	272.90 ± 2.73 ^f
D	43-70	Light brown	200.50	1091.78 ± 16.14 ^e	400.49 ± 10.31 ^g
E	71-92	Sticky brownish	390.20	2364.25 ± 0.55 ^a	175.96 ± 2.74 ^d
F	93	Sticky brownish	36.20	2026.54 ± 7.96 ^b	163.38 ± 2.45 ^d
G	94-98	Yellowish brown	1615.60	1600.55 ± 5.23 ^c	184.48 ± 2.87 ^e
H	99-108	Light brown powder	3261.90	1227.74 ± 18.32 ^d	111.51 ± 0.87^c
I	109-116	Yellowish brown	418.30	1571.49 ± 18.25 ^c	56.89 ± 0.32^a
J	117-179	Sticky brownish	708.80	536.40 ± 8.56 ^f	176.64 ± 0.93 ^d
K	180-220	Sticky brownish	544.00	1505.15 ± 29.88 ^c	64.86 ± 0.55^b



Plate 4.7.4.1: DPPH• antioxidant activity of pooled ethyl acetate column sub-fractions A – K of *Musa acuminata* (Simili radjah) leaf

Table 4.7.4.2: Yield of sub-fractions from H loaded on sephadex column

S/N	Sub-fractions	Yield (mg)
1	HA (1 – 5)	12.35
2	HB (6 – 7)	28.80
3	HC (8 – 11)	221.10
4	HD (12 – 14)	1239.90
5	HE (15)	27.50
6	HF (16 – 23)	609.00
7	HG (24 – 27)	113.90
8	HH (28 – 31)	44.30
9	HI (32 – 41)	35.50
10	HJ (42 – 55)	32.00
11	HK (56 – 83)	869.00

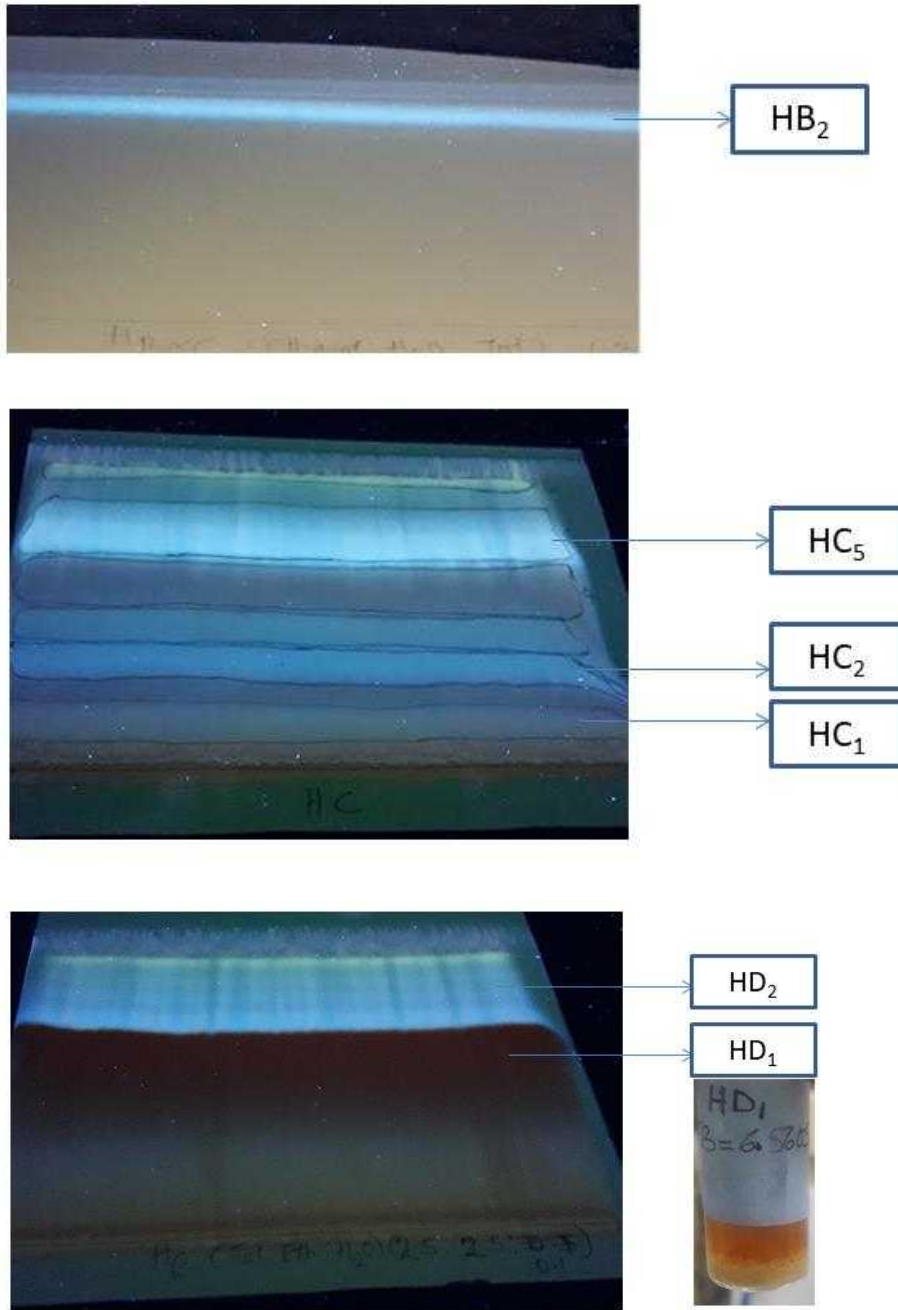


Figure 4.7.4.2: Preparative Thin layer chromatography of HB, HC and HD

Table 4.7.4.3: Biological activities of compounds in the sub-fraction H: means of TPC, TFC, DPPH• antioxidant activity, α -GLD and α -AML inhibitory activities

Compounds	Yield (mg)	TPC (mg GAE/g)	TFC (mg QE/g)	DPPH• IC ₅₀ (μ g/mL)	α -Glucosidase inhibition IC ₅₀ (μ g/mL)	α -Amylase inhibition IC ₅₀ (μ g/mL)
HB ₂	3.7	24.57 \pm 3.00 ^c	2.86 \pm 0.64 ^b	355.60 \pm 32.32 ^b	174.80 \pm 13.09 ^c	135.45 \pm 2.23 ^d
HC ₁	36.4	34.94 \pm 0.87^a	3.15 \pm 0.21^b	389.47 \pm 26.11 ^b	129.29 \pm 11.28 ^b	84.27 \pm 4.11^b
HC ₂	30.9	27.67 \pm 1.51 ^b	2.82 \pm 0.07 ^b	277.08 \pm 9.66 ^a	127.58 \pm 14.67^b	16.10 \pm 1.85^a
HC ₅	33.0	27.67 \pm 0.58 ^b	0.74 \pm 0.34 ^c	259.61 \pm 6.84^a	138.51 \pm 9.51 ^b	126.50 \pm 0.16 ^d
HD ₁	484.0	31.74 \pm 0.87^a	6.91 \pm 0.04^a	236.47 \pm 7.17^a	85.26 \pm 2.91^a	102.47 \pm 1.02 ^c
HD ₂	55.3	22.25 \pm 0.48 ^c	2.86 \pm 0.68 ^b	465.96 \pm 21.29 ^c	224.50 \pm 21.05 ^d	97.84 \pm 1.71 ^{bc}

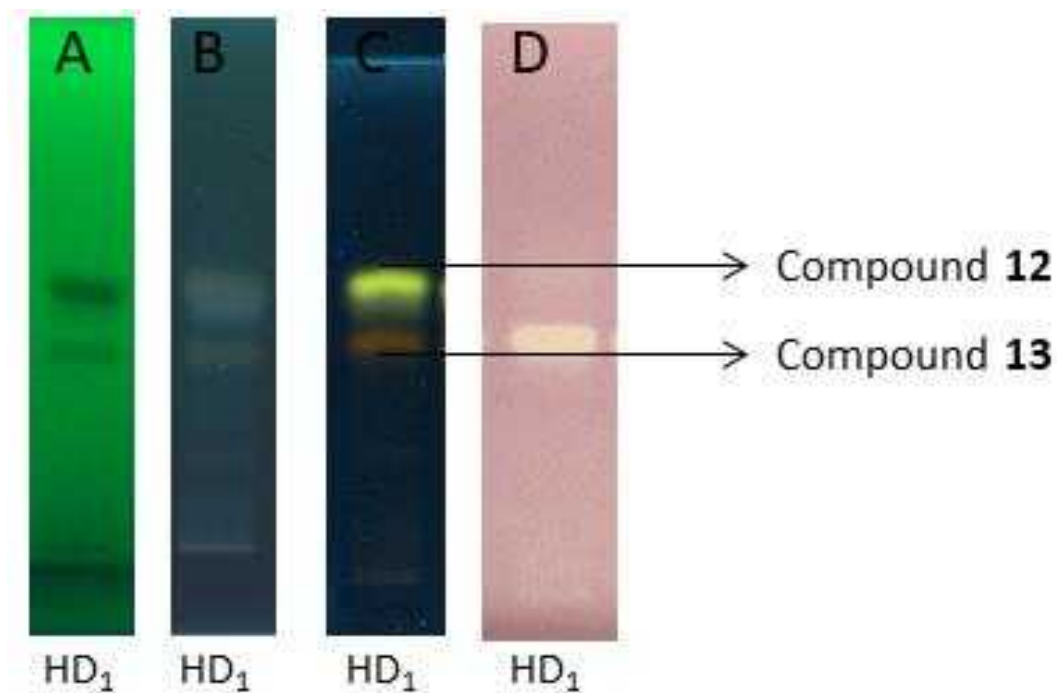


Figure 4.7.5.1: HD₁ on HPTLC fluorescence plate (Silica gel 60 F₂₅₄) developed in ethyl acetate: toluene: formic acid: H₂O (3.4: 0.5: 0.7: 0.5) and (A) viewed under 254 nm (B) viewed under 366 nm (C) derivatised in natural products reagents and viewed under 366 nm (D) derivatised in DPPH• and viewed under white light (transmittance mode).

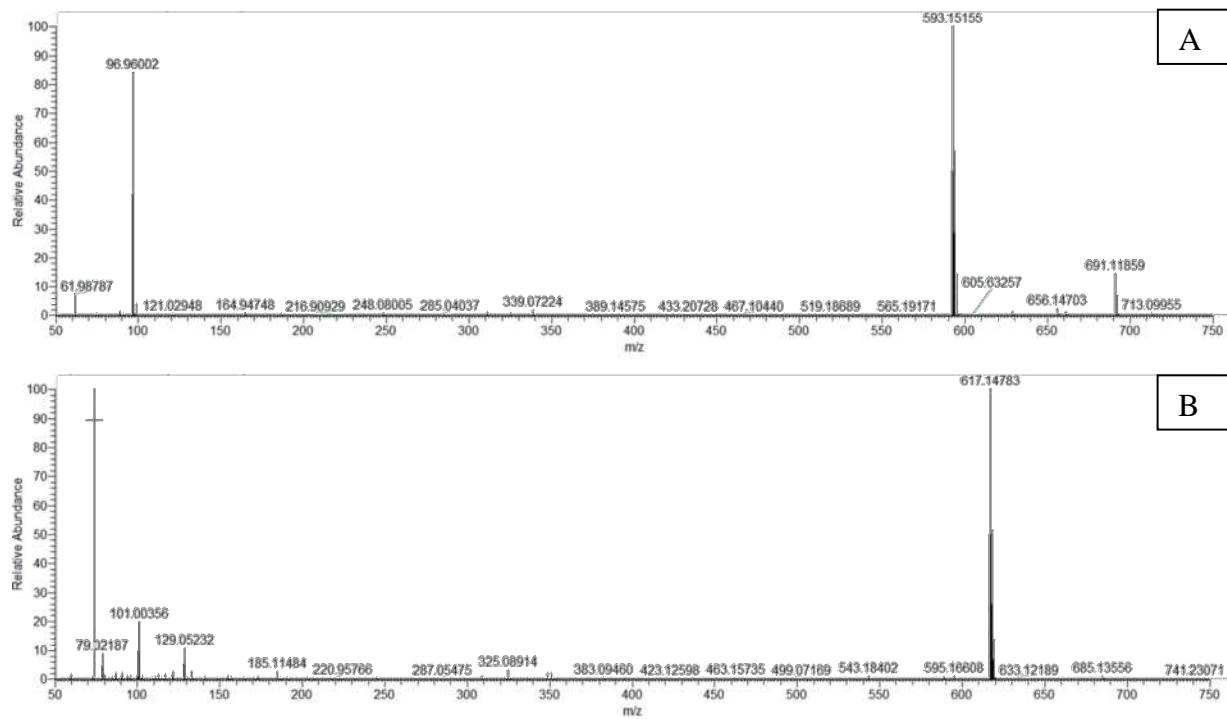


Figure 4.7.5.2: HPTLC-HRMS spectra of compound (12) recorded in the (A) ESI⁻ mode (B) ESI⁺ mode

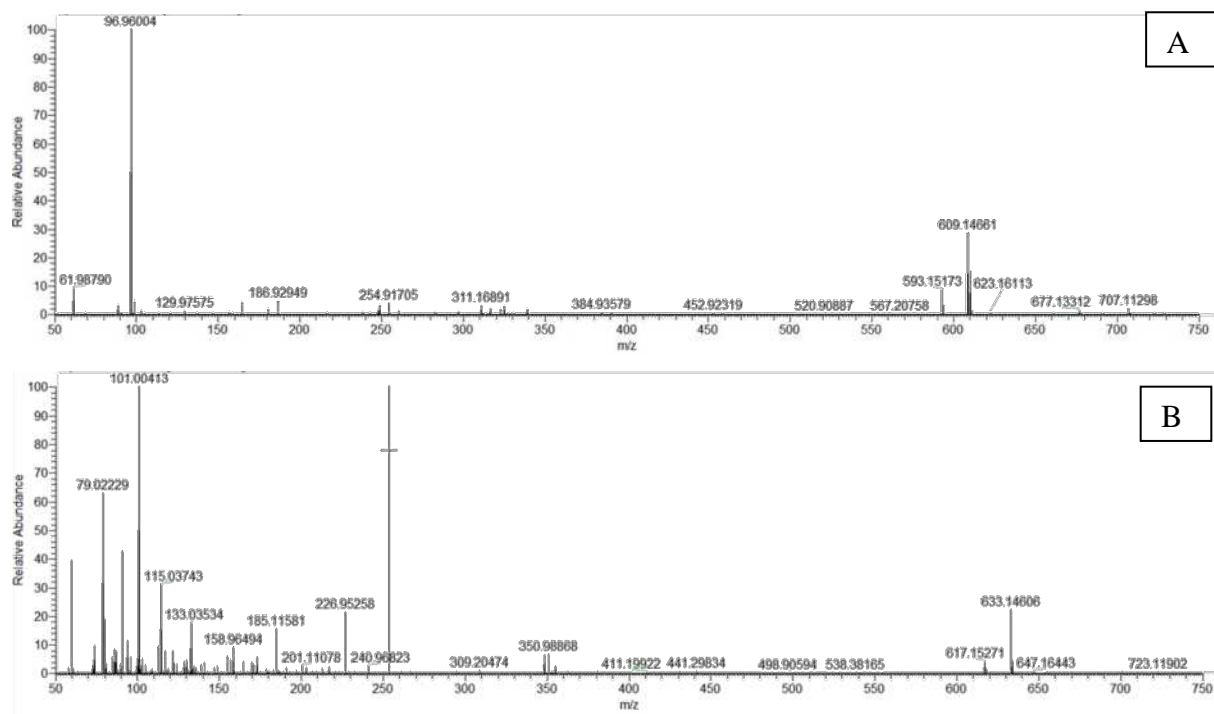


Figure 4.7.5.3: HPTLC-HRMS spectra of (**13**) recorded in the (A) ESI⁻ mode (B) ESI⁺ mode

Table 4.7.5.1: HPTLC-HRMS data of HD₁ compounds

Compound	Observed mass	Assignment	Sum formular	Mass error	Intens ity	Calculated mass	Exact formular	Identity
12	593.1515	[M-H] ⁻	C ₂₇ H ₂₉ O ₁₅ ⁻	2.251	8E7	594.1585	C ₂₇ H ₃₀ O ₁₅	Kaempferol-3- <i>O</i> -rutinoside
	691.1186	[M-HSO ₄] ⁻			1E7			
	617.1478	[M+Na] ⁺	C ₂₇ H ₃₀ O ₁₅ Na	2.299	2E8			
13	609.1466	[M-H] ⁻	C ₂₇ H ₂₉ O ₁₆ ⁻	0.5	5E6	610.1534	C ₂₇ H ₃₀ O ₁₆	Rutin
	633.1461	[M+Na] ⁺			9E6			

Table 4.7.5.2: ^1H , ^{13}C NMR and Distortionless Enhancement by Polarisation Transfer of Kaempferol-3-*O*-rutinoside (**12**)

No.	^1H $\delta_{\text{H}}^{\text{O}}$	$\delta_{\text{H}}^{\text{L}}$	^{13}C ($\delta_{\text{C}}^{\text{O}}$)	$\delta_{\text{C}}^{\text{L}}$	Carbon Type
2	-	-	159.4	159.4	C
3	-	-	135.5	135.5	C
4	-	-	179.3	179.4	C
5	-	-	161.5	163.0	C
6	6.21 (brs)	6.25 (d, $J = 2.1$)	100.1	100.1	CH
7	-	-	166.3	166.3	C
8	6.40 (brs)	6.45 (d, $J = 2.1$)	95.1	95.0	CH
9	-	-	158.5	158.6	C
10	-	-	105.6	105.6	C
1'	-	-	122.7	122.8	C
2'	8.06 (d, $J = 7.4$)	8.11 (d, $J = 8.9$)	132.4	132.4	CH
3'	6.90 (d, $J = 7.4$)	6.93 (d, $J = 8.9$)	116.2	116.1	CH
4'	-	-	161.5	161.5	C
5'	6.90 (d, $J = 7.4$)	6.93 (d, $J = 8.9$)	116.2	116.1	CH
6'	8.06 (d, $J = 7.4$)	8.11 (d, $J = 8.9$)	132.4	132.4	CH
1'' Glucose moiety	5.11 (d, $J = 7.4$)	5.17 (d, $J = 7.4$)	102.4	104.6	CH
2''	3.45 (m)	3.41-3.52 (m)	75.7	75.8	CH
3''	3.45 (m)	3.41-3.52 (m)	78.2	78.2	CH
4''	3.24 (m)	3.28-3.34 (m)	71.4	71.4	CH
5''	3.31 (m)	3.41-3.52 (m)	77.2	77.2	CH
6''	3.82 (d, $J = 10.8$) 3.31 (m)	3.85 (dd, $J = 11.0,$ 1.4) 3.41-3.52 (m)	69.7	68.6	CH ₂
1''' Rhamnose moiety	4.52 (brs)	4.56 (d, $J = 1.4$)	104.7	102.4	CH
2'''	3.55 (m)	3.67 (dd, $J = 9.5,$ 3.5)	72.3	72.1	CH
3'''	3.29 (m)	3.56 (dd, $J = 9.5,$ 3.5)	73.9	72.3	CH
4'''	3.65 (m)	3.28-3.34 (m)	72.3	73.9	CH
5'''	3.29 (m)	3.41-3.52 (m)	72.1	69.7	CH
6'''	1.13 (d, $J = 6.1$)	1.16 (d, $J = 6.2$)	17.9	17.9	CH ₃

Assignments were established from ^1H , ^{13}C and 2D NMR experiments; ^Oobserved spectrum; ^Lliterature value (Ganbaatar *et al.*, 2015)

Table 4.7.5.3: ^1H , ^{13}C NMR and Distortionless Enhancement by Polarisation Transfer of Quercetin-3-*O*-rutinoside (**13**)

No.	^1H $\delta_{\text{H}}^{\text{O}}$	$\delta_{\text{H}}^{\text{L}}$	^{13}C ($\delta_{\text{C}}^{\text{O}}$)	$\delta_{\text{C}}^{\text{L}}$	Carbon Type
2	-		159.4	159.5	C
3	-		135.5	135.7	C
4	-		179.3	179.5	C
5	-		162.9	163.2	C
6	6.21 (brs)	6.26 (d, $J = 2.1$)	100.1	100.0	CH
7	-		166.3	166.2	C
8	6.40 (brs)	6.45 (d, $J = 2.1$)	95.1	95.0	CH
9	-		159.4	158.5	C
10	-		105.6	105.7	C
1'	-		122.7	123.2	C
2'	7.69 (d, $J = 7.4$)	7.71 (d, $J = 2.2$)	117.7	117.8	CH
3'	-	-	146.0	146.0	C
4'	-	-	150.4	150.4	C
5'	6.90 (d, $J = 7.4$)	6.92 (d, $J = 8.4$)	116.2	116.2	CH
6'	7.65 (d, $J = 7.4$)	7.68 (dd, $J = 8.4, 2.2$)	123.6	123.7	CH
1'' Glucose moiety	5.11 (d, $J = 7.4$)	5.15 (d, $J = 7.8$)	104.8	104.8	CH
2''	3.45 (m)	3.38-3.53 (m)	75.7	75.9	CH
3''	3.45 (m)	3.38-3.53 (m)	77.2	77.4	CH
4''	3.27 (m)	3.29-3.33 (m)	71.4	71.5	CH
5''	3.31 (m)	3.38-3.53 (m)	78.1	78.3	CH
6''	3.82 (d, $J = 10.8$)	3.84 (dd, $J = 11.1, 1.5$)	68.6	68.7	CH2
	3.34 (m)	3.38-3.53 (m)			
1''' Rhamnose moiety	4.52 (brs)	4.56 (d, $J = 1.5$)	102.4	102.5	CH
2'''	3.52 (m)	3.67 (dd, $J = 3.4, 1.6$)	72.2	72.2	CH
3'''	3.25 (m)	3.58 (dd, $J = 9.5, 3.5$)	72.3	72.4	CH
4'''	3.65 (m)	3.29-3.33 (m)	73.9	74.1	CH
5'''	3.28 (m)	3.38-3.53 (m)	69.7	69.8	CH
6'''	1.13 (d, $J = 6.1$)	1.16 (d, $J = 6.2$)	17.9	18.0	CH3

Assignments were established from ^1H , ^{13}C and 2D NMR experiments; ^Oobserved spectrum; ^Lliterature value (Al-Majmaie *et al.*, 2019)

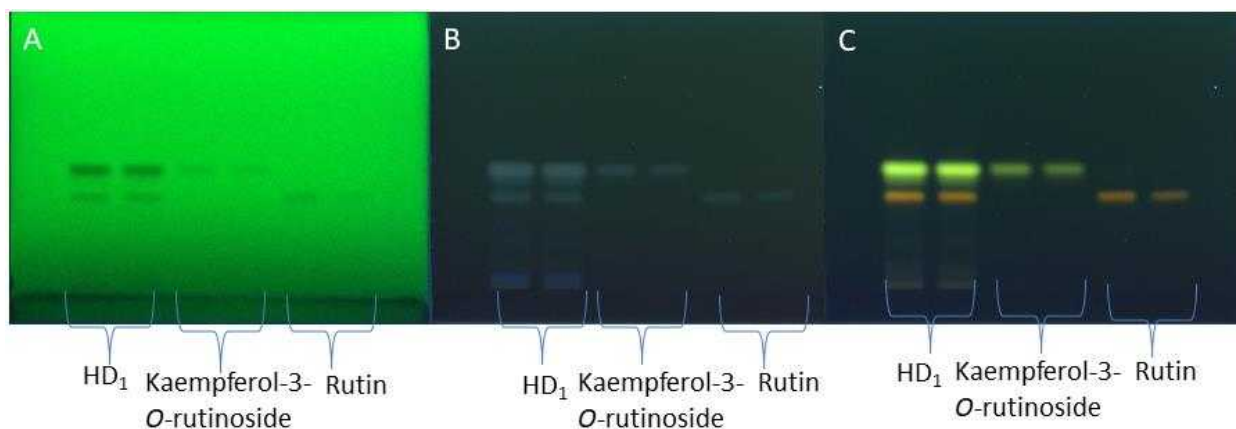


Figure 4.7.5.4: Confirmation of the two compounds in the subfraction HD₁ to be kaempferol-3-*O*-rutinoside (**12**) and rutin (**13**), having the same hR_F values of 32 and 25, respectively, as the standard compounds on the HPTLC plate documented at (A) UV 254 nm, (B) UV 366 nm and (C) after derivatisation with Neu's reagent at UV 366 nm.

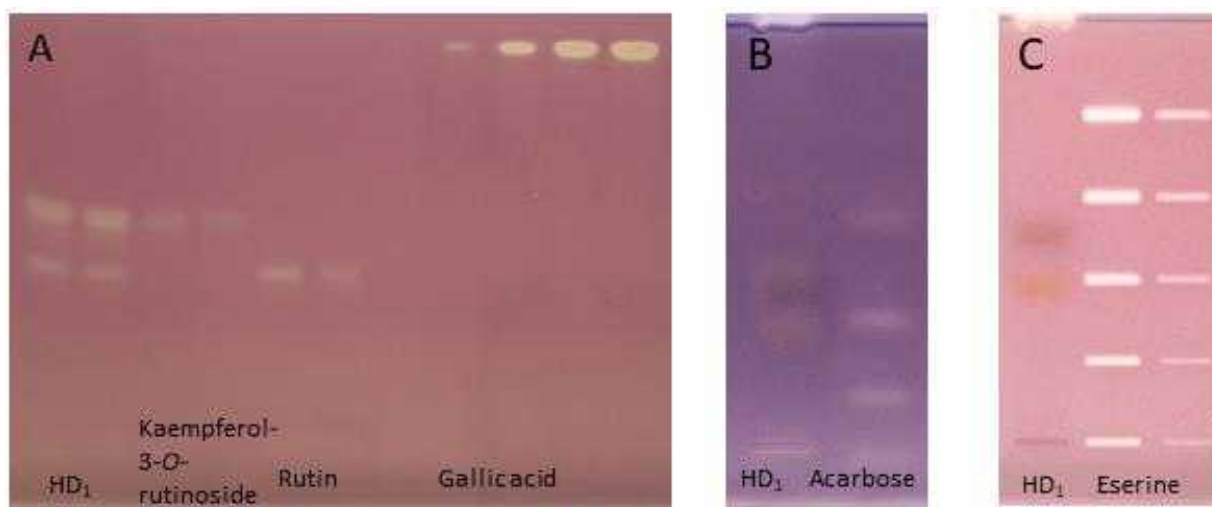


Figure 4.7.5.5: HPTLC-EDA autograms at white light illumination: Activities of the HD₁ isolates (**12** and **13**) detected by the (A) DPPH• radical scavenging, (B) α-glucosidase (C) and AChE assays (**12** and **13** showed no AChE inhibition)

Table 4.7.5.2: Mean antioxidant and antidiabetic activities ($n = 3$) of the compounds in HD₁ in comparison with the standards obtained by HPTLC densitometric measurement

Samples		Antioxidant activity (mg/g)	Antidiabetic activity (mg/g)
12	Kaempferol-3- <i>O</i> -rutinoside	372.81 ± 3.10	1.89
13	Quercetin-3- <i>O</i> -rutinoside	435.96 ± 5.42	3.61
Standards	Kaempferol-3- <i>O</i> -rutinoside	5150.87 ± 114.90	ND
	Quercetin-3- <i>O</i> -rutinoside	5556.08 ± 320.60	ND

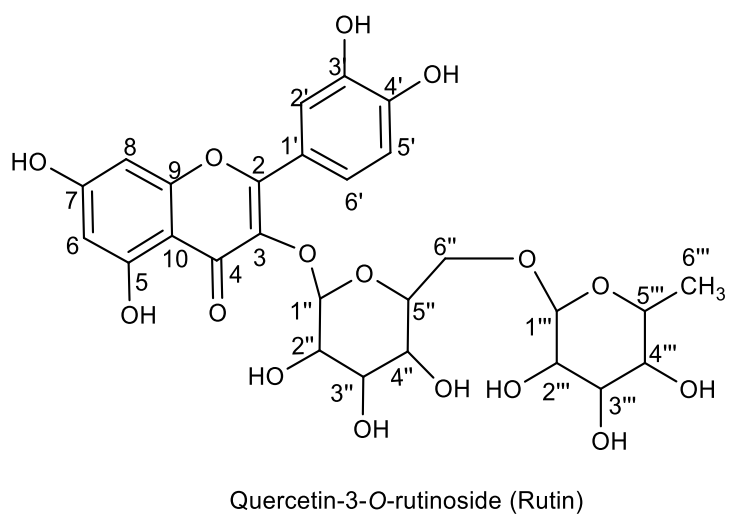
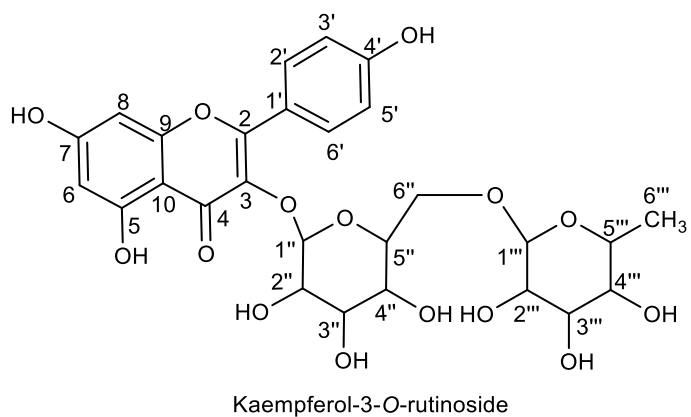


Figure 4.7.5.6: Molecular structures of the isolated compounds **12** and **13**

CHAPTER FIVE

DISCUSSIONS, CONCLUSIONS AND RECOMMENDATIONS

5.1 Discussion

5.1.1 Micropropagation and genetic fidelity assessment of the *Musa* spp. accessions

The result of the *in vitro* propagation confirmed the amenability of *Musa* species to *in vitro* plant tissue culture (PTC) technique. The routine protocol of the *in vitro* PTC laboratory of the genetic resources centre, IITA was successfully used for the micropropagation of the selected taxonomic reference accessions from IITA and *Musa sapientum* collected from the Botanical Garden, University of Ibadan. Fully-developed plantlets were obtained every 6-weeks subculture cycle (with root, shoot and leaves formation) using Murashige and Skoog media supplemented with 4.5 gL⁻¹ 6-Benzyl amino purine (BAP) and 0.18 mgL⁻¹ Indole acetic acid (IAA). The cultures were maintained under 25 °C temperature, 42 µmol/m²/s light intensity and 12 h photoperiod. Many other works have been reported on the micropropagation of *Musa* spp. especially from meristem which was used in this study (Kulkarni *et al.*, 2006; Makara *et al.*, 2010).

There was variation in the response of the different *Musa* spp. accessions, in terms of growth parameters. Some of the accessions grew comparatively very fast in the proliferation culture media while some accessions had a slow growth rate. It was noticed that the variation in the growth rate correlated with the genome groups of the accessions. Accessions, Foconah, P. Mas, Calcutta-4 and Simili radjah belonging to; AAB, AA, AAwild and ABB genome groups, respectively were the accession with the highest shoot length, number of leaves and number of shoots, while *Musa balbisiana* HND, Pelipita and Safet Velchi belonging to; BB, ABB and AABcv genome groups, respectively were the slow growing accessions (Table 4.1.1).

For the genetic fidelity and diversity study, the distribution of SNP markers on nuclear and mitochondrial genome, the distribution of minor allele frequency and the distribution of heterozygosity proportion gave the information about the polymorphism and heterozygosity of the SNP markers used for the study. They were able to depict variations in the banana genome used for the study. The genetic fidelity and molecular relationship among the accessions using DArTseq SNP analysis revealed that almost the entire *in vitro*-grown *Musa* species accessions were true-to-type, which simply means they are not genetically different from the parent plants. This was indicated by the neighbour joining tree where the *in vitro*-grown accessions were clustered together with their corresponding field accessions (Figure 4.2.4). This genetic similarity assessment of micropropagated material, confirming the absence of molecular variation with the field plants, is a prerequisite for the use of PTC technique for mass propagation of medicinal plants (Salvi *et al.*, 2001). The trueness-to-type of *in vitro* propagated *Musa* spp. accessions suggests that PTC can be reliably used for large-scale biomass production of *Musa* spp. plant materials within a relatively very short time and for the supply of secondary metabolites. The DArTseq SNP analysis also revealed the clustering of the accessions based on their genetic similarity. *Musa sapientum*, whose genome group was originally unknown, was clustered with the AAB bananas, suggesting that it belongs to the AAB genome group. Molecular markers have been widely used in a lot of crops and medicinal plants for genetic relationship analysis. Mishra *et al.* (2015) successfully propagated *Canna indica*, a medicinal plant, *in vitro*. They used molecular markers (ISSR and RAPD) to assess the trueness-to-type of the micropropagated plants and the *in vitro*-grown materials were reported to be true-to-type with the parent plants, showing monomorphic bands. Other molecular markers (SSR, ISSR, RAPD) have been used to assess the genetic fidelity of *Musa* species (Rout *et al.*, 2009; Sales and Butardo, 2014) but very few studies have used SNP markers for the assessment of genetic variation in *Musa* spp. Nowadays, SNP markers are the most widely accepted in worldwide molecular research (Rabbi *et al.*, 2015), validating the choice of using SNP markers generated from a high-throughput next-generation sequencing method, (DArTseq) to assess the genetic relationship of selected *Musa* spp. in this study.

5.1.2 Extraction yield and biological assays of field and *in vitro*-grown accessions

Methanol served as an efficient extraction solvent in this study. The extraction yield varied considerably among the different samples. The extraction yield of field samples ranged from 6.94% to 15.84%, while the extraction yield of micropropagated samples ranged from 16.54% to 64.00% (Table 4.3.1). This showed that *in vitro* propagated *Musa* species leaf can provide better extract yield than the field samples. This is in support of the utilisation of *in vitro* PTC techniques for the supply of plant materials for secondary metabolites extraction. Al-Manasrah (2012) reported a similar result where *Crataegus aronia* was successfully propagated *in vitro* and the *in vitro* leaves and callus gave higher extraction yield than the field leaves.

Total phenolic content (TPC) and total flavonoid content (TFC) varied considerably among the accessions. Many of the accessions had high phenolic content, ranging from 2.43 ± 0.30 to 124.52 ± 12.72 mgGAE/g of extract, while the TFC ranged from 0.40 ± 0.06 to 60.14 ± 6.30 mgQE/g of extract. Field and *in vitro*-grown samples of Simili radjah (ABB) had the highest TPC, while both field and *in vitro*-grown samples of *Musa balbisiana* Tani (BBwild), *Musa balbisiana* HND (BBwild) and Dole (ABB) had consistently low TPC and TFC (Table 4.4.3.1). Across all the tested accessions, *in vitro*-grown samples had higher TPC whereas, field-grown leaf samples had higher TFC.

All the samples showed a dose dependent DPPH• antioxidant activity, revealed by reduction of the purple coloured, stable DPPH• radical to the yellow-coloured diphenylpicrylhydrazine. Concentration values of the extract that can give 50% inhibition (IC₅₀) ranged from 10.68 ± 0.27 to 257.92 ± 2.25 µg/mL. *In vitro*-grown samples showed the highest antioxidant activity when compared to their field counterpart. Similar result was obtained from previous study (Ayoola *et al.*, 2017). Using the FRAP method, the trolox equivalent ranged from 4.34 ± 0.12 to 152.16 ± 2.80 mgTE/g of extract with *in vitro*-grown samples, also exhibiting higher antioxidant activity. However, *Musa balbisiana* Tani (BBwild) and *Musa balbisiana* HND (BBwild) showed low antioxidant potential in these assays.

Different antioxidant assay methods were employed because it is assumed that more than one assay would better reflect the antioxidant potential of a complex mixture of secondary metabolites such as plant extracts, which were used in this study (Brito *et al.*, 2014). Each assay would also contribute to the understanding of the mechanism of the antioxidant activity. The correlation between the antioxidant assays with the phytochemical composition among the field samples was generally lower than the correlation among the *in vitro*-grown samples, in line with the result obtained from the accessions tested in the previous study (Ayoola *et al.*, 2017). The result revealed a relatively good correlation between the DPPH• and FRAP assays among both the field ($r = 0.61$) and *in vitro* ($r = 0.66$) grown accessions (Table 4.4.4.1). For the *in vitro*-grown samples, there was a strong correlation between the total phenolic content (TPC) and antioxidant activity (DPPH•); as well as between TPC and ferric reducing antioxidant power (FRAP) but a weak correlation between TFC and DPPH•. Teixeira *et al.* (2017) also noticed a strong correlation between TPC and antioxidant assays in all their studied medicinal plants but a weak correlation between TFC and antioxidants. This indicates that other phenolic compounds, apart from the flavonoids, are responsible for the strong antioxidant capacity of the samples. For the anticholinesterase activity, most of the *in vitro*-grown samples gave better acetylcholinesterase (AChE) inhibitory activity than the field ones. Micropropagated Calcutta-4 (IC_{50} is $11.53 \pm 6.12 \mu\text{g/mL}$), showed better activity than even the standard, eserine (IC_{50} is $31.23 \pm 7.33 \mu\text{g/mL}$). There is paucity of information on the anticholinesterase activity of *Musa* spp. leaves. This result therefore is in support of the ethnomedicinal claims of the utilisation of *Musa* species in treatment of neurodegenerative disorders.

Generally, this study revealed that the *in vitro*-grown leaves possess higher phenolic content, antioxidant and anticholinesterase activity which were up to three times higher in some cases than the field samples. Puente-Garza *et al.* (2105) reported similar result from the micropropagated leaves of *Agave salvia*, a medicinal and commercial Mexican plant. They observed that the micropropagated leaves had a TPC and antioxidant activity, which were 30% and three times higher than the wild plants, respectively. Extracts of *in vitro* leaves of *Lessertia frutescence*, a South African medicinal plant, had abundant phenolics, flavonoids and alkaloids when compared to the field leaves (Shaik *et al.*, 2011). Phenolic

compounds are known to be triggered in plants as a response to stress condition (Almaráz-Abarca *et al.*, 2013). This could be the reason why *in vitro*-grown materials, which is exposed to many stresses (physical, chemical and biotic), had higher total phenolic content and antioxidant activity than the field materials.

5.1.3 Chemical profile of field, *in vitro* and acclimatised samples using high performance thin layer chromatography

A very polar mobile phase comprising ethyl acetate: toluene: formic acid: water (3.4: 0.5: 0.7: 0.5) gave the best separation of the different *Musa* species components (Figure 4.5.1.1). This showed that the samples contain polar compounds.

For the first time, HPTLC was used to reveal the chemical fingerprint of *Musa* species field accessions in comparison with *in vitro*-grown accessions. Both free and conjugated sugars forms were found in all the samples when derivatised with DPA, as has been reported by Mohapatra *et al.* (2010).

Derivatisation in natural products (Neu's) reagents revealed the pattern of phenolics and flavonoids in the *Musa* spp. Phenolic compounds are reported to have wide pharmacological activities such as antimicrobial (Mandalari *et al.*, 2007), antioxidant (Ghasemzadeh *et al.*, 2012), antidiabetic (Lu *et al.*, 2011), and antiulcer (Matsuda *et al.*, 2003). Phenolic compounds were found to be abundant in *in vitro*-grown samples (Figure 4.5.2.1). This is in support of the result obtained from the cuvette assay with the *in vitro* accessions giving higher TPC than the field grown accessions. Also, the flavonoids were revealed as dark bands at 254 nm but after derivatisation in neu's reagents they appeared as green and orange bands. The flavonoids compounds were detected only in the field samples, not in the *in vitro*-grown materials. Interestingly, this result is also in consonance with what was obtained previously from the cuvette assay where field accessions gave higher total flavonoid content than the *in vitro*-grown samples.

Derivatisation in DPPH[•], revealed the presence of antioxidant compounds in *Musa* spp. *In vitro*-grown samples, which have many phenolic compounds, had many antioxidant compounds unlike the field grown accessions having flavonoids but reduced number of antioxidant compounds. This is in support of the result of the correlation among the

bioassays and this implies that other compounds (phenolics) are responsible for the antioxidant property of the plant samples, while flavonoids contributed little to the antioxidant property.

Similarly, the HPTLC method revealed the variation in the chemical profiles of the different samples from different origin with different genome groups. Just like the result obtained from the cuvette spectrophotometric assays, the samples with the high TPC, TFC, DPPH• and FRAP values also had many antioxidative bands (higher peak area values) after HPTLC derivatisation in DPPH•, while samples with low cuvette assay values had fewer bands. *In vitro*-grown accessions gave the highest peak area values from HPTLC quantification. These *in vitro*-grown accessions that are rich in phenolics and antioxidant can be explored for natural products isolation.

5.1.4 Effect directed analysis with (EDA) HPTLC

So far, the biological activities of *Musa* spp. such as antidiabetic activity of the fruit (Kumar *et al.*, 2013), anticholinesterase potential of the fruits and leaves (Ayoola *et al.*, 2017) and antimicrobial activity of peel and leaf (Alisi *et al.*, 2008) have been reported using cuvette spectrophotometric assays. In this study, HPTLC was hyphenated with cholinesterase, glucosidase, Gram-negative (*A. fischeri*) and Gram-positive (*B. subtilis*) bacteria and genotoxicity assays. The results from the present study showed for the first time the biological profiles of *Musa* spp. accessions using HPTLC coupled with effect directed analysis (EDA). This also allowed the comparison of the biological profiles of plants grown in different environments (field, *in vitro* and *ex vitro* or acclimatised). The HPTLC-EDA tool helped to clearly separate and identify the bioactive constituents, which is not possible with cuvette assay that gives a sum parameter.

Two mobile phases were used so as to capture all the bioactive metabolites in the samples. The first is a very polar and acidic mobile phase (Ethyl acetate: Toluene: Formic acid: Water; 3.4: 0.5: 0.7: 0.5), while the second is a medium and non-acidic mobile phase (Toluene: ethylacetate: methanol 6:3:1).

Cholinesterase inhibitors were identified in the *Musa* spp. accessions. Cholinesterase inhibitors are known to be important drugs for treating neurological diseases such as

Alzheimer's disease. Acetylcholinesterase (AChE) and butyrylcholinesterase (BChE) are key enzymes found in human neurological system. The AChE is responsible for the breakdown of acetylcholine into choline and acetic acid, which leads to a reduced acetylcholine level in the body (Schneider *et al.*, 2009). The body has a way of balancing that reaction but in disease condition, cholinesterase inhibitor is usually needed. Plants containing AChE and BChE inhibitors are good sources of neurodegenerative diseases drug (Hostettmann *et al.*, 2006). Three major compounds with hR_F (retention factor * 100) 15, 44 and 83 were identified as AChE and BChE inhibitors and were observed from *in vitro*-grown materials when the polar mobile phase was used, while one major compound with hR_F 63 was identified to inhibit AChE and BChE in almost all the tested samples with increased band intensity in the acclimatised accessions, when the medium-polar mobile phase was used.

The inhibition of alpha-glucosidase, β -glucosidase and alpha-amylase (three (3) enzymes present in the digestive system) is linked to antidiabetic effect. The enzymes are responsible for the breakdown of carbohydrates to glucose thereby increasing the blood glucose level in diabetes patients. The inhibition of these enzymes plays a major role in diabetes management as they decrease the hydrolysis of carbohydrates (Rabasa-Lhoret and Chiasson, 2004; Abeysekera *et al.*, 2007). Combination of HPTLC with glucosidase assay revealed compounds with alpha-glucosidase and β -glucosidase inhibition in the tested *Musa* spp. samples. Two major inhibitor compounds were detected from *in vitro*-grown samples when the polar and acidic mobile phase was used. Using the same mobile phase for α -amylase, no zones of inhibition was observed, except at the solvent front in sample E3 (Zebrina). Therefore, the medium-polar mobile phase was used alternatively to reduce the elution power, which revealed two (2) zones of inhibition in all the samples at hR_F 40 and 63.

Antimicrobials were discovered in *Musa* spp. samples analysed with HPTLC-EDA. Several studies on antimicrobial properties of different *Musa* spp parts, using agar well diffusion assay have been reported (Asuquo and Udobi, 2016; Umamaheswari *et al.*, 2017). However, this study reported for the first time, the inhibition of these microorganisms via HPTLC-EDA. The effect-directed analysis of *B. subtilis* assay, using the

medium-polar mobile phase, revealed one main inhibition zone (hR_F 63) with a very intense band in almost all the samples. For *Aliivibrio fischeri* bioassay, antimicrobials are detected based on their impact on the luminescence of *A. fischeri* bacteria. Antimicrobials appear as dark (inhibiting) or bright (enhancing) zones on an instantly luminescent plate background. Many dark zones of inhibition were seen in the different *Musa* spp. accessions with increasing intensity as the time increases.

Some of the accessions (Pelipita (J), *M. balbisiana* Tani (K), Dole (L), *M. balbisiana* HND (N). and Igitsiri O.) did not show any inhibition zones in both α - and β -glucosidase assays and similar results were observed in the cholinesterase assay. *Musa balbisiana* Tani, Dole, *M. balbisiana* HND and Igitsiri are the accessions with weak or no zones of inhibition in the antimicrobial assays. These were the same accessions with low biological activity when analysed with the UV-spectrophotometric assays. This could be related to the genome group they belong to.

In summary, four compounds were detected to have multiple bioactivities. Using the polar and acidic mobile phase, 3 compounds (1, 2 and 3) were identified to have acetylcholinesterase inhibitory, butyrylcholinesterase inhibitory and antioxidant activities. Those 3 compounds were detected only in the *in vitro*-grown accessions. Two of them (1 and 2) additionally have α -glucosidase and β -glucosidase inhibitory activities. Aslam *et al.* (2009) stated that vincristine (an alkaloid) was higher in *in vitro*-grown tissues of *Catharanthus roseus* compared to the *ex vitro* plants when they were quantified using HPLC. Another compound, (compound 4), was detected when the medium-polar and non-acidic mobile phase was used. It has no antioxidant property but exhibited acetylcholinesterase inhibition, butyrylcholinesterase inhibition, alpha-amylase inhibition and antimicrobial activities.

5.1.5 Absence of toxins as determined by the mutagenotoxicity assay

The newly developed genotoxicity assay was used to assess the plant samples for the presence of toxins. No toxic agents were detected in the plant samples at the concentrations tested. The positive control, 4-nitroquinoline-1-oxide (a toxic chemical), appeared as white fluorescence at 366 nm after the bioassay, while the samples even at

higher concentration gave no such fluorescence using both the polar and medium-polar mobile phase for the assay (Figure 4.5.3.3). *In vivo* animal model studies have been used to report the toxicity profile of some parts of *Musa paradisiaca* L. The juice from the pseudostem of *Musa paradisiaca* was found not toxic (Abirami *et al.*, 2014); Asuquo and Udobi (2016) found out that the ethanol extract of the leaf is slightly toxic, while Ugbogu *et al.* (2018) reported that the unripe fruit extract is non-toxic and safe for pharmaceutical use.

5.1.6 Characterisation of active zones via HPTLC-High resolution mass spectrometry (HRMS)

The multipotent compounds 1, 2 and 3 were obtained from only *in vitro*-grown samples developed in the polar and acidic mobile phase (Figure 4.5.3.4). The tentative assignment of the compounds was based on their base peak, HPTLC derivatisation and literature. Compound 1 (hR_F 15), which is a blue fluorescent compound at UV 366 nm gave a base peak at m/z 133.0606, which was assigned as $[M+H]^+$ with calculated molecular formula as $C_4H_9O_3N_2$. The sodium adduct was seen at m/z 155.0424 ($[M+Na]^+$) ($C_4H_8O_3N_2Na$). In the negative mode, the base peak was at m/z 131.0461 assigned as $[M-H]^-$ with a molecular formula $C_4H_7O_3N_2$. Thus, the actual molecular formula of compound 1 is $C_4H_8O_3N_2$. This molecular formula fits to an amino acid (different forms of asparagine, alanine and glycine anhydride). Though aspartic acid and other amino acids have been reported to be present in the pulp (Barua and Das, 2013) and peel (Khawas and Deka, 2016) of *Musa* spp., further experiments (selectivity of the mobile phase needs to be adjusted) are needed to clarify the observed effects.

Compound 2 (hR_F 44), having a strong antioxidant property, showed a characteristic blue colour after derivatisation with the Neu's reagent. The base peak was at m/z 166. $[M+H]^+$ with $C_9H_{12}NO_2$ as molecular formula. In the negative mode, the respective molecular ion peak $[M-H]^-$ was at m/z 146.9660. Thus, the formula of compound 2 ($C_9H_{11}NO_2$) corresponds to that of a simple aromatic ring (benzene) with an amino group, carbonyl and hydroxyl group attached which could be 4-aminohydrocinnamic acid, phenylalanine, 2-amino-3,4-dimethylbenzoic acid or 2-(4-methylphenoxy) acetamide. Compounds 1 and 2

showed strong antioxidant activity, strong AChE and BChE inhibition but moderate α and β -glucosidase inhibitory activity, based on the EDA results.

Compound 3 (hR_F 83) is not UV sensitive and gave a characteristic yellow colour surrounded by blue colour after derivatisation in Neu's reagent. In the positive ionisation mode, the recorded mass spectra of this zone showed a base peak at m/z 242.0783, assigned as $[M+Na]^+$ and $C_{12}H_{13}O_3NNa$. The dimer of this compound was seen at m/z 461.1676 and assigned as $[2M+Na]^+$. In the negative mode, the base peak was at m/z 218.0823 $[M-H]^-$ with its dimer $[2M-H]^-$ at m/z 437.1717. Thus, the actual molecular formula of this compound was calculated as $C_{12}H_{13}O_3N$. From literature, this compound was found to be an alkaloid with pyrrolidine base, most likely aniracetam. Pyrrolidine alkaloids are used as anticholinergic drugs. From the EDA results, compound 3 showed no α and β -glucosidase inhibitory activity but moderate antioxidant activity and very strong AChE and BChE inhibition. This is the first time that such alkaloid is reported in Musaceae family. Many alkaloids from plants such as rivastigmine, galanthamine and huperzine A have been reported for their anticholinesterase activity (Mukherjee *et al.*, 2007a).

The multipotent compound 4 (hR_F 63) was obtained when the medium-polar mobile phase was used. It was present in all the samples and more abundant in acclimatised plant materials as given by the peak area and intensity of the bands (zones of inhibition) (Figure 4.5.3.5). Compound 4 showed a characteristic purple colour when derivatised in *p*-anisaldehyde. The mass spectra of this band showed a molecular ion peak at m/z 277.2175, which was assigned as $[M-H]^-$ with the formula $C_{18}H_{29}O_2$. In the positive mode, the respective sodium adduct of this compound was seen at m/z 301.2132. Other unassigned fragments were also observed. The actual molecular formula of this compound was found to be $C_{18}H_{30}O_2$, indicating linolenic acid (octadeca-9,12,15-trienoic acid). By co-chromatography of the sample and the purchased standard (linolenic acid), compound 4 was confirmed to be linolenic acid. This fatty acid was detected in fruits (Vilela *et al.*, 2014) and leaves (Sonibare *et al.*, 2018) of different *Musa* spp. cultivars. This polyunsaturated fatty acid is an essential fatty acid that cannot be synthesised by the human body and therefore, must be supplied by external sources. *Musa* spp. is shown to

be an excellent source of this fatty acid. In this study, this fatty acid is reported to have multiple bioactivities such as strong AChE, BChE, *B. subtilis* and *A. fischeri* and a weak α -amylase inhibitory property but no antioxidant property. These multiple bioactivities of linolenic acid were confirmed in parallel studies on *Primula* species (Mahran *et al.*, 2019). The identification of important bioactive metabolites in micropropagated accessions suggests that *in vitro* plant tissue culture techniques can be used to increase the production of bioactive metabolites in *Musa* species. Elicitation experiments were therefore carried out on selected accessions to see if the antioxidant activity of the accessions with low biological activity can be increased.

5.1.7 Elicitation experiments and their effect on increasing the total phenolic content and antioxidant compounds

Since *in vitro* plant tissue culture of the *Musa* spp., accessions produced more active secondary metabolites; it is evident that there is the possibility to explore the influence of this phenomenon by manipulating the culture conditions. Different *in vitro* plant tissue culture parameters were explored to boost the accumulation of secondary metabolites.

5.1.7.1 Effect of sugar increase on the accumulation of antioxidant metabolites

Increase in the sugar level of the culture medium was explored in this work. Fazal *et al.* (2016) stated that sugar is one of the nutrient sources that provides energy and can affect the physiological activities and metabolism during plant growth *in vitro*. Sugar is a vital component of the MS mineral-based culture medium, serving as carbon and energy source. In this study, different sugar concentrations (30 – 50 gL⁻¹) were tested and the influence on plant growth and accumulation of antioxidant compounds were determined. For all the accessions tested, increased sugar doses increased the total phenolic content (TPC) of the plant material. Similar pattern of bioactive compounds was observed with the different sugar doses but with varying intensities. For Foconah, the total phenolic content increased 4.89 times, from 39.43 to 138.64 ngGAE/g of extract when 30 and 50 g/L of sugar were used, respectively. For other studied accessions, the increment in TPC ranged from 1.23 to 2.78 folds when sugar concentration was increased (Table 4.6.1.1). Previous studies reported also increase in the TPC when higher doses of sucrose were added to the

culture media (Cui *et al.*, 2010). Given the fact that sugar induces osmotic stress, it can be hypothesised that this effect leads to increase in phenolics accumulation in plant cells, thus increase in bioactive compounds.

The increase in sugar, especially at 40 and 45 g/L, augmented the average number of shoots and average number of leaves (ANL) produced by the different accessions after 6 weeks of sub-culture. However, ANL of some accessions decreased when 50 g/L of sugar was supplemented to the *in vitro* culture medium. It can be concluded that optimum sugar level to boost bioactive compound production in *Musa* spp., without affecting their growth can be estimated, in this case, as 40 or 45 g/L. The optimum sugar level for plant growth and accumulation of secondary metabolites can vary for different plant species. Previous studies suggested that optimum sucrose level for cell biomass accumulation is not always the same in liquid cultures (Cui *et al.*, 2010). Fazal *et al.* (2014) reported that sucrose level of 20 and 25 g/L among other concentrations (0 – 50 g/L) increased the bioamass accumulation in the suspension cultures of *Prunella vulgaris* L. This confirmed as well that accumulation of cell biomass and growth rate are influenced by the plant species and the type of explant, but also by the sugar concentration (Suan See *et al.*, 2011).

5.1.7.2 Reduction in temperature enhanced the accumulation of antioxidant metabolites

Secondary metabolites and antioxidant activity of plants are affected by the modification of environmental (light, temperature and humidity) conditions (Wang *et al.*, 2008). The effect of three (3) temperature conditions (26, 20 and 15 °C) on the accumulation of antioxidant compounds was examined in this work. For all the accessions tested, plants grown at 20 °C gave a higher total phenolic content followed by plants grown at 15 °C and lastly plants grown at 26 °C (control temperature conditions). Growing the *Musa* spp. accessions at 20 °C was able to increase the TPC of all *Musa* spp. samples, even for the accessions with initially very low antioxidant activity. The TPC of Simili radjah increased from 6.30 to 18.48 ngGAE/g of extract which is 2.9 folds increment when it was grown at 26 and 20 °C, respectively. For Dole, the accession with a very low biological activity, the total phenolic content was increased from 8.59 to 41.57 ngGAE/g of extract (4.84 times higher) when it was grown at 26 and 20 °C, respectively (Table 4.6.2.1). The reduction in temperature however reduced the growth rate of the accessions. Plants grown at 26 °C had

the highest shoot length, leaves number and shoots number followed by plants grown at 20 °C temperature conditions. Plants grown at 15 °C had a very slow growth rate. Ochoa-Villarreal *et al.* (2016) reported that the growth of plant cells is inversely related to the production of natural products; therefore, it is necessary to find a dual system that would support plant growth and at the same time secondary metabolites production. Plants grown at 20 °C gave the highest antioxidant activity with a relatively moderate growth rate. This seems to be an optimum condition for plant cell growth and also secondary metabolites production with antioxidant activity, as per the results of this study.

5.1.7.3 Elicitation of antioxidant secondary metabolites using jasmonic acid

Jasmonic acid is an endogenous plant hormone involved in plant stress response. It is known as a signaling molecule that stimulates the biosynthesis and secondary metabolites accumulation in plants (Pauwels *et al.*, 2009). Jasmonic acid was used in some plants for the accumulation of important secondary metabolites like ginsenoside, vinblastine, nicotine and taxol, among others. The effect of different doses of jasmonic acid (50- 200 µM) on the TPC of six (6) *Musa* spp. accessions was tested. The TPC and the antioxidant compounds increased with the increase in the concentration of the jasmonic acid added to the *Musa* proliferation media when compared with the control. Although, for all the accessions tested, there was no qualitative difference in the antioxidant compounds produced by the control plants and the elicited accessions, but there was a quantitative increase in the TPC and the antioxidant bands intensity from the HPTLC measurement. For accessions, *Musa balbisiana* HND and Dole with a previously low antioxidant activity, jasmonic acid increased the TPC of the accessions (2.24 and 1.68 folds higher than their respective controls) (Table 4.6.3.1). It is obvious that that the addition of jasmonic acid to the media did not especially affect negatively the growth rate of the accessions because for some of the accessions, the average number of leaves produced was higher or equivalent as the control plantlets when the highest dose of jasmonic acid was added to the culture media. This observation corresponds to the work of Jalalpour *et al.* (2014) who reported that jasmonic acid enhanced the accumulation of phenolics and flavonoids in *Taxus baccata* cell culture. However, Ali *et al.* (2015) observed that higher

doses (2 mg/L) of methyl jasmonate and jasmonic acid inhibited the accumulation of phenolic compounds in suspension cultures of *Artemisia absinthium* L.

5.1.7.4 Glucosidase and cholinesterase inhibitors and no toxic compounds in selected elicited samples

Acetylcholinesterase and α -glucosidase inhibitors are used in the Alzheimer's disease and diabetes mellitus management (Lane *et al.*, 2006; Hanefeld and Schaper, 2007) and information on their presence in the studied accessions was of interest. In the HPTLC-enzyme assay autogram, enzyme inhibitors were revealed as colorless (white) zones on a purple background. In all five selected accessions (selected accessions had high total phenolic content in the different elicitation experiments), two acetylcholinesterase and two α -glucosidase inhibiting compound zones were found when 10 μ g/band extract was applied. Acetylcholinesterase was inhibited most intense at hR_F (retention factor * 100) 42 but also hR_F 28 and α -glucosidase most intense at hR_F 34 but also hR_F 42 (Figure 4.6.4.1). A recently developed genotoxic assay (Meyer *et al.*, 2021) was applied to study the presence of potential genotoxic compounds. The same chromatographic HPTLC system was used but on RP 18 W plates which ensures band sharpness even after 3 hours of incubation in the aqueous bioassay (Klingelhöfer and Morlock, 2014). The separated bands were similarly distributed along the migration distance and thus the transfer to the apolar plate was successful (Figure 4.6.4.2). The HPTLC-genotoxicity assay showed that there is no strong genotoxic compound in the elicited *Musa* spp. accessions for the applied extract amount of 10 μ g/band.

5.1.7.5 Characterisation of elicited antioxidant compounds using HPTLC-HRMS

Seven antioxidant zones (5-11) detected in the elicited accession (Red Dacca grown at 20 °C) were further characterised by elution into the HESI-HRMS system via an elution head-based interface and recording of HRMS spectra. Compound zones 5 (hR_F 40) and 6 (hR_F 42) appeared as blue fluorescent compounds at UV 366 nm after application of the natural product reagent, and as intense bright bands after application of the DPPH• reagent. Thus, these zones were assumed to be flavonoids, phenolic acids or polyphenols with a strong antioxidant activity. Compound zone 5 showed a base peak at m/z 180.1009

[M+H]⁺ in the positive ionisation mode and a mass signal at m/z 146.9661 [M-H]⁻ in the negative ionisation mode (Table 4.6.5.1). Compound zone 6, which additionally inhibited acetylcholinesterase and α -glucosidase, showed a base peak at m/z 137.0595 [M+H]⁺ and could be a phenolic compound like piceol. For compound zones 7 (hR_F 4) and 8 (hR_F 12), the same deprotonated molecule at m/z 202.9416 [M-H]⁻ was obtained, whereas some deprotonated molecules [M+H]⁺ were at m/z 133.0341 and 138.0546 (molecular formula C₇H₈NO₂⁺), respectively. Compound zone 9 (hR_F 32) showed the protonated molecule (base peak) at m/z 237.1239 [M+H]⁺ and molecular formula C₁₂H₁₇O₃N₂⁺ as well as its respective deprotonated molecule at m/z 235.1088 [M-H]⁻ and molecular formula C₁₂H₁₅O₃N₂⁻. Some compound zones were most likely coeluting with amino acids like zone 7 with arginine (m/z 175.1183 [M+H]⁺), zone 8 with glutamine (m/z 147.0760 [M+H]⁺) and zone 10 (hR_F 58) with leucine (m/z 132.1017 [M+H]⁺). Compound zone 11 (hR_F 71) can be a pyrrolidinone derivative like aniracetam with a base peak at m/z 218.082 [M-H]⁻ and molecular formula C₁₂H₁₂O₃N⁻. Phenolic and amine compounds have been reported to be present in *Musa* spp. (Pereira and Maraschin, 2015). However, further investigation is needed for structure elucidation of the antioxidants.

5.1.8 Biological activities of the crude and partitioned fraction of the fruit and leaf of *Musa acuminata*

Leaf and fruit of *Musa acuminata* (Simili radjah, ABB) were shown in this study to have antioxidant, anti-inflammatory, anticholinesterase and antidiabetic properties. Many studies have reported the antioxidant and antidiabetic property of different *Musa* species with a lot of research done on the antidiabetic activity of the inflorescence part, e.g. fruits and flowers (Adedayo *et al.*, 2016). Vilhena *et al.* (2018) did a review on the antidiabetic property of *Musa* spp. They found 16 studies reporting the antidiabetic property of the inflorescence part (flowers and bract), which all supported the ethnomedicinal claim that cooked flowers are able to treat diabetes mellitus. Furthermore, this present study compared the antidiabetic activity of the fruit and leaves, showing the leaf fractions having better activity than the fruit. The mode of inhibition, as depicted by the Lineweaver Burk plot, revealed a non-competitive α -amylase inhibition and an uncompetitive mode of α -glucosidase inhibition, for the fruit fractions. Moreover, for the leaf fractions, there was

a constant V_{\max} value (0.0019 mM/min) for both the extract and control with a decrease in K_m values from 0.028 (extract) to 0.020 mM (control), suggesting a competitive α -amylase mode of inhibition. However, the α -glucosidase mode of inhibition of the leaf fractions is uncompetitive. The uncompetitive mode of inhibition suggests that the extract binds close to the enzyme active site, therefore lowering both the k_m and V_{\max} values while the non-competitive mode of inhibition implies that some bioactive compounds in the extract binds at other sites instead of the active site of the enzyme (here, K_m is constant for both extract and control, V_{\max} is reduced). This allows for its binding to the enzyme-substrate complex and thus, interferes with the product. On the other hand, the competitive inhibition of the enzyme suggests that the bioactive compounds compete with the substrate for binding at the active site of the enzyme, indicative of the plant potential (as inhibitor) in slowing down the breakdown of poly- and oligosaccharides to disaccharides.

Other studies have reported the anti-inflammatory activity of the peel of some *Musa* species using nitric oxide inhibitory assay, formalin induced paw inflammation in rat and blood cell membrane stabilization method (Yuei *et al.*, 2016; Ramya *et al.*, 2017). This study assessed the anti-inflammatory activity of *Musa acuminata* fruits and leaves, which is particularly used traditionally for wound healing and ulcer. The putative anti-inflammatory action, determined in this study, is by the inhibition of the 15-LOX enzyme, considered as the key enzyme in the metabolism of arachidonic acid, responsible for leukotrienes formation involved in pathophysiology of chronic inflammatory and allergic diseases. The results showed that the ethyl acetate and *n*-butanol fractions of the *Musa* spp. leaves had better anti-inflammatory activity than even the positive control, quercetin.

Reports of the anticholinesterase activity of *Musa* species are very scarce. In this study, the anticholinesterase activity observed from leaves extract was higher than the fruits. These observations are in line with the results of the previous study (Ayoola *et al.*, 2017). The anticholinesterase activity of the different fractions was further compared to determine where the activity lies and it was discovered that the non-polar fractions (dichloromethane and *n*-hexane) had little or no anti-AChE activity, whereas the polar components of both the fruit and leaves had higher activity with the EAF of the leaf giving

the best result (Table 4.7.3.5.1). This result supports the ethnomedicinal claim of the use of *Musa* spp. in neurodegenerative disorders management.

Extensive review has been done on the bioactive constituents from the fruit, sap, peel of banana (Pothavorn *et al.*, 2010). In this study, it was discovered that the leaf samples had better antioxidant, anticholinesterase, antidiabetic and anti-inflammatory activity than the fruits. This confirms previous study revealing the better efficiency of leaf extracts in terms of antioxidant activity and TPC, compared to fruit extracts, for all the *Musa* species tested (Ayoola *et al.*, 2017). This suggests that research focus should also be on the leaf, especially for phytochemicals isolation.

The polar fractions (methanol and ethyl acetate) in this study were shown to possess better antioxidant, anticholinesterase, anti-inflammatory and antidiabetic activities suggesting that many of the bioactive compounds are polar in nature, reason why they are found in the polar fractions. This is in congruent with the result of other studies (Nakamura *et al.*, 2017; Faraone *et al.*, 2018). Moreso, phenolic compounds, including flavonoids, are known to exhibit antioxidant activities. Other researchers have also found out that phenolic compounds are soluble in polar solvents like alcohol, acetone (Luo *et al.*, 2002). Ethyl acetate fractions (EAF) were identified to have the highest TPC, antioxidant, anticholinesterase, antidiabetic and anti-inflammatory activities. A similar result was reported by Mariem *et al.* (2014) where the EAF of *Retama raetam* plant gave the highest biological activity and was selected for the identification of main compounds.

5.1.9 Characterisation of HD₁ isolates (compounds 12 and 13) using HPTLC-HRMS and NMR

Ethyl acetate fraction (EAF) of the leaf of *Musa acuminata* with the best antioxidant, antidiabetic, anti-inflammatory and anticholinesterase activities, was chosen for bioactive compounds isolation. The result of the TLC profile of all the fractions also revealed that the ethyl acetate fraction contains polar components. The EAF afforded sub-fraction H, which was further purified using sephadex thin column and this afforded sub-fraction HD₁ with the highest antioxidant and antidiabetic activities.

The HPTLC was used to separate HD₁, which is a yellow powder and shown to contain two flavonoids from the derivatisation in natural products reagents. HPTLC-HRMS characterisation of the first compound (**12**) showed a base peak at m/z 593.1515 and was assigned as [M-H]⁻ with the formula C₂₇H₂₉O₁₅⁻. The actual formula is C₂₇H₃₀O₁₅ which is kaempferol-3-*O*-rutinoside. The mass spectra of the second compound (**13**) showed a molecular ion peak at m/z 609.1464 and was assigned as [M-H]⁻ with the formula C₂₇H₂₉O₁₆⁻. The actual formula is C₂₇H₃₀O₁₆ which is quercetin-3-*O*-rutinoside (rutin). The identification of these compounds was confirmed by comparing their retardation factors (R_f) with those of the purchased corresponding standards. Kaempferol-3-*O*-rutinoside appeared as a yellow band while rutin showed as an orange band, when derivatised in Neu's reagent. The two compounds kaempferol-3-*O*-rutinoside (**12**) and rutin (**13**) have close R_f values 0.32 and 0.25, respectively, which are same as those of the standards. Al-Majmaie *et al.* (2019) isolated rutin and other rutin derivatives from *Ruta chalepensis*. They reported that HRMS-ESI data of rutin in the negative ionisation mode gave a base peak m/z at 609.1456 assigned as [M-H]⁻ with the formula C₂₇H₂₉O₁₆⁻, which is same as what was observed in this study. Ganbaatar *et al.* (2015) also isolated kaempferol-3-*O*-rutinoside and rutin as yellow powders from *Polygonum odoratum* and found their mass spectrometry base peak positive ion m/z at 595 ([M+H]⁺) and 633([M+Na]⁺), respectively which is similar to our results.

The structures of the two compounds were also assigned from the proton and ¹³C NMR. They are structurally similar with the same disaccharide sugar (rutinoside) comprising two sugar moieties (rhamnose and glucose). The only difference in their structure is an additional OH group attached to the B ring at carbon 3' of rutin, which gives it its better antioxidant activity than kaempferol-3-*O*-rutinoside as seen in the HPTLC-DPPH[•] assay result. All the protons of the two sugar moieties were found at chemical shifts (δ) between 3.2 and 5.2 ppm. The signal of the anomeric glucose proton of rhamnose is at δ 4.5 ppm which is a doublet while that of the anomeric proton of glucose is at δ 5.2 ppm. The signal of the expected methyl group attached to the rhamnose is seen in the upfield region at δ 1.1 ppm. It is a doublet with a coupling constant (*J*) of 6.1 Hz. The signals were well enhanced because of the overlapping of the two compounds. The proton signals at the

aromatic region is similar to that of a typical flavonoid (Bello *et al.*, 2011). For the kaempferol-3-*O*-rutinoside, the other proton signals are; broad singlets at δ 6.2, 6.4 and two doublets overlapping (appearing at the same chemical shift) at δ 6.9 ($J= 7.4$) and 8.0 ppm ($J= 7.4$); because the protons are symmetrical. These signals correspond to protons attached to carbons at positions C-6, C-8, C-2', C-3', C-5' and C-6' as seen in the structure (Fig. 4.7.5.7). For rutin, the only difference in the proton NMR assignment are the signals seen at chemical shifts 7.69 and 7.65 ppm which are doublets attached respectively to the C-2' and C-6' carbons of rutin. These data correspond to those reported in literature (Leong *et al.*, 2008). From the ^{13}C NMR spectrum, the only methyl signal at carbon C-6''' of the rhamnose sugar was confirmed at chemical shift 17.8 ppm. The methine group (10) (CH) carbons on the disaccharide moiety are found at δ 102.3, 78.1, 75.7, 71.4, 77.1, 104.7, 72.2, 73.9, 72.3 and 72.0 ppm. The only CH₂ (methylene) group was assigned as δ 69.2 which corresponds to carbon C-6'' of the glucose moiety. The signals of quaternary carbons on the A ring are at δ 161.4, 166.3, 159.4 and 105.5 ppm; those on the B ring are at δ 122.7 and 161.4 ppm; while those on the C ring are at 158.5, 135.5 and 179.3 ppm. This corresponds to data reported in the literature (Abdel-Raziq *et al.*, 2016).

The ethyl acetate fraction of *Musa acuminata* is rich in kaempferol-3-*O*-rutinoside and quercetin-3-*O*-rutinoside (rutin), justifying its antioxidant, anti-inflammatory and antidiabetic activities. Plants containing Kaempferol and quercetin are reported to have antidiabetic properties (Tusevski *et al.*, 2018). Kappel *et al.* (2013) also reported that rutin is a major compound with antidiabetic property in the *Musa paradisiaca* L. leaf. Kaempferol and its glucoside has been reported to have many biological activities such as antimicrobial and anti-inflammatory activities and they were detected in many plant families, including Musaceae (Calderón-Montaña *et al.*, 2011). Quercetin-3-*O*-rutinoside is known as a strong antioxidant agent and possesses antimicrobial activity (Al-Majmaie *et al.*, 2019). Kaempferol-3-*O*-rutinoside and quercetin-3-*O*-rutinoside were shown to have antidiabetic and antioxidant activity from this study but quercetin-3-*O*-rutinoside has a higher and very potent antioxidant activity as seen in the HPTLC derivatisation in DPPH•. These two compounds were shown to have no anticholinesterase activity. Abdel-

Raziq *et al.* (2016) also reported the isolation of flavonoids from the ethyl acetate fraction of *Musa cavendishii* leaf, which were stated to have α -amylase inhibitory activity.

In this study, fractionation allowed the identification of the most active compounds. This study showed that *Musa acuminata* leaves contain important flavonoids with antioxidant, anti-inflammatory and antidiabetic properties. Attention should therefore be drawn towards the leaf of *Musa* spp. for the isolation of important bioactive compounds by the pharmaceutical industries.

5.2 Contributions to Knowledge

1. Genetic fidelity of *in vitro*-grown accessions was established.
2. The genome group of *Musa sapientum* from the Botanical Garden, University of Ibadan is now known to be AAB from the genetic similarity study.
3. Accumulation of bioactive metabolites in *Musa* spp. was higher *in vitro* environment.
4. The chemical and biological fingerprint of 15 field, *in vitro*-grown and acclimatised accessions from the taxonomic reference *Musa* spp collection, containing *Musa acuminata* and *Musa balbisiana*, were revealed for the first time using High-performance thin layer chromatography (HPTLC).
5. The effect directed analysis allowed the identification of four compounds (asparagine, phenolic compound, pyrrolidine alkaloid, linolenic acid) with multiple bioactivities (antioxidant, anticholinesterase, antidiabetic and antimicrobial) in *Musa* spp.
6. Asparagine, phenolic compound, pyrrolidine alkaloid were detected only from *in vitro* samples and this study reported for the first time pyrrolidine alkaloid in Musaceae family
7. Plant tissue culture elicitation experiment was shown in this study to be able to increase bioactive metabolites in plants.
8. The leaves of *Musa* species possess more biological activities than the fruits.
9. The HPTLC hyphenated with high-resolution mass spectrometry was used in this study to identify and characterise the bioactive compounds.

10. The leaves of *Musa* species are rich in kaempferol-3-*O*-rutinoside and rutin. These compounds have antioxidant and antidiabetic activities.

5.3 CONCLUSIONS

Musa species were chosen for this study based on an ethnobotanical survey on the plants used for the treatment of neurodegenerative diseases and subsequent literature review. The wide medicinal importance of *Musa* spp. necessitated its rapid mass propagation, through *in vitro* plant tissue culture techniques. This study demonstrated the amenability of *Musa* spp. to micropropagation and showed that biomass production of plant materials for bioactive compounds extraction is possible within a short time using *in vitro* propagation. This method is not restrained by environmental conditions and can also give good and better extraction yield when compared to materials from the field. The genetic fidelity of the accessions confirmed true-to-type validates the use of *in vitro* plant tissue culture as an alternative method for large scale production of plant material and supply of bioactive constituents. From the genetic relationship among the accessions, the genome group of *Musa sapientum* from the Botanical Garden, University of Ibadan was identified as AAB banana.

All the *in vitro*-grown leaves had higher TPC, antioxidant and anticholinesterase activities than field samples from the UV spectrophotometric assay. This was confirmed by the high throughput high-performance thin layer chromatographic (HPTLC) method. The HPTLC linked to bioassays allowed the analysis of up to 22 samples simultaneously within a short time. This hyphenation helped to identify the bioactive compounds in a complex sample in contrast to sum parameter given by the spectrophotometric assays. The HPTLC-effect directed analysis (EDA) revealed the compounds with antioxidant, antidiabetic, anticholinesterase and antimicrobial activities. This supports the ethnomedicinal claim of the use of *Musa* spp. in the treatment of many diseases. Summarily, four multipotent compounds were identified. Compounds 1, 2 and 3 which are asparagine, a phenolic compound and aniracetam (pyrrolidine alkaloid) were observed only from *in vitro*-grown samples while compound 4 (linolenic acid) was detected in all the samples but abundant in acclimatised accessions. The field accessions were however richer in flavonoids. The

HPTLC was effective for bioactivity-guided characterisation of the bioactive constituents in *Musa* spp. accessions.

Elicitation of *in vitro* shoot culture of *Musa* spp. were used, for the first time in this study, to increase the phenolic content and antioxidant activity of *Musa* spp. Increasing the sugar levels (40, 45 or 50 g/L), reducing temperature condition to 20 °C and adding jasmonic acid (200 µM) to the *in vitro* plant tissue culture proliferation medium were able to elicit compounds with relatively higher antioxidant activity. These elicitors can be useful tools for the enhancement of the production of secondary metabolites in *Musa* spp. The elicitors used also triggered the production of amine compounds and alkaloids with antioxidant, antidiabetic and anticholinesterase activities in *Musa* species, firstly reported in Musaceae family. This work demonstrated that *in vitro* plant tissue culture is a reliable alternative system for sustainable and consistent production of bioactive metabolites with high antioxidant activity. These elicitation methods can be further utilised to target the production of important and novel pharmaceuticals on a commercial scale. In addition to the opportunity, given by micropropagation, to have a synchronised, standardised, controlled and reliable system, this method of secondary metabolite production would enhance the rational use of natural resources and reduce the dependence of the pharmaceutical industry on field or wild collection of plant materials; thereby conserving the natural resources.

Finally, from the bioassay guided isolation, from the best field sample of *Musa acuminata* (Simili radjah), the leaf sample was found to be more biologically active than the fruit. Many studies have focused on the isolation of secondary metabolites from fruits, peel and other parts of *Musa* species, with less work on the leaf. This study, which is the first of its kind, compared the bioactivity of the leaf and fruit of *Musa acuminata*. All the leaf fractions exhibited higher antioxidant, anti-inflammatory, anticholinesterase and antidiabetic activity than fruit fractions. Among all the six fractions (aqueous methanol, crude methanol, *n*-butanol, ethyl acetate (EAF), dichloromethane, *n*-hexane fraction), the EAF gave the highest antioxidant, anti-inflammatory, anticholinesterase and antidiabetic activities. The ethyl acetate fraction of *Musa acuminata* is rich in kaempferol-3-*O*-

rutinoside and quercetin-3-*O*-rutinoside (rutin), justifying its antioxidant, anti-inflammatory and antidiabetic activities.

5.4 RECOMMENDATIONS

From the results of this study, the following are recommended;

1. *Musa* species are popularly known as food and used as medicine. They are reported to have many medicinal applications. For the supply of phytochemicals, nutraceutical and bioactive secondary metabolites, attention should be drawn towards the leaf tissues. More studies on the biological activities of *Musa* spp. leaves should be done, as much as previous emphasis on fruit, pulp and peel.
2. Attention should be shifted to the use of *in vitro* plant tissue culture for the production of useful secondary metabolites as this study revealed the presence of anticholinergic alkaloid only from *in vitro*-grown samples. They also displayed higher total phenolic content and antioxidant activity.
3. More elicitation experiments can be performed to determine the effect of other stress and elicitors on secondary metabolites production, taking into consideration their optimal levels or concentrations.
4. The genes responsible for important secondary metabolites production *in vitro* culture system can be determined using transcriptome and functional genomics. This would enhance bio-engineering for efficient production of important medicinal compounds.

REFERENCES

- Abad, T., McNaughton-Smith, G., Fletcher, W. Q., Echeverri, F., Diaz-Penate, R., Tabraue, C., ... and Luis, J. G. (2000). Isolation of (S)-(+)-naproxene from *Musa acuminata*. Inhibitory effect of naproxene and its 7-methoxy isomer on constitutive COX-1 and inducible COX-2. *Planta Medica* 66.5: 471-473.
- Abdel-Raziq, M. S., Bar, F. M. A., and Gohar, A. A. (2016). Alpha-amylase Inhibitory Compounds from *Musa cavendishii*. *British Journal of Pharmaceutical Research* 13.4: 1-10.
- Abdullah, F. C., Rahimi, L., Zakaria, Z. A., and Ibrahim, A. L. (2014). Hepatoprotective, Antiulcerogenic, Cytotoxic and Antioxidant Activities of *Musa acuminata* Peel and Pulp In: Gurib-Fakim, A. (Ed.), *Novel Plant Bioresources: Applications in Food, Medicine and Cosmetics* John Wiley & Sons, UK. doi: 10.1002/9781118460566.ch26.
- Abeyssekera, W. K. S. M., Chandrasekera, A., and Liyanage, P. K. (2007). Amylase and glucosidase enzyme inhibitory activity of ginger (*Zingiber officinale* Roscoe) an *in vitro* study. *Tropical Agricultural Research* 19: 128-135.
- Abirami, J., Brindha, P. and Raj C. D. (2014). Evaluation of Toxicity Profiles of *Musa Paradisiaca* L (Pseudostem) Juice. *International Journal of Pharmacy and Pharmaceutical Science* 6: 9–11.
- Adebayo, S. A., Dzoyem, J. P., Shai, L. J., and Eloff, J. N. (2015). The anti-inflammatory and antioxidant activity of 25 plant species used traditionally to treat pain in southern African. *BMC Complementary and Alternative medicine* 15.1: 159.
- Adedayo, B. C., Oboh, G., Oyeleye, S. I., and Olasehinde, T. A. (2016). Antioxidant and antihyperglycemic properties of three banana cultivars (*Musa* spp.). *Scientifica* 2016.
- Adeniji, T. A., Sanni, L. O., Barimalaa, I. S., and Hart, A. D. (2006). Determination of micronutrients and colour variability among new plantain and banana hybrids flour. *World Journal of Chemistry* 1.1: 23-27.
- Ali, H., Houghton, P. J., and Soumyanath, A. (2006). α -Amylase inhibitory activity of some Malaysian plants used to treat diabetes; with particular reference to *Phyllanthus amarus*. *Journal of Ethnopharmacology* 107: 449–455.
- Ali, M., Abbasi, B. H., and Ali, G. S. (2015). Elicitation of antioxidant secondary metabolites with jasmonates and gibberellic acid in cell suspension cultures of *Artemisia absinthium* L. *Plant Cell, Tissue and Organ Culture (PCTOC)* 120.3: 1099-1106.
- Alisi, C. S., Nwanyanwu, C. E., Akujobi, C. O., and Ibegbulem, C. O. (2008). Inhibition of dehydrogenase activity in pathogenic bacteria isolates by aqueous extracts of *Musa paradisiaca* (Var Sapiantum). *African Journal of Biotechnology* 7.12: 1821-1825.

- Al-Majmaie, S., Nahar, L., Sharples, G. P., Wadi, K., and Sarker, S. D. (2019). Isolation and antimicrobial activity of rutin and its derivatives from *Ruta chalepensis* (Rutaceae) growing in Iraq. *Records of Natural Products* 13.1: 64-70.
- Al-Manasrah, W. S. (2012). *In vitro* propagation of *Crataegus aronia* L. and secondary metabolites detection. *Biotechnology Master program*. (Palestine Polytechnique University, Hebron, 2012) <http://biotech.ppu.edu/sites/default/files/thesis/Wala%20Shuaib%20Al-%20Manasrah.pdf>.
- Almaraz-Abarca, N., Delgado-Alvarado, E. A., Ávila-Reyes, J. A., Uribe-Soto, J. N., and González-Valdez, L. S. (2013). The phenols of the genus *Agave* (Agavaceae). *Journal of Biomaterials and Nanobiotechnology* 4.3: 9.
- Altemimi, A., Lakhssassi, N., Baharlouei, A., Watson, D., and Lightfoot, D. (2017). Phytochemicals: Extraction, isolation, and identification of bioactive compounds from plant extracts. *Plants* 6.4: 42.
- Amutha, K., and Selvakumari, U. (2016). Wound healing activity of methanolic stem extract of *Musa paradisiaca* Linn. (Banana) in Wistar albino rats. *International Wound Journal* 13.5: 763-767.
- Anand, S. (2010). Various approaches for secondary metabolite production through plant tissue culture. *Pharmacia* 1.1: 1-7.
- Apriasari, M. L., Endariantari, A., and Oktaviyanti, I. K. (2015). The effect of 25% Mauli banana stem extract gel to increase the epithel thickness of wound healing process in oral mucosa. *Dental Journal (Majalah Kedokteran Gigi)* 48.3: 150-153.
- Aslam, J., Mujib, A., Nasim, S. A., and Sharma, M. P. (2009). Screening of vincristine yield in *ex vitro* and *in vitro* somatic embryos derived plantlets of *Catharanthus roseus* L.(G) Don. *Scientia Horticulturae* 119.3: 325-329.
- Asuquo, E. G., and Udobi, C. E. (2016). Antibacterial and toxicity studies of the ethanol extract of *Musa paradisiaca* leaf. *Cogent Biology* 2.1: 1219248.
- Atta-Ur-Rahman and Choudhary, M. I. (2001). Bioactive natural products as a potential source of new pharmacophores. A theory of memory. *Pure and Applied Chemistry* 73.3: 555-560.
- Ayoola, I. O., Gueye, B., Sonibare, M. A., Abberton, M. T. (2017). Antioxidant activity and acetylcholinesterase inhibition of field and *in vitro* grown *Musa* L. species. *Journal of Food Measurement and Characterisation* 11.2: 488-499.
- Azadniya, E., and Morlock, G. E. (2018). Bioprofiling of *Salvia miltiorrhiza* via planar chromatography linked to (bio) assays, high resolution mass spectrometry and nuclear magnetic resonance spectroscopy. *Journal of Chromatography A* 1533: 180-192.

- Azmir, J., Zaidul, I. S. M., Rahman, M. M., Sharif, K. M., Mohamed, A., Sahena, F., ... and Omar, A. K. M. (2013). Techniques for extraction of bioactive compounds from plant materials: A review. *Journal of Food Engineering* 117.4: 426-436.
- Bailey, C. J. (2003). New approaches to the pharmacotherapy of diabetes. *Textbook of diabetes* 2: 73-1.
- Barua, N., and Das, M. (2013). An overview on pharmacological activities of *Musa sapientum* and *Musa paradisiaca*. *International Journal of Pharma Professional's Research* 4.2: 852-858.
- Bello, I. A., Ndukwe, G. I., Audu, O. T., and Habila, J. D. (2011). A bioactive flavonoid from *Pavetta crassipes* K. Schum. *Organic and Medicinal Chemistry Letters* 1.1: 14.
- Bhattacharyya, P., Kumar, V., and Van Staden, J. (2017a). Assessment of genetic stability amongst micropropagated *Ansellia africana*, a vulnerable medicinal orchid species of Africa using SCoT markers. *South African Journal of Botany* 108: 294-302.
- Bose, B., Kumaria, S., Choudhury, H., and Tandon, P. (2016). Assessment of genetic homogeneity and analysis of phytomedicinal potential in micropropagated plants of *Nardostachys jatamansi*, a critically endangered, medicinal plant of alpine Himalayas. *Plant Cell, Tissue and Organ Culture (PCTOC)* 124.2: 331-349.
- Bradbury, P. J., Zhang, Z., Kroon, D. E., Casstevens, T. M., Ramdoss, Y., and Buckler, E. S. (2007). TASSEL: software for association mapping of complex traits in diverse samples. *Bioinformatics* 23.19: 2633-2635.
- Brito, A., Ramirez, J., Areche, C., Sepúlveda, B., and Simirgiotis, M. (2014). HPLC-UV-MS profiles of phenolic compounds and antioxidant activity of fruits from three *Citrus* species consumed in Northern Chile. *Molecules* 19.11: 17400-17421.
- Brosseau, C. L., Gambardella, A., Casadio, F., Grzywacz, C. M., Wouters, J., and Van Duyne, R. P. (2009). Ad-hoc surface-enhanced Raman spectroscopy methodologies for the detection of artist dyestuffs: thin layer chromatography-surface enhanced Raman spectroscopy and in situ on the fiber analysis. *Analytical Chemistry* 81.8: 3056-3062.
- Bulich, A. A. (1979). Use of luminescent bacteria for determining toxicity in aquatic environments. In *Aquatic Toxicology: Proceedings of the Second Annual Symposium on Aquatic Toxicology*. ASTM International.
- Büyükokuroğlu, M. E., Gülçin, I., Oktay, M., and Küfrevioğlu, O. I. (2001). *In vitro* antioxidant properties of dantrolene sodium. *Pharmacological Research* 44.6: 491-494.
- Calderon-Montano, J. M., Burgos-Morón, E., Pérez-Guerrero, C., and López-Lázaro, M. (2011). A review on the dietary flavonoid kaempferol. *Mini Reviews in Medicinal Chemistry* 11.4: 298-344.

- Chemat, F., Tomao, V., and Viot, M. (2008). Ultrasound-assisted extraction in food analysis. *Handbook of food analysis instruments* 85-103.
- Choi, H. K., Kim, S. I., Son, J. S., Hong, S. S., Lee, H. S., and Lee, H. J. (2000). Enhancement of paclitaxel production by temperature shift in suspension culture of *Taxus chinensis*. *Enzyme and Microbial Technology* 27.8: 593-598.
- Choma, I., and Jesionek, W. (2015). TLC-direct bioautography as a high throughput method for detection of antimicrobials in plants. *Chromatography* 2.2: 225-238.
- Christenhusz, M. J. M., and Byng, J. W. (2016). The number of known plants species in the world and its annual increase. *Phytotaxa* 261.3: 201–217.
- Christophoridou, S., Dais, P., Tseng, L. H., and Spraul, M. (2005). Separation and identification of phenolic compounds in olive oil by coupling high-performance liquid chromatography with postcolumn solid-phase extraction to nuclear magnetic resonance spectroscopy (LC-SPE-NMR). *Journal of Agricultural and Food Chemistry* 53.12: 4667-4679.
- Conforti, F., Sosa, S., Marrelli, M., Menichini, F., Statti, G. A., Uzunov, D., ... and Della Loggia, R. (2008). *In vivo* anti-inflammatory and *in vitro* antioxidant activities of Mediterranean dietary plants. *Journal of Ethnopharmacology* 116.1: 144-151.
- Crowson, C. S., Liao, K. P., Davis III, J. M., Solomon, D. H., Matteson, E. L., Knutson, K. L., ... and Gabriel, S. E. (2013). Rheumatoid arthritis and cardiovascular disease. *American Heart Journal* 166.4: 622-628.
- Cui, X. H., Murthy, H. N., Wu, C. H., and Paek, K. Y. (2010). Sucrose-induced osmotic stress affects biomass, metabolite, and antioxidant levels in root suspension cultures of *Hypericum perforatum* L. *Plant Cell, Tissue and Organ Culture (PCTOC)* 103.1: 7-14.
- Davey, M. W., Van den Bergh, I., Markham, R., Swennen, R., and Keulemans, J. (2009b). Genetic variability in *Musa* fruit provitamin A carotenoids, lutein and mineral micronutrient contents. *Food Chemistry* 115.3: 806-813.
- Dayanand, G., Sharma, A., Ahmed, M., Jyothi, P. P., and Rani, M. (2015). Effect of banana on blood pressure of hypertensive individuals: a cross sectional study from Pokhara, Nepal. *Medical Science* 3.2: 233-237.
- De Capdeville, G., Júnior, M. T. S., Szinay, D., Diniz, L. E. C., Wijnker, E., Swennen, R., ... and De Jong, H. (2009). The potential of high-resolution BAC-FISH in banana breeding. *Euphytica* 166.3: 431-443.
- De Langhe, E. (2009). Relevance of banana seeds in archaeology. *Ethnobotany Research and Applications* 7: 271-281.
- Devi, S. P., Kumaria, S., Rao, S. R., and Tandon, P. (2014). Single primer amplification reaction (SPAR) methods reveal subsequent increase in genetic variations in

- micropropagated plants of *Nepenthes khasiana* Hook. f. maintained for three consecutive regenerations. *Gene* 538.1: 23-29.
- Doyle, J. J. (1990). A rapid total DNA preparation procedure for fresh plant tissue. *Focus* 12: 13-15.
- Ebrahimzadeh, M. A., Nabavi, S. F., and Nabavi, S. M. (2009). Antioxidant activities of methanol extract of *Sambucus ebulus* L. flower. *Pakistan Journal of Biological Sciences* 12.5: 447.
- Ellman, G. L., Courtney, K. D., Andres Jr, V., and Featherstone, R. M. (1961). A new and rapid colorimetric determination of acetylcholinesterase activity. *Biochemical Pharmacology* 7.2: 88-95.
- Elufioye, T. O., Obuotor, E. M., Sennuga, A. T., Agbedahunsi, J. M., and Adesanya, S. A. (2010). Acetylcholinesterase and butyrylcholinesterase inhibitory activity of some selected Nigerian medicinal plants. *Revista Brasileira de Farmacognosia* 20.4: 472-477.
- Emaga, T. H., Andrianaivo, R. H., Wathelet, B., Tchango, J. T., and Paquot, M. (2007). Effects of the stage of maturation and varieties on the chemical composition of banana and plantain peels. *Food Chemistry* 103.2: 590-600.
- Espinosa-Leal, C. A., Puente-Garza, C. A., and García-Lara, S. (2018). *In vitro* plant tissue culture: means for production of biological active compounds. *Planta* 248.1: 1-18.
- European Committee for Standardization (2009). Water quality – Determination of the inhibitory effect of water samples on the light emission of *Vibrio fischeri* (Luminescent bacteria test) DIN EN ISO 11348-1:2009-05. Berlin: Beuth Verlag.
- Faraone, I., Rai, D., Chiummiento, L., Fernandez, E., Choudhary, A., Prinzo, F., and Milella, L. (2018). Antioxidant Activity and Phytochemical Characterization of *Senecio clivicolus* Wedd. *Molecules*, 23.10: 2497.
- Fazal, H., Abbasi, B. H., and Ahmad, N. (2014). Optimization of adventitious root culture for production of biomass and secondary metabolites in *Prunella vulgaris* L. *Applied Biochemistry and Biotechnology* 174.6: 2086-2095.
- Fazal, H., Abbasi, B. H., Ahmad, N., Ali, M., and Ali, S. (2016). Sucrose induced osmotic stress and photoperiod regimes enhanced the biomass and production of antioxidant secondary metabolites in shake-flask suspension cultures of *Prunella vulgaris* L. *Plant Cell, Tissue and Organ Culture (PCTOC)* 124.3: 573-581.
- Fett-Neto, A. G., Melanson, S. J., Nicholson, S. A., Pennington, J. J., and DiCosmo, F. (1994). Improved taxol yield by aromatic carboxylic acid and amino acid feeding to cell cultures of *Taxus cuspidata*. *Biotechnology and Bioengineering* 44.8: 967-971.
- Gamborg, O. L., Miller, R., and Ojima, K. (1968). Nutrient requirements of suspension cultures of soybean root cells. *Experimental Cell Research* 50.1: 151-158.

- Ganbaatar, C., Gruner, M., Mishig, D., Duger, R., Schmidt, A. W., and Knölker, H. J. (2015). Flavonoid Glycosides from the Aerial Parts of *Polygonatum odoratum* (Mill.) Druce Growing in Mongolia. *Open Natural Products Journal* 8: 1-7.
- Gaspar, T., Kevers, C., Penel, C., Greppin, H., Reid, D. M., and Thorpe, T. A. (1996). Plant hormones and plant growth regulators in plant tissue culture. *In Vitro Cellular and Developmental Biology-Plant* 32.4: 272-289.
- Georgiev, M., Pavlov, A., and Ilieva, M. (2006). Selection of high rosmarinic acid producing *Lavandula vera* MM cell lines. *Process Biochemistry* 41.9: 2068-2071.
- Ghasemzadeh, A., Omidvar, V., and Jaafar, H. Z. (2012). Polyphenolic content and their antioxidant activity in leaf extract of sweet potato (*Ipomoea batatas*). *Journal of Medicinal Plants Research* 6.15: 2971-2976.
- Glavnik, V., Vovk, I., and Albreht, A. (2017). High performance thin-layer chromatography–mass spectrometry of Japanese knotweed flavan-3-ols and proanthocyanidins on silica gel plates. *Journal of Chromatography A* 1482: 97-108.
- Gonçalves, S., and Romano, A. (2018). Production of Plant Secondary Metabolites by Using Biotechnological Tools. In *Secondary Metabolites-Sources and Applications*. IntechOpen. 81-99.
- Govindaraju, S., and Arulselvi, P. I. (2018). Effect of cytokinin combined elicitors (l-phenylalanine, salicylic acid and chitosan) on *in vitro* propagation, secondary metabolites and molecular characterization of medicinal herb–*Coleus aromaticus* Benth (L). *Journal of the Saudi Society of Agricultural Sciences* 17.4: 435-444.
- Grzegorzczak, I., Matkowski, A., and Wysokińska, H. (2007). Antioxidant activity of extracts from *in vitro* cultures of *Salvia officinalis* L. *Food Chemistry* 104.2: 536-541.
- Guerriero, G., Berni, R., Muñoz-Sanchez, J., Apone, F., Abdel-Salam, E., Qahtan, A., ... and Siddiqui, K. (2018). Production of plant secondary metabolites: Examples, tips and suggestions for biotechnologists. *Genes* 9.6: 309.
- Gueye B., Adeyemi A., Debiru M., Akinyemi B., Olagunju M., Okeowo A., Otukpa S., Dumet D., (2012) Standard Operation Procedures (SOP) for IITA *in vitro* genebank Nigeria. *IITA Annual Report* 59.
- Haq, I. U., and Dahot, M. U. (2007). Effect of permanent and temporary immersion systems on banana micro-propagation. *Pakistan Journal of Botany* 39.5: 1763-1772.
- Helliot, B., Panis, B., Poumay, Y., Swennen, R., Lepoivre, P., and Frison, E. (2002). Cryopreservation for the elimination of cucumber mosaic and banana streak viruses from banana (*Musa* spp.). *Plant Cell Reports* 20.12: 1117-1122.
- Holková, I., Bezáková, L., Bilka, F., Balažová, A., Vanko, M., and Blanáriková, V. (2010). Involvement of lipoxygenase in elicitor-stimulated sanguinarine

- accumulation in *Papaver somniferum* suspension cultures. *Plant Physiology and Biochemistry* 48.10-11: 887-892.
- Hossain, M. S., Alam, M. B., Asadujjaman, M., Zahan, R., Islam, M. M., Mazumder, M. E. H., and Haque, M. E. (2011). Antidiarrheal, antioxidant and antimicrobial activities of the *Musa sapientum* Seed. *Avicenna Journal of Medical Biotechnology* 3.2: 95.
- Hostettmann, K., Borloz, A., Urbain, A., and Marston, A. (2006). Natural product inhibitors of acetylcholinesterase. *Current Organic Chemistry* 10.8: 825-847.
- Houghton, P. J., Howes, M. J., Lee, C. C., and Steventon, G. (2007). Uses and abuses of *in vitro* tests in ethnopharmacology: visualizing an elephant. *Journal of Ethnopharmacology* 110.3: 391-400.
- Hu, F. X., and Zhong, J. J. (2008). Jasmonic acid mediates gene transcription of ginsenoside biosynthesis in cell cultures of *Panax notoginseng* treated with chemically synthesized 2-hydroxyethyl jasmonate. *Process Biochemistry* 43.1: 113-118.
- Hussain, M. S., Fareed, S., Saba Ansari, M., Rahman, A., Ahmad, I. Z., and Saeed, M. (2012). Current approaches toward production of secondary plant metabolites. *Journal of Pharmacy and Bioallied Sciences* 4.1: 10-20.
- Ingale, S., Joshi, S. J., and Gupte, A. (2014). Production of bioethanol using agricultural waste: banana pseudo stem. *Brazilian Journal of Microbiology* 45.3: 885-892.
- Ingale, S. P., Ingale, P. L., and Joshi, A. M. (2009). Analgesic activity of the stem of *Musa sapientum* Linn. *Journal of Pharmaceutical Research* 2.9: 1381-1382.
- Ivan, A. R. 2005. *Musa sapientum*, In: Medicinal plants of the world, Humana Press In, Totowa, New Jersey, 319.
- Jain, D. L., Baheti, A. M., Parakh, S. R., Ingale, S. P., and Ingale, P. L. (2007). Study of antacid and diuretic activity of ash and extracts of *Musa sapientum* L. fruit peel. *Pharmacognosy Magazine* 3.10: 116-119.
- Jalalpour, Z., Shabani, L., Afghani, L., Sharifi-Tehrani, M., and Amini, S. A. (2014). Stimulatory effect of methyl jasmonate and squalenstatin on phenolic metabolism through induction of LOX activity in cell suspension culture of yew. *Turkish Journal of Biology* 38.1: 76-82.
- Jamshidi-Aidji, M., and Morlock, G. E. (2015). Bioprofiling of unknown antibiotics in herbal extracts: Development of a streamlined direct bioautography using *Bacillus subtilis* linked to mass spectrometry. *Journal of Chromatography A* 1420: 110-118.
- Jamshidi-Aidji, M., and Morlock, G. E. (2016). From bioprofiling and characterization to bioquantification of natural antibiotics by direct bioautography linked to high-resolution mass spectrometry: exemplarily shown for *Salvia miltiorrhiza* root. *Analytical Chemistry* 88.22: 10979-10986.

- Jamshidi-Aidji, M., and Morlock, G. E. (2018). Fast Equivalency Estimation of Unknown Enzyme Inhibitors *in Situ* the Effect-Directed Fingerprint, Shown for *Bacillus* Lipopeptide Extracts. *Analytical Chemistry* 90.24: 14260-14268.
- Jamshidi Aijdi, M., Macho, J., Müller, M., Morlock, G. E. (2019). Effect-directed profiling of aqueous, fermented plant preparations via high-performance thin-layer chromatography combined with *in situ* assays and high-resolution mass spectrometry. *Journal of Liquid Chromatography and Related Technology* in print.
- Jekayinoluwa, T., Gueye, B., Bhattacharjee, R., Osibanjo, O., Shah, T., Abberton, M. (2019). Agromorphologic, genetic and methylation profiling of *Dioscorea* and *Musa* species multiplied under three micropropagation systems. *PloS one* 14(5): e0216717.
- Kaimoyo, E., Farag, M. A., Sumner, L. W., Wasmann, C., Cuello, J. L., and VanEtten, H. (2008). Sub-lethal Levels of Electric Current Elicit the Biosynthesis of Plant Secondary Metabolites. *Biotechnology Progress* 24.2: 377-384.
- Kanazawa, K., and Sakakibara, H. (2000). High content of dopamine, a strong antioxidant, in cavendish banana. *Journal of Agricultural and Food Chemistry* 48.3: 844-848.
- Kappel, V. D., Cazarolli, L. H., Pereira, D. F., Postal, B. G., Madoglio, F. A., Buss, Z. D. S., ... and Silva, F. R. (2013). Beneficial effects of banana leaves (*Musa x paradisiaca*) on glucose homeostasis: multiple sites of action. *Revista Brasileira de Farmacognosia* 23.4: 706-715.
- Karuppiah, P., and Mustafa, M. (2013). Antibacterial and antioxidant activities of *Musa* spp. leaf extracts against multidrug resistant clinical pathogens causing nosocomial infection. *Asian Pacific Journal of Tropical Biomedicine* 3.9: 737-742.
- Karuppusamy, S. (2009). A review on trends in production of secondary metabolites from higher plants by *in vitro* tissue, organ and cell cultures. *Journal of Medicinal Plants Research* 3.13: 1222-1239.
- Khatoon, M., Islam, E., Islam, R., Abdur Rahman, A. and Alam, k. (2013). Estimation of total phenol and *in vitro* antioxidant activity of *Albizia procera* leaves. *BMC Research Notes* 6: 121-127.
- Khawas, P., and Deka, S. C. (2016). Comparative Nutritional, Functional, Morphological, and Diffractogram Study on Culinary Banana (*Musa* ABB) Peel at Various Stages of Development. *International Journal of Food Properties* 19.12: 2832-2853.
- Kim, Y. M., Jeong, Y. K., Wang, M. H., Lee, W. Y., and Rhee, H. I. (2005). Inhibitory effect of pine extract on α -glucosidase activity and postprandial hyperglycemia. *Nutrition* 21.6: 756-761.
- Komaraiah, P., Kishor, P. K., Carlsson, M., Magnusson, K. E., and Mandenius, C. F. (2005). Enhancement of anthraquinone accumulation in *Morinda citrifolia* suspension cultures. *Plant Science* 168.5: 1337-1344.
- Krentz, A. J., and Bailey, C. J. (2005). Oral antidiabetic agents. *Drugs* 65.3: 385-411.

- Krings, U., and Berger, R. G. (1998). Biotechnological production of flavours and fragrances. *Applied Microbiology and Biotechnology* 49.1: 1-8.
- Krüger, S., Urmann, O., and Morlock, G. E. (2013). Development of a planar chromatographic method for quantitation of anthocyanes in pomace, feed, juice and wine. *Journal of Chromatography A* 1289: 105-118.
- Kulkarni, V. M., Suprasanna, P., and Bapat, V. A. (2006). Plant regeneration through multiple shoot formation and somatic embryogenesis in a commercially important and endangered Indian banana cv. Rajeli. *Current Science* 90.6: 842-846.
- Kumar, K. S., Bhowmik, D., Duraivel, S., and Umadevi, M. (2012). Traditional and medicinal uses of banana. *Journal of Pharmacognosy and Phytochemistry* 1.3: 51-63.
- Kumar, M., Gautam, M. K., Singh, A., and Goel, R. K. (2013). Healing effects of *Musa sapientum* var. *paradisiaca* in diabetic rats with co-occurring gastric ulcer: cytokines and growth factor by PCR amplification. *BMC Complementary and Alternative Medicine* 13.1: 305.
- Kwon, Y. I., Apostolidis, E., and Shetty, K. (2008). Inhibitory potential of wine and tea against α -amylase and α -glucosidase for management of hyperglycemia linked to type 2 diabetes. *Journal of Food Biochemistry* 32.1: 15-31.
- Lane, R. M., Potkin, S. G., and Enz, A. (2006). Targeting acetylcholinesterase and butyrylcholinesterase in dementia. *International Journal of Neuropsychopharmacology* 9.1: 101-124.
- Lee, Y. L., Sagare, A. P., Lee, C. Y., Feng, H. T., Ko, Y. C., Shaw, J. F., and Tsay H. S. (2001). Formation of protoberberine-type alkaloids by the tubers of somatic embryo-derived plants of *Corydalis yanhusuo*. *Planta Medica* 67: 839-842.
- Lee, Y., Lee, D. E., Lee, H. S., Kim, S. K., Lee, W. S., Kim, S. H., and Kim, M. W. (2011). Influence of auxins, cytokinins, and nitrogen on production of rutin from callus and adventitious roots of the white mulberry tree (*Morus alba* L.). *Plant Cell, Tissue and Organ Culture (PCTOC)* 105.1: 9-19.
- Leong, C. N. A., Tako, M., Hanashiro, I., and Tamaki, H. (2008). Antioxidant flavonoid glycosides from the leaves of *Ficus pumila* L. *Food Chemistry* 109.2: 415-420.
- Lewis, D. A., and Shaw, G. P. (2001). A natural flavonoid and synthetic analogues protect the gastric mucosa from aspirin-induced erosions. *The Journal of Nutritional Biochemistry* 12.2: 95-100.
- Lewis, D. A., Fields, W. N., and Shaw, G. P. (1999). A natural flavonoid present in unripe plantain banana pulp (*Musa sapientum* L. var. *paradisiaca*) protects the gastric mucosa from aspirin-induced erosions. *Journal of Ethnopharmacology* 65.3: 283-288.

- Li, Q., Deng, M., Zhang, J., Zhao, W., Song, Y., Li, Q., and Huang, Q. (2013). Shoot organogenesis and plant regeneration from leaf explants of *Lysionotus serratus* D. Don. *The Scientific World Journal* 2013: 1-7.
- Li, Y. C., and Tao, W. Y. (2009). Effects of paclitaxel-producing fungal endophytes on growth and paclitaxel formation of *Taxus cuspidata* cells. *Plant Growth Regulation* 58.1: 97-105.
- Linsmaier, E. M., and Skoog, F. (1965). Organic growth factor requirements of tobacco tissue cultures. *Physiologia Plantarum* 18.1: 100-127.
- Lloyd, G., and McCown, B. (1980). Commercially-feasible micropropagation of mountain laurel, *Kalmia latifolia*, by use of shoot-tip culture. *Commercially-feasible micropropagation of mountain laurel, Kalmia latifolia, by use of shoot-tip culture* 30: 421-427.
- Lu, Z., Jia, Q., Wang, R., Wu, X., Wu, Y., Huang, C., and Li, Y. (2011). Hypoglycemic activities of A-and B-type procyanidin oligomer-rich extracts from different Cinnamon barks. *Phytomedicine* 18.4: 298-302.
- Luo, X. D., Basile, M. J., and Kennelly, E. J. (2002). Polyphenolic antioxidants from the fruits of *Chrysophyllum cainito* L.(star apple). *Journal of Agricultural and Food Chemistry* 50.6: 1379-1382.
- Mahran, E., El Gamal, I., Keusgen, M., and Morlock, G. E. (2019). Effect-directed analysis by high-performance thin-layer chromatography for bioactive metabolites tracking in *Primula veris* flower and *Primula boveana* leaf extracts. *Journal of Chromatography A* 1605: 460371.
- Makara, A. M., Rubaihayo, P. R., and Magambo, M. J. S. (2010). Carry-over effect of Thidiazuron on banana *in vitro* proliferation at different culture cycles and light incubation conditions. *African Journal of Biotechnology* 9.21: 3079-3085.
- Malin, A. S., Qi, D., Shu, X. O., Gao, Y. T., Friedmann, J. M., Jin, F., and Zheng, W. (2003). Intake of fruits, vegetables and selected micronutrients in relation to the risk of breast cancer. *International Journal of Cancer* 105.3: 413-418.
- Mandalari, G., Bennett, R. N., Bisignano, G., Trombetta, D., Saija, A., Faulds, C. B., ... and Nardad, A. (2007). Antimicrobial activity of flavonoids extracted from bergamot (*Citrus bergamia* Risso) peel, a byproduct of the essential oil industry. *Journal of Applied Microbiology* 103.6: 2056-2064.
- Mangathayaru, K., Umeshankar, G., Muralitharan, G., Cordairayen, E., Vasantha, J. (2004). Antimicrobial activity of some indigenous plants. *Indian Journal of Pharmaceutical Sciences* 66: 123.
- Maridass, M., and De Britto, A. J. (2008). Origins of plant derived medicines. *Ethnobotanical Leaflets* 2008.1: 44.
- Mariem, S., Hanen, F., Inès, J., Mejdi, S., and Riadh, K. (2014). Phenolic profile,

- biological activities and fraction analysis of the medicinal halophyte *Retama raetam*. *South African Journal of Botany* 94: 114-121.
- Marston, A. (2011). Thin-layer chromatography with biological detection in phytochemistry. *Journal of Chromatography A* 1218.19: 2676-2683.
- Matsuda, H., Pongpiriyadacha, Y., Morikawa, T., Ochi, M., and Yoshikawa, M. (2003). Gastroprotective effects of phenylpropanoids from the rhizomes of *Alpinia galanga* in rats: structural requirements and mode of action. *European Journal of Pharmacology* 471.1: 59-67.
- McCue, P. P., and Shetty, K. (2004). Inhibitory effects of rosmarinic acid extracts on porcine pancreatic amylase in vitro. *Asia Pacific Journal of Clinical Nutrition* 13.1: 101-106.
- Meyer, D., Marin-Kuan, M., Debon, E., Serrant, P., Cottet-Fontannaz, C., Schilter, B., Morlock, G. E. (2021). Detection of low levels of genotoxic compounds in food contact materials using an alternative HPTLC-SOS-Umu-C Assay. *ALTEX - Alternatives to animal experimentation* DOI: <https://doi.org/10.14573/altex.2006201>.
- Mishra, T., Goyal, A., and Sen, A. (2015). Somatic embryogenesis and genetic fidelity study of the micropropagated medicinal species, *Canna indica*. *Horticulturae* 1.1: 3-13.
- Mohapatra, D., Mishra, S., and Sutar, N. (2010). Banana and its by-product utilisation: an overview. *Journal of Scientific and Industrial Research* 69: 323-329.
- Móricz, Á. M., Jamshidi-Aidji, M., Krüzselyi, D., Darcsi, A., Böszörményi, A., Csontos, P., ... and Morlock, G. E. (2019). Distinction and valorization of 30 root extracts of five goldenrod (*Solidago*) species. *Journal of Chromatography A* 460602 in print.
- Morlock, G., and Schwack, W. (2010). Coupling of planar chromatography to mass spectrometry. *TrAC Trends in Analytical Chemistry* 29.10: 1157-1171.
- Morlock, G., and Schwack, W. (2010). Hyphenations in planar chromatography. *Journal of Chromatography A* 1217.43: 6600-6609.
- Mukherjee, P. K., Kumar, V., Mal, M., and Houghton, P. J. (2007a). Acetylcholinesterase inhibitors from plants. *Phytomedicine* 14.4: 289-300.
- Mulabagal, V., and Tsay, H. S. (2004). Plant cell cultures-an alternative and efficient source for the production of biologically important secondary metabolites. *International Journal of Applied Science and Engineering* 2.1: 29-48.
- Murashige, T., and Skoog, F. (1962). A revised medium for rapid growth and bioassays with tobacco tissue cultures. *Physiologia Plantarum* 15.3: 473-497.
- Murthy, H. N., Lee, E. J., and Paek, K. Y. (2014). Production of secondary metabolites from cell and organ cultures: strategies and approaches for biomass improvement

- and metabolite accumulation. *Plant Cell, Tissue and Organ Culture (PCTOC)* 118.1: 1-16.
- Musa, K. H., Abdullah, A., Jusoh, K., and Subramaniam, V. (2011). Antioxidant activity of pink-flesh guava (*Psidium guajava* L.): effect of extraction techniques and solvents. *Food Analytical Methods* 4.1: 100-107.
- Nakamura, M., Ra, J. H., Jee, Y., and Kim, J. S. (2017). Impact of different partitioned solvents on chemical composition and bioavailability of *Sasa quelpaertensis* Nakai leaf extract. *Journal of Food and Drug Analysis* 25.2: 316-326.
- Nalawade, S. M., and Tsay, H. S. (2004). *In vitro* propagation of some important Chinese medicinal plants and their sustainable usage. *In Vitro Cellular and Developmental Biology-Plant* 40.2: 143-154.
- Namdeo, A. G. (2007). Plant cell elicitation for production of secondary metabolites: a review. *Pharmacognosy Review*, 1.1: 69-79.
- Nirmala, M., Girija, K., Lakshman, K., and Divya, T. (2012). Hepatoprotective activity of *Musa paradisiaca* on experimental animal models. *Asian Pacific Journal of Tropical Biomedicine* 2.1: 11-15.
- Oboh, G., and Rocha, J. B. T. (2007). Antioxidant in foods: a new challenge for food processors. *Leading Edge Antioxidants Research* 35-64.
- Ochoa-Villarreal, M., Howat, S., Hong, S., Jang, M. O., Jin, Y. W., Lee, E. K., and Loake, G. J. (2016). Plant cell culture strategies for the production of natural products. *BMB Reports* 49.3: 149.
- Ojewole, J. A. O., and Adewunmi, C. O. (2003). Hypoglycemic effect of methanolic extract of *Musa paradisiaca* (Musaceae) green fruits in normal and diabetic mice. *Methods and Findings in Experimental and Clinical Pharmacology* 25.6: 453-456.
- Onasanwo, S. A., Emikpe, B. O., Ajah, A. A., and Elufioye, T. O. (2013). Anti-ulcer and ulcer healing potentials of *Musa sapientum* peel extract in the laboratory rodents. *Pharmacognosy Research* 5.3: 173.
- Onyenekwe, P. C., Okereke, O. E., and Owolewa, S. O. (2013). Phytochemical screening and effect of *Musa paradisiaca* stem extrude on rat haematological parameters. *Current Research Journal of Biological Sciences* 5.1: 26-29.
- Padam, B. S., Tin, H. S., Chye, F. Y., and Abdullah, M. I. (2014). Banana by-products: an under-utilized renewable food biomass with great potential. *Journal of Food Science and Technology* 51.12: 3527-3545.
- Pagare, S., Bhatia, M., Tripathi, N., Pagare, S., and Bansal, Y. K. (2015). Secondary metabolites of plants and their role: Overview. *Current Trends in Biotechnology and Pharmacy* 9.3: 293-304.

- Palacio, L., Cantero, J. J., Cusidó, R., and Goleniowski, M. (2011). Phenolic compound production by *Larrea divaricata* Cav. plant cell cultures and effect of precursor feeding. *Process Biochemistry* 46.1: 418-422.
- Park, Y. G., Kim, S. J., Kang, Y. M., Jung, H. Y., Prasad, D. T., Kim, S. W., ... and Choi, M. S. (2004). Production of ginkgolides and bilobalide from optimized the *Ginkgo biloba* cell culture. *Biotechnology and Bioprocess Engineering* 9.1: 41-46.
- Pauwels, L., Inzé, D., and Goossens, A. (2009). Jasmonate-inducible gene: what does it mean?. *Trends in Plant Science* 14.2: 87-91.
- Pereira, A., and Maraschin, M. (2015). Banana (*Musa* spp) from peel to pulp: ethnopharmacology, source of bioactive compounds and its relevance for human health. *Journal of Ethnopharmacology* 160: 149-163.
- Porta, H., and Rocha-Sosa, M. (2002). Plant lipoxygenases. Physiological and molecular features. *Plant Physiology* 130.1: 15-21.
- Pothavorn, P., Kitdamrongsont, K., Swangpol, S., Wongniam, S., Atawongsa, K., Svasti, J., and Somana, J. (2010). Sap phytochemical compositions of some bananas in Thailand. *Journal of Agricultural and Food Chemistry* 58.15: 8782-8787.
- Prabha, P., Karpagam, T., Varalakshmi, B., and Packiavathy, A. S. C. (2011). Indigenous anti-ulcer activity of *Musa sapientum* on peptic ulcer. *Pharmacognosy Research* 3.4: 232.
- Praveen, N., and Murthy, H. N. (2010). Production of withanolide-A from adventitious root cultures of *Withania somnifera*. *Acta Physiologiae Plantarum* 32.5: 1017-1022.
- Praveen, N., and Murthy, H. N. (2012). Synthesis of withanolide A depends on carbon source and medium pH in hairy root cultures of *Withania somnifera*. *Industrial Crops and Products* 35.1: 241-243.
- Puente-Garza, C. A., Gutiérrez-Mora, A., and García-Lara, S. (2015). Micropropagation of *Agave salmiana*: means to production of antioxidant and bioactive principles. *Frontiers in Plant Science* 6: 1026.
- Rabasa-Lhoret, R., and Chiasson, J. L. (2004). Alpha-glucosidase inhibitors. W: De Fronzo RA, Ferrannini E., Keen H., Zimmet P. (red.) International textbook of diabetes mellitus. John Wiley and Sons, New Jersey.
- Rabbi, I. Y., Kulakow, P. A., Manu-Aduening, J. A., Dankyi, A. A., Asibuo, J. Y., Parkes, E. Y., ... and Reyes, B. (2015). Tracking crop varieties using genotyping-by-sequencing markers: a case study using cassava (*Manihot esculenta* Crantz). *BMC Genetics* 16.1: 115.
- Rådmark, O., and Samuelsson, B. (2007). 5-lipoxygenase: regulation and possible involvement in atherosclerosis. *Prostaglandins and Other Lipid Mediators* 83.3: 162-174.

- Ragasa, C. Y., Martinez, A., Chua, J. E. Y., and Rideout, J. A. (2007). A Triterpene from *Musa errans*. *Philippine Journal of Sciences* 136.2: 167-171.
- Ramachandra, R. S., and Ravishankar, G. A. (2002). Biotransformation of isoeugenol to vanilla flavor metabolites and capsaicin in freely suspended and immobilized cell cultures of *Capsicum frutescens*: study of the influence of β -cyclodextrin and fungal elicitor. *Process Biochemistry* 35: 341-348.
- Ramesha, B. T., Amna, T., Ravikanth, G., Gunaga, R. P., Vasudeva, R., Ganeshaiyah, K. N., ... and Qazi, G. N. (2008). Prospecting for camptothecines from *Nothapodytes nimmoniana* in the Western Ghats, South India: identification of high-yielding sources of camptothecin and new families of camptothecines. *Journal of Chromatographic Science* 46.4: 362-368.
- Ramya, S., Saraswathi, U., and Malathi, M. (2017). *In vitro* anti-inflammatory activity of different varieties of *Musa sapientum* (banana) peel extract extract". *International Journal of Current Research* 9: 47300-47302.
- Rao, S. R., and Ravishankar, G. A. (1999). Biotransformation of isoeugenol to vanilla flavour metabolites and capsaicin in suspended and immobilized cell cultures of *Capsicum frutescens*: study of the influence of β -cyclodextrin and fungal elicitor. *Process Biochemistry* 35.3-4: 341-348.
- Rao, S. R., and Ravishankar, G. A. (2002). Plant cell cultures: chemical factories of secondary metabolites. *Biotechnology Advances* 20.2: 101-153.
- Rashidkhani, B., Lindblad, P., and Wolk, A. (2005). Fruits, vegetables and risk of renal cell carcinoma: a prospective study of Swedish women. *International Journal of Cancer* 113.3: 451-455.
- Raskin, I., Ribnicky, D. M., Komarnytsky, S., Ilic, N., Poulev, A., Borisjuk, N., ... and O'Neal, J. M. (2002). Plants and human health in the twenty-first century. *Trends in Biotechnology* 20.12: 522-531.
- Rates, S. M. K. (2001). Plants as source of drugs. *Toxicon* 39.5: 603-613.
- Ravishankar, G. A., and Ramachandra Rao, S. (2000). Biotechnological Production of Phyto-Pharmaceuticals. *Journal of Biochemistry Molecular Biology and Biophysics* 4: 73-102.
- Re, R., Pellegrini, N., Proteggente, A., Pannala, A., Yang, M., and Rice-Evans, C. (1999). Antioxidant activity applying an improved ABTS radical cation decolorization assay. *Free Radical Biology and Medicine* 26.9-10: 1231-1237.
- Rosida, S. S., Sukardiman, and Khotib, J. (2014). The increasing of VEGF expression and re-epithelialisation on dermal wound healing process after treatment of banana peel extract (*Musa acuminata* Colla). *International Journal of Pharmacy Pharmaceutical Sciences* 6.11: 427-30.

- Rout, G. R., Samantaray, S., and Das, P. (2000). *In vitro* manipulation and propagation of medicinal plants. *Biotechnology Advances* 18.2: 91-120.
- Rout, G. R., Senapati, S. K., Aparajita, S., and Palai, S. K. (2009). Studies on genetic identification and genetic fidelity of cultivated banana using ISSR markers. *Plant Omics* 2.6: 250.
- Sales, E. K., and Butardo, N. G. (2014). Molecular analysis of somaclonal variation in tissue culture derived bananas using MSAP and SSR markers. *International Journal of Biotechnology and Bioengineering* 8.6: 615-622.
- Salvi, N. D., George, L., and Eapen, S. (2001). Plant regeneration from leaf base callus of turmeric and random amplified polymorphic DNA analysis of regenerated plants. *Plant Cell, Tissue and Organ Culture (PCTOC)* 66.2: 113-119.
- Sánchez-Sampedro, M. A., Fernández-Tárrago, J., and Corchete, P. (2005a). Yeast extract and methyl jasmonate-induced silymarin production in cell cultures of *Silybum marianum* (L.) Gaertn. *Journal of biotechnology* 119.1: 60-69.
- Sasidharan, S., Chen, Y., Saravanan, D., Sundram, K. M., and Latha, L. Y. (2011). Extraction, isolation and characterization of bioactive compounds from plants' extracts. *African Journal of Traditional, Complementary and Alternative Medicines* 8.1: 1-10.
- Sasikumar, S., Raveendar, S., Premkumar, A., Ignacimuthu, S., and Agastian, P. (2009). Micropropagation of *Baliospermum montanum* (Willd.) Muell. Arg.—A threatened medicinal plant. *Indian Journal of Biotechnology* 8.2: 223-226.
- Savali, A. S., Bhinge, S. D., and Chitapurkar, H. R. (2011). Evaluation of hair growth promoting activity of *Musa paradisiaca* unripe fruit extract. *Journal of Natural Pharmaceuticals* 2.3: 120-124.
- Schenk, R. U., and Hildebrandt, A. C. (1972). Medium and techniques for induction and growth of monocotyledonous and dicotyledonous plant cell cultures. *Canadian Journal of Botany* 50.1: 199-204.
- Schneider, J. A., Arvanitakis, Z., Leurgans, S. E., and Bennett, D. A. (2009). The neuropathology of probable Alzheimer disease and mild cognitive impairment. *Annals of Neurology: Official Journal of the American Neurological Association and the Child Neurology Society* 66.2: 200-208.
- Selli, S., Gubbuk, H., Kafkas, E., and Gunes, E. (2012). Comparison of aroma compounds in Dwarf Cavendish banana (*Musa* spp. AAA) grown from open-field and protected cultivation area. *Scientia Horticulturae* 141: 76-82.
- Shaik, S., Singh, N., and Nicholas, A. (2011). HPLC and GC analyses of *in vitro*-grown leaves of the cancer bush *Lessertia* (*Sutherlandia*) *frutescens* L. reveal higher yields of bioactive compounds. *Plant Cell, Tissue and Organ Culture (PCTOC)* 105.3: 431-438.

- Shankar, K., Chavan, L., Shinde, S., and Patil, B. (2011). An improved DNA extraction protocol from four *in vitro* banana cultivars. *Asian Journal of Biotechnology* 3.1: 84-90.
- Sheng, Z., Dai, H., Pan, S., Ai, B., Zheng, L., Zheng, X., ... and Xu, Z. (2017). Phytosterols in banana (*Musa* spp.) flower inhibit α -glucosidase and α -amylase hydrolyses and glycation reaction. *International Journal of Food Science and Technology* 52.1: 171-179.
- Simmonds, N. W., and Shepherd, K. (1955). The taxonomy and origins of the cultivated bananas. *Botanical Journal of the Linnean Society* 55.359: 302-312.
- Smetanska, I. (2008). Production of secondary metabolites using plant cell cultures. In *Food biotechnology* Springer, Berlin, Heidelberg, (pp. 187-228)..
- Someya, S., Yoshiki, Y., and Okubo, K. (2002). Antioxidant compounds from bananas (*Musa cavendish*). *Food Chemistry* 79.3: 351-354.
- Sonibare, M. A., and Ayoola, I. O. (2015). Medicinal plants used in the treatment of neurodegenerative disorders in some parts of Southwest Nigeria. *African Journal of Pharmacy and Pharmacology* 9.38: 956-965.
- Sonibare, M. A., Ayoola, I. O., Gueye, B., Abberton, M. T., D'Souza, R., and Kuhnert, N. (2018). Leaves metabolomic profiling of *Musa acuminata* accessions using UPLC–QTOF–MS/MS and their antioxidant activity. *Journal of Food Measurement and Characterisation* 12.2: 1093-1106.
- Srivastava, M. M. (2011). An overview of HPTLC: A modern analytical technique with excellent potential for automation, optimization, hyphenation, and multidimensional applications. In *High-performance thin-layer chromatography (HPTLC)* (pp. 3-24). Springer, Berlin, Heidelberg.
- Srivastava, S., and Srivastava, A. K. (2014). Effect of elicitors and precursors on azadirachtin production in hairy root culture of *Azadirachta indica*. *Applied biochemistry and biotechnology* 172.4: 2286-2297.
- Su, Y. H., Liu, Y. B., and Zhang, X. S. (2011). Auxin–cytokinin interaction regulates meristem development. *Molecular Plant* 4.4: 616-625.
- Suan See, K., Bhatt, A., and Lai Keng, C. (2011). Effect of sucrose and methyl jasmonate on biomass and anthocyanin production in cell suspension culture of *Melastoma malabathricum* (Melastomaceae). *Revista de Biologia Tropical* 59.2: 597-606.
- Susanti, D., Sirat, H. M., Ahmad, F., Ali, R. M., Aimi, N., and Kitajima, M. (2007). Antioxidant and cytotoxic flavonoids from the flowers of *Melastoma malabathricum* L. *Food Chemistry* 103.3: 710-716.
- Tassoni, A., Durante, L., and Ferri, M. (2012). Combined elicitation of methyl-jasmonate and red light on stilbene and anthocyanin biosynthesis. *Journal of Plant Physiology* 169.8: 775-781.

- Team, R. C. (2013). R: A language and environment for statistical computing.
- Teixeira, T. S., Vale, R. C., Almeida, R. R., Ferreira, T. P. S., and Guimarães, L. G. L. (2017). Antioxidant potential and its correlation with the contents of phenolic compounds and flavonoids of methanolic extracts from different medicinal plants. *Revista Virtual de Química* 9.4: 1546-1559.
- Thangaraj, P. (2016). Pharmacological assays of plant-based natural products. Geneva, Switzerland: Springer.
- Tsamo, C. V. P., Herent, M. F., Tomekpe, K., Emaga, T. H., Quetin-Leclercq, J., Rogez, H., ... and Andre, C. (2015). Phenolic profiling in the pulp and peel of nine plantain cultivars (*Musa* spp.). *Food Chemistry* 167: 197-204.
- Tsao, R., and Deng, Z. (2004). Separation procedures for naturally occurring antioxidant phytochemicals. *Journal of Chromatography B* 812.1-2: 85-99.
- Tusevski, O., Krstikj, M., Stanoeva, J. P., Stefova, M., and Simic, S. G. (2018). Phenolic profile and biological activity of *Hypericum perforatum* L.: Can roots be considered as a new source of natural compounds?. *South African Journal of Botany* 117: 301-310.
- Ugbogu, E. A., Ude, V. C., Elekwa, I., Arunsi, U. O., Uche-Ikonne, C., and Nwakanma, C. (2018). Toxicological profile of the aqueous-fermented extract of *Musa paradisiaca* in rats. *Avicenna Journal of Phytomedicine* 8.6: 478.
- Uhegbu, F. O., Imo, C., and Onwuegbuchulam, C. H. (2016). Hypoglycemic, Hypolipidemic and Antioxidant Activities of *Musa paradisiaca*, Normalis (Plantain) Supplemented Diet on Alloxan Induced-diabetic Albino Rats. *Asian Journal of Biochemistry* 11.3: 162-167.
- Umamaheswari, A., Puratchikody, A., Prabu, S. L., and Jayapriya, T. (2017). Phytochemical screening and antimicrobial effect of *Musa acuminata* bract. *International Research Journal of Pharmacy* 8.8: 41-44.
- Urbano, M., De Castro, M. D. L., Pérez, P. M., García-Olmo, J., and Gomez-Nieto, M. A. (2006). Ultraviolet-visible spectroscopy and pattern recognition methods for differentiation and classification of wines. *Food Chemistry* 97.1: 166-175.
- Urbanska, N., Giebultowicz, J., Olszowska, O., and Szypula, W. J. (2014). The growth and saponin production of *Platycodon grandiflorum* (Jacq.) A. DC.(Chinese bellflower) hairy roots cultures maintained in shake flasks and mist bioreactor. *Acta Societatis Botanicorum Poloniae* 83.3: 229-237.
- Vanisree, M., Lee, C. Y., Lo, S. F., Nalawade, S. M., Lin, C. Y., and Tsay, H. S. (2004). Studies on the production of some important secondary metabolites from medicinal plants by plant tissue cultures. *Botanical Bulletin of the Academia Sinica* 45.1: 1-22.
- Vilela, C., Santos, S. A., Villaverde, J. J., Oliveira, L., Nunes, A., Cordeiro, N., Freire, C. S. R., and Silvestre, A. J. (2014). Lipophilic phytochemicals from banana fruits of

- several *Musa* species. *Food Chemistry* 162: 247-252.
- Vilhena, O. R., Fachi, M. M., Marson, B. M., Dias, B. L., Pontes, F. L., Tonin, F. S., and Pontarolo, R. (2018). Antidiabetic potential of *Musa* spp. inflorescence: a systematic review. *Journal of Pharmacy and Pharmacology* 70.12: 1583-1595.
- Waghmare, S. G., Pawar, K. R., Tabe, R. H. and Jamdade, A. S. (2017). Somatic embryogenesis in strawberry (*Fragaria ananassa* Var. Camarosa). *Global Journal of Bio-science and Biotechnology* 6.2: 309-313.
- Wang, J. W., Xia, Z. H., Chu, J. H., and Tan, R. X. (2004). Simultaneous production of anthocyanin and triterpenoids in suspension cultures of *Perilla frutescens*. *Enzyme and Microbial Technology* 34.7: 651-656.
- Wang, S. Y., Bowman, L., and Ding, M. (2008). Methyl jasmonate enhances antioxidant activity and flavonoid content in blackberries (*Rubus* spp.) and promotes antiproliferation of human cancer cells. *Food Chemistry* 107.3: 1261-1269.
- Wang, W., and Zhong, J. J. (2002). Manipulation of ginsenoside heterogeneity in cell cultures of *Panax notoginseng* by addition of jasmonates. *Journal of Bioscience and Bioengineering* 93.1: 48-53.
- Wenzl, P., Carling, J., Kudrna, D., Jaccoud, D., Huttner, E., Kleinhofs, A., and Kilian, A. (2004). Diversity Arrays Technology (DArT) for whole-genome profiling of barley. *Proceedings of the National Academy of Sciences* 101.26: 9915-9920.
- Wiktorowska, E., Długosz, M., and Janiszowska, W. (2010). Significant enhancement of oleanolic acid accumulation by biotic elicitors in cell suspension cultures of *Calendula officinalis* L. *Enzyme and Microbial Technology* 46.1: 14-20.
- World Health Organization. (2009). Diarrhoea: why children are still dying and what can be done.
- Xu, M., and Dong, J. (2005a). Elicitor-induced nitric oxide burst is essential for triggering catharanthine synthesis in *Catharanthus roseus* suspension cells. *Applied Microbiology and Biotechnology* 67.1: 40-44.
- Yadav, J. P., Saini, S., Kalia, A. N., and Dangi, A. S. (2008). Hypoglycemic and hypolipidemic activity of ethanolic extract of *Salvadora oleoides* in normal and alloxan-induced diabetic rats. *Indian Journal of Pharmacology* 40.1: 23.
- Yakubu, M. T., Nurudeen, Q. O., Salimon, S. S., Yakubu, M. O., Jimoh, R. O., Nafiu, M. O., ... and Williams, F. E. (2015). Antidiarrhoeal activity of *Musa paradisiaca* sap in Wistar rats. *Evidence-Based Complementary and Alternative Medicine* 2015: 1-9.
- Yue, W., Ming, Q. L., Lin, B., Rahman, K., Zheng, C. J., Han, T., and Qin, L. P. (2016). Medicinal plant cell suspension cultures: pharmaceutical applications and high-yielding strategies for the desired secondary metabolites. *Critical Reviews in Biotechnology* 36.2: 215-232.

- Yuei, L. P., Singaram, N., and Hassan, H. (2016). Study of anti-inflammatory and analgesic activity of *Musa* spp. peel. DOI: 10.13140/RG.2.2.33612.10884
- Zakpaa, H. D., Al-Hassan, A., and Adubofour, J. (2010). An investigation into the feasibility of production and characterization of starch from apantu plantain (giant horn) grown in Ghana. *African Journal of Food Science* 4.9: 571-577.
- Zhang, C. H., Fevereiro, P. S., He, G., and Chen, Z. (2007). Enhanced paclitaxel productivity and release capacity of *Taxus chinensis* cell suspension cultures adapted to chitosan. *Plant Science* 172.1: 158-163.
- Zhang, C. P., Zheng, H. Q., Liu, G., and Hu, F. L. (2011). Development and validation of HPLC method for determination of salicin in poplar buds: Application for screening of counterfeit propolis. *Food Chemistry* 127.1: 345-350.

Appendices

Table 1: Imputation report of missing data with six different algorithms of 150.5K SNP in 56 banana samples

Imputation Report

- Plugin Version: (21)
- Imputed File: gd2l_ppca_imputed.csv

Imputation methods timings and scores

Alg	Time	smc
ppca	7.814	0.98609
svd	5.673	0.9859732
nipals	2.992	0.9851168
random	4.222	0.7091946
em	3.834	0.4533588
knn	.503	0.3771913

Process

Each imputation method was ran on the dataset with an additional 10.0% introduced missing values. The imputed, introduced missing values are then compared to the original dataset to calculate a [Simple Matching Coefficient \(SMC\)](#). As the winning candidate, the highest scoring method is then used to imputed the original dataset.

Table 2: Peak area of HPTLC-Effect directed analysis of field, *in vitro* and acclimatised*Musa* spp. accessions

Sample ID	Sample code	Peak area						
		DPPH* (PAMP)	AChE (PAMP)	AChE (NAMP)	BChE (PAMP)	BChE (NAMP)	α -glucosidase	β -glucosidase
Simili radjah_F	A ₁	34795.4	0	1819.9	3195.6	1235.4	180.2	4030.3
Simili radjah_IV	A ₂	66699.4	6450.5	2536.6	13608.2	1632.1	3027.3	9606.3
Simili radjah_Acc	A ₃	0	0	8850.2	0	8300.6	0	0
Foconah_F	B ₁	19124.9	0	6938.7	2864.1	7330.4	0	2267.5
Foconah_IV	B ₂	52620.1	1076.6	5990.5	13560.6	5004	933.3	5993
Foconah_Acc	B ₃	0	0	6559.2	0	6304.7	0	0
P. Mas_F	C ₁	20295.7	0	4657.5	3373.9	5086.4	0	0
P. Mas_IV	C ₂	49792.3	5283.9	6638.5	14130.3	7872.2	1915.9	2301.7
P. Mas_Acc	C ₃	0	0	9079.6	0	10379.1	0	0
P. Jaribuaya_F	D ₁	17978.2	0	4751.4	2534.1	5434.7	0	0
P. Jaribuaya_IV	D ₂	51853	5138.6	6661.9	16144.1	7073.4	2423.4	1130.3
P. Jaribuaya_Acc	D ₃	0	0	9419.1	0	12237.8	0	0
Zebrina_F	E ₁	18420.4	0	7228.9	2666.4	9109.9	0	0
Zebrina_IV	E ₂	52340.7	5443.2	8336.3	18465.9	8622.7	3281.5	3407.9
Zebrina_Acc	E ₃	0	0	2278.6	0	6306.4	0	0
Calcutta-4_F	F ₁	0	0	4741	1343.3	6062.8	0	0
Calcutta-4_IV	F ₂	82254.8	7649	1072.2	15017.6	806	3999	3111.9
Calcutta-4_Acc	F ₃	4145.9	0	9958.7	0	10158.9	0	0
Gros michel_F	G ₁	13130	0	3543.4	2535.6	2439.3	0	0
Gros michel_IV	G ₂	31052.5	787.3	7286.2	12397.7	5492.5	0	2306.5
Gros michel_Acc	G ₃	0	0	3292.5	0	2066.9	0	0

Red Dacca_F	H ₁	7621.1	0	9493.6	0	4261.3	0	0
Red Dacca_IV	H ₂	61559	12435.9	6034.1	18542.1	1919.8	8574.7	8352.3
Red Dacca_Acc	H ₃	0	0	9809.3	0	6471.3	0	0
P. Ceylan_F	I ₁	2706.3	0	4597.6	0	3010.8	0	0
P. Ceylan_IV	I ₂	49174.6	4840.5	2199.7	7207.5	1795.6	2334.3	0
P. Ceylan_Acc	I ₃	0	2161.9	10576	0	10719.6	0	0
Pelipita_F	J ₁	17422.4	0	4818.1	0	3622.3	0	0
Pelipita_IV	J ₂	27732	2945.6	4662.4	8798.8	2806.2	536.2	0
Pelipita_Acc	J ₃	0	1689.1	7279.4	0	6947.2	0	0
M. balbisiana Tani_F	K ₁	16145.2	2077.7	1768.2	0	1384.8	0	0
M. balbisiana Tani_IV	K ₂	17027.9	3567	2669.8	4686	3123.2	0	0
M. balbisiana Tani_Acc	K ₃	0	0	3484.6	0	3114.9	0	0
Dole_F	L ₁	12848.7	2912.9	3331.5	0	2846	0	0
Dole_IV	L ₂	12814	3459.3	6321.7	0	5239.3	0	0
Dole_Acc	L ₃	0	0	5830.7	0	7455.3	0	0
Safet velchi_F	M ₁	15183.6	2136.9	4304.1	0	3746.6	0	0
Safet velchi_IV	M ₂	43395.7	12016.3	5140.3	12232.4	4112.8	1747.2	0
Safet velchi_Acc	M ₃	0	0	4048.3	0	9252.4	0	0
M. balbisiana HND_F	N ₁	9160.7	0	1494.6	0	829.8	0	0
M. balbisiana HND_IV	N ₂	9963.4	111.9	3053.9	0	1634	0	0
Igitsiri_F	O ₁	15728.8	555.7	5062.4	0	3407.2	0	0
Igitsiri_IV	O ₂	38427	5078.7	4811.4	6878	2356.4	2789.8	2438.4

Table 3: Means of ABTS and hydroxyl radical scavenging activities of *Musa acuminata* (Siili radjah) leaf and fruit crude extracts and fractions

S/N	Fractions	Hydroxyl IC ₅₀ (µg/mL)	ABTS IC ₅₀ (µg/mL)
Leaf			
1	CME	10.16 ± 1.03 ^a	240.00 ± 0.42 ^a
2	NHF	22.56 ± 1.01 ^b	466.70 ± 14.97 ^c
3	DCM	55.17 ± 1.79 ^c	470.80 ± 13.36 ^c
4	EAF	12.05 ± 0.86 ^a	187.30 ± 0.13 ^a
5	NBF	11.26 ± 1.04 ^a	206.10 ± 1.67 ^a
6	AMF	56.88 ± 13.16 ^c	1332.00 ± 50.63 ^d
Fruit			
7	CME	187.10 ± 1.86 ^c	452.70 ± 18.24 ^c
8	NHF	183.60 ± 2.10 ^c	560.30 ± 0.92 ^d
9	DCM	253.60 ± 3.41 ^d	480.50 ± 7.08 ^c
10	EAF	188.10 ± 2.07 ^c	541.20 ± 5.85 ^d
11	NBF	249.20 ± 12.24 ^d	465.10 ± 7.12 ^c
12	AMF	115.70 ± 5.50 ^b	628.30 ± 31.89 ^c
Gallic acid		58.71 ± 1.94 ^a	199.50 ± 0.79 ^a
Ascorbic acid		124.90 ± 2.53 ^a	349.60 ± 1.04 ^b

Table 4: Antidiabetic activity of *Musa acuminata* (Siili radjah) leaf and fruit crude extracts and fractions

S/N	Fractions	α -amylase IC ₅₀ ($\mu\text{g mL}^{-1}$)	α -glucosidase IC ₅₀ ($\mu\text{g mL}^{-1}$)
Leaf			
1	CME	490.50 \pm 10.86 ^b	91.22 \pm 5.14 ^c
2	NHF	337.80 \pm 3.51 ^a	182.80 \pm 6.33 ^d
3	DCM	448.10 \pm 12.07 ^b	99.13 \pm 8.84 ^c
4	EAF	444.30 \pm 4.00 ^b	4.94 \pm 1.61 ^a
5	NBF	1210.00 \pm 41.18 ^c	53.63 \pm 2.80 ^b
6	AMF	300.10 \pm 1.41 ^a	24.10 \pm 3.39 ^b
Fruit			
7	CME	713.10 \pm 5.77 ^d	200.90 \pm 7.45 ^a
8	NHF	1292.00 \pm 10.46 ^f	590.20 \pm 71.4 ^d
9	DCM	706.20 \pm 9.91 ^d	298.40 \pm 17.02 ^b
10	EAF	297.90 \pm 1.28 ^a	277.00 \pm 5.04 ^b
11	NBF	777.80 \pm 5.68 ^e	505.40 \pm 6.05 ^c
12	AMF	521.70 \pm 3.66 ^c	192.70 \pm 2.52 ^a
Acarbose		332.50 \pm 1.91 ^b	265.20 \pm 6.00 ^b

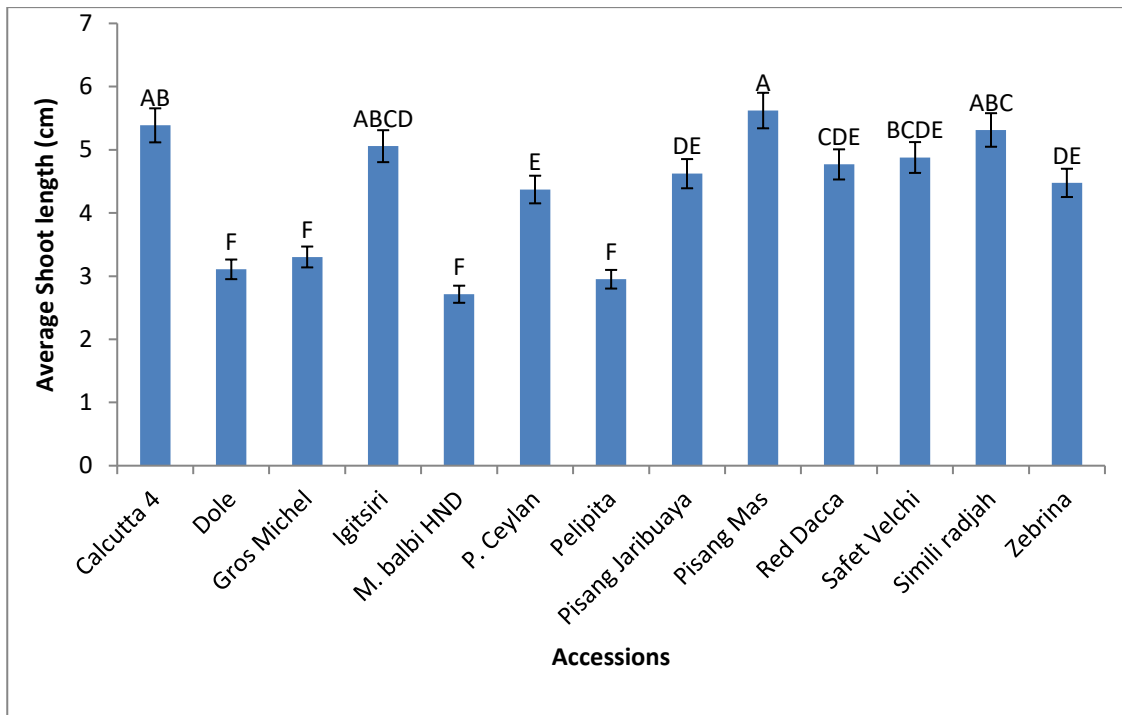


Figure 1: Average Shoot length (cm) of the different tissue culture-grown accessions

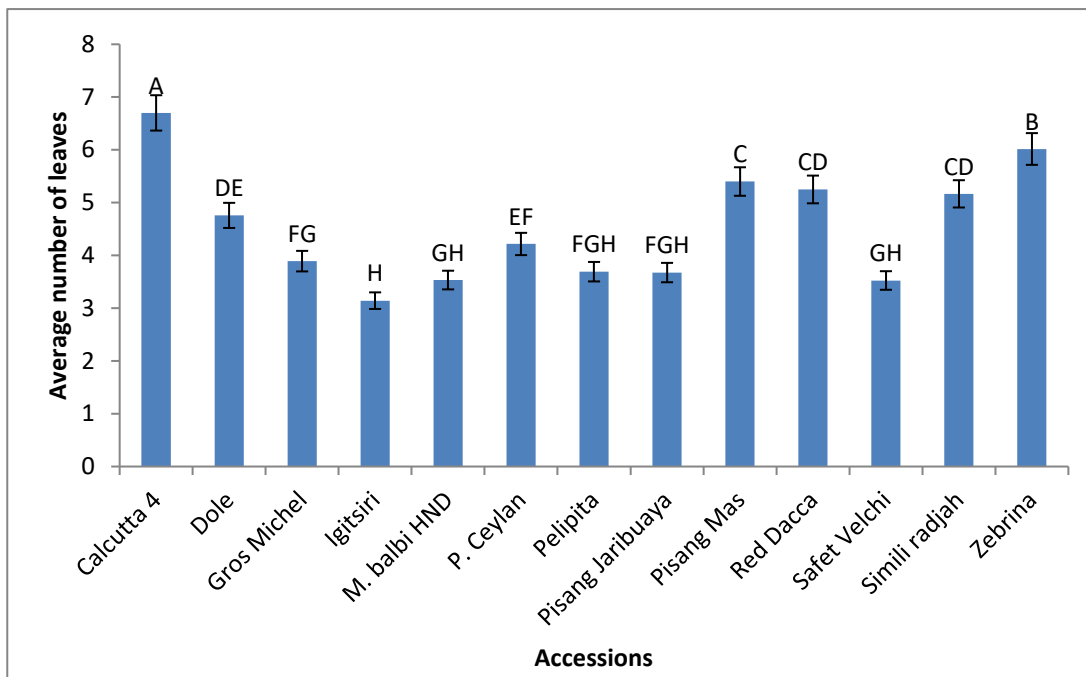


Figure 2: Average number of leaves of the different tissue culture-grown accessions

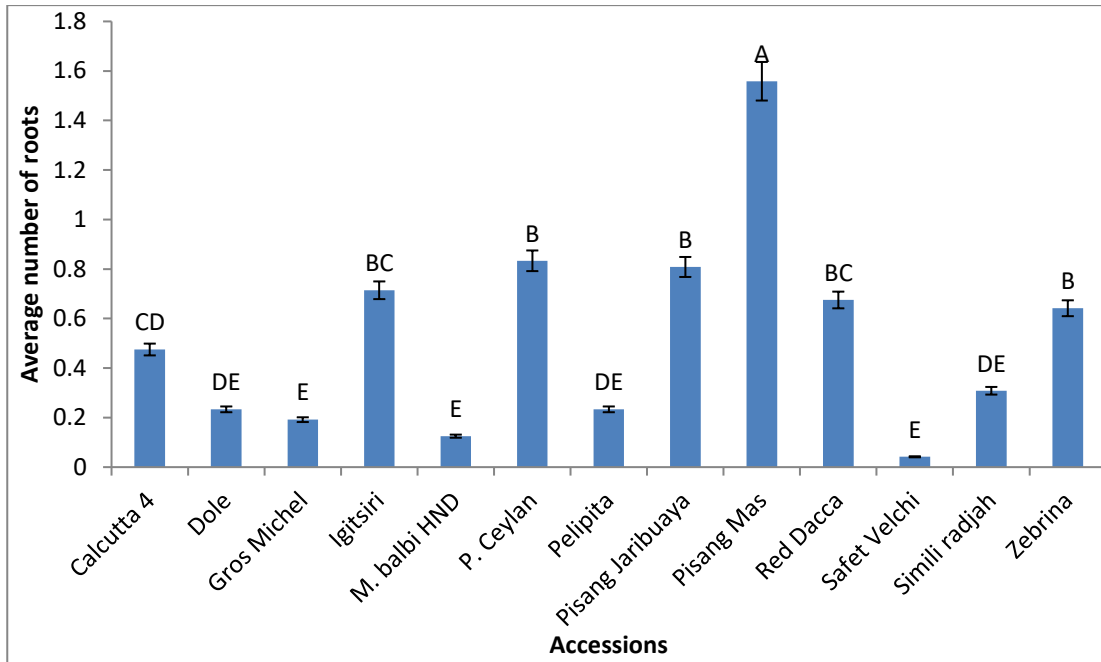


Figure 3: Average number of roots of the different tissue culture-grown accessions

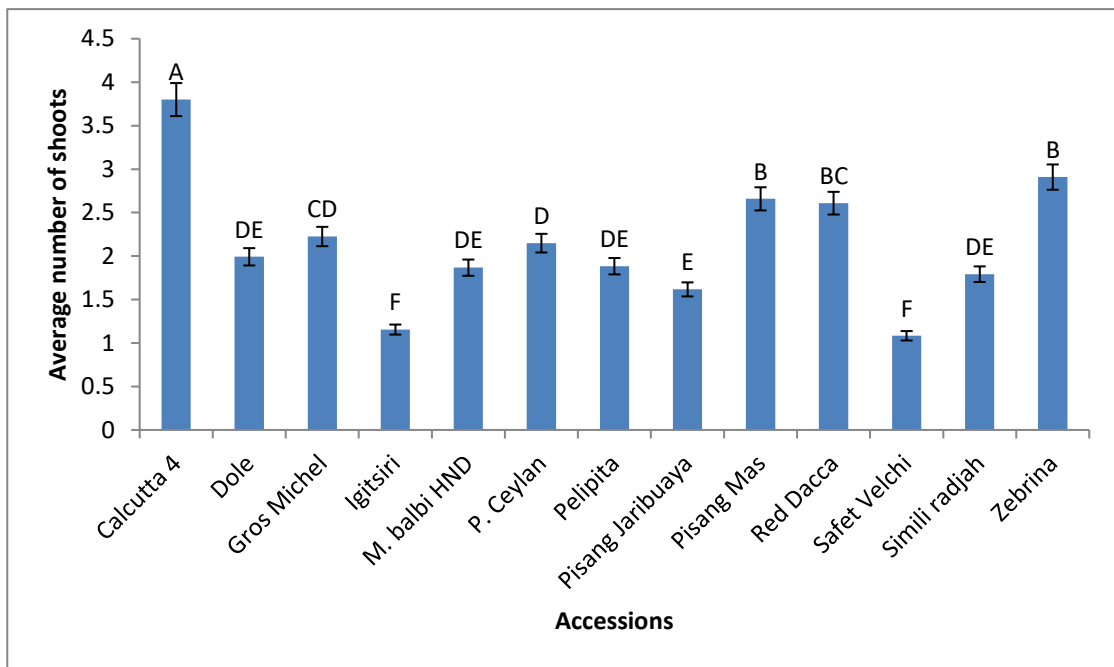


Figure 4: Average number of shoots of the different tissue culture-grown accession

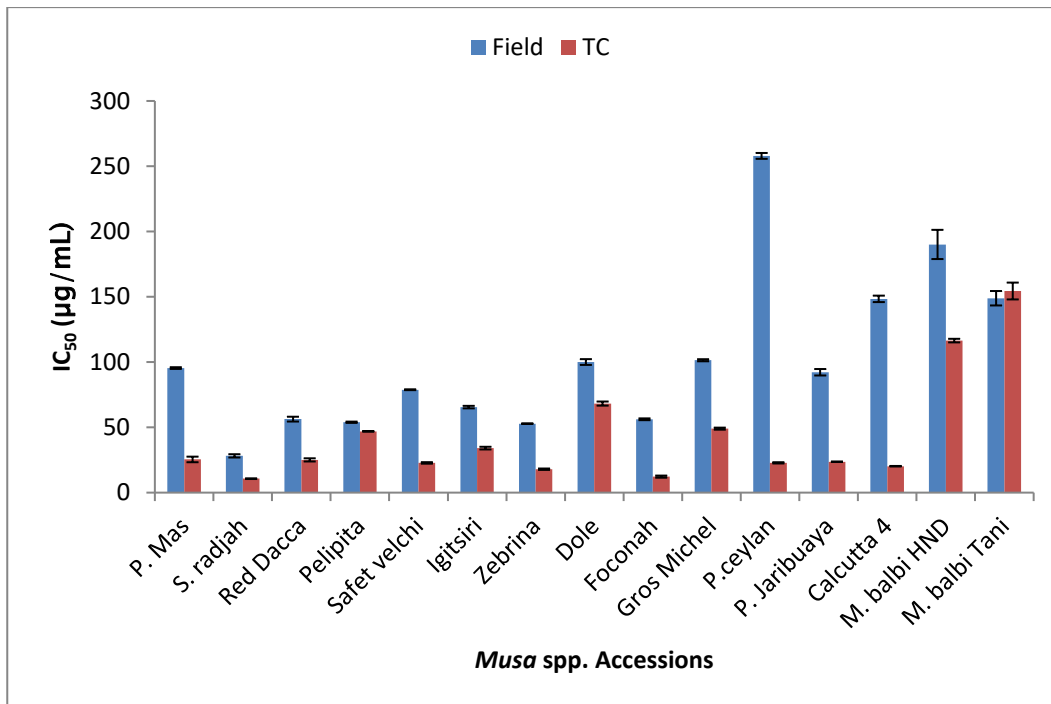


Figure 5: DPPH• IC₅₀ values of field and tissue culture accessions

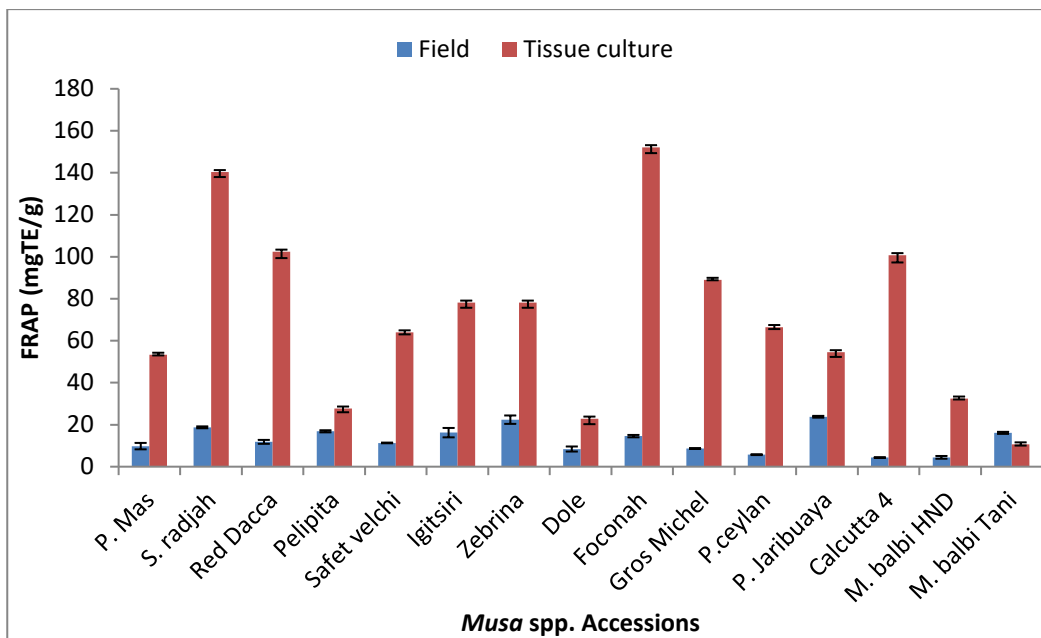


Figure 6: Ferric reducing antioxidant power of field and tissue culture-grown accessions

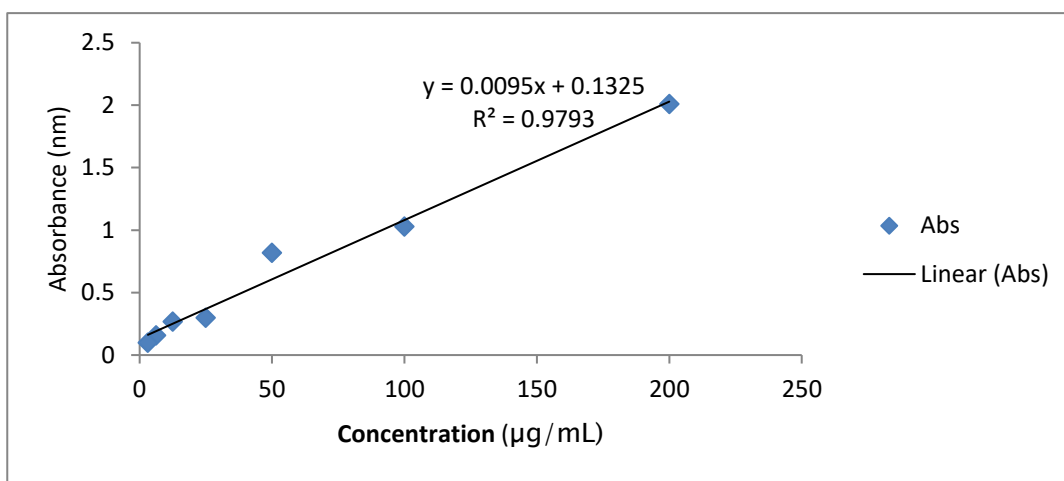


Figure 7: Gallic acid calibration curve for TPC

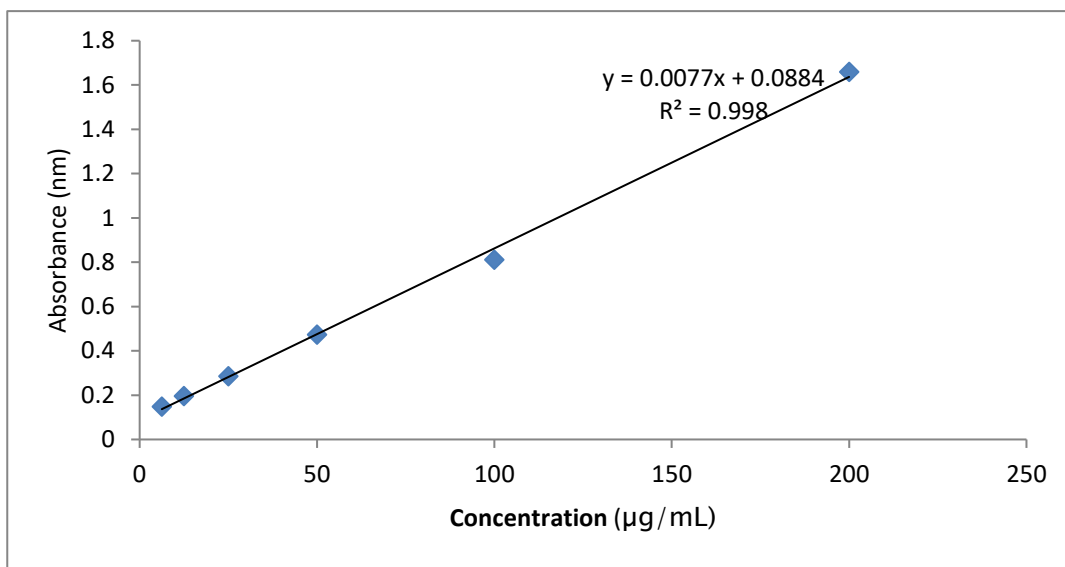


Figure 8: Quercetin calibration curve for TFC

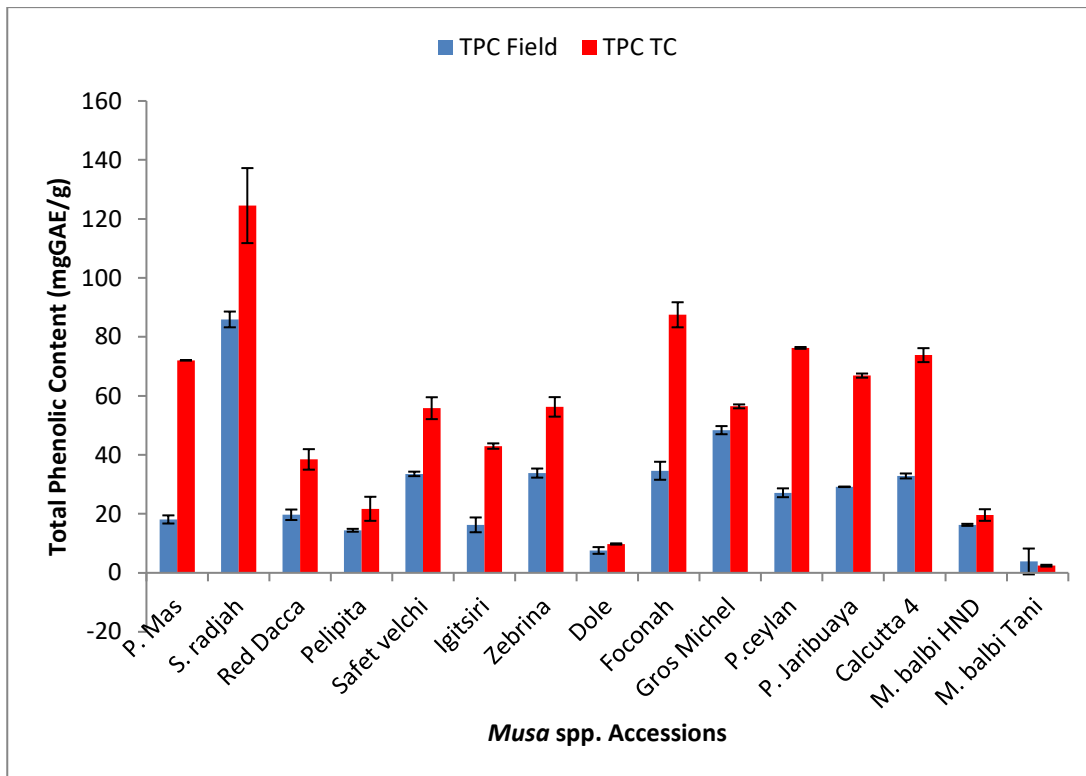


Figure 9: Total phenolic contents of field and tissue culture-grown accessions

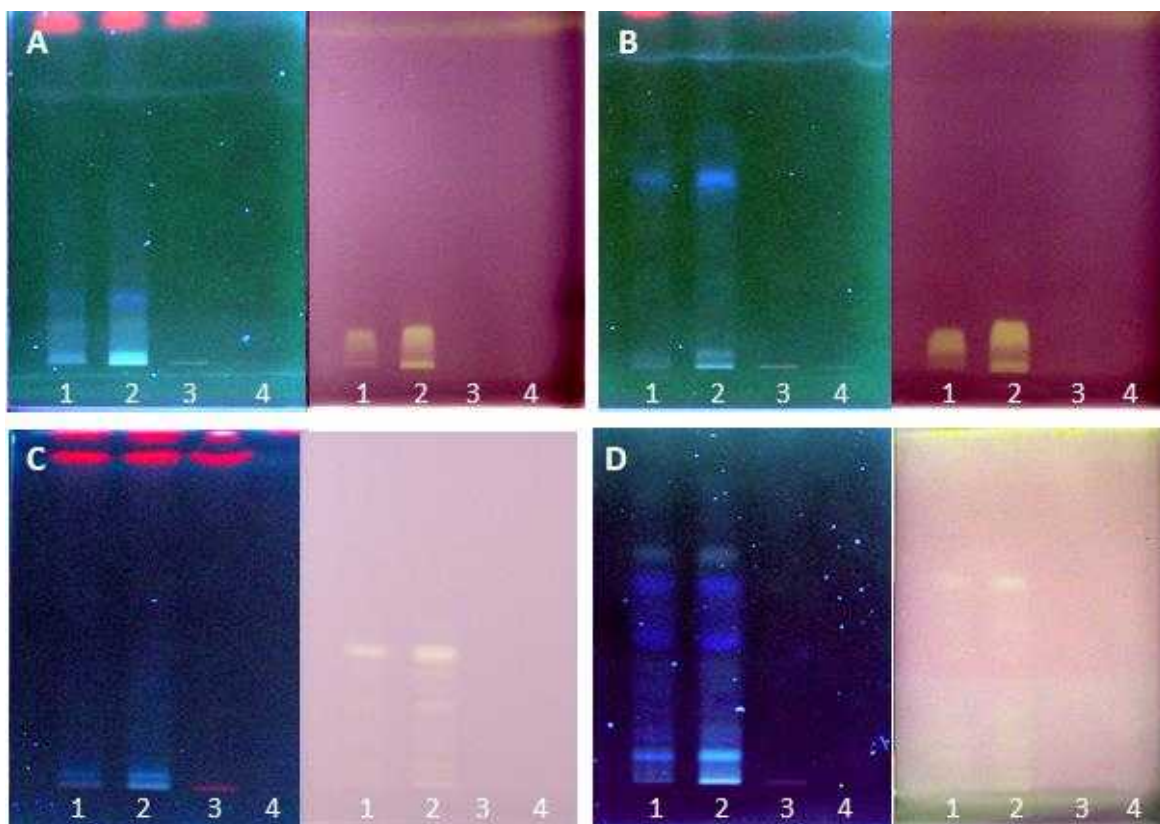


Figure 10: HPTLC-UV/FLD chromatograms of the accession Foconah extracted with (1) methanol, (2) ethanol - water 7:3, (3) ethyl acetate and (4) *n*-hexane and developed with (A) ethanol - water 4:0.5:0.5, (B) ethanol - water 4:1, (C) ethyl acetate - toluene - formic acid - water 6.4:1.6:1.2:0.8 (D) ethyl acetate - toluene - formic acid - water 6.8:1:1.4:1, all detected at UV 366 nm and after DPPH[•] assay documented at white light illumination

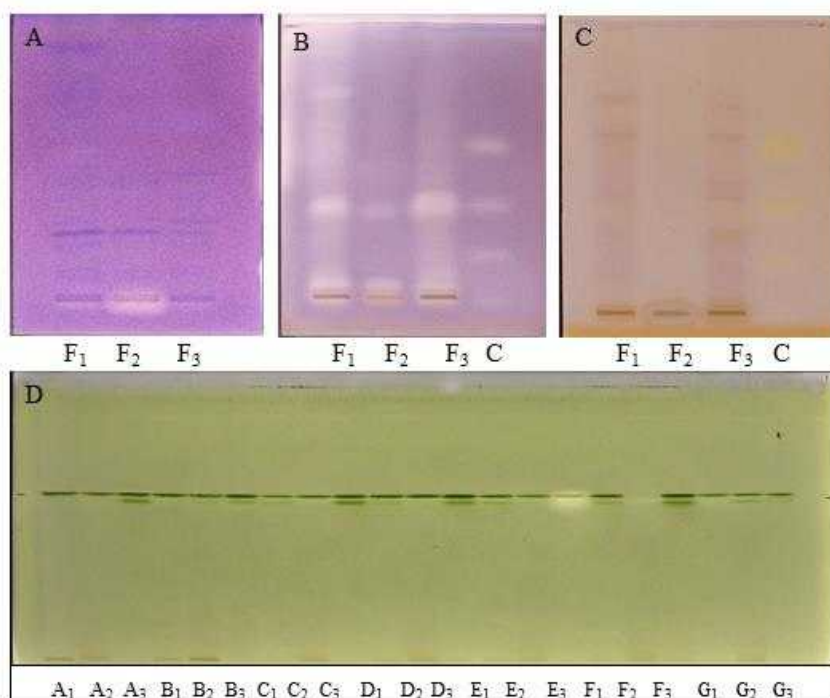


Figure 11: HPTLC chromatogram showing α -glucosidase inhibition of F1, F2, F3 (Calcutta-4, field, *in vitro* and acclimatised samples) developed in (A) toluene (T): ethyl acetate (EA): methanol 6: 3: 1; (B) T: EA: 4: 1 (C) β -glucosidase inhibition of F1, F2, F3 developed in T: EA: 4:1 (D) α -amylase inhibition of samples A-H developed in EA: T: FA: water (3.4: 0.5: 0.7: 0.5). Track C is the positive control, acarbose.

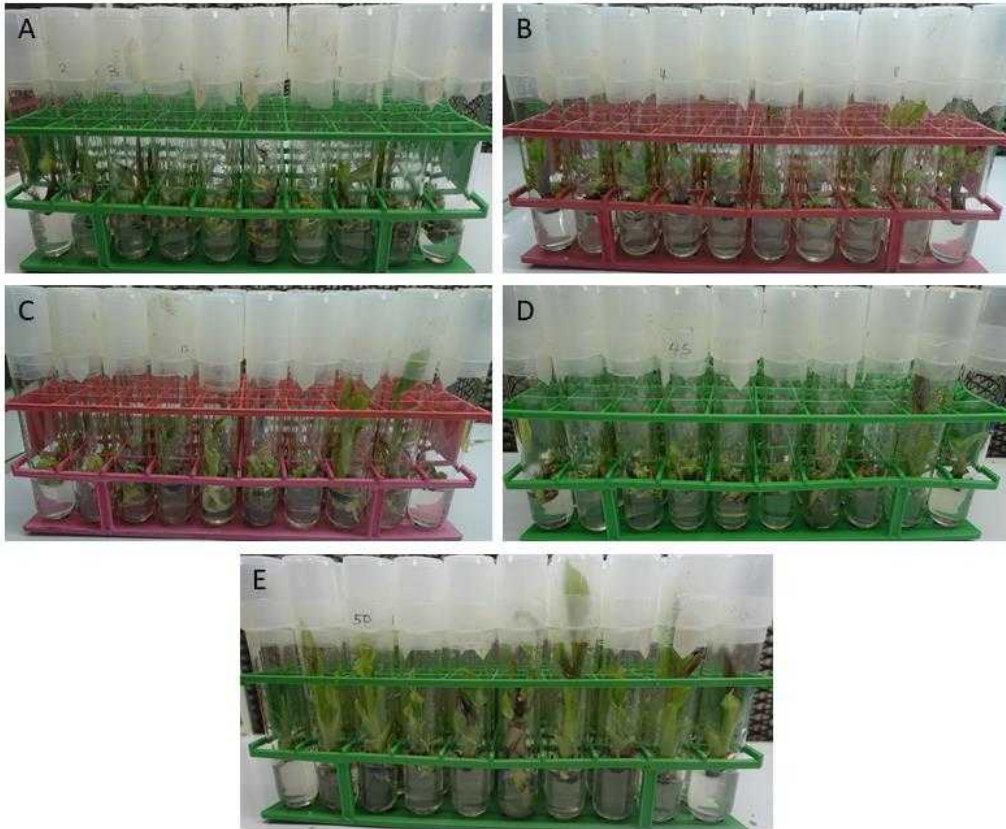


Figure 12: *Musa* spp. accession grown on media with different doses of sugar used as elicitor (A) 30 g/L, control (B) 35 gL⁻¹ (C) 40 gL⁻¹ (D) 45 gL⁻¹ (E) 50 gL⁻¹



Figure 13: *Musa* spp. accession grown on proliferation media but incubated at (A) 26 °C (control) (B) 20 °C and (C) 15 °C

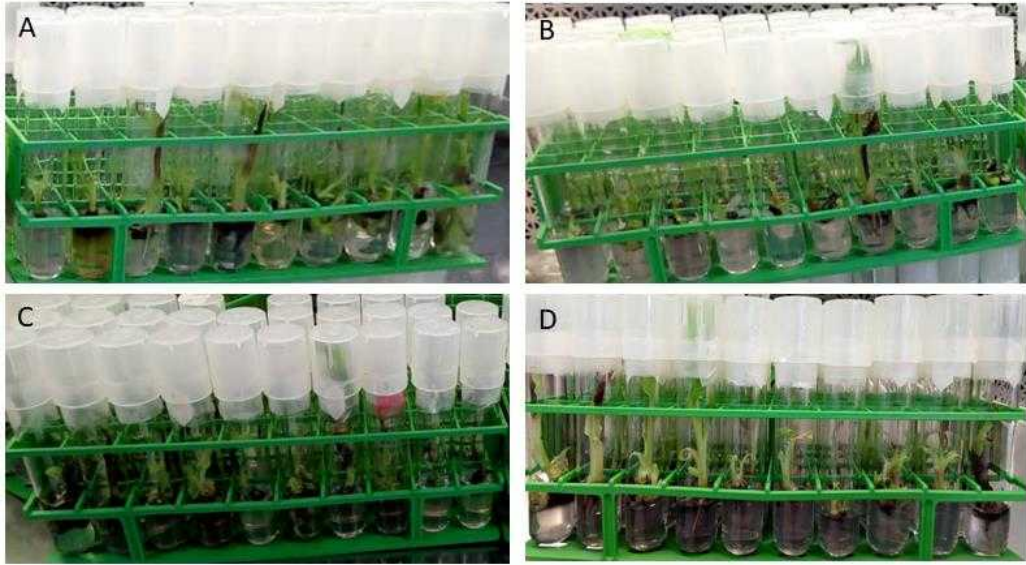


Figure 14: *Musa* spp. accession grown on media with different doses of jasmonic acid (JA) used as elicitor (A) control, 0 μM JA (B) 50 μM JA (C) 100 μM JA (D) 200 μM JA

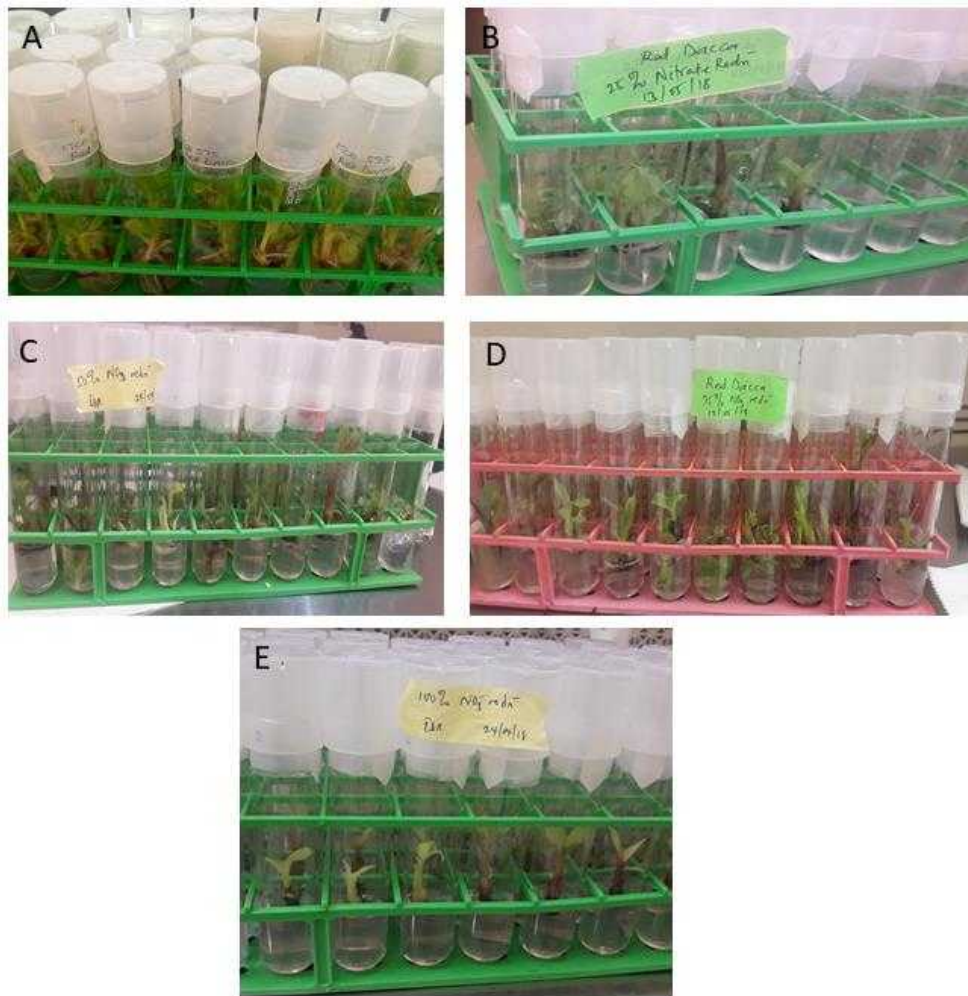


Figure 15: *Musa* spp. accession (Red Dacca) grown on media with reduction in the nitrate source component of the media by (A) 0% (control) (B) twenty five percent (C) fifty percent (D) seventy five percent (E) 100%

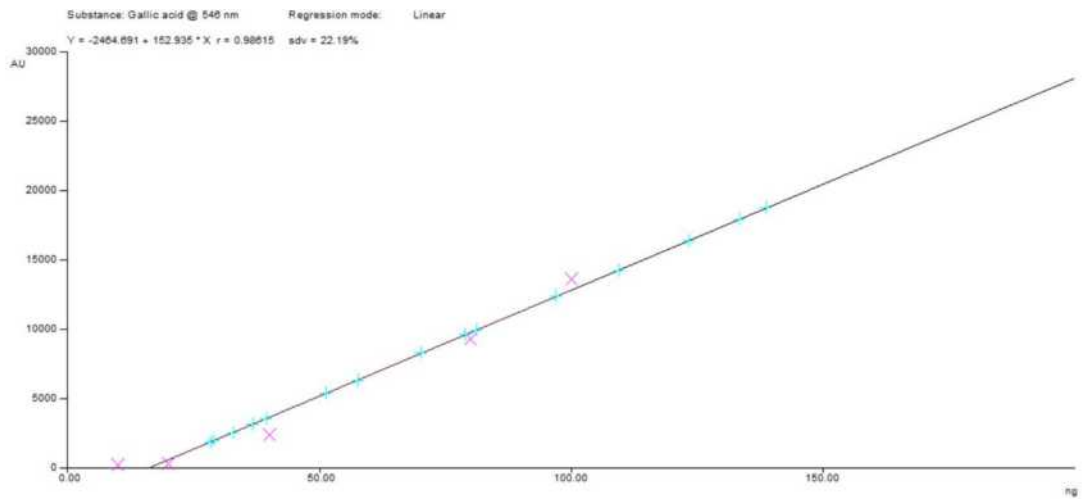


Figure 16: Sugar (1 – 15) calibration curve Sample. Sample conc: 1000 ng, GA conc: 10 – 1000 ng $Y = 152.935X - 2464.691$ $r = 0.98615$ $sdv = 22.19\%$

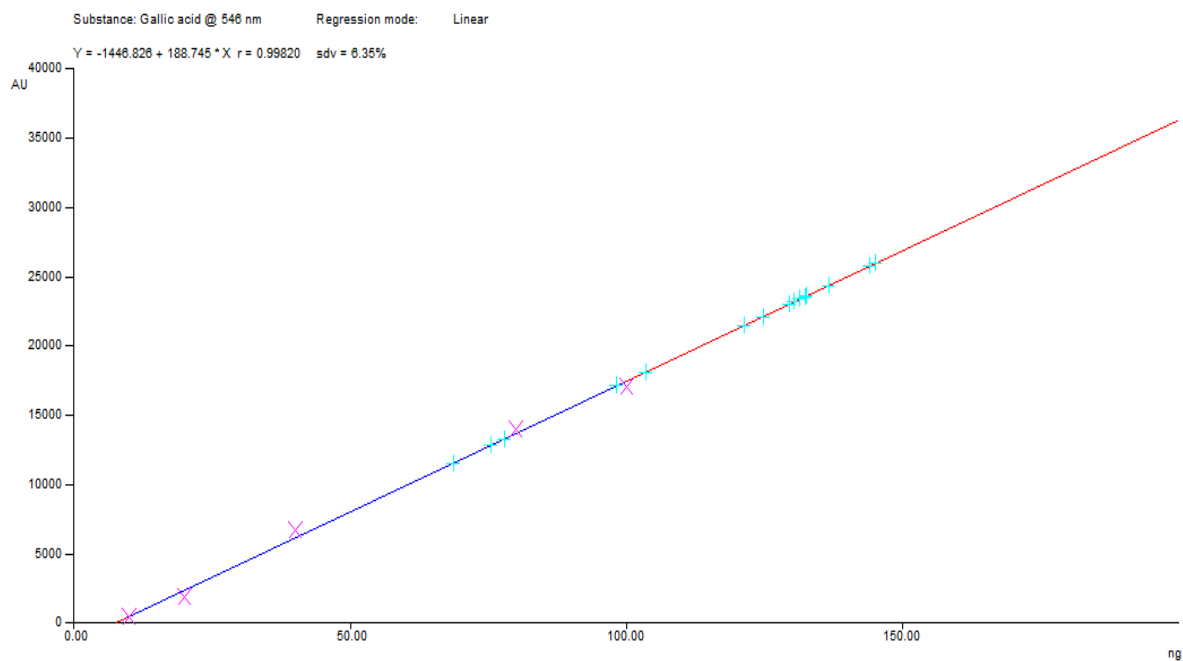


Figure 17: Sugar (16 – 30) calibration curve, conc: 1000 ng, GA conc: 10 – 1000 ng

$$Y = 188.745X - 1446.826 \quad r = 0.99820 \quad sdv = 6.35\%$$

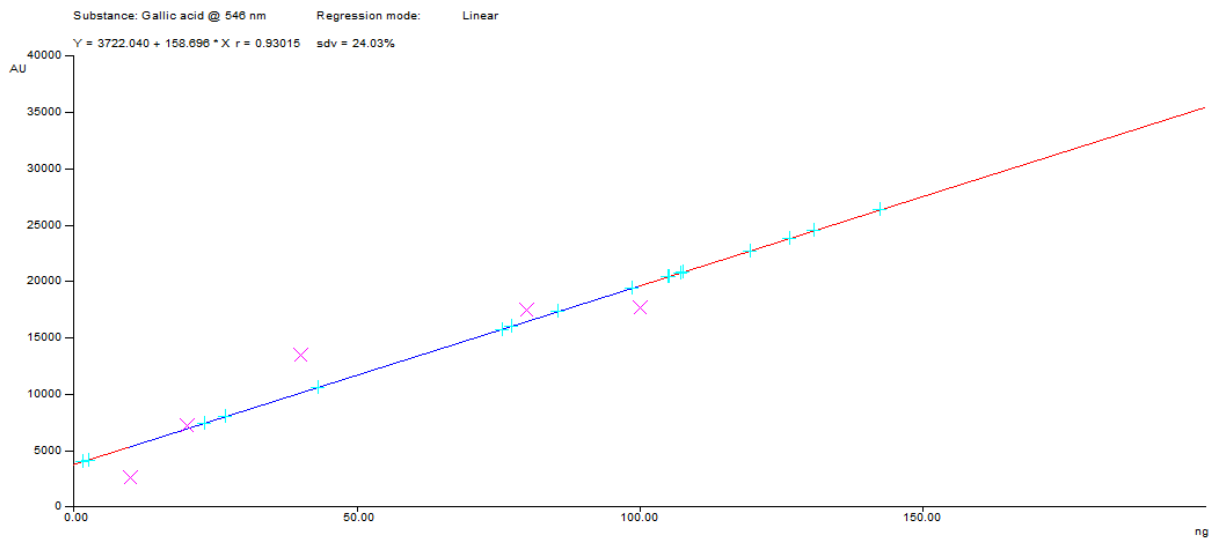


Figure 18: Temperature GA calibration curves (10 – 100 ng) Sample conc: 1000 ng

$Y = 158.7X + 3722$ $r = 0.93015$ $Sdv = 24.03\%$

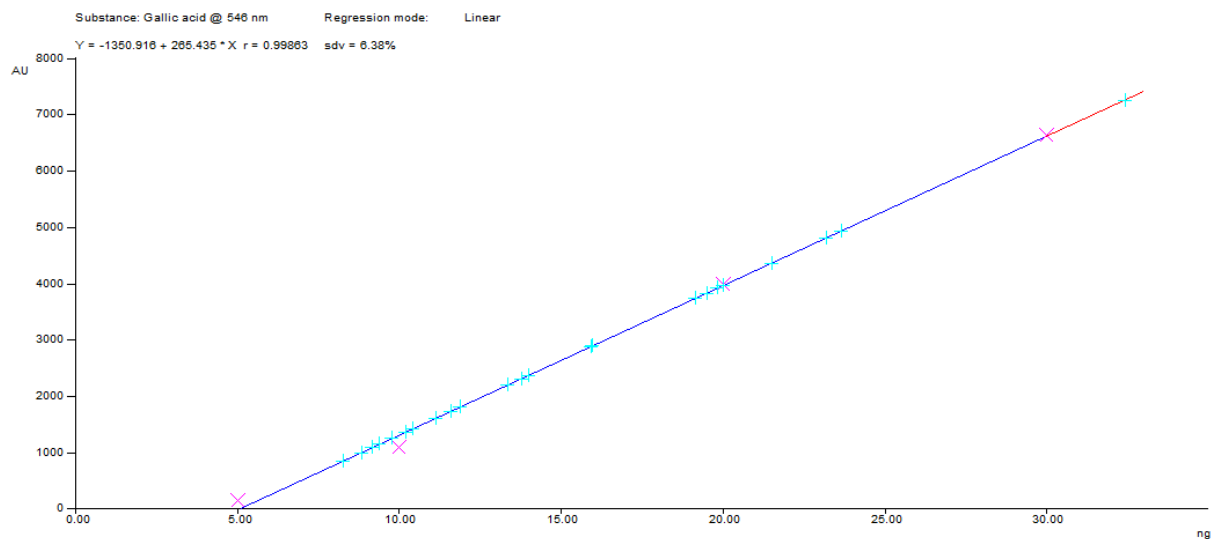


Figure 19: Jasmonic acid calibration curve (5-30 ng) Sample conc: 400 ng/ul

$$Y = 265.435X - 1350.92, r = 0.99863 \text{ sdv} = 6.38\%$$

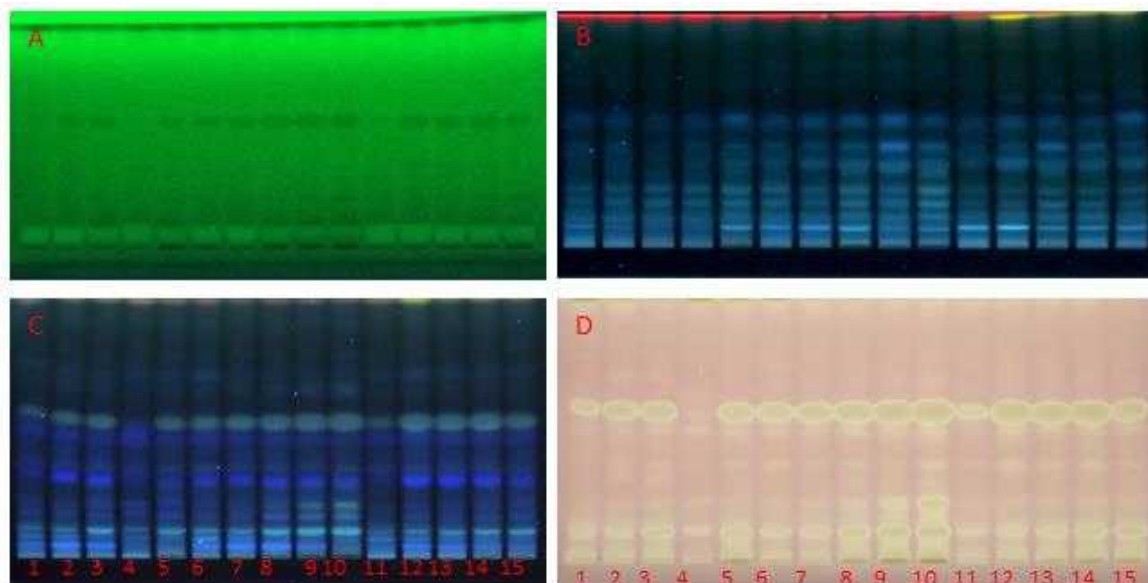


Figure 20: HPTLC chromatograms of elicited accessions using different sugar doses (30, 35, 40, 45, 50 g/L) for each accession. Each track represents individual accession 1-15 as listed in Table 4.6.1.1. The plates were developed in EA: toluene: FA: H₂O (3.4: 0.5: 0.7: 0.5) and documented (A) (A) at short wavelength, (B) at long wavelength, (C) after derivatisation in natural product (neu's) reagent and visualised at 366 nm, (D) after derivatisation in DPPH[•]. 10 µL/band was applied in each case.

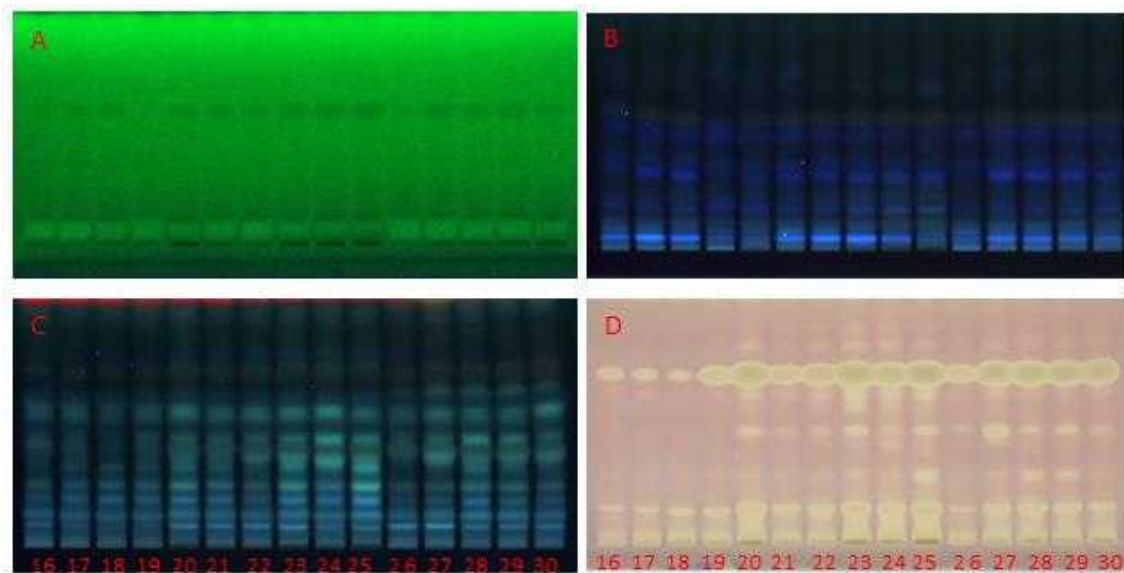


Figure 21: HPTLC chromatograms of elicited accessions using different sugar doses (30, 35, 40, 45, 50 g/L) for each accession. Each track represents individual accession 16-30 as listed in Table 4.6.1.1. The plates were developed in EA: toluene: FA: H₂O (3.4: 0.5: 0.7: 0.5) and documented (A) at short wavelength, (B) at long wavelength, (C) after derivatisation in natural product (neu's) reagent and visualised at 366 nm, (D) after derivatisation in DPPH•. 10 µL/band was applied in each case.

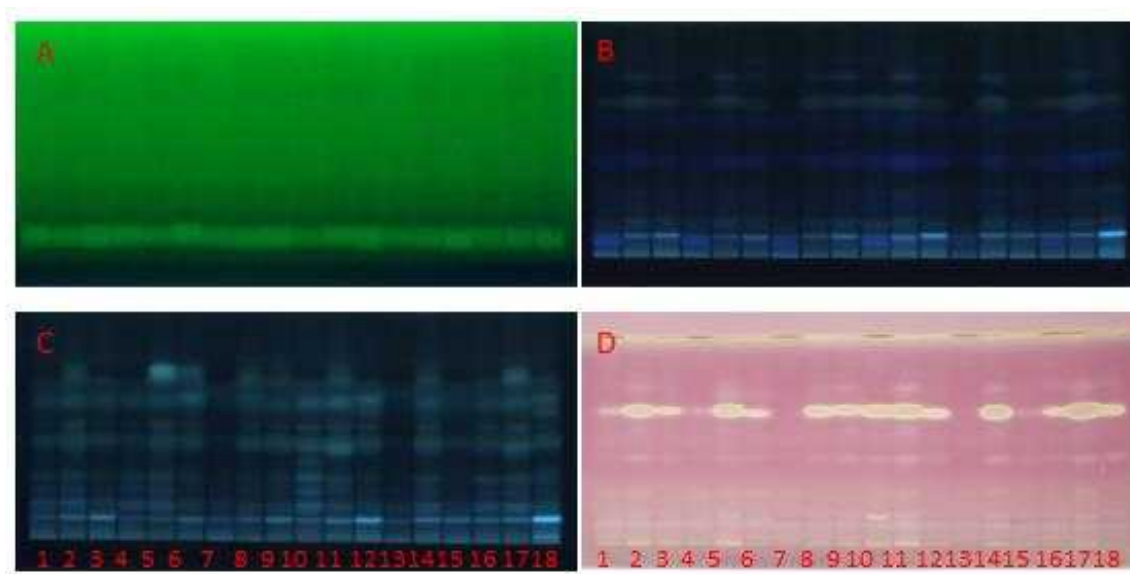


Figure 22: HPTLC chromatograms of elicited accessions grown under different temperature conditions (26, 20 and 15 °C). Each track represents individual accession as listed in Table 4.6.2.1. The plates were developed in EA: toluene: FA: H₂O (3.4: 0.5: 0.7: 0.5) and documented (A) at short wavelength, (B) at long wavelength, (C) after derivatisation in natural product (neu's) reagent and visualised at 366 nm, (D) after derivatisation in DPPH[•]. 10 µL/band was applied in each case.

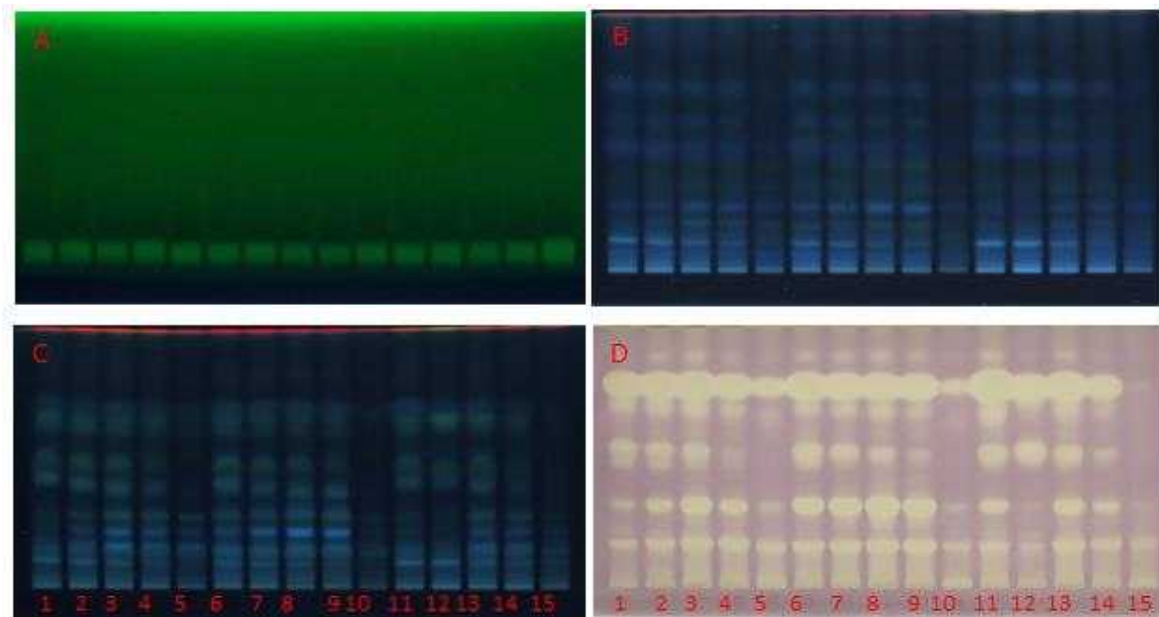


Figure 23: HPTLC chromatograms of elicited accessions grown in media with reduced nitrate components (Control, 25%, 50%, 75% and 100% nitrate reduction). Each track represents individual accession. The plates were developed in EA: toluene: FA: H₂O (3.4: 0.5: 0.7: 0.5) and documented (A) at short wavelength, (B) at long wavelength, (C) after derivatisation in natural product (neu's) reagent and visualised at 366 nm, (D) after derivatisation in DPPH•. 10 µL/band was applied in each case.

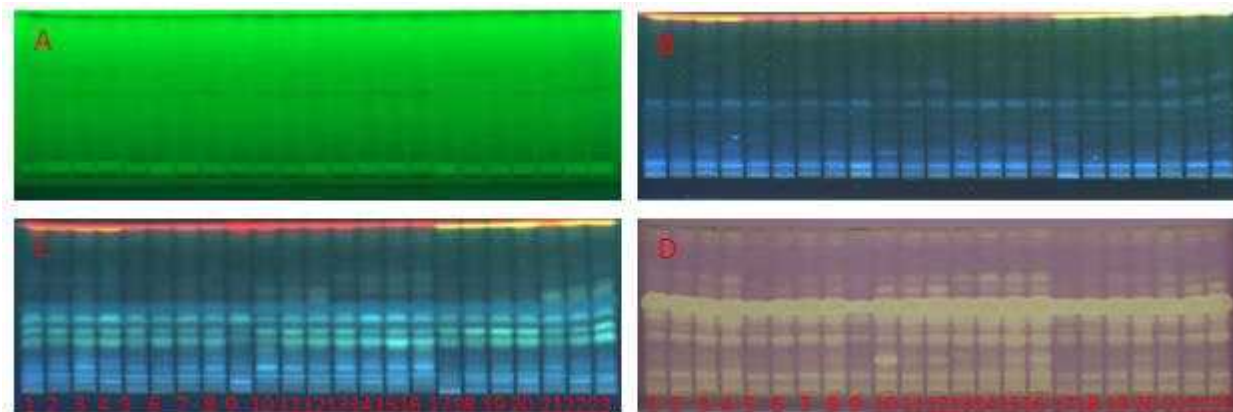


Figure 24: HPTLC chromatograms of elicited accessions using different doses of jasmonic acid (control, 50, 100 and 200 μM). Each track represents individual accession as listed in Table 4.6.3.1. The plates were developed in EA: toluene: FA: H_2O (3.4: 0.5: 0.7: 0.5) and documented (A) at short wavelength, (B) at long wavelength, (C) after derivatisation in natural product (neu's) reagent and visualised at 366 nm, (D) after derivatisation in DPPH \cdot . 10 μL /band was applied in each case.

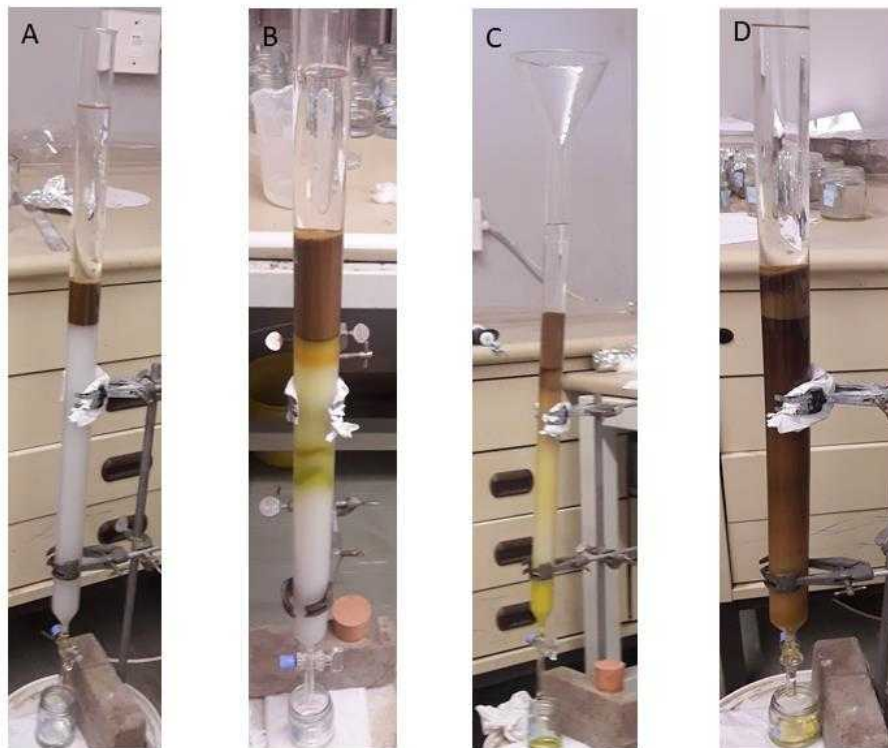


Figure 25: Column chromatography of ethyl acetate fraction; (A) immediately after packing (B) after elution with mixture of *n*-hexane (Hex) and EA (C) after elution with hex and EA but higher EA ratio (D) after elution with ethyl acetate and methanol but higher ethyl acetate ratio



Figure 26: Picture of collected sub-fractions from the silica gel column of the EA fraction of *Musa acuminata* leaf

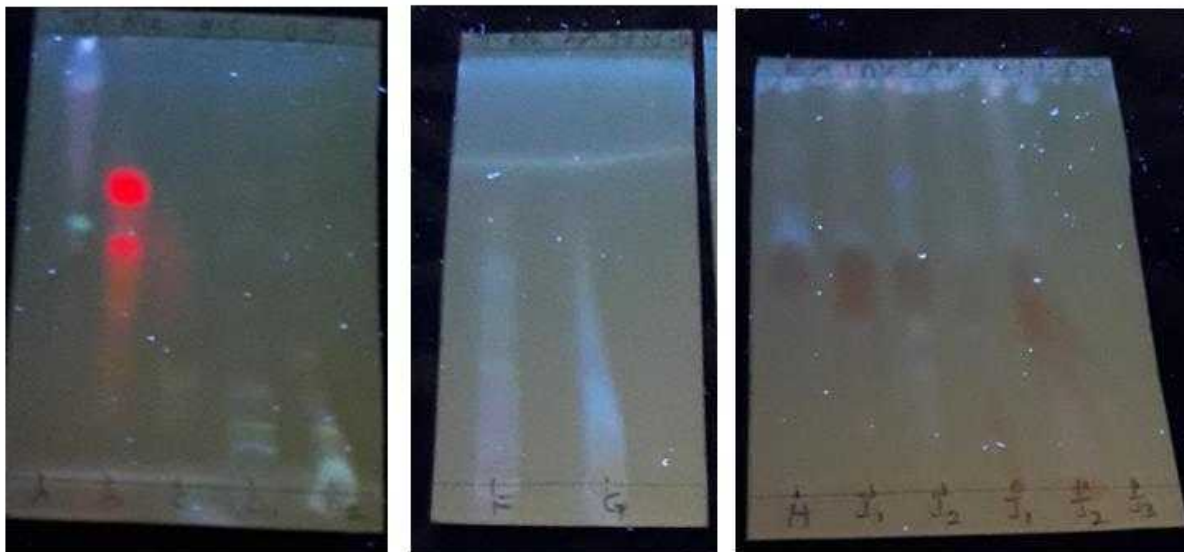


Figure 27: TLC of pooled sub-fractions A-K from the silica gel column of the EA fraction of *Musa acuminata* leaf



Figure 28: TLC of pooled sub-fractions A-K from the sephadex column chromatography of sub-fraction H

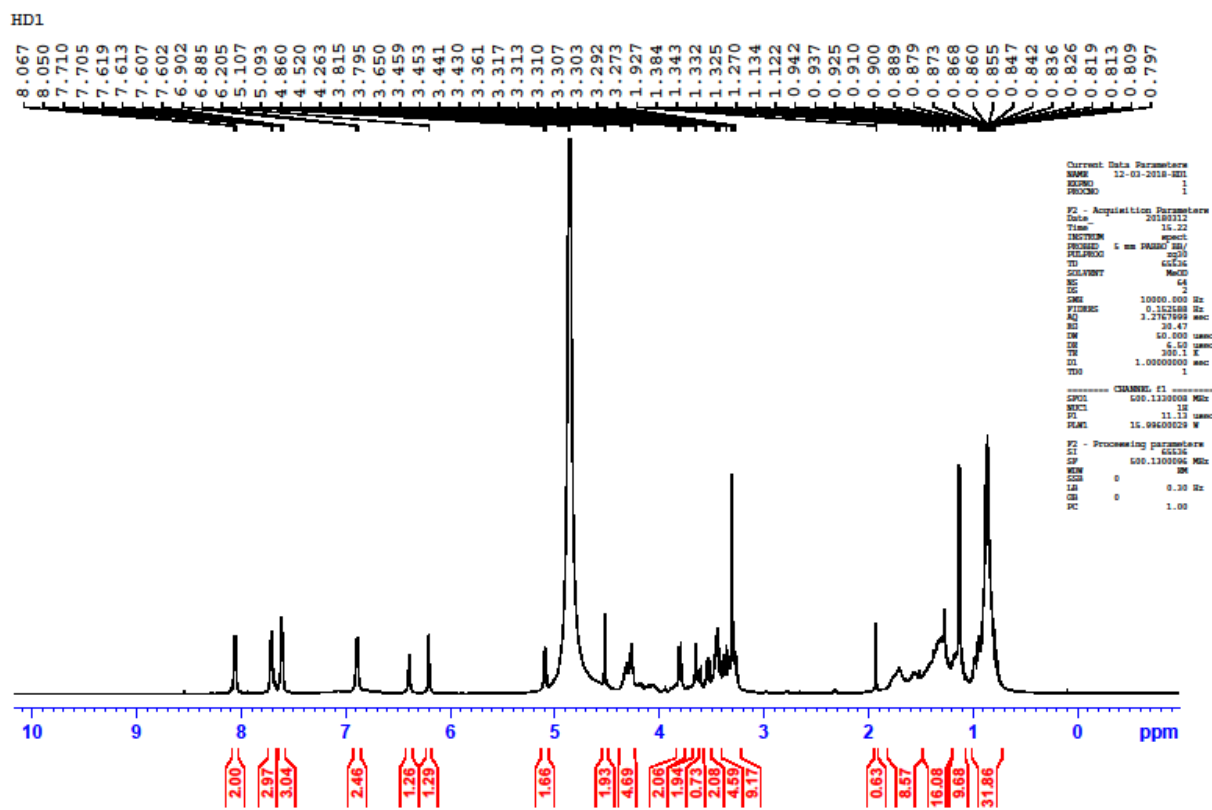


Figure 29: ^1H NMR full spectral of compound HD₁

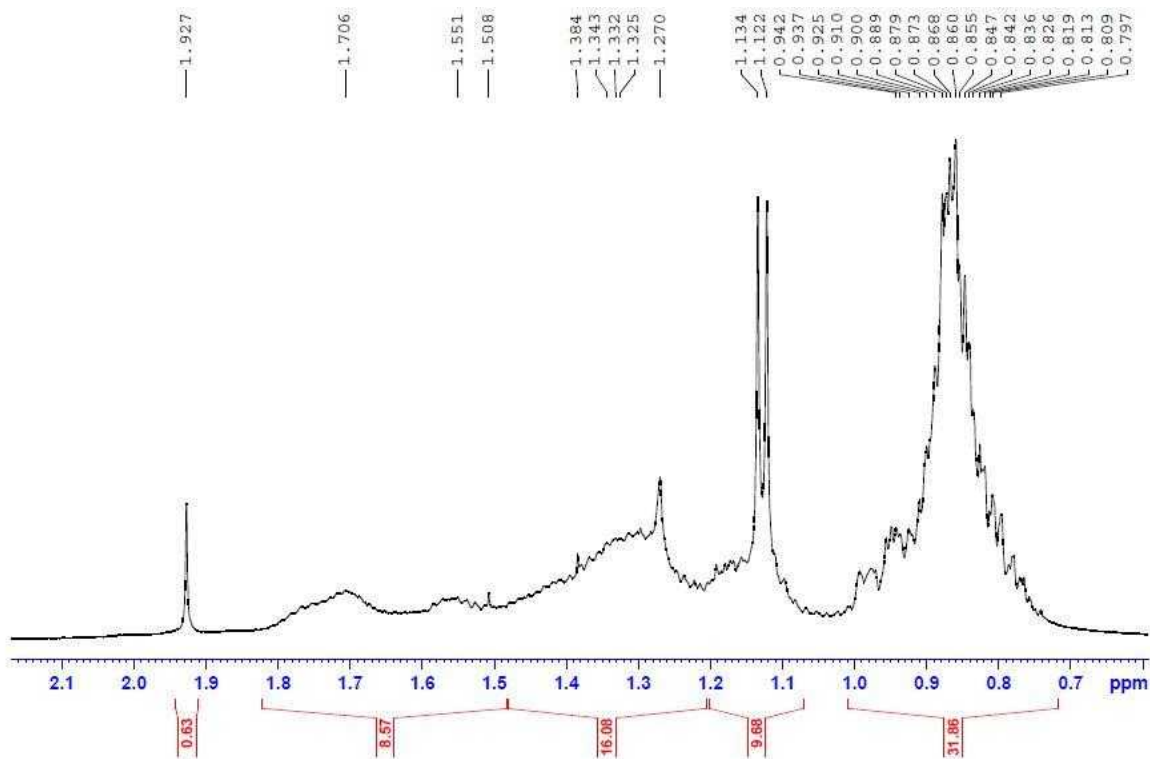


Figure 30: Expanded ^1H NMR spectral of compound HD_1 showing peaks found between 0.7 and 2.1 ppm chemical shifts

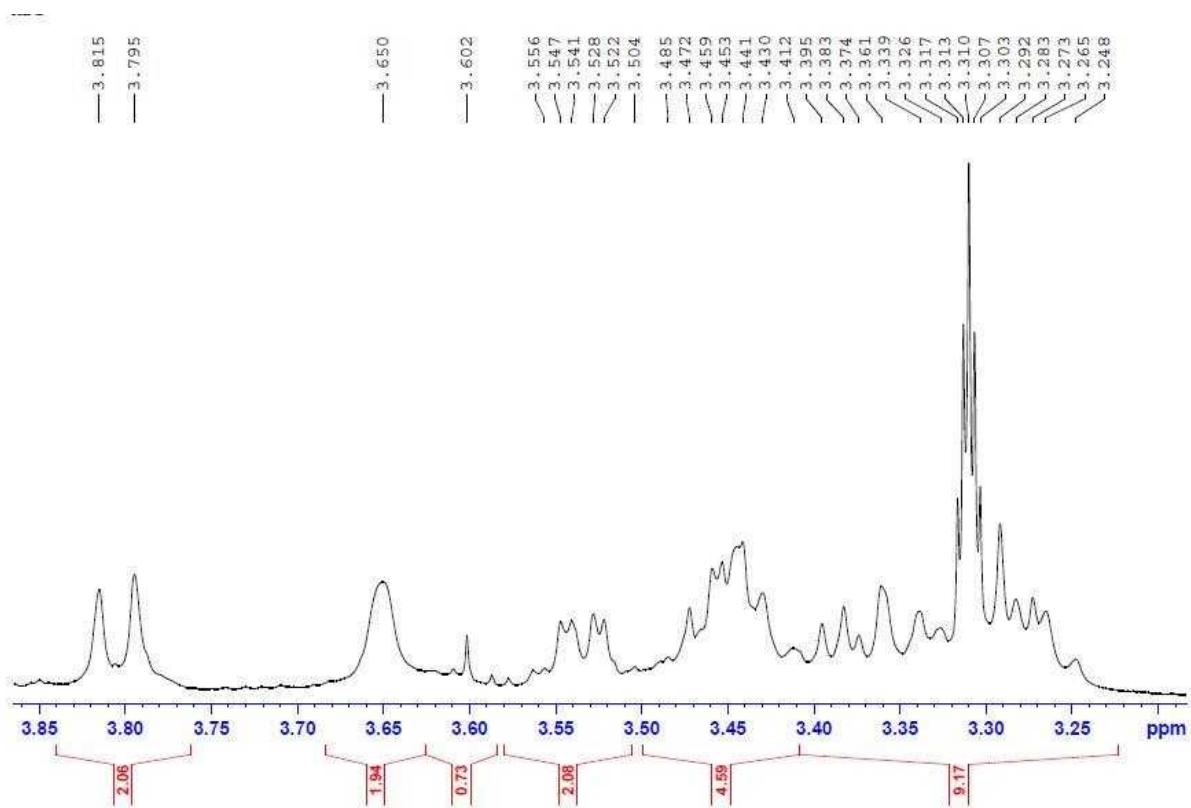


Figure 31: Expanded ^1H NMR spectral of compound HD_1 showing peaks found between 3.25 and 3.85 ppm chemical shifts

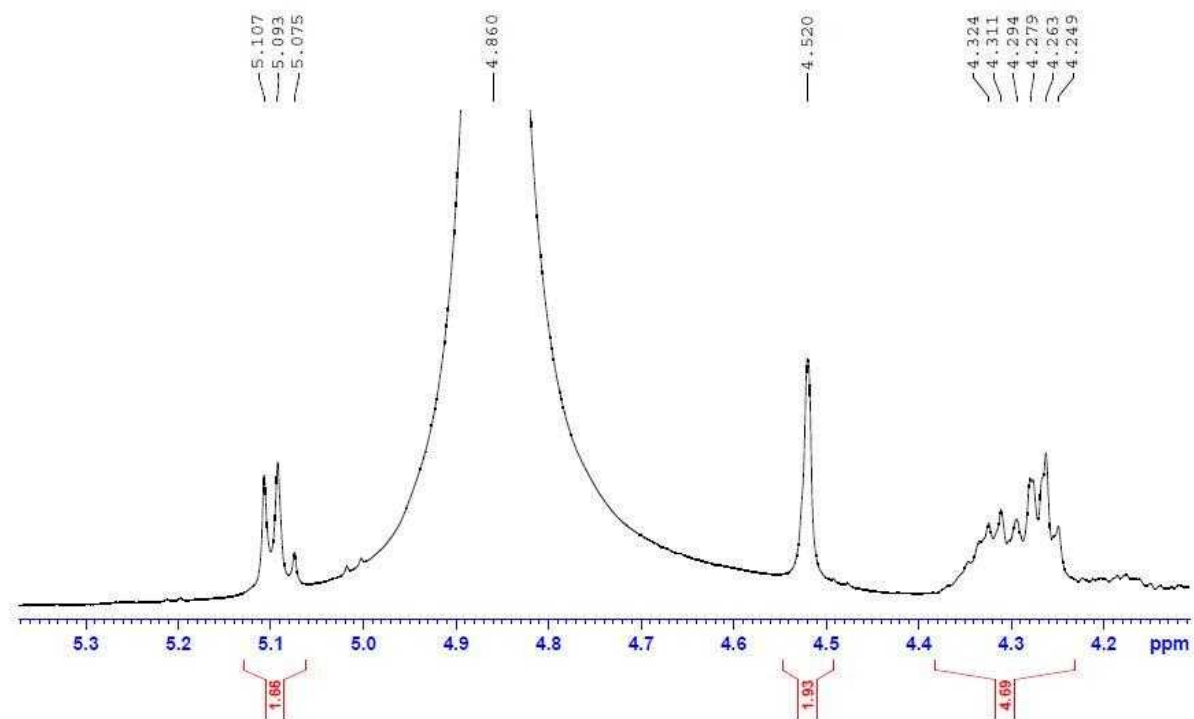


Figure 32: Expanded ¹H NMR spectral of compound HD₁ showing peaks found between chemical shifts 4.2 and 5.3 ppm

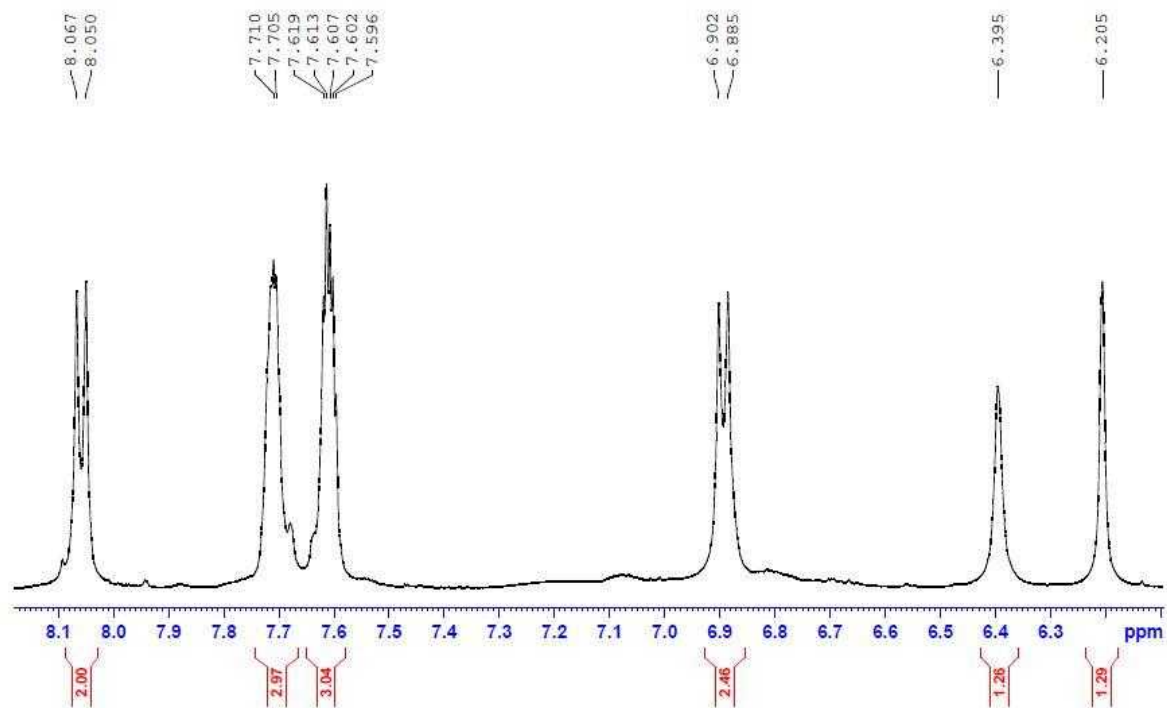


Figure 33: Proton NMR spectral of compound HD₁ showing peaks found between chemical shifts 6.3 and 8.1 ppm

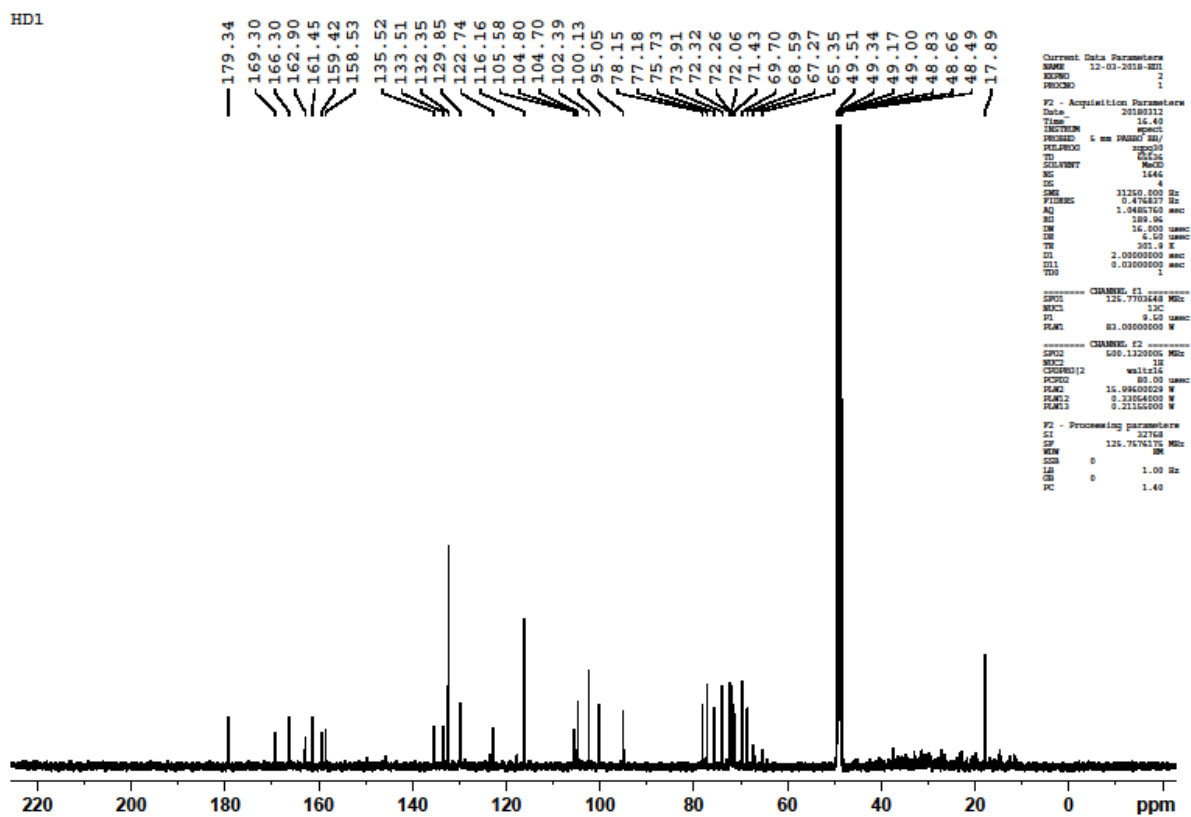


Figure 34: Carbon-13 NMR full spectral of compound HD₁

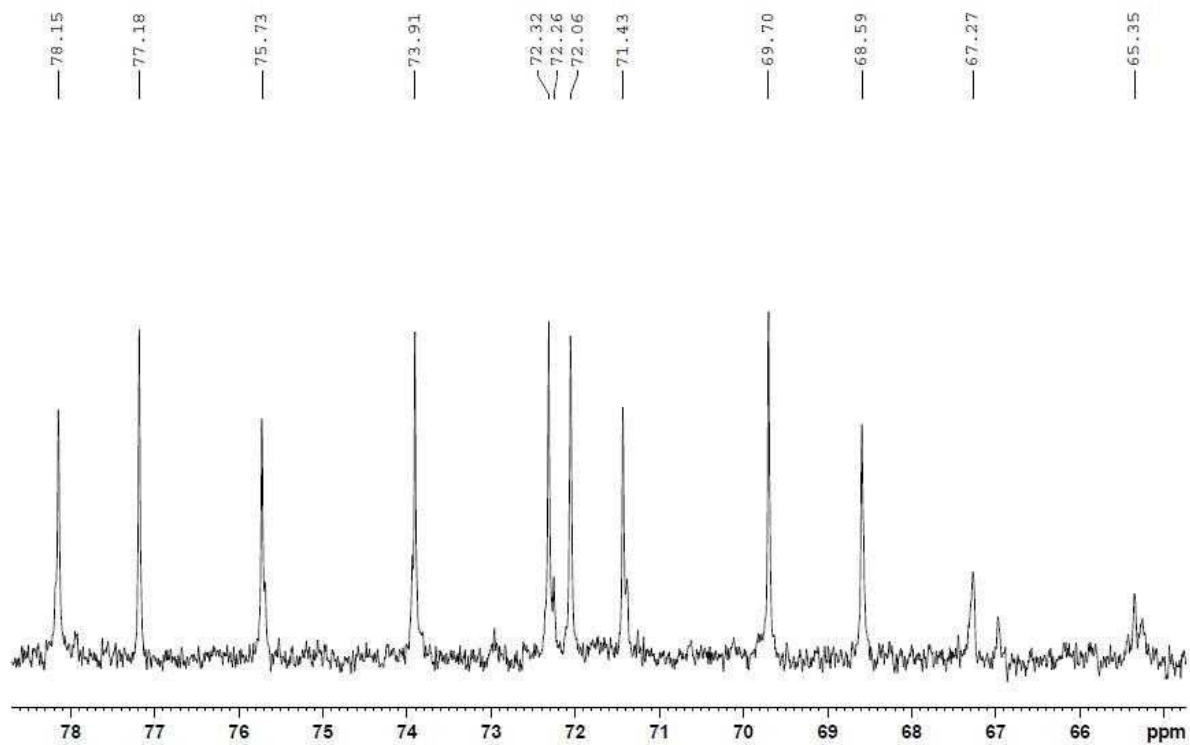


Figure 35: Expanded ^{13}C NMR spectral of compound HD₁ showing peaks found between chemical shifts 66 and 78 ppm

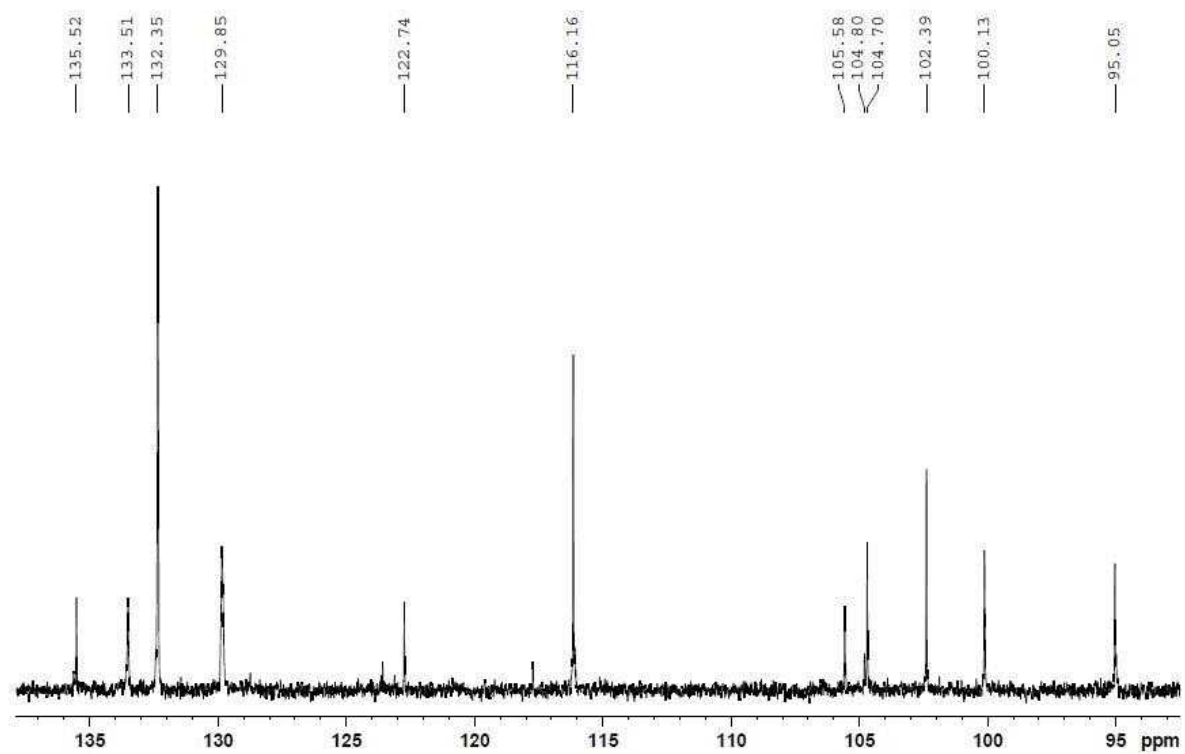


Figure 36: Expanded ^{13}C NMR spectral of compound HD₁ showing peaks found between chemical shifts 95 and 135 ppm

HD1

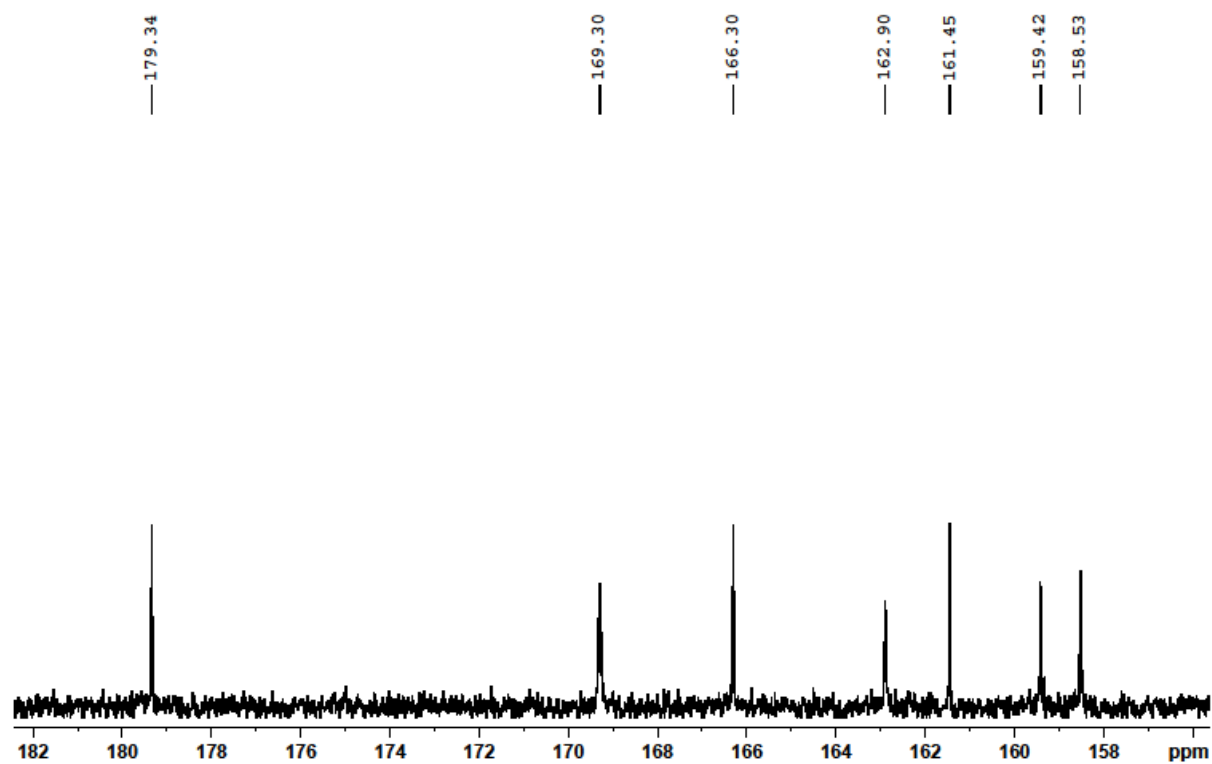


Figure 37: Expanded ^{13}C NMR spectral of compound HD₁ showing peaks found between chemical shifts 158 and 182 ppm

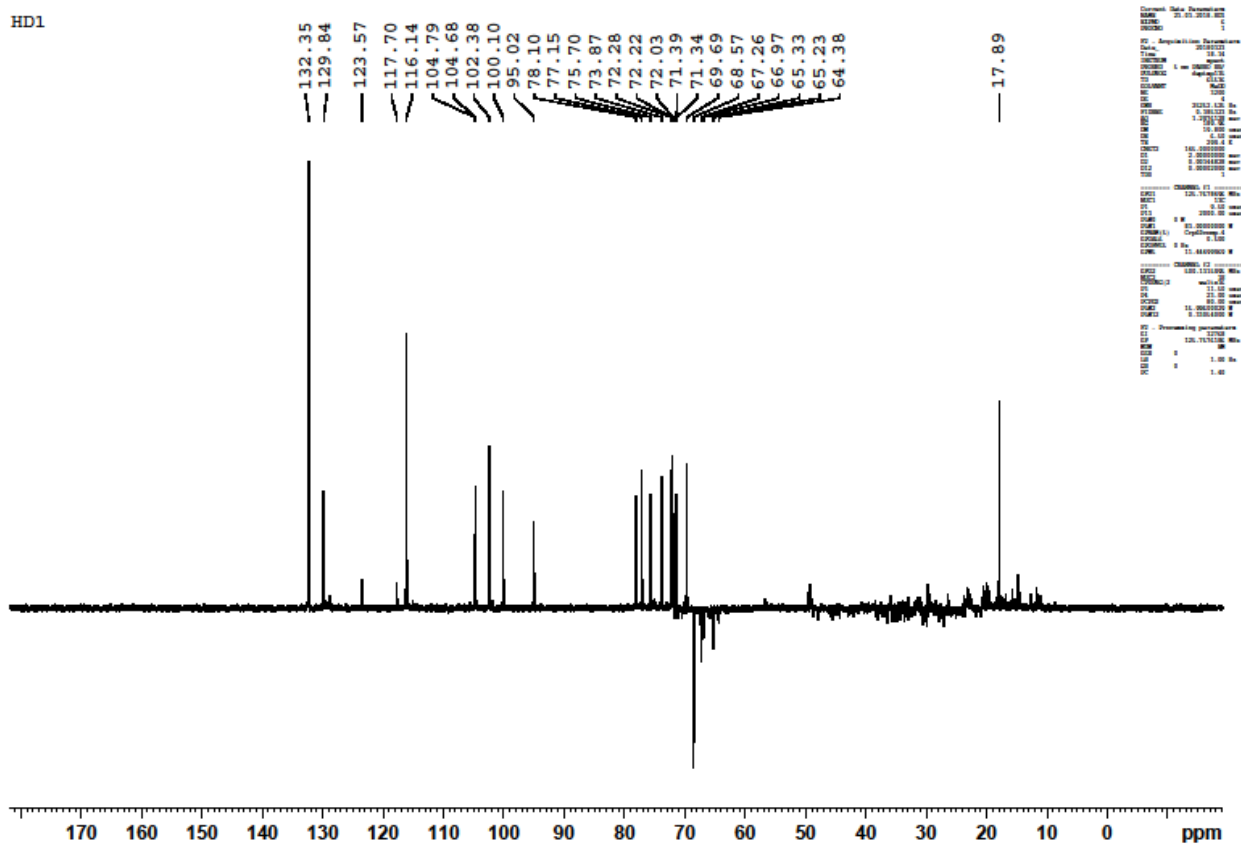


Figure 38: Distortionless Enhancement by Polarisation Transfer (DEPT) spectral of compound HD₁

HD1

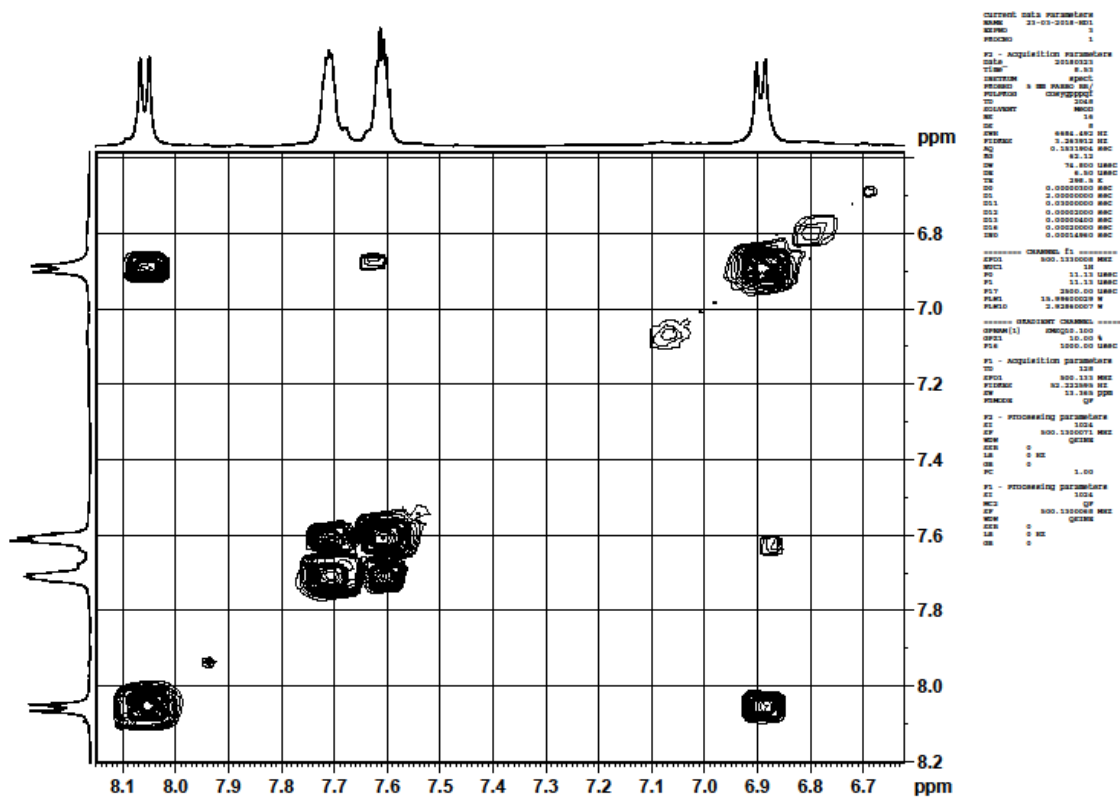


Figure 40: Expanded Correlation spectroscopy (COSY) spectral of compound HD₁

HD1

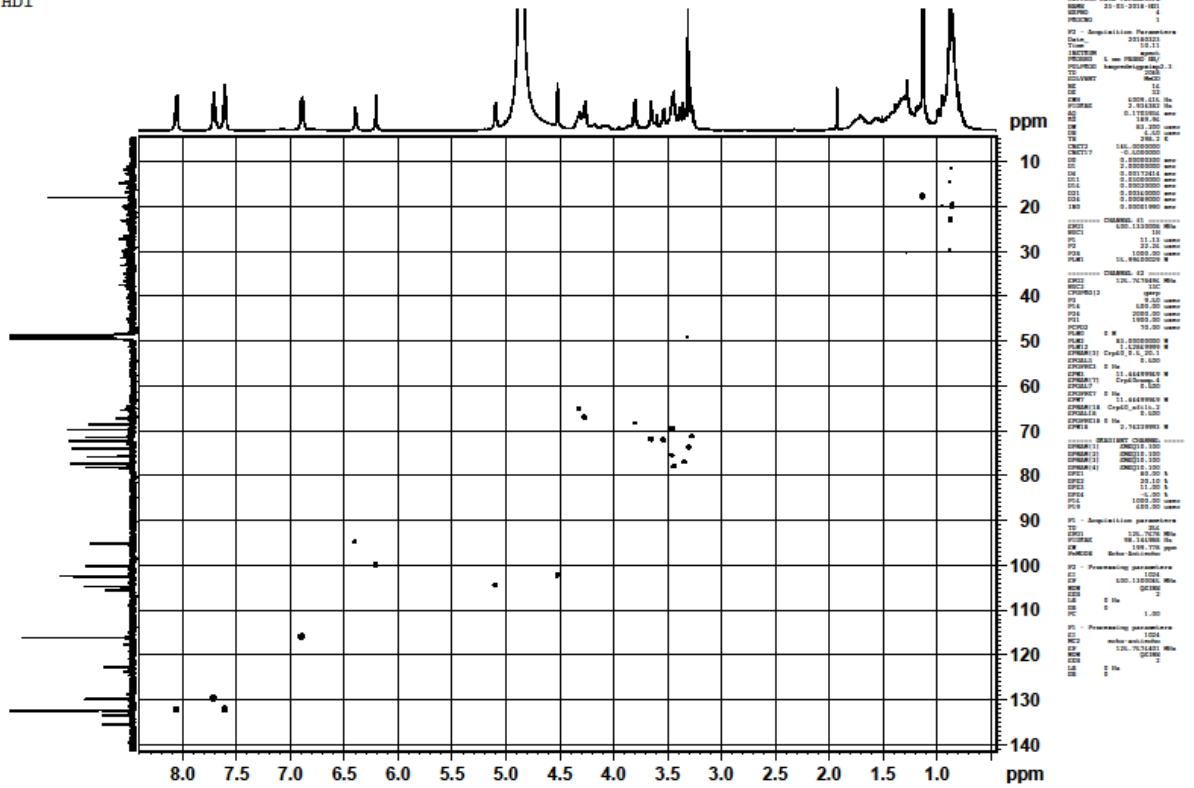


Figure 42: HSQC spectral of compound HD₁

HD1

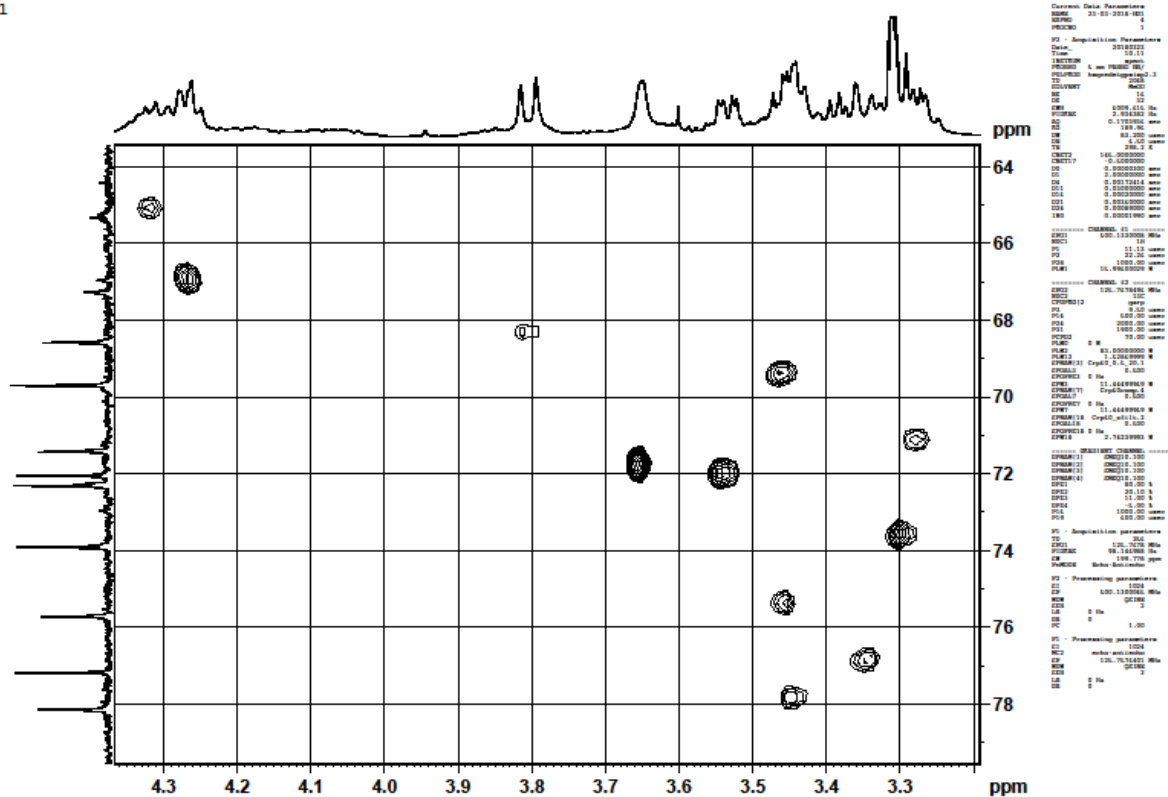


Figure 43: Expanded HSQC spectral of compound HD₁



Effect-directed profiling and identification of bioactive metabolites from field, *in vitro*-grown and acclimatized *Musa* spp. accessions using high-performance thin-layer chromatography-mass spectrometry

Ibukun O. Ayoola-Oresanya^{a,b,c}, Mubo A. Sonibare^a, Badara Gueye^b, Rajneesh Paliwal^b, Michael T. Abberton^b, Gertrud E. Morlock^{c,*}

^a Department of Pharmacognosy, Faculty of Pharmacy, University of Ibadan, Ibadan, Nigeria

^b Genetic Resources Centre, International Institute of Tropical Agriculture, Ibadan, Nigeria

^c Department of Food Science, Institute of Nutritional Science, Justus Liebig University Giessen, Giessen, Germany

ARTICLE INFO

Article history:

Received 19 October 2019

Revised 5 December 2019

Accepted 6 December 2019

Available online 9 December 2019

Keywords:

Musa spp.

Antioxidants

Effect-directed analysis

In vitro culture

Genetic fidelity

HPTLC-HRMS

ABSTRACT

Bananas and plantains (*Musa* spp.) are used as nutritious foods, and at the same time, are a source of phytoconstituents for the pharmaceutical industry. As biological activities of especially the pulp and peel of *Musa* spp. have been documented, this study investigated the variation in the secondary metabolite profiles of the leaves from field, *in vitro*-grown and acclimatized accessions. The genetic fidelity of the diverse accessions was assessed using diversity array technology sequencing. It showed that the *in vitro*-grown accessions were true-to-type with the field samples. The antioxidant and anticholinesterase activities of the samples from different culture systems (field and *in vitro*) were evaluated by UV-spectrophotometry and compared to high-performance thin-layer chromatography-effect-directed analysis (HPTLC-EDA). The latter was applied for the first time for effect-directed profiling of the polar and medium polar sample components via different biochemical and biological assays. Compound zones showed acetyl-/butyrylcholinesterase inhibition (zones 1–4), α -/ β -glucosidase inhibition (zones 1 and 2) as well as antioxidative (zones 1–3) and antimicrobial (zone 4) activities. Structures were preliminary assigned by HPTLC-HRMS. The HPTLC was effective for bioactivity-guided characterization of the bioactive constituents in *Musa* spp. accessions. Accumulation of useful metabolites, especially compounds with antioxidant and anticholinesterase properties, was higher in samples from *in vitro* system. This validated the use of plant tissue culturing as an alternative method for large scale production of plant material and supply of bioactive constituents.

© 2019 Published by Elsevier B.V.

1. Introduction

High-performance thin-layer chromatography (HPTLC) is a robust, simple, rapid, and efficient tool in the quantitative analysis of compounds. It enables a highly sensitive high-throughput screening for the rapid analysis of a large number of compounds [1]. It is widely used for quality control of medicinal plants and characterization of metabolites. Bioassays with cuvette, petri dish and microtiter plates gives a sum of parameters, which can be due to antagonistic or synergistic effects but the specific compounds responsible for the bioactivity are unknown. Biological and biochemical assays can be combined with chromatography and reveal the bioactivity of single compounds. The effect-directed analysis

(EDA), in combination with chromatography, makes detection and characterization of bioactive compounds in plant samples easier. Thus, thousands of compounds in a complex plant mixture are reduced to few important bioactive ones [2]. Several researchers have developed HPTLC-enzyme inhibition assays and other bioassays, e.g., cholinesterase and glucosidase inhibition [3,4]. In the past, to get structural information about unknown compounds, HPLC was in most cases combined with high-resolution mass spectrometry (HRMS) [5], while the hyphenation of HPTLC with spectrometric/spectroscopic detectors received little attention in analytical chemistry [6]. The isolation and online transfer of zones of interest to a mass spectrometer became easier with the availability of the first TLC-MS interface introduced in 2009 [7]. More so, it was possible with MS² experiments to assign molecule ions and their fragment ions. This powerful hyphenation of HPTLC to HRMS ensured a fast, quantitative, reproducible, high-throughput, precise

* Corresponding author.

E-mail address: Gertrud.Morlock@uni-giessen.de (G.E. Morlock).

and cheap analysis [8]. However, the complete structure elucidation of a molecule requires in addition nuclear magnetic resonance (NMR) analysis [9], especially in the case of a new and novel compound. These techniques are important, especially in the recent search for bioactive molecules in *Musa* spp.

Musa spp. (bananas and plantains), belonging to the family Musaceae, are not only important food crops but have also been reported for various medicinal uses. Traditionally, dried fruits of banana, the flowers and roots are used orally for diabetes [10]; the extracts from the leaves are used for wound healing [11] and fruit as a mild laxative [12]. Other pharmacological activities, reported for different parts of *Musa* spp., include anti-ulcer, hypoglycemic and antimicrobial activities among others [13,14]. It is therefore an important species for the production of bioactive secondary metabolites. Plant tissue culture is an alternative method of plant material supply for the production of desirable medicinal compounds from *Musa* spp. leaves. It is a less destructive source of plant material compared to field and also ensures sustainable conservation and rational utilization of biodiversity [15]. *In vitro* plant tissue culture tool can be a reliable supplemental method to traditional agriculture in the industrial production of bioactive plant metabolites [16]. However, true-to-type clonal fidelity is one of the most important pre-requisites in the micropropagation of plant species. The occurrence of cryptic genetic defects potentially arising via somaclonal variation in plants regenerated *in vitro* can limit the broader utility of the micropropagation system [17]. Therefore, it is necessary to establish genetic uniformity of micropropagated plants to confirm the quality of the plantlets for its commercial utility.

In the past, other chromatographic methods have been used for the detection of phytochemicals in *Musa* spp. Thin-layer chromatography (TLC) analysis was used to confirm the presence of flavanoids in the *Musa* spp. extract [18]. Anthocyanins and their derivatives have also been identified from different parts of *Musa*. The volatile fractions of the pulp and whole fruit of two banana cultivars were characterized by [19] using headspace solid phase micro-extraction (HS-SPME) and gas chromatography-mass spectrometry (GC-MS). Vilela et al. [20] also identified fatty acids and sterols in the pulp of different banana cultivars using GC-MS. Sonibare et al. [21] characterized field-grown *Musa acuminata* leaves using ultra performance liquid chromatography quadrupole time of flight (UPLC-QToF)-MS. This analysis revealed the presence of flavonoids, fatty acids and sugars. Phytoanticipin, a strong antifungal agent, was isolated in *Musa* spp. using bioassay-guided vacuum liquid chromatography (VLC) purification and LC-MS for characterization [22]. Several researchers have also reported various biological activities of *Musa* spp. using majorly cuvette assays, spectrophotometric methods and *in vivo* animal models [13,14,23]. Report on HPTLC analysis of *Musa* in literature is scarce; Bonnet et al. [24] reported the use of an HPTLC method for the quantification of dopamine in the peel of the Cavendish banana.

HPTLC-EDA-HRMS has not been exploited for a straightforward characterization of bioactive secondary metabolites in *Musa* spp. so far. Thus in this study, HPTLC was hyphenated to acetyl and butyryl cholinesterase, α -glucosidase, β -glucosidase, α -amylase, *Aliivibrio fischeri*, *Bacillus subtilis* and *Salmonella thyphimurium* assays, which was aimed at identifying bioactive molecules with multiple biological activities in *Musa* spp. The suitability of HPTLC for a high throughput bioprofiling was evaluated on 15 different taxonomic reference *Musa* spp. accessions comprising different genome groups of *Musa acuminata* and *Musa balbisiana*, which are representatives of *Musa* spp. global biodiversity. This was combined with a comparative study of the bioactivity of field, *in vitro*-grown and acclimatized taxonomic reference accessions reported for the first time.

2. Material and methods

2.1. Reagents and chemicals

All chemicals used in the study were of analytical grade. They include gallic acid, anhydrous sodium carbonate, sodium acetate, aluminum chloride, sodium hydroxide, Fast Blue B salt, acetic acid, citric acid, α -naphthyl acetate, acetylcholinesterase (AChE) lyophilisate (*Electrophorus electricus*, electric eel), butyrylcholinesterase (BChE) from horse serum, hydrochloric acid (32%), α -glucosidase from *Saccharomyces cerevisiae* (1000 U/vial), α -amylase from hog pancreas (50 U/mg), sodium chloride, sodium monohydrogen phosphate, bovine serum albumin (BSA), tris(hydroxymethyl)aminomethane (TRIS), eserine, Folin-Ciocalteu reagent, quercetin, acetylthiocholine iodide (ATCI), 5,5'-dithiobis [2-nitrobenzoic acid] (DTNB), 2,2-diphenyl-1-picrylhydrazyl (DPPH[•]), 2,4,6-Tri(2-pyridyl)-s-triazine (TPTZ), ferric chloride hexahydrate, ascorbic acid, 6-hydroxy-2,5,7,8-tetramethylchroman-2-carboxylic acid (trolox), physostigmine, acarbose, imidazole, 2-naphthyl- α -D-glucopyranoside, 2-chloro-p-nitrophenyl- α -D-maltotriose (CNP-G3) and formic acid, were obtained from Sigma-Aldrich (Steinheim, Germany). 2-Naphthyl- β -D-glucopyranoside (95%) and β -glucosidase from almonds (3040 U/mg) were provided by ABCR, Karlsruhe, Germany. 1-Naphthyl acetate was obtained from AppliChem, Darmstadt, Germany. 3-(4,5-Dimethylthiazol-2-yl)-2,5-diphenyltetrazoliumbromide (MTT, $\geq 98\%$), methanol, ethanol (95%), ethyl acetate, *Bacillus subtilis* spores (BGA, ATCC 6633), and toluene as well as HPTLC plates silica gel 60 F₂₅₄, 20 × 10 cm, were purchased from Merck, Darmstadt, Germany. Luminescent marine bacteria *Aliivibrio fischeri* (DSM no. 5171) were obtained from the Leibniz Institute, DSMZ, German Collection of Microorganisms and Cell Cultures (Braunschweig, Germany). Natural products reagent (NP, diphenylboryloxyethylamine or diphenylboric acid β -ethylamino ester) were purchased from Carl Roth, Karlsruhe, Germany.

2.2. Plant materials

Accessions from the *Musa* taxonomic reference collection (15) were collected from the Genetic Resource Centre, International Institute of Tropical Agriculture (IITA), Ibadan, Nigeria. These accessions were selected based on their genome group. They comprise *Musa acuminata* and *Musa balbisiana* species, which are representatives of *Musa* biodiversity. More accessions, landraces (10) from IITA and a *Musa sapientum* accession from the Botanical Garden of the University of Ibadan were also selected for the genetic fidelity study. The passport data of the *Musa* spp. used is given in Table S-1.

2.3. In vitro propagation and acclimatization

All the *in vitro* materials used were obtained through meristem regeneration from suckers of the accessions, collected from the field and established *in vitro* culture using the IITA *in vitro* genebank routine protocol [25]. The sterilization and *in vitro* propagation protocol used is as described by Ayoola et al. [26], using Murashige and Skoog basal medium supplemented with growth hormones (0.18 mg/L of indole-acetic acid and 4.5 mg/L of benzyl amino purine) [27]. Plantlets with a well-developed root were carefully washed free of agar, transferred to a prepared pot containing sterile top soil and covered with a wet plastic bag for humidity. Pots were maintained in an insect-proof room with a warm and bright environment. The plastic bags were removed after 10 weeks and plantlets were left to grow for up to 7 months.

2.4. DNA extraction and diversity array technology sequencing (DARtseq) single-nucleotide polymorphism (SNP) analysis

Genomic DNA was obtained from each field (26) and *in vitro*-grown (26) accessions using 150 mg of young leaves from both field and *in vitro* samples according to CTAB protocol [28] with some modifications [29]. The quality and quantity of all the extracted DNA samples were checked on Nanodrop spectrophotometer and further confirmed on 1% agarose gel run in TAE buffer at 100 V. A total of 56 high quality DNA samples (50 μ L of 100 ng μ L⁻¹) including four technical replicates as control for sequencing error from three accessions Orishele (field), Simili radjah (both field and *in vitro*) and Safet velchi (*in vitro*) (Table S-1) were sent to Diversity Array Technology (<http://www.diversityarrays.com>), Canberra, Australia to generate SNP markers. SNP markers was generated using next generation high-throughput DARtseq approach which represents a combination of both complexity reduction using restriction enzymes method [30]. Sequence generated in FASTQ files were further processed using proprietary DARt analytical pipelines. The discovered SNP were run against the phytozome database 'Musa acuminata DH Pahang v2' which was used as the reference genome. A total of 150556 SNP was derived from DARtseq approach and further filtered based only on minor allele frequency (MAF) >0.01 as there was no missing data after imputation. Data filter, MAF, heterozygosity analysis, pairwise identity-by-state (IBS) genetic distance matrix and genetic relationship cladogram analysis-based IBS matrix using neighbor-joining (NJ) method were completed using Tassel 5.2.25 software [31]. Heterozygosity results were taken into Excel to generate MAF and heterozygosity distribution plot. Similarly, IBS genetic distance matrix was used in R-program [32] with ggplot and gplots packages.

2.5. Preparation of plant extracts

Young leaves from the field (the first and second leaves), 6 weeks old *in vitro*-grown leaves and 7 months old acclimatized leaves were collected, freeze dried and separately milled into powder. Powdered field samples (50 g), 3 g *in vitro*-grown and 5 g acclimatized samples were weighed. They were extracted in methanol (plant sample-to-methanol 1:10, w/v). Extracts were filtered and concentrated *in vacuo*. These residues were stored at 4 °C and 2.5 mg each were re-dissolved in 1 mL methanol for HPTLC analysis.

2.6. UV spectrophotometry for evaluation of antioxidative activity

2.6.1. Total phenolic content (TPC) and total flavonoid content (TFC)

The method of Khatoon et al. [33] was used to evaluate the total phenolic content (TPC) of all the extracts. Blue colored complex are formed when samples containing phenolic compounds were reduced by the Folin-Ciocalteu reagent. Total phenolic content was expressed as mg gallic acid equivalent (GAE)/g extract which was calculated from the regression equation of gallic acid calibration curve ($y = 0.0095x + 0.1325$, $r^2 = 0.9793$). Aluminum chloride colorimetric method was used to evaluate the total flavonoid contents of the plant samples [34]. The TFC was expressed as mg quercetin equivalent (QE)/g extract, calculated from standard curves ($y = 0.0077x + 0.0884$, $r^2 = 0.9980$) prepared with 6.25–200 μ g quercetin/mL.

2.6.2. DPPH[•] cuvette assay

The antioxidant potential of the extracts was determined by their ability to scavenge the stable radical DPPH[•] according to the method described by Susanti et al. [35] and Ayoola et al. [26] with slight modifications. Briefly, 3 mL of freshly prepared DPPH[•] solution (0.1 mM) in methanol was mixed with 2 mL of the ex-

tract/standard at different concentrations (1.6 to 100.0 μ g/mL). Absorbance was measured at 517 nm using a UV/visible spectrophotometer after incubation at room temperature for 30 min in the dark. The experiment was carried out in triplicate. The percentage inhibition of DPPH[•] free radical scavenging activity was calculated using the following equation:

$$\% \text{ inhibition} = \left[\frac{\text{absorbance of control} - \text{absorbance of test sample}}{\text{absorbance of control}} \right] \times 100\%$$

The antioxidant activity of each sample was expressed in terms of IC₅₀ (micromolar concentration required to inhibit DPPH[•] radical formation by 50%), which was calculated from the linear regression curve.

2.6.3. Ferric reducing antioxidant power (FRAP) cuvette assay

The determination of antioxidant activity through FRAP was carried out according to literature [21,36]. The FRAP reagent was freshly prepared using 300 mM acetate buffer, pH 3.6 (3.1 g sodium acetate trihydrate, plus 16 mL glacial acid made up to 1:1 with distilled water). TPTZ (10 mM) in 40 mM hydrochloric acid and 20 mM ferric chloride hexahydrate in the ratio of 10:1:1 was used as the working reagent. The FRAP reagent (2.85 mL) was added to 200 μ L extracts and the absorbances were taken at 595 nm wavelength with a spectrophotometer after 30 min. The calibration curve of trolox was used to estimate the activity capacity expressed as mg trolox equivalents per g extract (mg TE/g extract).

2.6.4. Anticholinesterase cuvette assay

The inhibition of acetylcholinesterase was determined spectrophotometrically using the modified Ellman's colorimetric method [37,38]. Samples, eserine, DTNB and substrate (acetylcholine iodide, ATCI) were dissolved in phosphate buffer (pH 8.0). In a 96-well plate, the reaction mixture consisted of 40 μ L phosphate buffer (pH 8.0), 20 μ L of varying concentrations of the test samples (0.1 to 1 mg/mL of sample and 0.06 to 0.5 mg/mL of positive control, eserine) and 20 μ L of the enzyme (0.26 U/mL). The reaction mixture was incubated for 30 min at 37 °C, and then 100 μ L of 3 mM DTNB was added. The reaction was initiated by the addition of 20 μ L of 15 mM ATCI. The rate of hydrolysis of ATCI was then determined spectrophotometrically by measuring the change in the absorbance per minute ($\Delta A/\text{min}$) due to the formation of the yellow 5-thio-2-nitrobenzoate anion at 405 nm over a period of 4 min at 30 s interval. Buffer was mixed with the enzyme alongside other reagents and served as negative control. The experiments were carried out in triplicate and percentage inhibition was calculated as follows: $\Delta A = (1 - a/b) \times 100$, where a is $\Delta A/\text{min}$ of test sample and b is $\Delta A/\text{min}$ of negative control. IC₅₀ was calculated from the linear regression curve by plotting the percentage inhibition against extract concentration.

2.7. Statistical analysis

Each antioxidant activity assay was done three times from the same extract in order to determine their reproducibility. Analysis of variance was used to test any difference in antioxidant activities resulting from these methods. Duncan's new multiple range test was used to determine significant differences. Correlations among data obtained were calculated using Pearson's correlation coefficient (r).

2.8. HPTLC-EDA method

2.8.1. Separation system

Apart from the cholinesterase assay (15 or 25 μ L/band), 10 μ L/band were sprayed on the HPTLC plate for all other assays by an automatic TLC sampler (ATS 4, CAMAG, Muttenz, Switzerland)

using 7-mm bands, 8-mm distance from the lower edge and automatic track distance. After mobile phase development, a polar, acidic solvent system (ethyl acetate - toluene - formic acid - water, 3.4: 0.5: 0.7: 0.5) as well as a medium polar solvent system (toluene - ethyl acetate - methanol, 6: 3: 1) were used to separate most of the plant components. The development was done in an unsaturated 20 cm × 10 cm Twin Trough Chamber (CAMAG) up to a migration distance of 60 mm, which took ca. 30 min. The chromatogram was documented by the TLC Visualizer Documentation System (CAMAG) UV lamp at UV 254 nm and 366 nm (CAMAG).

2.8.2. Post-chromatographic derivatization

The chromatogram developed in the polar, acidic mobile phase was derivatized using a reagent sequence. After intermediate drying, the same plate was dipped (1) first in NP reagent, (2) followed by ninhydrin reagent and (3) lastly diphenylamine aniline (DPA) reagent. The plates were heated on the TLC Plate Heater (CAMAG) at 110 °C for 3 to 5 min before dipping in NP reagent, and thereafter documented at UV 366 nm. After immersion in either ninhydrin or DPA reagents, the plates were heated at 110 °C for 3 to 5 min and documented at white light illumination. The chromatograms developed in the medium polar mobile phase were immersed in *p*-anisaldehyde sulfuric acid reagent and heated at 110 °C for 3 to 5 min. For all, immersion time was 2 s at a 2.0-cm/s immersion speed using the TLC Immersion Device, CAMAG.

2.8.3. Neutralization of chromatograms

After development in the acidic mobile phase, chromatograms were neutralized using the Derivatizer (CAMAG) according to Elufoye et al. [38]. Briefly, before the assay application, the chromatograms were dried in a stream of cold air, and phosphate buffer (8%, pH 7.5) was piezoelectrically sprayed on the plates, followed by plate drying in the Automatic Development Chamber (ADC 2, CAMAG).

2.8.4. HPTLC-DPPH[•] assay

The chromatogram was immersed (immersion speed 2.0 cm/s and immersion time 5 s) in 0.02% methanolic DPPH[•] solution. The chromatogram was documented at white light illumination (reflection and transmission mode) after 1, 10 and 30 min. The absorbance of the chromatogram was measured at 546 nm using the mercury lamp in the fluorescence mode without optical filter.

2.8.5. HPTLC-AChE/BChE inhibition assays

The cholinesterase inhibition profiling was performed according to Azadnija et al. [39]. The sample volume sprayed as 7-mm bands was 25 µL/band for the polar, acidic mobile phase, but 15 µL/band for the medium polar mobile phase, while the other HPTLC conditions remained the same as described. The positive control was a methanolic physostigmine solution (0.1 to 1 ng/band). Briefly, the neutralized chromatogram was piezoelectrically sprayed with 1 mL TRIS buffer 0.05 M, pH 7.8, then with 3 mL enzyme solution (6.66 AChE units/mL or 3.34 BChE units/mL in 100 mL TRIS buffer, 0.05 M, pH 7.8, containing 1 mg/mL BSA). The plate was incubated at 37 °C for 25 min and piezoelectrically sprayed with the substrate solution (90 mg α -naphthyl acetate and 160 mg Fast Blue B salt in 90 mL water - ethanol, 2:1), followed by drying at room temperature. White inhibition zones were detected on a purple background at white light illumination (transmission and reflection modes).

2.8.6. HPTLC- α -glucosidase, β -glucosidase and α -amylase inhibition assays

The glucosidase inhibition profiling were performed according to Jamshidi Aijdi et al. [40]. As ethanolic positive control solutions, acarbose (3 to 18 µg/band) or imidazole (3 to 7 µg/band)

were used. Concisely, 2 mL substrate solution (60 mg 2-naphthyl- α -D-glucopyranoside or respective β -anomer in 50 mL ethanol) were piezoelectrically sprayed on the neutralized chromatogram and air-dried for 2 min. The plate was pre-wetted with 1 mL sodium acetate buffer (pH 7.5). Then, 2 mL enzyme solution (100 units α -glucosidase or 200 units β -glucosidase in 10 mL buffer) were sprayed. The plate was placed horizontally in a pre-prepared humidity box and incubated at 37 °C for 15 min for α -glucosidase or 30 min for β -glucosidase. Finally, 0.5 mL of an aqueous Fast Blue B salt solution (2 mg/mL) was sprayed on the chromatogram. Plate images were taken directly and after plate drying (via the ADC 2 humidity control) at white light illumination (transmission and reflection modes). Enzyme inhibitors were detected as white zones on a purple background. For the HPTLC- α -amylase inhibition assay, plates were dipped into the ethanolic substrate solution (1.4 mg/mL CNP-G3), dried for 2 min (hair dryer) and immersed in the enzyme solution (1.2 mg/mL α -amylase in sodium acetate buffer, pH 7.5). After 15 min incubation at 37 °C in a moistened polypropylene box, the autogram was dried and documented at white light illumination. Active compounds were detectable as bright zones against a yellowish green background [41].

2.8.7. HPTLC-Bacillus subtilis bioassay

The Gram-positive antibacterial profiling was performed according to Jamshidi-Aidji and Morlock [42]. The positive control was a methanolic tetracycline solution (0.4 to 1.2 ng/band). Briefly, the chromatogram developed in the medium polar mobile phase was dipped for 7 s at an immersion speed of 3 cm/s into the *B. subtilis* suspension (optical density at 600 nm of 0.8), incubated at 37 °C for 2 h and then visualized by immersion into a 0.2% PBS-buffered MTT solution for 1 s at an immersion speed of 3.5 cm/s and incubated at 37 °C for 30 min, followed by heating at 50 °C for 10 min. Active microorganisms reduced the MTT into the purple formazan. Thus, white antimicrobial zones were observed on a purple background [43] and documented at white light illumination (reflection mode).

2.8.8. HPTLC-Aliivibrio fischeri bioassay

The Gram-negative antimicrobial profiling was performed according to Krüger et al. [44]. The positive control (PC) was a methanolic caffeine solution (0.5 to 6 µg/band). Briefly, the chromatogram developed in the medium polar mobile phase was immersed for 2 s into the luminescent *A. fischeri* suspension prepared according to European Committee for Standardization [45] (the proper luminescence was visually checked by shaking the flask in a dark room). The change over time of the instantly luminescent bioautogram was monitored for 30 min and documented with the BioLuminizer (CAMAG) using an exposure time of 30 s and 1 min trigger intervals. Dark zones indicated the luminescence inhibition of the bacteria and thus a lower bacterial metabolic activity [46].

2.8.9. HPTLC-SOS-Umu-C bioassay

A genotoxic assay with *Salmonella thyphimurium* bacteria (SOS-Umu-C bioassay), newly developed in a parallel research study [47], was applied on the samples to indicate any genotoxic substances or mutagens in the samples. The standard 4-nitroquinoline-1-oxide was used as a positive control.

2.9. HPTLC-ESI-HRMS

The HPTLC plates were pre-washed by development (up to 9.5 cm each) twice with methanol-formic acid 10:1 (V/V), followed with acetonitrile-methanol 2:1 (V/V) [48]. The *Musa* spp. leaf extracts were applied in triplicate (as three sets) and developed. The chromatogram was cut (smartCut Plate Cutter, CAMAG). The first

section was used for the bioassay, the second section for derivatization (with either natural product reagent for the polar, acidic mobile phase or anisaldehyde sulfuric acid reagent for the medium polar mobile phase), while the third section was for HRMS recording. For the latter, the positions of the active zones were transferred on the chromatogram for HRMS and marked at UV 254 or 366 nm using a soft pencil. The zones were eluted with methanol (flow rate 0.1 mL/min) using the TLC-MS Interface 2 (CAMAG) or Plate Express (Advion, Ithaca, NY) coupled to the QExactive Plus mass spectrometer (Thermo Fisher Scientific, Dreieich, Germany). Full scan mass spectra (m/z 50–800) were recorded in the positive and negative ionization modes with the following settings: ESI voltage 3.3 kV, capillary temperature 320 °C, and collision energy 35 eV. Nitrogen was produced by a SF2 compressor (Atlas Copco Kompressoren and Drucklufttechnik, Essen, Germany). Data evaluation and background subtraction were performed by Xcalibur 3.0.63 software (Thermo Fisher Scientific).

3. Results and discussion

3.1. *In vitro* propagation and genetic conformity between field- and *in vitro*-grown *Musa* spp. accessions

The results of this study confirmed that biomass production from *Musa* spp. is possible within a short time using *in vitro* propagation (Fig. S-1). This method is not restrained by environmental conditions and can also give good extraction yield, like field material. This method confirms the amenability of *Musa* spp. to plant tissue culture reported by several studies [49–51].

From the DArTseq analysis, a total of 150.5 K SNP markers were generated with imputation for missing markers and further filtered for $MAF > 0.01$ and retained 114285 SNPs which was used for the genetic fidelity study. Out of 114 K SNP, 93524 SNP were distributed all over 11 chromosomes of banana genome (Table S-2) and 20064 SNPs were not aligned on reference genome, while 697 SNPs were distributed on 12 chromosomes of mitochondrial genome. Minor allele frequency ranged from 0.018 to 0.50 (Fig. S-2). The proportion of heterozygous ranged from 0.009 to 0.2436 (Fig. S-3) in both field and *in vitro* samples and the average heterozygosity proportion was 0.12. The pairwise genetic distance matrix among the *Musa* spp. accessions ranged from 0.0199 to 0.4968 between the 56 field- and *in vitro*-grown samples (Fig. S-4). The pairwise IBS genetic distance found 23 out of the 26 accessions true to type between *in vitro* and field material except Egjoga, P. raja and P. Jaribuaya accessions and seen in the Neighbor Joining (NJ) clustering based on IBS genetic distance matrix (Fig. 1). The genetic distance based on NJ-tree mapping showed that the true-to-type field and *in vitro*-grown accessions were grouped together based on their genetic similarity. Similar result was obtained from the heterozygosity proportion distribution of the 56 banana samples. Molecular markers (e.g., SSR, ISSR and RAPD) have been widely used in crops for genetic relationship analysis [52–54] including SNP markers [55–56] that are most widely accepted nowadays in worldwide molecular research. This study suggests that banana accessions, which are true-to-type between field and *in vitro* lines, can be used for large biomass production of *Musa* spp. within a short time using *in vitro* plant tissue culture and supply of secondary metabolites.

3.2. Total phenolic (TPC) and flavonoid (TFC) content

The total phenolic and total flavonoid content varied considerably among the accessions. Many of the accessions have high phenolic content. The total phenolic content ranged from 2.4 ± 0.3 to 124.5 ± 12.7 mg GAE/g extract with both field and *in vitro*-grown simili radjah (ABB) having the highest phenolic content, while the

total flavonoid content ranged from 0.4 ± 0.1 to 60.1 ± 6.3 mg QE/g extract (Table 1). Field and *in vitro*-grown *Musa balbisiana* Tani (BBwild), *Musa balbisiana* HND (BBwild) and Dole (ABB) had consistently low total phenolic and total flavonoid contents. Across all the tested accessions, *in vitro*-grown samples had higher total phenolic content whereas, field-grown leaf samples had higher total flavonoid content.

3.3. Total antioxidative and anticholinesterase activity

All the samples showed a dose dependent DPPH[•] free radical scavenging activity by reducing the purple colored and stable DPPH[•] radical to the yellow-colored diphenylpicrylhydrazine. The values of the concentration of the extract that can give 50% inhibition (IC_{50}) ranged from 10.7 ± 0.3 to 257.9 ± 2.3 μ g/mL (Table 1). *In vitro*-grown samples gave the highest antioxidant activity when compared to their field counterpart. Similar result was obtained from previous study [25]. FRAP assays are widely used to determine the efficiency of antioxidant compounds in plants to compete with the FRAP reagent and reduce the ferric to the ferrous blue-colored TPTZ complex. The trolox equivalent ranged from 4.3 ± 0.1 to 152.2 ± 2.8 mg TE/g extract with *in vitro*-grown samples again having better antioxidant activity. *Musa balbisiana* Tani (BBwild) and *Musa balbisiana* HND (BBwild) exhibited low antioxidant potential in these assays. For the AChE inhibition, most of the *in vitro*-grown accessions gave better AChE inhibitory activity than the field accessions (Table 1). One of the *in vitro*-grown accessions, Calcutta 4 (IC_{50} : 11.5 ± 6.1 μ g/mL), gave a better activity than the reference standard eserine (IC_{50} : 31.2 ± 7.3 μ g/mL).

3.4. Correlation among the antioxidative cuvette assays

The correlation among the antioxidant assays as determined by Pearson's coefficient r is shown in Table S-3. Different antioxidant assay methods (DPPH[•] and FRAP) were employed in this study because it is assumed that more than one assay would reflect better the antioxidant potential of a complex mixture of secondary metabolites [57]. Each assay would also help to better know the mechanism of the antioxidant activity. The correlation of the antioxidant assays with the phytochemical composition among the field accessions was generally lower than the correlation among the *in vitro*-grown accessions (Table S-3 A). This is similar to the result obtained from the accessions tested in a previous study [26]. The result revealed a relatively good correlation between the DPPH[•] and FRAP assays among both, the field ($r = 0.61$) and *in vitro* ($r = 0.66$) grown accessions. For the *in vitro*-grown samples, there was a strong correlation between TPC and DPPH[•], and between TPC and FRAP, but a weak correlation between TFC and DPPH[•]. Teixeira et al. [58] also noticed a strong correlation between TPC and antioxidant assays in all their studied medicinal plants but a weak correlation between TFC and antioxidants. This indicates that other phenolic compounds apart from the flavonoids are responsible for the strong antioxidant capacity of the samples.

3.5. HPTLC method

For the first time, HPTLC was used to reveal the chemical fingerprint of *Musa* species field accessions in comparison with *in vitro*-grown accessions. Polar solvent systems were investigated due to prior information noted from the cuvette assay about the high phenolic content of the *Musa* spp accessions. Among the different mobile phases tested (Fig. S-5), a polar, acidic mobile phase comprising of ethyl acetate – toluene – formic acid – water (3.4: 0.5: 0.7: 0.5) gave the best separation and was used. The derivatization with the NP reagent revealed the fingerprint of phenolic compounds and flavonoids in the *Musa* spp. Phenolic compounds

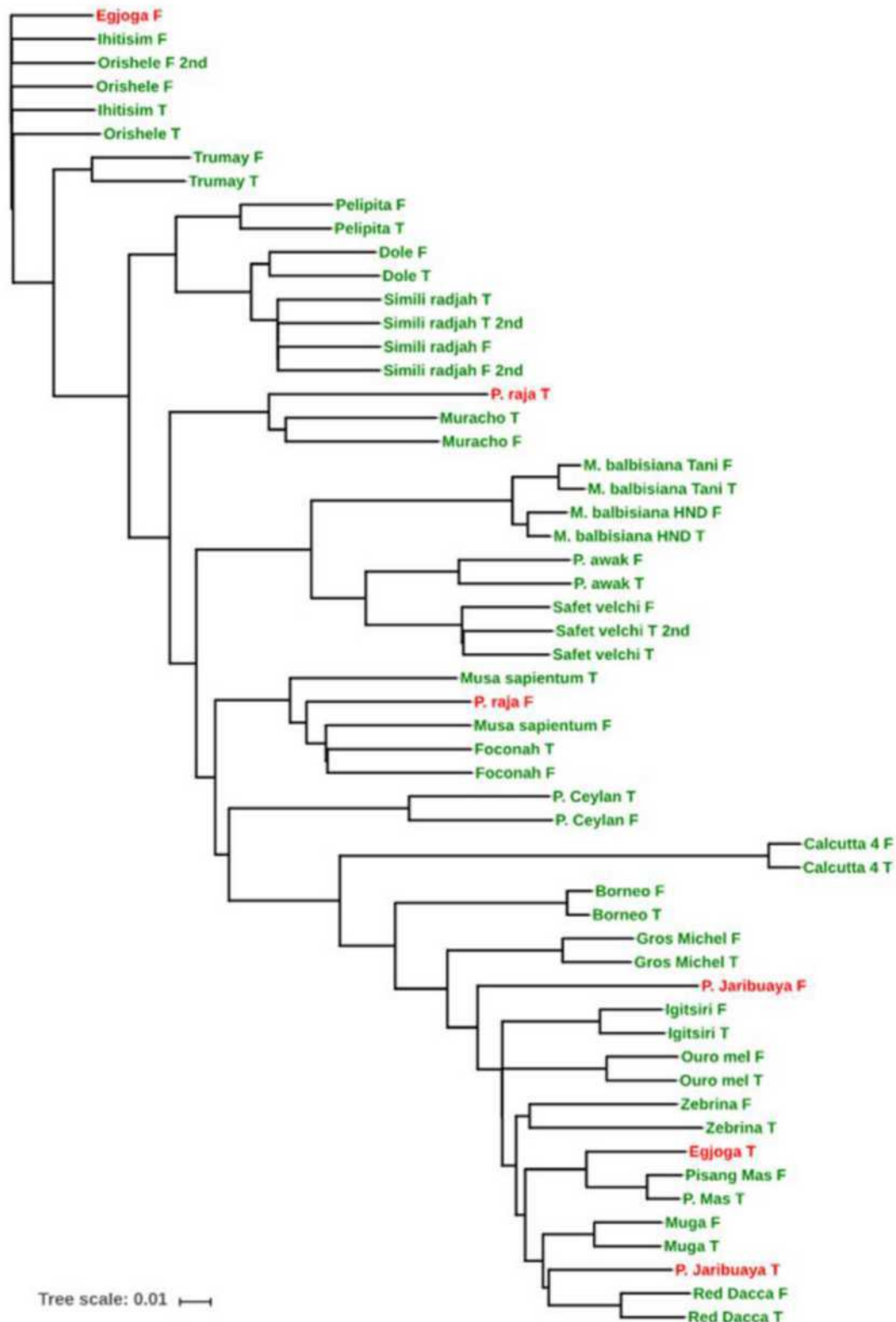


Fig. 1. Neighbor joining tree of field and *in vitro*-grown *Musa* spp. accessions using 150 k SNP markers.

are known to have a wide pharmacological activity range, such as antimicrobial [59], antioxidant [60], anti-inflammatory [61], antidiabetic [62], and antiulcer [63] properties among others. Phenolic compounds were found to be abundant from *in vitro*-grown samples (Fig. 2C). This is in support of the result obtained from the

cuvette assay with the *in vitro* accessions giving higher TPC than the field-grown accessions. Also, the flavonoids shown as dark UV-absorbing bands at 254 nm and as green and orange fluorescent bands after derivatization in the NP reagent are seen in the field accessions, but not in the *in vitro*-grown accessions (Fig. 2C). Inter-

Table 1

Means ($n=3$) of total phenolic content (TPC), flavonoid content (TFC), FRAP antioxidant potential, IC₅₀ of DPPH[•] free radical scavenging and AChE inhibitory activity of field-grown and *in vitro*-grown *Musa* spp. accessions.

No	Accession	Gen group	TPC (mg GAE/g)		TFC (mg QE/g)		FRAP (mg TE/g)		DPPH IC ₅₀ (µg/mL)		AChE IC ₅₀ (µg/mL)	
			Field	<i>In vitro</i>	Field	<i>In vitro</i>	Field	<i>In vitro</i>	Field	<i>In vitro</i>	Field	<i>In vitro</i>
1	P. Mas	AA	18.1 ± 2.7 ^e	72.1 ± 0.1 ^c	9.6 ± 3.1 ^f	3.4 ± 0.0 ^f	9.8 ± 1.5 ^c	53.3 ± 0.3 g	95.4 ± 0.7 ^{ef}	25.4 ± 2.1 ^d	219.1 ± 13.8^a	137.2 ± 23.8 ^b
2	Simili Radjah	ABB	85.9 ± 1.4^a	124.5 ± 12.7^a	30.3 ± 2.7 ^b	11.3 ± 0.7 ^b	18.8 ± 0.4 ^b	140.3 ± 2.3^b	28.2 ± 1.3^a	10.7 ± 0.3^a	610.6 ± 127.1 ^c	541.3 ± 81.1 ^d
3	Red Dacca	AAA	19.7 ± 3.1 ^e	38.5 ± 3.5 ^e	24.0 ± 1.7 ^c	3.8 ± 0.2 ^e	11.8 ± 0.9 ^e	102.4 ± 3.0 ^c	56.3 ± 1.8 ^b	25.1 ± 1.2 ^d	376.3 ± 40.2 ^c	282.3 ± 59.8 ^c
4	Pelipita	ABB	14.4 ± 1.5 ^{ef}	21.7 ± 4.1 ^f	24.1 ± 1.8 ^c	2.5 ± 0.1 g	16.9 ± 0.5 ^c	27.7 ± 1.7 ⁱ	53.9 ± 0.5 ^b	46.9 ± 0.1 ^f	282.7 ± 19.4 ^b	429.0 ± 54.0 ^d
5	Safet Velchi	AABcv	33.6 ± 0.8 ^c	55.8 ± 3.7 ^d	3.6 ± 0.9 ^h	0.5 ± 0.3 g	11.3 ± 0.2 ^e	63.9 ± 0.9 ^f	78.8 ± 0.3 ^d	22.8 ± 0.6 ^{cd}	687.0 ± 26.1 ^c	1050.0 ± 274.1 ^e
6	Igitsiri	AAA	16.3 ± 0.8 ^e	43.0 ± 0.9 ^{cd}	9.4 ± 0.5 ^f	1.3 ± 0.1 g	16.2 ± 2.2 ^c	78.1 ± 2.4 ^e	65.5 ± 1.0 ^c	34.1 ± 1.0 ^f	430.8 ± 45.6 ^c	791.3 ± 36.1 ^e
7	Zebrina	AAwild	33.8 ± 0.1 ^c	56.3 ± 3.3 ^d	11.6 ± 0.3 ^e	1.6 ± 0.2 g	22.4 ± 2.0 ^a	52.3 ± 3.0 g	52.8 ± 0.1 ^b	17.9 ± 0.5 ^{bc}	419.0 ± 15.1 ^c	633.5 ± 71.8 ^d
8	Dole	ABB	7.6 ± 1.5 g	9.8 ± 0.2 ^{fg}	4.3 ± 0.2 g	0.6 ± 0.2 g	8.4 ± 1.2 ^e	22.9 ± 2.6 ⁱ	100.0 ± 2.2 ^{ef}	68.2 ± 1.6 g	2170.0 ± 372.9 g	771.5 ± 16.4 ^e
9	Foconah	AAB	34.6 ± 1.8 ^c	87.5 ± 4.3^b	11.4 ± 0.5 ^e	14.6 ± 1.4^a	14.6 ± 0.6 ^d	152.2 ± 2.8^a	56.2 ± 0.7 ^b	12.2 ± 0.8 ^{ab}	514.3 ± 90.3 ^c	289.4 ± 9.8 ^c
10	Gros Michel	AAA	48.4 ± 1.4^b	56.5 ± 0.7 ^d	60.1 ± 6.3^a	0.4 ± 0.1 g	8.6 ± 0.2 ^e	89.0 ± 0.2 ^d	101.4 ± 0.8 ^f	49.0 ± 0.8 ^f	1637.0 ± 253.1 g	434.6 ± 37.5 ^d
11	P. Ceylan	AAB	27.2 ± 2.5 ^d	76.3 ± 0.3 ^{bc}	28.7 ± 2.0 ^c	8.6 ± 0.2 ^c	5.7 ± 0.2 ^f	66.5 ± 0.9 ^f	257.9 ± 2.3 ⁱ	22.8 ± 0.5 ^{cd}	555.7 ± 17.8 ^c	420.9 ± 37.2 ^d
12	P. Jaribuaya	AA	29.2 ± 0.4 ^{cd}	66.9 ± 0.7 ^{cd}	11.1 ± 0.6 ^e	2.4 ± 0.6 g	23.8 ± 0.4 ^a	54.5 ± 2.2 g	92.2 ± 2.5 ^e	23.7 ± 0.2 ^{cd}	981.8 ± 62.6 ^d	494.0 ± 46.2 ^d
13	Calcutta 4	AAwild	32.9 ± 0.5 ^c	75.6 ± 2.4 ^c	4.2 ± 0.2 g	5.5 ± 0.7 ^d	4.3 ± 0.1 ^f	100.7 ± 3.5 ^c	148.4 ± 2.5 g	20.2 ± 0.2 ^{cd}	1124.0 ± 31.3 ^e	11.5 ± 0.1^a
14	M. balbi HND	BBwild	16.3 ± 1.1 ^e	19.6 ± 2.0 ^f	18.8 ± 2.6 ^d	1.1 ± 0.3 g	4.4 ± 0.7 ^f	32.4 ± 0.4 ^h	190.1 ± 11.2 ^h	116.4 ± 1.4 ^h	1280.0 ± 91.9 ^f	1181.0 ± 91.3 ^e
15	M. balbi Tani	BBwild	3.9 ± 0.4 ^h	2.4 ± 0.3 g	30.8 ± 2.8 ^b	1.1 ± 0.6 g	16.1 ± 0.5 ^c	10.6 ± 0.5 ^j	148.9 ± 5.5 g	154.4 ± 6.4 ⁱ	752.3 ± 45.3 ^c	780.4 ± 21.5 ^e

Means ($n=3$) with the same letter in the same column are not significantly different at $P<0.05$. IC₅₀ of gallic acid at 1.7 ± 0.0 µg/mL, ascorbic acid at 3.7 ± 0.1 µg/mL and serine at 31.2 ± 7.3 µg/mL.

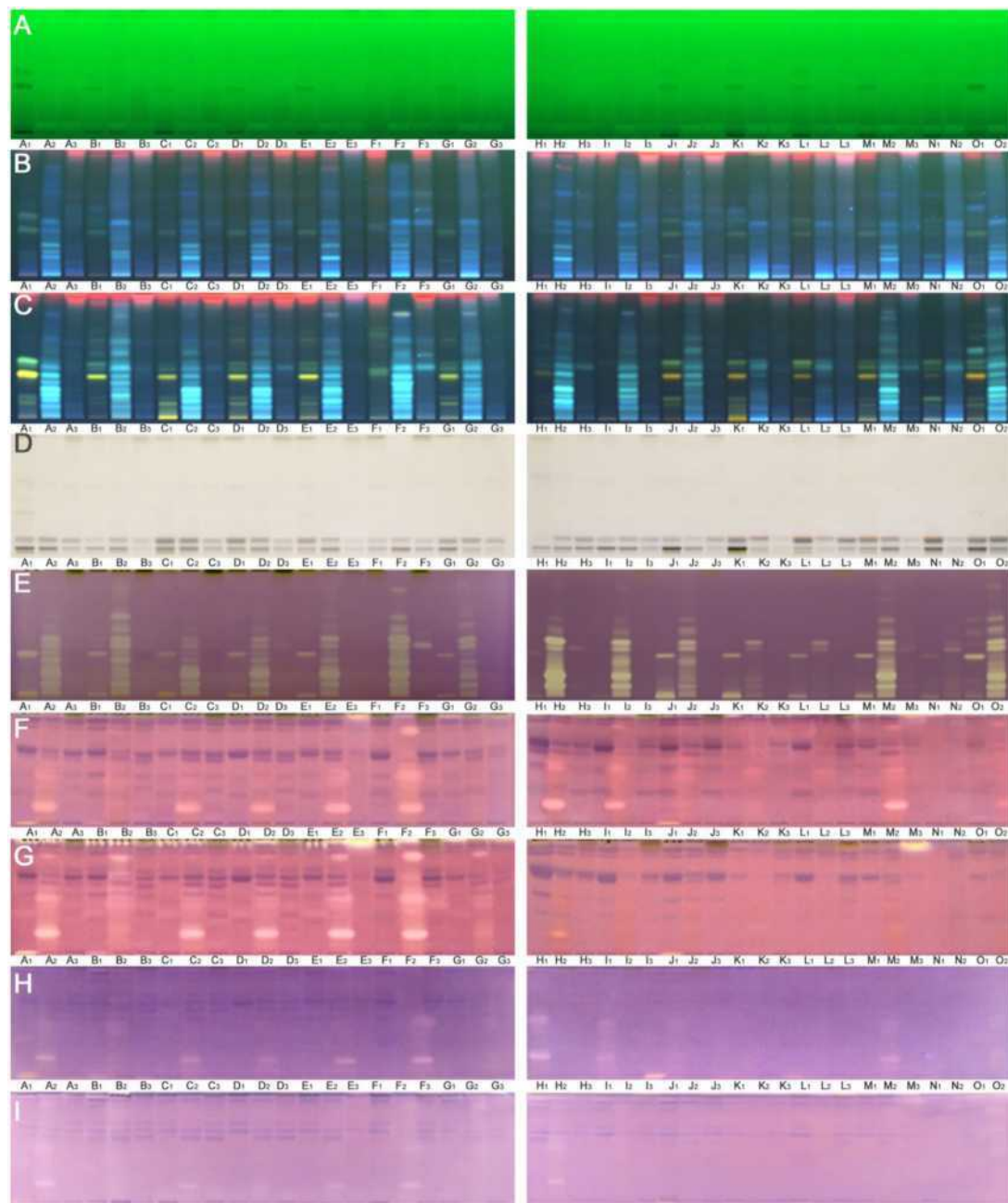


Fig. 2. HPTLC-UV/FLD-EDA fingerprints of field, *in vitro*-grown and acclimatized *Musa* spp. accessions (A1-O2 as assigned in Table S-1; 10 μ L/band, except for AChE/BChE 25 μ L/band) on silica gel HPTLC plates with ethyl acetate - toluene - formic acid - water, 3.4:0.5:0.7:0.5, documented (A) at UV 254 nm, (B) at UV 366 nm, (C) after derivatization using a reagent sequence starting with natural product reagent visualized at UV 366 nm, followed by ninhydrin reagent (no zones evident; not depicted) and lastly (D) diphenylamine reagent, (E) after derivatization by DPPH[•] reagent as well as after (F) AChE, (G) BChE, (H) α -glucosidase and (I) β -glucosidase assays, all latter (E-I) documented at white light illumination.

estingly, this result is also in consonance with what was obtained previously from the cuvette assay. Field accessions gave higher total flavonoid content than the *in vitro*-grown accessions. The pattern obtained by derivatization with the DPA reagent is seen in Fig. 2D. Sugars were found in all samples when derivatized with this reagent selective for saccharides and glycosides. This underlines previous studies [64], in which sugars have been reported to be present in the leaves of *Musa* spp.

3.6. Effect-directed analysis by HPTLC-EDA

So far, the biological activities of *Musa* spp. such as antidiabetic activity of the fruit [65], anticholinesterase potential

of the fruits and leaves [26] and antimicrobial activity of peel and leaf [14] have been reported using cuvette spectrophotometric assays and other *in vitro* and *in vivo* assays. For the first time, the present study shows the biological profiles of *Musa* spp. accessions using HPTLC-EDA. This work also compared the biological profiles of plants grown in different environments (field, *in vitro* and green house). The HPTLC-EDA helped to identify and observe clearly the compounds responsible for each biological activity, which is not possible with cuvette assays (sum parameter). In this study, HPTLC was hyphenated to DPPH[•], AChE, BChE, α -glucosidase, β -glucosidase, α -amylase, *Aliivibrio fischeri*, *Bacillus subtilis* and *Salmonella thyphimurium* assays.

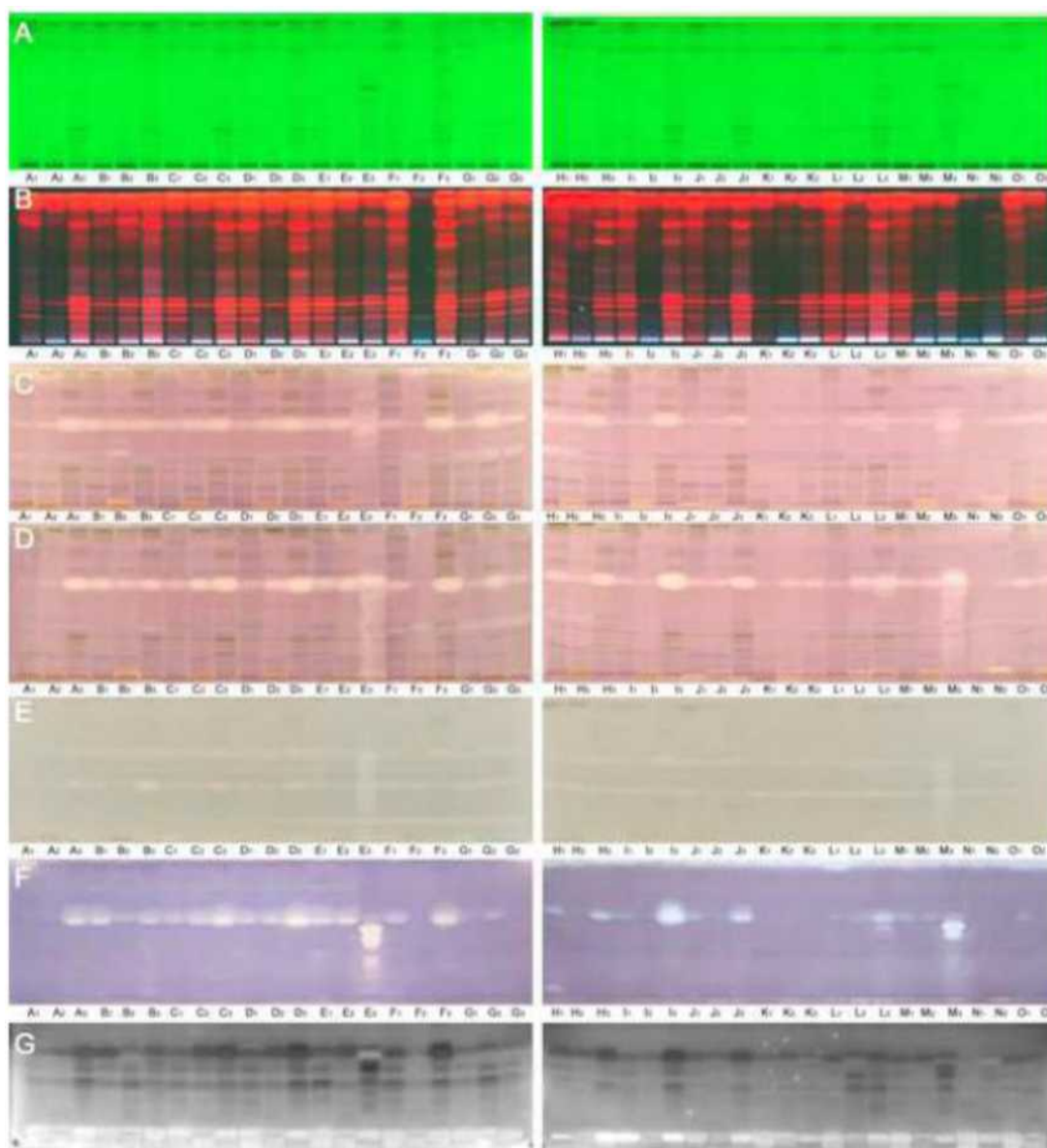


Fig. 3. HPTLC-UV/FLD-EDA fingerprints of field, *in vitro*-grown and acclimatized *Musa* spp. accessions (A1-O2 as assigned in Table S-1; 10 μ L/band, except for AChE/BChE 15 μ L/band) on silica gel HPTLC plates with toluene - ethyl acetate - methanol, 6:3:1, documented at (A) UV 254 nm, (B) UV 366 nm, and white light illumination after (C) AChE, (D) BChE, (E) α -amylase, (F) *B. subtilis*, and (G) *A. fischeri* assays.

3.6.1. Radical scavenging activity

The derivatization with the DPPH[•] reagent revealed the presence of antioxidant compounds in *Musa* spp. as a pattern of whitish bands on a purple background (Fig. 2E). *In vitro*-grown accessions, which have many phenolic compounds, have many whitish radical scavenging bands unlike the field-grown accessions with flavonoids but reduced number and intensity of whitish zones. This joins the result of the correlation among the assays. The phenolic compounds are responsible for the antioxidant property of the plant samples, while the flavonoids contributed less. Similarly, the HPTLC-DPPH[•] method revealed the variation in the chemical profile of samples from different origin with different genome group. Just like the result obtained from the cuvette spectrophotometric assays, the samples with the high TPC, TFC, DPPH[•] and FRAP values also have many whitish radical scavenging bands after derivatization with the DPPH[•] reagent, while samples with low cuvette assay values have fewer bands (Fig. 2E). *In vitro* grown accessions gave the highest peak area values of the radical scav-

enging compounds (Table S-4). These *in vitro*-grown accessions that are rich in phenolics and antioxidants can be explored for natural products isolation.

3.6.2. Detection of AChE and BChE inhibitors

Compounds that can inhibit cholinesterase enzymes were found in the *Musa* spp. accessions tested (Figs. 2 and 3). Cholinesterase inhibitors are known to be important drugs for treating neurological disorders such as Alzheimer's diseases. Key enzymes found in the human neurological system are AChE and BChE. For example, AChE is responsible for the breakdown of acetylcholine into choline and acetic acid, which leads to the reduction in the acetylcholine level in the body [66]. The body has a way of balancing the situation, but in disease condition, a cholinesterase inhibitor is usually needed. Plants containing AChE and BChE inhibitors are good sources of neurodegenerative diseases drug development [67].

The AChE and BChE inhibitors are seen as white bands on a purple background. With the polar, acidic mobile phase (ethyl ac-

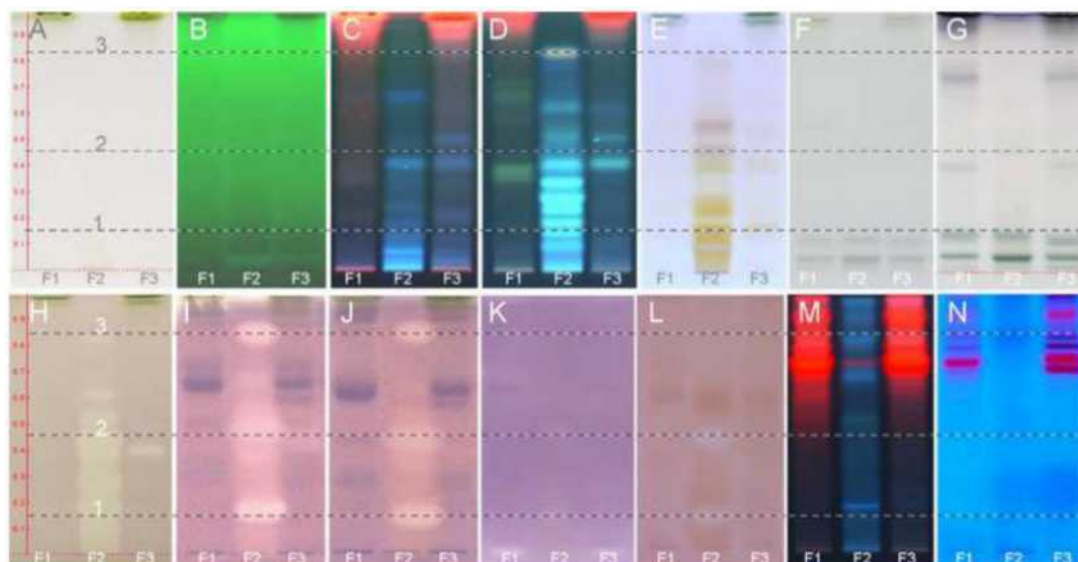


Fig. 4. Detailed comparison of active compounds 1–3 in the HPTLC fingerprints (as in Fig. 2) for *Musa* spp. leaf extract F1–F3, detected at (A) white light illumination (B) UV 254 nm, (C) UV 366 nm, (D) after derivatization using a reagent sequence starting with natural product reagent at 366 nm, followed by (E) ninhydrin reagent and lastly (F) diphenylamine reagent, (G) after derivatization with *p*-anisaldehyde, (H) DPPH• as well as after (I) AChE, (J) BChE, (K) α -glucosidase, and (L) β -glucosidase inhibition assays; same applied (15 μ L/band) on HPTLC RP18 W plate (M) at UV 366 nm and (N) after genotoxicity assay at UV 366 nm.

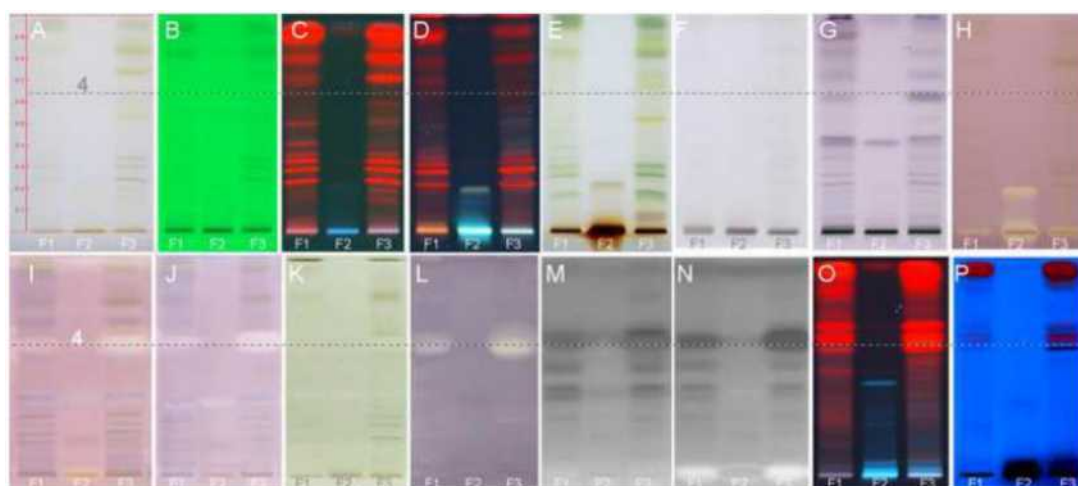


Fig. 5. Detailed comparison of active compound 4 in the HPTLC fingerprints (as in Fig. 3) for *Musa* spp. leaf extract F1–F3, detected (A) at white light illumination (B) at UV 254 nm, (C) at UV 366 nm, after derivatization using a reagent sequence (D) starting with natural product reagent at 366 nm, followed by (E) ninhydrin reagent and lastly (F) diphenylamine reagent, (G) after derivatization with *p*-anisaldehyde, (H) DPPH• as well as after (I) AChE, (J) BChE, (K) α -amylase inhibition assays, all latter documented at white light illumination, and after bioassays (L) *B. subtilis* and (M) *A. fischeri* after 3 min and (N) 30 min (both as bioluminescence image); same applied (15 μ L/band) on HPTLC RP18 W plate (O) at UV 366 nm and (P) after genotoxicity assay at UV 366 nm.

etate – toluene – formic acid – water, 3.4: 0.5: 0.7: 0.5), three major compounds (Fig. 4) at hR_f values 15, 44 and 83 were identified as AChE and BChE inhibitors and were observed from *in vitro*-grown accessions. White bands were noticed at the solvent front so the elution power was reduced. With the medium polar mobile phase (toluene – ethyl acetate – methanol, 6:3:1), one major compound (Fig. 5) with hR_f 63 was identified to inhibit AChE and BChE in almost all the samples tested with higher band intensity in the acclimatized accessions. In some samples (I to O, except J1 on start zone and M3 in front), no inhibitor compounds were detected when the polar mobile phase was used, suggesting that those samples do not contain any BChE inhibitory compound (Fig. 2).

3.6.3. Detection of α - β -glucosidase and α -amylase inhibitors

The inhibition of α -glucosidase, β -glucosidase and α -amylase is linked to the antidiabetic effect. These three enzymes are found

in the digestive system. They are responsible for the breakdown of carbohydrates to glucose thereby increasing the blood glucose level in diabetes patients. The inhibition of these enzymes plays an important role in the management of diabetes, reducing the hydrolysis of carbohydrates [68,69]. HPTLC combined with glucosidase assays revealed compounds with α -glucosidase and β -glucosidase inhibitory activity in the tested *Musa* spp. accessions. Two major compounds were identified from *in vitro*-grown accessions when the polar, acidic mobile phase (ethyl acetate – toluene – formic acid – water, 3.4: 0.5: 0.7: 0.5) was used. They appeared as white bands on a purple background (Fig. 2H and I). Some of the accessions: Pelipita (J), *M. balbisiana* Tani (K), Dole (L), *M. balbisiana* HND (N) and Igitsiri (O) did not show any inhibition zones in both α - and β -glucosidase assays, and similar results were observed in the cholinesterase assay. The zones of inhibition for the field-grown and acclimatized accessions were seen at the appli-

Table 2
HPTLC-HRMS data of bioactive compounds in the selected samples F₂ and F₃.

Sample	Com-pound	hR _F	Observed mass (<i>m/z</i>)	Assignment	Molecular formula	Mass error (ppm)	Intensity	Formula	Potential candidate (s)
F ₂	1	15	131.0461	[M-H] ⁻	C ₄ H ₇ O ₃ N ₂	7.78	5.89E+07	C ₄ H ₈ O ₃ N ₂	asparagine
			133.0606	[M+H] ⁺	C ₄ H ₉ O ₃ N ₂	1.343	9.26E+08		
	2	44	146.966	[M-H] ⁻			9.13E+07	C ₉ H ₁₁ NO ₂	4-aminohydrocinnamic acid, phenylalanine, 2-amino-3,4-dimethylbenzoic acid, 2-(4-methylphenoxy) acetamide
			166.0866	[M+H] ⁺	C ₉ H ₁₂ NO ₂	1.956	5.61E+08		
	3	83	218.0823	[M-H] ⁻	C ₁₂ H ₁₂ O ₃ N	4.632	1.90E+08	C ₁₂ H ₁₃ O ₃ N	pyrrolidinone, aniracetam
			437.1717	[2M-H] ⁻			5.62E+07		
242.0783			[M+Na] ⁺	C ₁₂ H ₁₃ O ₃ NNa	1.754	2.95E+08			
461.1676			[2M+Na] ⁺			6.04E+07			
F ₃	4	63	277.2175	[M2-H] ⁻	C ₁₈ H ₂₉ O ₂	2.795	1.38E+08	C ₁₈ H ₃₀ O ₂	linolenic acid
			301.2132	[M2+Na] ⁺			1.84E+07		
			171.1028	[M-H] ⁻	C ₉ H ₁₅ O ₃	4.154	1.21E+08	C ₉ H ₁₅ O ₃	
			195.099	[M+Na] ⁺	C ₉ H ₁₆ O ₃ Na	4.377	7.50E+07		

cation zone when the polar, acidic mobile phase was used. As a white shimmering was noticed at the solvent front (Fig. S-6A), further less polar mobile phases were tested and revealed further inhibition zones (Fig. S-6C). For α -amylase, a clear inhibition zone was detected at the solvent front for sample E3 (Zebrina, Fig. S-6E), whereas for other samples, the white shimmering at the solvent front was weaker. In order to reduce the elution power, the medium polar mobile phase was tested. This revealed two zones of inhibition, at hR_F 40 and 63, which were in all samples more or less intense (Fig. 3E).

3.6.4. Detection of antimicrobials

There are several reports on the antimicrobial properties of different parts of *Musa* spp. using agar well diffusion assay [70,71], but for the first time, the inhibition of these microorganisms was reported via HPTLC-EDA analysis. The HPTLC-*B. subtilis* bioassay (Gram-positive bacteria) revealed one main antibacterial zone (hR_F 63) with a very intense band in almost all the samples (Figs. 3F and 5L). The acclimatized samples gave more intense bands. *M. balbisiana* Tani, Dole, *M. balbisiana* HND and Igitsiri were the accessions with weak or no inhibition zones (Fig. 3F). For the HPTLC-*Aliivibrio fischeri* bioassay (Gram-negative bacteria), antimicrobials were detected based on their impact on the bioluminescence (metabolic activity) of *A. fischeri* bacteria, appearing as dark (inhibiting) or bright (enhancing) zones on an instantly luminescent bacterial plate background. Many dark zones of inhibition were observed in the different *Musa* spp. accessions (Fig. 3G) with increasing intensity as the time increased.

3.6.5. Absence of genotoxins

The HPTLC-genotoxicity assay via *Salmonella thyphimurium* bacteria (SOS-Umu-C bioassay) [47] applied to the plant samples showed that the *Musa* spp. contained no genotoxic compounds for the given highest amount of 38 μ g methanolic extract applied (15 μ L/band of a 2.5 mg/mL solution, Fig. S-7). The toxic positive control 4-nitroquinoline-1-oxide appeared as blue fluorescence at UV 366 nm, while the samples even at a higher amount on the plate gave no such fluorescence after development with both mobile phases (Fig. S-7). *In vivo* animal model studies have been used to report the toxicity profile of some parts of *Musa paradisiaca* L. The juice from the pseudostem of *Musa paradisiaca* was reported to be non-toxic [72]. The ethanol extract of the leaf was found to be slightly toxic with an LD₅₀ of 490 mg/kg body weight of the mice [70], while the unripe fruit extract was non-toxic and safe for pharmaceutical use [73]. These findings support our results. In HPTLC, still higher sample volumes can be analyzed to lower the detectability, but was not performed in this study.

3.7. Characterization of active zones via HPTLC-HRMS

The multipotent active zones were characterized by HPTLC-HRMS after online elution via an elution head-based interface. The multipotent compounds 1 to 3 were obtained from only *in vitro* grown accessions developed in the polar, acidic mobile phase (Fig. 4). The band of compound 3 was very intense *in vitro*-grown Calcutta 4 (F₂), but was not visible or absent in some accessions (*M. balbisiana* Tani, Dole and *M. balbisiana* HND). Calcutta 4 field (F₁), *in vitro* (F₂) and acclimatized extracts (F₃) were considered as representative samples based on the HPTLC-EDA assay results. The following tentative assignment of the compounds was based on the respective base peak in the HPTLC-HRMS spectrum, HPTLC derivatization and literature data (Table 2).

Compound 1 (hR_F 15) which is a blue fluorescent compound at UV 366 nm (Fig. 4) gave a base peak at *m/z* 133.0606, which was assigned as [M+H]⁺ (Fig. 6) with C₄H₉O₃N₂ as calculated molecular formula. The sodium adduct was seen at *m/z* 155.0424 [M+Na]⁺ (C₄H₈O₃N₂Na). In the negative mode, the base peak at *m/z* 131.0461, assigned as [M-H]⁻ (C₄H₇O₃N₂), underlined the previous result. Thus, the actual molecular formula of compound 1 was preliminary assigned to be C₄H₈O₃N₂. This molecular formula fit to an amino acid (different forms of asparagine, alanine and glycine anhydride). Though aspartic acid and other amino acids have been reported to be present in the pulp [74] and peel [75] of *Musa* spp., further experiments (selectivity of the mobile phase needs to be adjusted) are needed to clarify the observed effects. Compound 1 showed strong radical scavenging (antioxidant) activity and strong AChE and BChE inhibition, but moderate α - and β -glucosidase inhibition based on the HPTLC-EDA results (Fig. 4).

Compound 2 (hR_F 44) showed a characteristic blue color after derivatization with the NP reagent. It showed the same effects as compound 1. The base peak at *m/z* 166.0866 was assigned to be [M+H]⁺ with C₉H₁₂NO₂ as molecular formula. In the negative mode, the respective base peak [M-H]⁻ was at *m/z* 146.9660. Thus, the formula of compound 2 (C₉H₁₁NO₂) corresponds to that of a simple aromatic ring (benzene) with an amino group, carbonyl and hydroxyl group attached which could be 4-aminohydrocinnamic acid, phenylalanine, 2-amino-3,4-dimethylbenzoic acid or 2-(4-methylphenoxy) acetamide.

Compound 3 (hR_F 83) was not UV sensitive and gave a characteristic yellow color surrounded by blue color after derivatization in NP reagent (Fig. 4). In the positive ionization mode, the recorded mass spectra of this zone showed a base peak at *m/z* 242.0783, which was assigned as [M+Na]⁺ (C₁₂H₁₃O₃NNa). The dimer of this compound was seen at *m/z* 461.1676 and assigned as [2M+Na]⁺ (Fig. 6). In the negative mode, the respective base peak was at *m/z*

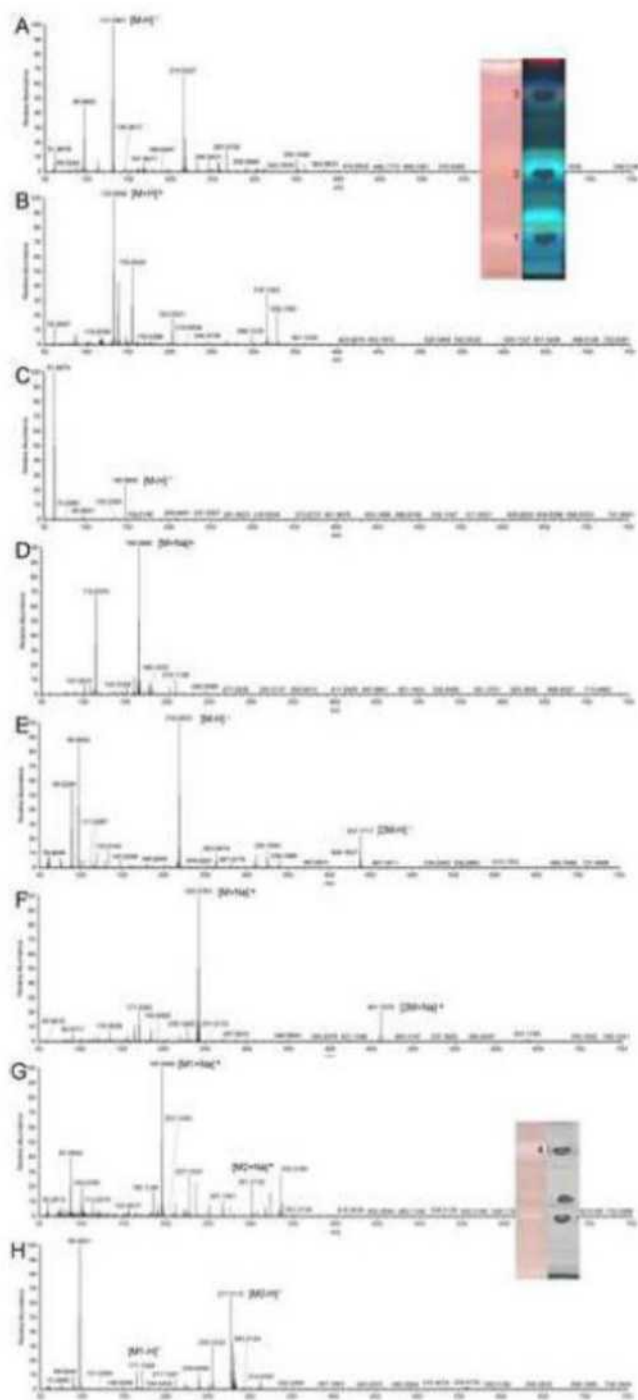


Fig. 6. HPTLC-HRMS spectra of compounds 1–3 in sample extract F_2 (A–F; conditions as in Fig. 3, 25 $\mu\text{L}/\text{band}$) and compound 4 in sample extract F_3 (G and H; conditions as in Fig. 4; 15 $\mu\text{L}/\text{band}$); for zone marking, a plate stripe was supplied to the AChE assay, and after zone elution, the plate stripe was immersed into a suited derivatization reagents to check proper positioning.

218.0823 $[\text{M}-\text{H}]^-$ with its dimer $[\text{2M}-\text{H}]^-$ at m/z 437.1717. Thus, the actual molecular formula of this compound was $\text{C}_{12}\text{H}_{13}\text{O}_3\text{N}$. From literature, this compound was found to be an alkaloid with a pyrrolidine base. It is most likely aniracetam. Pyrrolidine alkaloids are used as anticholinergic drugs. Based on the HPTLC-EDA results, compound 3 showed a moderate antioxidant activity, a very strong AChE and BChE, but no α - and β -glucosidase inhibition. Many alkaloids from plants such as rivastigmine, galantamine and hu-

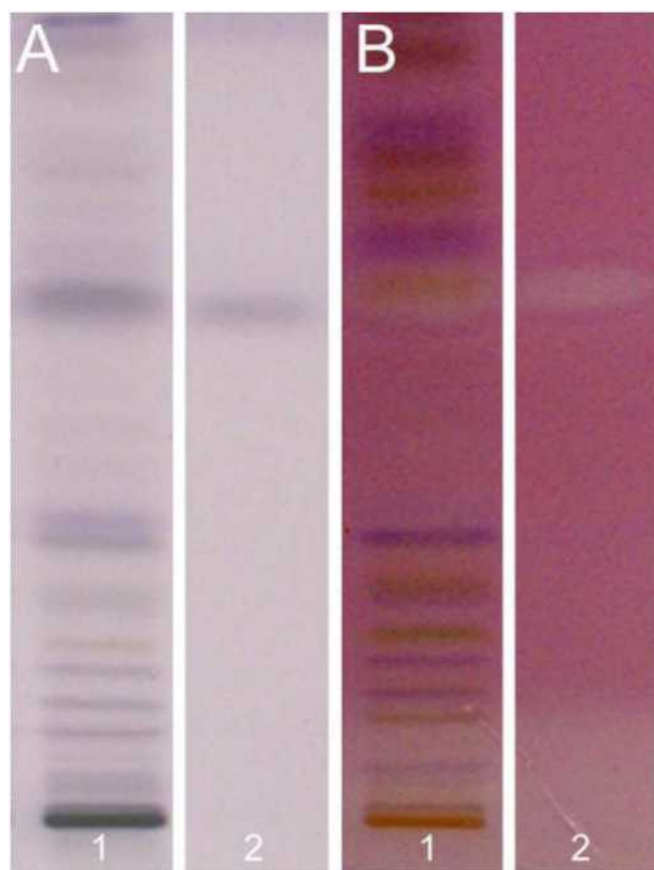


Fig. 7. Co-chromatography of sample extract F_4 , track 1 (10 $\mu\text{L}/\text{band}$), standard linolenic acid, track 2 (100 $\text{ng}/\mu\text{L}$, 0.1 mg/ml methanol, 5 μL applied) confirmed compound 4 to be linolenic acid (A) derivatized in *p*-anisaldehyde reagent and (B) after AChE assay.

perzine A have been reported for their anticholinesterase activity [76,77]. In *Musa* spp. and in Musaceae family, pyrrolidine alkaloids have not been reported so far and this suggested preliminary assignment is new.

The multipotent compound 4 (hR_f 63) was present in all the samples and abundant in acclimatized accessions based on the peak area. It was obtained from sample extract F_3 developed in the medium polar mobile phase (Fig. 5). Compound 4 showed a characteristic purple color when derivatized with the *p*-anisaldehyde reagent. The mass spectra of this zone showed a base peak at m/z 277.2175, which was assigned as $[\text{M}-\text{H}]^-$ with the formula $\text{C}_{18}\text{H}_{29}\text{O}_2$. In the positive mode, the respective sodium adduct of this compound was seen at m/z 301.2132. Other unassigned fragments were also seen (Fig. 6G and H). The actual molecular formula of this compound was found to be $\text{C}_{18}\text{H}_{30}\text{O}_2$, indicating linolenic acid (octadeca-9,12,15-trienoic acid). By co-chromatography of the sample and the standard (Fig. 7), compound 4 was confirmed to be linolenic acid. This fatty acid has been reported to be present in the fruits of different *Musa* spp. cultivars [78] also in the leaves [21]. This polyunsaturated fatty acid is an essential fatty acid that cannot be synthesized by the human body and therefore, must be supplied by external sources. *Musa* spp. is shown to be an excellent source of this fatty acid. In this study, this fatty acid is reported to have multiple bioactivities. It showed strong AChE, BChE, *B. subtilis* and *A. fischeri* inhibitory properties, but a weak α -amylase inhibition and no radical scavenging (antioxidant) activity. These multiple bioactivities of linolenic acid were confirmed in parallel studies on *Primula* species in our group [79].

Conclusions

This study for the first time provided the chemical, enzymatic and biological fingerprints of *Musa* spp. using hyphenated HPTLC. Up to 22 samples were simultaneously analyzed within a short time. It presented a simple, fast and streamlined workflow for the detection and characterization of multipotent secondary metabolites in *Musa* spp. This straightforward hyphenation helped to detect, characterize and even identify individual bioactive compounds in the complex extracts. The results of the HPTLC-EDA analysis confirmed the sum parameter results obtained by spectrophotometric cuvette assays. The samples with an overall high TPC and antioxidant activity were also seen to have many antioxidative bands with high peak area signals, while the samples with low TPC and antioxidant activity were seen to have fewer bands in many of the HPTLC-EDA autograms. The *in vitro*-grown accessions had the best antioxidant property and contained compounds 1 to 3, which were not detected in the field and the acclimatized samples. Compound 4 (linolenic acid) was found in all the samples, but was abundant in acclimatized accessions. This study confirmed the use of *Musa* spp. tissue cultures as an alternative mean of plant material supply for the pharmaceutical industry and demonstrated a suitable bioanalytical tool for activity control.

Author contributions

I. Ayoola-Oresanya did most experiments (partly done by master student N. Hockamp at JLU Giessen) and wrote the manuscript draft, revised by all authors except for R. Paliwal. M. Sonibare supervised the UV-spectrophotometric assays. B. Gueye supervised the *in vitro* cultivation, R. Paliwal did the DNA sequence analysis, M. Abberton organized the SNP sequencing, and G. Morlock supervised the HPTLC research performed at JLU Giessen.

Declaration of Competing Interest

The authors declare that they have no known competing financial interests or personal relationships that could have appeared to influence the work reported in this paper.

The authors declare no conflict of interest.

Acknowledgments

This work was supported by the German Academic Exchange Service, Germany (DAAD) short-term grant given to I. Ayoola-Oresanya for her stay at JLU Giessen. The authors are grateful to the Food Science group at JLU Giessen for assistance, especially to N. Hockamp. Instrumentation was partially funded by the Deutsche Forschungsgemeinschaft (DFG, German Research Foundation) - INST 162/471-1 FUGG; INST 162/536-1 FUGG.

Supplementary materials


Supplementary material associated with this article can be found, in the online version, at doi:10.1016/j.chroma.2019.460774.

References

- [1] I. Choma, W. Jesionek, TLC-direct bioautography as a high throughput method for detection of antimicrobials in plants, *Chromatography* 2 (2015) 225–238.
- [2] G.E. Morlock, Instrumental methods for the analysis and identification of bioactive molecules, in: ACS Symposium Series, 1185, 2013, pp. 101–121, doi:10.1021/bk-2014-1185.ch005.
- [3] M. Jamshidi-Aidji, G.E. Morlock, From bioprofiling and characterization to bioquantification of natural antibiotics by direct bioautography linked to high-resolution mass spectrometry: exemplarily shown for *salvia miltiorrhiza* root, *Anal. Chem.* 88 (2016) 10979–10986, doi:10.1021/acs.analchem.6b02648.
- [4] Á.M. Móricz, P.G. Ott, G.E. Morlock, Discovered acetylcholinesterase inhibition and antibacterial activity of polyacetylenes in tansy root extract via effect-directed chromatographic fingerprints, *J. Chromatogr. A.* 1543 (2018) 73–80, doi:10.1016/j.chroma.2018.02.038.
- [5] T. Müller, S. Vergeiner, B. Krättiler, Structure elucidation of chlorophyllcatabolites (phyllobilins) by ESI-mass spectrometry – pseudo-molecular ions and fragmentation analysis of a nonfluorescent chlorophyll catabolite (NCC), *Int. J. Mass Spectrom.* 365–366 (2014) 48–55.
- [6] I. Yüce, G.E. Morlock, Streamlined structure elucidation of an unknown compound in a pigment formulation, *J. Chromatogr. A.* 1469 (2016) 120–127, doi:10.1016/j.chroma.2016.09.040.
- [7] H. Luftmann, M. Aranda, G.E. Morlock, Automated interface for hyphenation of planar chromatography with mass spectrometry, *Rapid Commun. Mass Spectrom.* 21 (2007) 3772–3776.
- [8] G. Morlock, W. Schwack, Hyphenations in planar chromatography, *J. Chromatogr. A* 1217 (2010) 6600–6609.
- [9] W.H. Perera Córdova, S.G. Leitão, G. Cunha-Filho, R.A. Bosch, I.P. Alonso, R. Pereda-Miranda, R. Gervou, N.A. Touza, L.E.M. Quintas, F. Noêl, Bufadienolides from parotoid gland secretions of Cuban toad *Peltophyryne fustiger* (Bufonidae): inhibition of human kidney Na⁺/K⁺-ATPase activity, *Toxicol.* 110 (2016) 27–34.
- [10] E.O. Adewoye, V.O. Taiwo, F.A. Olayioye, Anti-oxidant and anti-hyperglycemic activities of *Musa sapientum* root extracts in alloxan-induced diabetic rats, *Afr. J. Med. Med. Sci.* 38 (2009) 109–117.
- [11] P.K. Agarwal, A. Singh, K. Gaurav, S. Goel, H.D. Khanna, R.K. Goel, Evaluation of wound healing activity of extracts of plantain banana (*Musa sapientum* var. *paradisica*) in rats, *Indian J. Exp. Biol.* 47 (2009) 322–340.
- [12] K.P.S. Kumar, D. Bhowmik, S. Duraivel, M. Umadevi, Traditional and medicinal uses of banana, *J. Pharmacog. Phytochem.* 1 (2012) 51–63.
- [13] J.A.O. Ojewole, C.O. Adewunmi, Hypoglycemic effect of methanolic extract of *Musa paradisica* (Musaceae) green fruits in normal and diabetic mice, *Meth. Exp. Find. Clin. Pharmacol.* 25 (2003) 453–456.
- [14] C.S. Alisi, C.E. Nwanyanwu, C.O. Akujobi, C.O. Ibegbulum, Inhibition of dehydrogenase activity in pathogenic bacteria isolates by aqueous extracts of *Musa paradisica* (Var *Sapientum*), *Afr. J. Biotechnol.* (2008) 7.
- [15] M.R. Zuzarte, A.M. Dinis, C. Cavaleiro, L.R. Salgueiro, J.M. Canhoto, Trichomes, essential oils and *in vitro* propagation of *Lavandula pedunculata* (Lamiaceae), *Ind. Crops Prod.* 32 (2010) 580–587.
- [16] S. Ramachandra Rao, G.A. Ravishankar, Plant cell cultures: chemical factories of secondary metabolites, *Biotechnol. Adv.* 20 (2002) 101–153, doi:10.1016/S0734-9750(02)00007-1.
- [17] N.D. Salvi, L. George, S. Eapen, Plant regeneration from leaf base callus of turmeric and random amplified polymorphic DNA analysis of regenerated plants, *Plant Cell. Tissue Organ Cult.* 66 (2001) 113–119.
- [18] R.K. Sahaa, S. Acharyaa, S.S.H. Shovon, P. Royb, Medicinal activities of the leaves of *Musa sapientum* var. *sylvestris* *in vitro*, *Asian Pac. J. Trop. Biomed.* 3 (6) (2013) 476–482.
- [19] H.V. de Vasconcelos Facundo, D. dos Santos Garruti, C.T. dos Santos Dias, B.R. Cordenunsi, F.M. Lajolo, Influence of different banana cultivars on volatile compounds during ripening in cold storage, *Food Res. Int.* 49 (2012) 626–633.
- [20] C. Vilela, S.A.O. Santos, J.J. Villaverde, L. Oliveira, A. Nunes, N. Cordeiro, C.S.R. Freire, A.J.D. Silvestre, Lipophilic phytochemicals from banana fruits of several *Musa* species, *Food Chem* 162 (2014) 247–252, doi:10.1016/j.foodchem.2014.04.050.
- [21] M.A. Sonibare, I.O. Ayoola, B. Gueye, M.T. Abberton, R. D'Souza, N. Kuhnert, Leaves metabolomic profiling of *Musa acuminata* accessions using UPLC – QTOF – MS / MS and their antioxidant activity, *J. Food Meas. Charact.* (2018), doi:10.1007/s11694-018-9725-4.
- [22] C.A. Cruz-cruz, G. Ramírez-tec, K. García-sosa, F. Escalante-erosa, L. Hill, A.E. Osbourn, L.M. Peña-rodríguez, Phytoanticipins from banana (*Musa acuminata* cv. Grande Naine) plants, with antifungal activity against *Mycosphaerella fijiensis*, the causal agent of black Sigatoka, (2010) 459–463, doi:10.1007/s10658-009-9561-9.
- [23] N.S. Mathew, P.S. Negi, Traditional uses, phytochemistry and pharmacology of wild banana (*Musa acuminata* Colla): a review, *J. Ethnopharmacol* 196 (2017) 124–140.
- [24] C.B. Bonnet, O. Hubert, D. Mbeguie-a-mbeguie, D. Pallet, A. Hiol, M. Reynes, P. Poucheret, Effect of physiological harvest stages on the composition of bioactive compounds in Cavendish bananas, *J. Zhejiang Univ. Sci. B* 14 (2013) 270–278, doi:10.1631/jzus.B1200177.
- [25] B. Gueye, A. Adeyemi, M. Debiru, B. Akinyemi, M. Olagunju, A. Okeowo, S. Otukpa, D. Dumet, Standard Operation Procedures (SOP) For IITA *In Vitro* Genebank, IITA, Nigeria, 2012.
- [26] I.O. Ayoola, B. Gueye, M.A. Sonibare, M.T. Abberton, Antioxidant activity and acetylcholinesterase inhibition of field and *in vitro* grown *Musa* L. species, *J. Food Meas. Charact.* 11 (2017) 488–499, doi:10.1007/s11694-016-9416-y.
- [27] T. Murashige, F. Skoog, A revised medium for rapid growth and bio assays with tobacco tissue cultures, *Physiol. Plant.* 15 (1962) 473–497.
- [28] J.J. Doyle, Isolation of plant DNA from fresh tissue, *Focus (Madison)* 12 (1990) 13–15.
- [29] K. Shankar, L. Chavan, S. Shinde, B. Patil, An improved DNA extraction protocol from four *in vitro* banana cultivars, *Asian J. Biotechnol.* 3 (2011) 84–90.
- [30] P. Wenzl, J. Carling, D. Kudrna, D. Jaccoud, E. Huttner, A. Kleinhofs, A. Kilian, Diversity arrays technology (DArT) for whole-genome profiling of barley, *Proc. Natl. Acad. Sci.* 101 (2004) 9915–9920.

- [31] P.J. Bradbury, Z. Zhang, D.E. Kroon, T.M. Casstevens, Y. Ramdoss, E.S. Buckler, TASSEL: software for association mapping of complex traits in diverse samples, *Bioinformatics* 23 (2007) 2633–2635.
- [32] R.C. Team, R: a language and environment for statistical computing, (2013).
- [33] M. Khatoun, E. Islam, R. Islam, A.A. Rahman, A.H.M.K. Alam, P. Khondkar, M. Rashid, S. Parvin, Estimation of total phenol and *in vitro* antioxidant activity of *Albizia procera* leaves, *BMC Res. Notes* 6 (2013) 1, doi:10.1186/1756-0500-6-121.
- [34] H. Fathi, M.A. Ebrahimzadeh, Antioxidant and free radical scavenging activities of *Hypericum perforatum* L.(st. John's wort), *Int. J. For. Soil Eros.* 3 (2013) 68–72.
- [35] D. Susanti, H.M. Sirat, F. Ahmad, R.M. Ali, N. Aimi, M. Kitajima, Antioxidant and cytotoxic flavonoids from the flowers of *Melastoma malabathricum* L, *Food Chem.* 103 (2007) 710–716.
- [36] K.H. Musa, A. Abdullah, K. Jusoh, V. Subramaniam, Antioxidant activity of pink-flesh guava (*Psidium guajava* L.): effect of extraction techniques and solvents, *Food Anal. Method.* 4 (2011) 100–107.
- [37] G.L. Ellman, K.D. Courtney, V. Andres Jr, R.M. Featherstone, A new and rapid colorimetric determination of acetylcholinesterase activity, *Biochem. Pharmacol.* 7 (2) (1961) 88–95.
- [38] T.O. Elufioye, E.M. Obuotor, A.T. Sennuga, J.M. Agbedahunsi, S.A. Adesanya, Acetylcholinesterase and butyrylcholinesterase inhibitory activity of some selected Nigerian medicinal plants, *Rev. Bras. Farmacogn.* 20 (4) (2010) 472–477.
- [39] E. Azadnia, G.E. Morlock, Bioprofiling of *salvia miltiorrhiza* via planar chromatography linked to (bio)assays, high resolution mass spectrometry and nuclear magnetic resonance spectroscopy, *J. Chromatogr. A* 1533 (2018) 180–192, doi:10.1016/j.chroma.2017.12.014.
- [40] M. Jamshidi Aijdi, J. Macho, M. Müller, G.E. Morlock, Effect-directed profiling of aqueous, fermented plant preparations via high-performance thin-layer chromatography combined with *in situ* assays and high-resolution mass spectrometry, *J. Liq. Relat. Techn.* (2019) 1–8.
- [41] Á.M. Mórícz, M. Jamshidi-Aidji, D. Krüzelyi, A. Darcsi, A. Böszörményi, P. Csontos, S. Béni, P.G. Ott, G.E. Morlock, Distinction and valorization of 30 root extracts of five goldenrod (*Solidago*) species, *J. Chromatogr. A* (2019) in print.
- [42] M. Jamshidi-Aidji, G.E. Morlock, Bioprofiling of unknown antibiotics in herbal extracts: development of a streamlined direct bioautography using *Bacillus subtilis* linked to mass spectrometry, *J. Chromatogr. A* 1420 (2015) 110–118.
- [43] A. Marston, Thin-layer chromatography with biological detection in phytochemistry, *J. Chromatogr. A* 1218 (2011) 2676–2683.
- [44] S. Krüger, O. Urmann, G.E. Morlock, Development of a planarchromatographic method for quantitation of anthocyanes in pomace, feedjuice and wine, *J. Chromatogr. A* 1289 (2013) 105–118 <http://dx.doi.org/10.1016/j.chroma.2013.03.005>.
- [45] European Committee for Standardization, Water quality – Determination of the inhibitory effect of water samples on the light emission of *Vibrio fischeri* (Luminescent bacteria test) DIN EN ISO 11348-1:2009-05 (2009).
- [46] A.A. Bulich, Use of luminescent bacteria for determining toxicity in aquatic environments ASTM International, in: *Aquatic Toxicology: Proceedings of the Second Annual Symposium on Aquatic Toxicology*, 1979.
- [47] D. Meyer, M. Marin-Kuan, E. Debon, P. Serrant, C. Bezançon, B. Schilte, G.E. Morlock, Breakthrough Genotoxicity Assay: New validated HPTLC-SOS-Umu-C assay versus state-of-the-art assays, in submission
- [48] V. Glavnik, I. Vovk, A. Albreht, High performance thin-layer chromatography-mass spectrometry of Japanese knotweed flavan-3-ols and proanthocyanidins on silica gel plates, *J. Chromatogr. A* (2017) 1482, doi:10.1016/j.chroma.2016.12.059.
- [49] H. Strosse, H. Schoofs, B. Panis, E. Andre, K. Reyniers, R. Swennen, Development of embryogenic cell suspensions from shoot meristematic tissue in bananas and plantains (*Musa* spp.), *Plant Sci.* 170 (2006) 104–112.
- [50] H. Strosse, E. Andre, L. Sági, R. Swennen, B. Panis, Adventitious shoot formation is not inherent to micropropagation of banana as it is in maize, *Plant Cell. Tissue Organ Cult.* 95 (2008) 321.
- [51] A.M. Makara, P.R. Rubaihayo, M.J.S. Magambo, Carry-over effect of Thidiazuron on banana *in vitro* proliferation at different culture cycles and light incubation conditions, *Afr. J. Biotechnol.* 9 (2010) 3079–3085.
- [52] G.R. Rout, S.K. Senapati, S. Aparajita, S.K. Palai, Studies on genetic identification and genetic fidelity of cultivated banana using ISSR markers, *Plant Omics* 2 (2009) 250.
- [53] E.K. Sales, N.G. Butardo, Molecular analysis of somaclonal variation in tissue culture derived bananas using MSAP and SSR markers, *Int. J. Biol. Vet. Agric. Food Eng.* 8 (2014) 63–610.
- [54] T. Mishra, A.K. Goyal, A. Sen, Somatic embryogenesis and genetic fidelity study of the micropropagated medicinal species, *Canna indica*, *Horticulturæ*. 1 (2015) 3–13.
- [55] I.Y. Rabbi, P.A. Kulakow, J.A. Manu-Aduening, A.A. Dankyi, J.Y. Asibuo, E.Y. Parkes, T. Abdoulaye, G. Girma, M.A. Gedil, P. Ramu, Tracking crop varieties using genotyping-by-sequencing markers: a case study using cassava (*Manihot esculenta* Crantz), *BMC Genet.* 16 (2015) 115.
- [56] D. Ellis, O. Chavez, J.J. Coombs, J.V. Soto, R. Gomez, D.S. Douches, A. Panta, R. Silvestre, N.L. Anglin, Genetic identity in genebanks: application of the SolCAP 12K SNP array in fingerprinting and diversity analysis in the global in trust potato collection, *Genome* 61 (7) (2018) 523–537.
- [57] A. Brito, J.E. Ramirez, C. Areche, B. Sepúlveda, M.J. Simirgiotis, HPLC-UV-MS profiles of phenolic compounds and antioxidant activity of fruits from three citrus species consumed in Northern Chile, *Molecules* 19 (2014) 17400–17421, doi:10.3390/molecules191117400.
- [58] T.S. Teixeira, R.C. Vale, R.R. Almeida, T.P.S. Ferreira, L.G.L. Guimarães, Antioxidant potential and its correlation with the contents of phenolic compounds and flavonoids of methanolic extracts from different medicinal plants, *Rev. Virtual Química* 9 (2017) 1546–1559.
- [59] ... G. Mandalari, R.N. Bennett, G. Bisignano, D. Trombetta, A. Saija, C.B. Faulds, A. Narbad, Antimicrobial activity of flavonoids extracted from bergamot (*Citrus bergamia* Risso) peel, a byproduct of the essential oil industry, *J. Appl. Microbiol.* 103 (6) (2007) 2056–2064.
- [60] A. Ghasemzadeh, V. Omidvar, H.Z.E. Jaafar, Polyphenolic content and their antioxidant activity in leaf extract of sweet potato (*Ipomoea batatas*), *J. Med. Plants Res.* 6 (2012) 2971–2976.
- [61] C.A.C. Araujo, L.L. Leon, Biological activities of *Curcuma longa* L., *Mem. Inst. Oswaldo Cruz* 96 (2001) 723–728.
- [62] Z. Lu, Q. Jia, R. Wang, X. Wu, Y. Wu, C. Huang, Y. Li, Hypoglycemic activities of A- and B-type procyanidin oligomer-rich extracts from different Cinnamon barks, *Phytomedicine* 18 (2011) 298–302.
- [63] H. Matsuda, Y. Pongpiriyadacha, T. Morikawa, M. Ochi, M. Yoshikawa, Gastro-protective effects of phenylpropanoids from the rhizomes of *Alpinia galanga* in rats: structural requirements and mode of action, *Eur. J. Pharmacol.* 471 (2003) 59–67.
- [64] D. Mohapatra, S. Mishra, N. Sutar, Banana and its by-product utilisation: an overview, *J. Sci. Ind. Res.* 69 (2010) 323–329.
- [65] S. Kumar Karan, S.K. Mishra, D. Pal, A. Mondal, Isolation of β -sitosterol and evaluation of antidiabetic activity of *Aristolochia indica* in alloxan-induced diabetic mice with a reference to *in-vitro* antioxidant activity, *J. Med. Plants Res.* 6 (2012) 1219–1223, doi:10.5897/JMPR11.973.
- [66] J.A. Schneider, Z. Arvanitakis, S.E. Leurgans, D.A. Bennett, The neuropathology of probable Alzheimer disease and mild cognitive impairment, *Ann. Neurol. Off. J. Am. Neurol. Assoc. Child Neurol. Soc.* 66 (2009) 200–208.
- [67] K. Hostettmann, A. Borloz, A. Urbain, A. Marston, Natural product inhibitors of acetylcholinesterase, *Curr. Org. Chem.* 10 (2006) 825–847.
- [68] R. Rhabasa-Lhoret, J.L. Chiasson, Alpha-glucosidase inhibitors, in: R.A. DeFronzo, E. Ferrannini, H. Keen, P. Zimmet (Eds.), *International Textbook of Diabetes Mellitus*, Vol. 1, John Wiley, UK, 2004.
- [69] W. Abeyskera, A. Chandrasekera, P.K. Liyanage, Amylase and glucosidase enzyme inhibitory activity of ginger (*Zingiber officinale* Roscoe) an *in vitro* study, *Trop. Agric. Res.* 19 (2007) 128–135.
- [70] E.G. Asuquo, C.E. Udobi, Antibacterial and toxicity studies of the ethanol extract of *Musa paradisiaca* leaf, *Cogent Biol.* 2 (2016) 1219248.
- [71] A. Umamaheswari, A. Puratchikody, S.L. Prabu, T. Jayapriya, Phytochemical screening and antimicrobial effects of *Musa acuminata* bract, *Intl. Res. J.Pharm.* 8 (2017) 41–44, doi:10.7897/2230-8407.088142.
- [72] J. Abirami, P. Brindha, C.D. Raj, Evaluation of toxicity profiles of *Musa paradisiaca* L (Pseudostem) Juice, *Int. J. Pharm. Pharm. Sci.* 6 (2014) 9–11.
- [73] E.A. Ugbogu, V.C. Ude, I. Elekwa, U.O. Arunsi, C. Uche-Ikonne, C. Nwakanma, Toxicological profile of the aqueous-fermented extract of *Musa paradisiaca* in rats., *Avicenna J. Phytomedicine* 8 (2018) 478–487.
- [74] N. Barua, M. Das, An overview on the pharmacological activity of *Musa sapientum* and *Musa paradisiaca*, *Intl. J. Pharma Prof. Res.* 4 (2013) 986–992.
- [75] P. Khawas, S.C. Deka, Comparative nutritional, functional, morphological, and diffractogram study on culinary banana (*Musa ABB*) Peel at various stages of development, *Int. J. Food Prop.* 19 (2016) 2832–2853, doi:10.1080/10942912.2016.1141296.
- [76] S. López, J. Bastida, F. Viladomat, C. Codina, Acetylcholinesterase inhibitory activity of some Amaryllidaceae alkaloids and Narcissus extracts, *Life Sci.* 71 (2002) 2521–2529.
- [77] P.K. Mukherjee, V. Kumar, M. Mal, P.J. Houghton, Acetylcholinesterase inhibitors from plants, *Phytomed* 14 (2007) 289–300.
- [78] C. Vilela, S.A. Santos, J.J. Villaverde, L. Oliveira, A. Nunes, N. Cordeiro, C.S.R. Freire, A.J. Silvestre, Lipophilic phytochemicals from banana fruits of several *Musa* species, *Food Chem.* 162 (2014) 247–252.
- [79] E. Mahran, I. Elgamal, M. Keusgen, G. Morlock, Effect-directed analysis by high performance thin-layer chromatography for bioactive metabolites tracking in *Primula veris* flower and *Primula boveana* leaf extracts, *J. Chromatogr. A* 1605 (2019) in print.

Isolation of flavonoids from *Musa acuminata* Colla (Simili radjah, ABB) and the in vitro inhibitory effects of its leaf and fruit fractions on free radicals, acetylcholinesterase, 15-lipoxygenase, and carbohydrate hydrolyzing enzymes

Ibukun Oluwabukola Oresanya^{1,2,3,4}  | Mubo A. Sonibare¹ | Badara Gueye² | Fatai Oladunni Balogun³ | Salmon Adebayo³ | Anofi Omotayo Tom Ashafa³ | Gertrud Morlock⁴

¹Faculty of Pharmacy, Department of Pharmacognosy, University of Ibadan, Ibadan, Nigeria

²International Institute of Tropical Agriculture, Genetic Resources Centre, Ibadan, Nigeria

³Department of Plant Sciences, University of the Free State, Phuthsditjhaba, South Africa

⁴Chair of Food Science, Institute of Nutritional Science and Interdisciplinary Research Center, Justus Liebig University Giessen, Giessen, Germany

Correspondence

Mubo A. Sonibare, Faculty of Pharmacy, Department of Pharmacognosy, University of Ibadan, Ibadan, Nigeria.
Email: sonibaredeola@yahoo.com

Funding information

African-German Network of Excellence in Science Mobility Grant for Junior Researchers supported by BMBF and AvH; Deutscher Akademischer Austauschdienst, Grant/Award Number: 57378443

Abstract

Musa species are used traditionally for the management of many diseases. The study evaluated and compared anticholinesterase, anti-inflammatory, antioxidant, and antidiabetic activities of *Musa acuminata* (Simili radjah, ABB) fruits and leaves fractions and characterized the bioactive compounds using HPTLC-HRMS and NMR. Leaf fractions gave the higher biological activities than the fruit. Ethyl acetate fraction of the leaf had the highest total phenolic content (911.9 ± 1.7 mg GAE/g) and highest 2,2-diphenyl-1-picrylhydrazyl (DPPH) scavenging activity (IC_{50} , 9.0 ± 0.4 μ g/ml). It also gave the most effective inhibition of acetylcholinesterase (IC_{50} , 404.4 ± 8.0 μ g/ml) and α -glucosidase (IC_{50} , 4.9 ± 1.6 μ g/ml), but a moderate α -amylase inhibition (IC_{50} , 444.3 ± 4.0 μ g/ml). The anti-inflammatory activity of *n*-butanol (IC_{50} , 34.1 ± 2.6 μ g/ml) and ethyl acetate fractions (IC_{50} , 43.1 ± 11.3 μ g/ml) of the leaf were higher than the positive control, quercetin (IC_{50} , 54.8 ± 17.1 μ g/ml). Kaempferol-3-*O*-rutinoside and quercetin-3-*O*-rutinoside (rutin) were identified as the bioactive compounds with antioxidant and antidiabetic activities from the ethyl acetate fraction of *M. acuminata* leaf.

Practical applications

All parts of *Musa acuminata* are known to be useful ethnomedicinally even as food. The leaves are mostly used to serve food and used for wrapping purposes. However, this study concluded that *M. acuminata* leaf is rich in bioactive flavonoids such as kaempferol-3-*O*-rutinoside and rutin, with relatively high antioxidative, antidiabetic, and anti-inflammatory activities. Therefore, aside the fact that the leaves can serve as potential drug leads for pharmaceutical industries, it can also be embraced in the food sector to produce supplements and/or nutraceuticals in the management of Alzheimer's, diabetes and other inflammatory diseases.

This is an open access article under the terms of the Creative Commons Attribution-NonCommercial License, which permits use, distribution and reproduction in any medium, provided the original work is properly cited and is not used for commercial purposes.

© 2020 The Authors. *Journal of Food Biochemistry* published by Wiley Periodicals, Inc.

KEYWORDS

anticholinesterase, antidiabetic, antioxidant, flavonoid, HPTLC-HRMS, *Musa acuminata*

1 | INTRODUCTION

One of the major strategies to manage type 2-diabetes, accorded as one of the top most chronic diseases globally, is the inhibition of α -glucosidase and α -amylase, which are the two key carbohydrate hydrolyzing enzymes (Diamond, 2003; Kaushik, Satya, Khandelwal, & Naik, 2010). Inhibition of these two enzymes reduces the rate of glucose absorption therefore decreases the glucose level in the blood (Rabasa-Lhoret & Chiasson, 2004). Also, free radicals accumulation, culminating into oxidative stress, and inflammation, was reported to be risk factors in the pathophysiology of *diabetes mellitus* (Giacco & Brownlee, 2010) and Alzheimer's disease (AD) (Houghton, Howes, Lee, & Steventon, 2007). The link between the cholinergic system and inflammation mechanism has been reported, as acetylcholine, main neurotransmitter, was reported to reduce the release of cytokines in the parasympathetic anti-inflammatory pathway, by which the brain modulates systemic inflammatory responses to endotoxin (Borovikova et al., 2000). The brain of patients suffering from AD is believed to be under oxidative stress. Acetylcholinesterase inhibitors play an anti-inflammatory role through their action against the free radicals and amyloid toxicity, thereby decreasing the release of cytokines from activated microglia in the brain and blood (Tabet, 2006). Thus, the therapeutic use of natural products with antioxidative and anti-inflammatory potentials would be a good candidate for the treatment of diabetes and AD. Interestingly, the use of natural products, especially from plants in the management of diseases, has gained attention in recent times, partly because they are presumed to be less toxic, readily available, affordable, and with milder adverse side-effects unlike synthetic drugs such as acarbose (Ekor, 2014; Essa et al., 2019).

Musa acuminata (banana) is known as a nutritious food with a wide range of medicinal properties. Virtually all the various parts of the plant have multiple traditional uses. The peel, pulp, stem, root, sap, leaf, pseudo-stem bract, and flowers have been used traditionally to treat one ailment or the other (Joshi, 2000; Mathew & Negi, 2017; Sonibare & Ayoola, 2015). Many reports have investigated the pharmacological activities of different parts of different *Musa* spp. especially the fruit where most of the compounds were isolated. The peel is reported to have anti-ulcer property (Imam & Akter, 2011), while the peel, leaf, pulp, and sap have antimicrobial potential (Alisi, Nwyanwu, Akujobi, & Ibegbulem, 2008; Brooks, 2008; Singh, Bhat, & Singh, 2003;). Extensive research has been done on the pulp and peel of different *Musa* spp. Vu, Scarlett, and Vuong (2018) presented a review on the phenolic composition of the peel of different banana species. More than 40 phenolic compounds with potent antioxidant and antimicrobial activities have been revealed in the peel of different banana species. Bioactive compounds in the pulp and peel of different *Musa* species were also reported by Singh, Singh, Kaur, and Singh (2016). Four groups of phenolic compounds were identified in *Musa* spp., namely hydroxycinnamic acids, flavonols, flavan-3-ols (Rebello et al., 2014), and catecholamines (Kanazawa &

Sakakibara, 2000). The flavonoids detected in the pulp of banana include quercetin, myricetin, kaempferol, and cyaniding (Pothavorn et al., 2010). Unfortunately, there is paucity of information on the bioactive compounds isolated from the leaves of *Musa* spp. Although antidiabetic effect of some *Musa* spp have been studied (Adewoye, Ige, & Latona, 2011; Bhaskar, Shobha, Sambaiah, & Salimath, 2011; Kalita et al., 2016) particularly on the flower and inflorescence part.

This study presents, for the first time, a comparative evaluation of the antioxidant, anti-inflammatory, anticholinesterase, and antidiabetic potentials of the fruit and leaf fractions of *M. acuminata* (Simili radjah, ABB) as well as that of the isolated, flavonoid-rich compound. The study was done on *Musa acuminata* (Simili radjah, ABB), which has been reported to have relatively high total flavonoid and total phenolic content, and a DPPH' antioxidant activity, compared to other *Musa* species from different genome groups. High-performance thin-layer chromatography (HPTLC), directly combined with effect-directed analysis (EDA), was used in this study to separate and identify the active compounds following the column chromatography. Two different enzymatic assays and a radical scavenging assay were also performed in situ, on HPTLC adsorbent. HPTLC-high-resolution mass spectrometry (HRMS) was used to characterize and confirm the identity of the bioactive, isolated compounds.

2 | MATERIALS AND METHODS

2.1 | Reagents and chemicals

The reagents used in this study include gallic acid, anhydrous sodium carbonate, Folin-Ciocalteu reagent, DPPH', 2,2-azinobis-3-ethylbenzothiazoline-6-sulfonic acid (ABTS), potassium pyrosulphate, iron (II) sulphate, deoxyribose, hydrogen peroxide, phosphate buffer, trichloroacetic acid, thiobarbituric acid, acarbose, α -amylase, α -glucosidase, starch, dinitro salicylic acid, *p*-nitrophenyl glucopyranoside, quercetin, 15-lipoxygenase from *Glycine max*, 5,5'-dithio-bis-2-nitrobenzoic acid, eserine, acetylcholine iodide, and acetylcholinesterase (AChE, from electric eel, C3389) were purchased from Sigma-Aldrich (Steinheim, Germany and South Africa). Natural products reagent (diphenylboryloxyethylamine or diphenylboric acid β -ethylamino ester) were purchased from Carl Roth, Karlsruhe, Germany, while linoleic acid, sodium acetate, fast blue salt, and 2-naphthyl- α -D-glucopyranoside were obtained from Merck (Darmstadt, Germany). All chemicals used in the study were of analytical grade.

2.2 | Plant material, maceration, and liquid-liquid extraction

Leaves and fruits of *M. acuminata* (Simili radjah, ABB banana) were sampled from *Musa* spp. field bank of the IITA Genetic Resources Center, in

Ibadan (Nigeria). The International Transit Centre, ITC code is ITC0123 and accession number is TMB 136. Samples were freeze-dried and pulverized. Powdered leaves (1.06 kg) and fruit (1.96 kg) were macerated in methanol for 72 hr. Each of the samples was filtered and soaked again in 1 L of methanol for another 24 hr before filtering. The filtrates were pooled together and concentrated *in vacuo*. The dried methanolic extracts of the leaf (85 g) and fruit (33 g) were re-dissolved in a methanol - water (3:1, 200 ml) mixture and partitioned successively into *n*-hexane, dichloromethane, ethyl acetate, and *n*-butanol using 100 ml aliquots of 2.5 L *n*-hexane and 1 L each of the other solvents. All fractions obtained were concentrated and preserved at -4°C until use.

2.3 | Effect-directed *in vitro* assays

For analysis of the leaf and fruit crude extracts and fractions, different antioxidant, anticholinesterase, antidiabetic, and anti-inflammatory assays were carried out according to the following standard methods.

2.3.1 | Total phenolic and total flavonoid content

The total phenolic content was estimated as described by Khatoun et al. (2013). In summary, all the crude extracts and fractions (0.5 ml, 200 $\mu\text{g}/\text{ml}$) were mixed with 2.5 ml Folin-Ciocalteu's reagent (V/V) (1:10) and 2.0 ml of 7.5% sodium carbonate. The reaction mixture was incubated for 30 min at room temperature and the absorbance was measured at 765 nm using 752s UV-Vis spectrophotometer. The total phenolic content expressed as mg gallic acid equivalent (GAE)/g of extract was calculated from a gallic acid calibration curve ($y = 0.0078x + 0.0728$, $r^2 = 0.9946$), which was prepared using a methanolic gallic acid solution in the concentration range of 12.5 to 200 $\mu\text{g}/\text{ml}$. Colorimetric aluminum chloride method was used for total flavonoid contents (TFC) determination (Ayoola, Gueye, Sonibare, & Abberton, 2017). The TFC was expressed as mg quercetin equivalent (QE)/g of extract, calculated from the standard curves prepared with 6.25–200 μg quercetin/ml ($y = 0.0138x + 0.0568$, $r^2 = 0.9988$).

2.3.2 | Antioxidant assays

The antioxidant activity of all samples was determined by three different methods. The DPPH $^{\cdot}$ assay was done according to the method described by Susanti et al. (2007) and Ayoola et al. (2017). The ABTS assay was performed and hydroxyl radical scavenging activities were determined using the methods described by Re et al. (1999) and Oboh, Puntel, and Rocha (2007), respectively. Different concentrations of the extracts and standards (both 12.5 to 200.0 $\mu\text{g}/\text{ml}$) as well as isolated compounds (3.1 to 100.0 $\mu\text{g}/\text{ml}$) were used for the assays.

2.3.3 | Enzyme inhibitory assays

The AChE inhibition was determined spectrophotometrically using Ellman's colorimetric method (Ellman, Courtney, Andres, & Featherstone,

1961) modified by Ajayi, Aderogba, Obuotor, and Majinda (2019). All the samples, the positive control standard eserine, 5,5'-dithiobis-(2-nitrobenzoic acid), and the substrate acetylcholine iodide (ATCI) were dissolved in phosphate buffer (pH 8.0). In a 96-well plate, the reaction mixture consisted of 40 μl phosphate buffer (pH 8.0), 20 μl of varying concentrations of the test samples (0.1 to 1 mg/ml of sample or 0.06 to 0.5 mg/ml of eserine), and 20 μl of the enzyme (0.26 U/ml). The reaction mixture was incubated for 30 min at 37°C , and then 100 μl of 3 mM 5,5'-dithiobis-(2-nitrobenzoic acid) was added. The reaction was initiated by the addition of 20 μl of 15 mM ATCI. The rate of hydrolysis of ATCI was then determined spectrophotometrically by measuring the change in the absorbance per minute ($\Delta\text{A}/\text{min}$) due to the formation of the yellow 5-thio-2-nitrobenzoate anion at 405 nm over a period of 4 min at 30s intervals. Buffer was used in place of the test sample and used as a negative control. The experiments were carried out in triplicate and the percentage inhibition was calculated as follows: $(1 - a/b) \times 100$, where $a = \Delta\text{A}/\text{min}$ of test sample; $b = \Delta\text{A}/\text{min}$ of control; ΔA = change in absorbance. The α -amylase inhibitory assay was performed using the method reported by McCue and Shetty (2004), while the α -glucosidase inhibitory effect was determined according to the method described by Kim, Jeong, Wang, Lee, and Rhee (2005). The enzyme kinetics and inhibition modes of both α -amylase and α -glucosidase were determined according to the method described by Ali, Houghton, and Soumyanath (2006). The anti-inflammatory activity was determined by using the inhibition of 15-lipoxygenase (15-LOX) enzyme method of Adebayo, Dzoyem, Shai, and Eloff (2015). Samples or positive control were dissolved in methanol to a concentration of 12.5 to 200 $\mu\text{g}/\text{ml}$.

2.4 | Assay-guided isolation of bioactive compounds from the ethyl acetate fraction of the leaf

Leaf ethyl acetate fraction (6 g) was subjected to column chromatography on silica gel (particle/mesh size 230–400 μm , length 85 cm and diameter 3.5 cm). It was eluted with solvents of increasing polarity using *n*-hexane, ethyl acetate, and methanol. The fractions were collected (50 ml portions) and spotted on TLC plates silica gel 60 F $_{254}$ (20 \times 20 cm, Merck, Germany). The fractions were pooled together using the TLC profile and retention factor (R_f) as guide. A total of 220 fractions were collected and then pooled to 11 subfractions (A–K). The DPPH $^{\cdot}$ radical scavenging activity and total phenolic content of the subfractions were determined. The subfraction H was loaded on a sephadex column (LH-20, length 167 cm and diameter 2.5 cm), eluted with methanol and 10 ml portions were collected. A total of 83 fractions were collected and pooled to 11 subfractions (HA–HK). The subfraction HD with a very good yield and yellow precipitate was chosen for the preparative TLC and compound isolation.

2.5 | Nuclear magnetic resonance (NMR) spectroscopy

The NMR spectra were recorded on a Bruker Ascend-500 spectrometer (Bruker Biospin Co., Karlsruhe, Germany) with ^1H NMR at

400 MHz and ^{13}C NMR at 100 MHz. The isolated compound was prepared using deuterated methanol with tetramethylsilane (TMS) as internal standard in 5 mm NMR tubes. Chemical shifts were expressed in parts per million (δ) according to the TMS signal. 2D NMR spectroscopy (distortionless enhancement by polarization transfer, DEPT; homonuclear correlation spectroscopy, COSY; heteronuclear single-quantum coherence, HSQC; and heteronuclear multiple bond correlation, HMBC) was applied for assignment.

2.6 | HPTLC method

2.6.1 | Chromatographic system and detection

The flavonoid-rich compound (2.5 mg) was dissolved in methanol (1 ml) and applied on the HPTLC plate by the Automatic TLC Sampler (ATS 4 CAMAG, Muttenz, Switzerland). The sample was sprayed as 7-mm bands ($10\ \mu\text{l band}^{-1}$) onto the HPTLC plate at 8 mm distance from the bottom edge. The HPTLC separation was done in the Twin Trough Chamber (20 cm \times 10 cm, CAMAG) up to a migration distance of 60 mm using ethyl acetate - toluene - formic acid - water 6.8:1:1.4:1. The chromatogram was dried in a stream of cold air for 3 min and documented at UV 254 nm and 366 nm. For flavonoid detection, the chromatogram was immersed in the natural products reagent (0.5% methanolic solution of 2-aminoethyl diphenylborinate), followed by immersion in a 5% methanolic polyethylene

glycol 400 solution, and fluorescent compounds were documented at UV 366 nm. For detection of the radical scavenging activity, the chromatogram was immersed in a 0.2% methanolic DPPH $^{\cdot}$ solution, and the radical scavenging compounds were documented at white light illumination. Immersion was performed at an immersion speed of 3.0 cm/s for 2 s using the TLC Immersion Device and documentation by the TLC Visualizer Documentation System (both CAMAG).

2.6.2 | HPTLC-HRMS

The two flavonoid bands were online eluted with methanol (flow rate 0.1 ml/min) using the TLC-MS Interface 2 (CAMAG) or Plate Express (Advion, Ithaca, NY) coupled to the QExactive Plus mass spectrometer (Thermo Fisher Scientific, Dreieich, Germany). Full scan mass spectra (m/z 50–1,000) were recorded in the positive and negative ionization modes with the following settings: ESI voltage \pm 3.3 kV, capillary temperature 320°C, and collision energy 35 eV. Nitrogen was produced by a SF2 compressor (Atlas Copco Kompressoren and Drucklufttechnik, Essen, Germany). Data evaluation and background subtraction were performed by Xcalibur 3.0.63 software (Thermo Fisher Scientific). After the HPTLC-HRMS analysis, the standards kaempferol-3-O-rutinoside and rutin were prepared in the methanolic solutions (0.1 mg/ml). The standard solutions were developed alongside the isolated compounds for identity confirmation by chromatography.

TABLE 1 Means of total phenolic content (TPC), DPPH $^{\cdot}$, hydroxyl radical (OH $^{\cdot}$), 2,2-azinobis-3-ethylbenzothiazoline-6-sulfonic acid (ABTS $^{\cdot}$) radical scavenging, anti-inflammatory (15-LOX inhibition), and acetylcholinesterase (AChE) inhibitory activities of leaf and fruit crude extract and fractions

S/N	Fractions	TPC (mg GAE/g)	DPPH IC ₅₀ ($\mu\text{g/ml}$)	Hydroxyl IC ₅₀ ($\mu\text{g/ml}$)	ABTS IC ₅₀ ($\mu\text{g/ml}$)	15-LOX inhibition IC ₅₀ ($\mu\text{g/ml}$)	AChE inhibition IC ₅₀ ($\mu\text{g/ml}$)
Leaf							
1	CME	343.1 \pm 2.4 ^d	109.7 \pm 3.0 ^e	10.2 \pm 1.0 ^a	240.0 \pm 0.4 ^a	272.4 \pm 49.6 ^e	530.9 \pm 24.4 ^c
2	NHF	85.4 \pm 3.5 ^f	211.8 \pm 1.6 ^f	22.6 \pm 1.0 ^b	466.7 \pm 15.0 ^b	768.1 \pm 94.9 ^g	1,709.0 \pm 5.2 ^h
3	DCM	187.7 \pm 6.1 ^e	98.1 \pm 1.1 ^d	55.2 \pm 1.8 ^c	470.8 \pm 13.34 ^b	1,323.1 \pm 166.3 ^h	627.4 \pm 11.2 ^e
4	EAF	911.9 \pm 1.7 ^a	9.0 \pm 0.4 ^a	12.1 \pm 0.9 ^a	187.3 \pm 0.1 ^a	43.1 \pm 11.3 ^a	404.4 \pm 8.0 ^a
5	NBF	404.8 \pm 5.7 ^b	60.7 \pm 3.2 ^c	11.3 \pm 1.0 ^a	206.1 \pm 1.7 ^a	34.1 \pm 2.6 ^a	603.1 \pm 5.2 ^d
6	AMF	366.2 \pm 7.1 ^c	35.1 \pm 7.6 ^b	56.9 \pm 13.2 ^c	1,332.0 \pm 50.6 ^e	45.0 \pm 14.3 ^{ab}	698.8 \pm 29.1 ^f
Fruit							
7	CME	70.2 \pm 6.7 ^g	323.4 \pm 6.6 ⁱ	187.1 \pm 1.9 ^e	452.7 \pm 18.2 ^b	72.3 \pm 3.4 ^b	565.8 \pm 23.0 ^c
8	NHF	12.6 \pm 0.4 ^j	589.8 \pm 7.8 ^k	183.6 \pm 2.1 ^e	560.3 \pm 0.9 ^c	456.7 \pm 37.7 ^f	1,848.7 \pm 5.3 ⁱ
9	DCM	36.0 \pm 3.3 ⁱ	226.5 \pm 3.4 ^g	253.6 \pm 3.4 ^f	480.5 \pm 7.1 ^b	149.5 \pm 12.2 ^c	1,359.9 \pm 1.6 ^g
10	EAF	55.3 \pm 1.3 ^h	260.9 \pm 6.1 ^h	188.1 \pm 2.1 ^e	541.2 \pm 5.9 ^c	241.8 \pm 43.6 ^d	478.2 \pm 20.6 ^b
11	NBF	44.6 \pm 2.2 ⁱ	319.7 \pm 2.5 ⁱ	249.2 \pm 12.2 ^f	465.1 \pm 7.1 ^b	440.7 \pm 56.4 ^f	419.0 \pm 16.4 ^a
12	AMF	43.1 \pm 7.2 ⁱ	456.6 \pm 7.3 ^j	115.7 \pm 5.5 ^d	628.3 \pm 31.9 ^d	133.4 \pm 30.3 ^c	698.8 \pm 29.1 ^f

Note: Means ($n = 3$) bearing different superscript letters along the same column are significantly different ($p < .05$) from each other. IC₅₀ of gallic acid is 4.1 \pm 1.2 $\mu\text{g/ml}$ (DPPH $^{\cdot}$ positive control). IC₅₀ of gallic acid and ascorbic acid are 58.71 \pm 1.94 $\mu\text{g/ml}$ and 124.90 \pm 2.53 $\mu\text{g/ml}$, respectively (OH $^{\cdot}$ positive control). IC₅₀ of gallic acid and ascorbic acid are 199.50 \pm 0.79 $\mu\text{g/ml}$, and 349.60 \pm 1.04 $\mu\text{g/ml}$ (ABTS $^{\cdot}$ positive control). IC₅₀ values of quercetin and indomethacin are 54.8 \pm 17.1 $\mu\text{g/ml}$ and 229.2 \pm 33.2 $\mu\text{g/ml}$, respectively (15-LOX positive controls). IC₅₀ value of eserine is 26.5 \pm 1.6 $\mu\text{g/ml}$ (AChE inhibiting positive control).

2.6.3 | HPTLC-EDA-Vis and densitometric quantification

Solutions of gallic acid (0.1 mg/ml), acarbose (1 mg/ml), and physostigmine (0.1 mg/ml) were prepared for the DPPH[•] radical scavenging, α -glucosidase, and AChE assays, respectively. For the calibration curve, 1 to 15 μ l/band were applied as track pattern using the Free mode option of the ATS4 (CAMAG). The HPTLC-DPPH[•], HPTLC-AChE, and HPTLC- α -glucosidase assays were performed according to the methods of Jamshidi-Aidji, Macho, Mueller, and Morlock (2019), Azadnia and Morlock (2018) and Jamshidi-Aidji and Morlock (2018). The HPTLC-AChE assay was recently adjusted to the piezoelectric spraying using the Derivatizer (CAMAG) by Azadnia and Morlock (2019). Concisely, 2 ml of substrate (60 mg 2-naphtyl- α -D-glucopyranoside in 50 ml ethanol) were sprayed on the neutralized

chromatogram and air-dried for 2 min. The plate was pretreated with 1 ml sodium acetate buffer (pH 7.2–7.5). The enzyme solution (2 ml, 500 units of α -glucosidase in 50 ml buffer) was sprayed on the plate, which was then placed horizontally in a prepared humidity box and incubated at 37°C for 13 min. After the incubation, 0.5 ml of fast blue B salt solution was sprayed on the plate. After drying the plate using the ADC2 humidity control (filled with molecular sieve), images were taken under white light illumination (transmission and reflection modes). Enzyme inhibitors were detected as white inhibition zones on a purple background. The autograms were densitometrically scanned in an inverse scan mode for absorbance measurement at 546 nm using the mercury lamp (software trick to obtain positive peaks for the white inhibition zones: fluorescence mode and no optical filter). By evaluating the peak area, sample results were obtained in μ g per band, calculated from the gallic acid, acarbose,

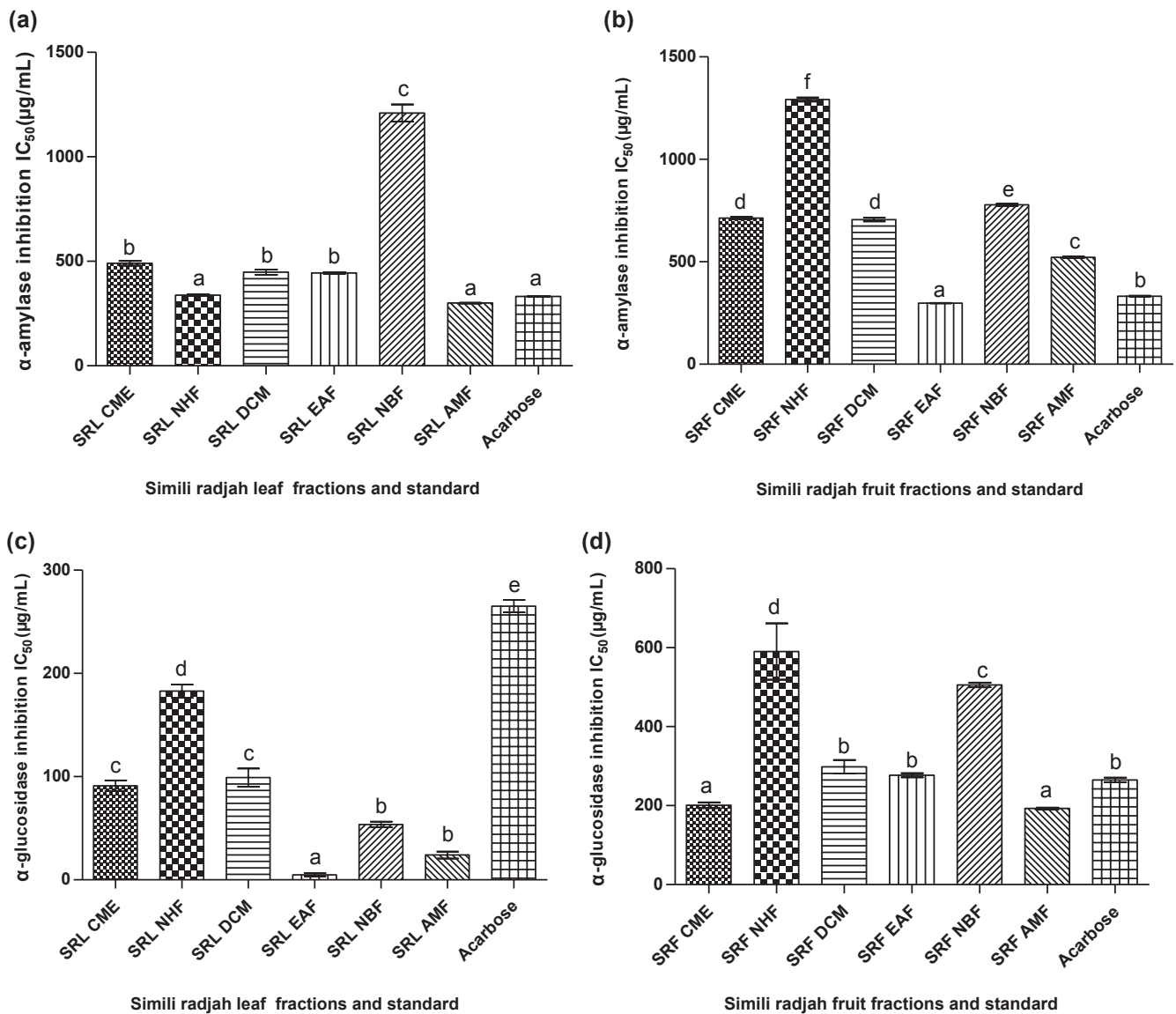


FIGURE 1 α -Amylase inhibitory activity of leaf (a) and fruit (b) fractions; α -glucosidase inhibitory activity of leaf (c) and fruit (d) fractions obtained by *n*-hexane (NHF), dichloromethane (DCM), ethyl acetate (EAF), *n*-butanol (NBF) and aqueous methanol (AMF) as well as crude extract (CME) and standard acarbose. Bars with different superscript letters are significantly different from each other ($p < .05$)

or physostigmine calibration curve taking into account the applied volume and sample solution concentration (mg/ml).

2.7 | Statistical analysis

All assays were carried out in triplicates, and the results obtained by linear regression analysis were reported as mean of IC_{50} (concentration of the sample that gave 50% activity/inhibition) and its standard error. One-way analysis of variance and turkey's test for mean comparison was done using the GraphPad Prism software (version 5.0 for windows, GraphPad Software, San Diego, CA).

3 | RESULTS

3.1 | Total phenolic content and antioxidant activity of the leaf and fruit fractions measured by DPPH[•], hydroxyl, and ABTS[•] radical scavenging assays

The results of the total phenolic content, DPPH[•] radical scavenging (antioxidant), anti-inflammatory, and anticholinesterase activities showed that leaf fractions presented better antioxidant, antidiabetic, and anti-inflammatory potentials than the fruit (Table 1). Among the leaf fractions, the ethyl acetate fraction had the highest total phenolic

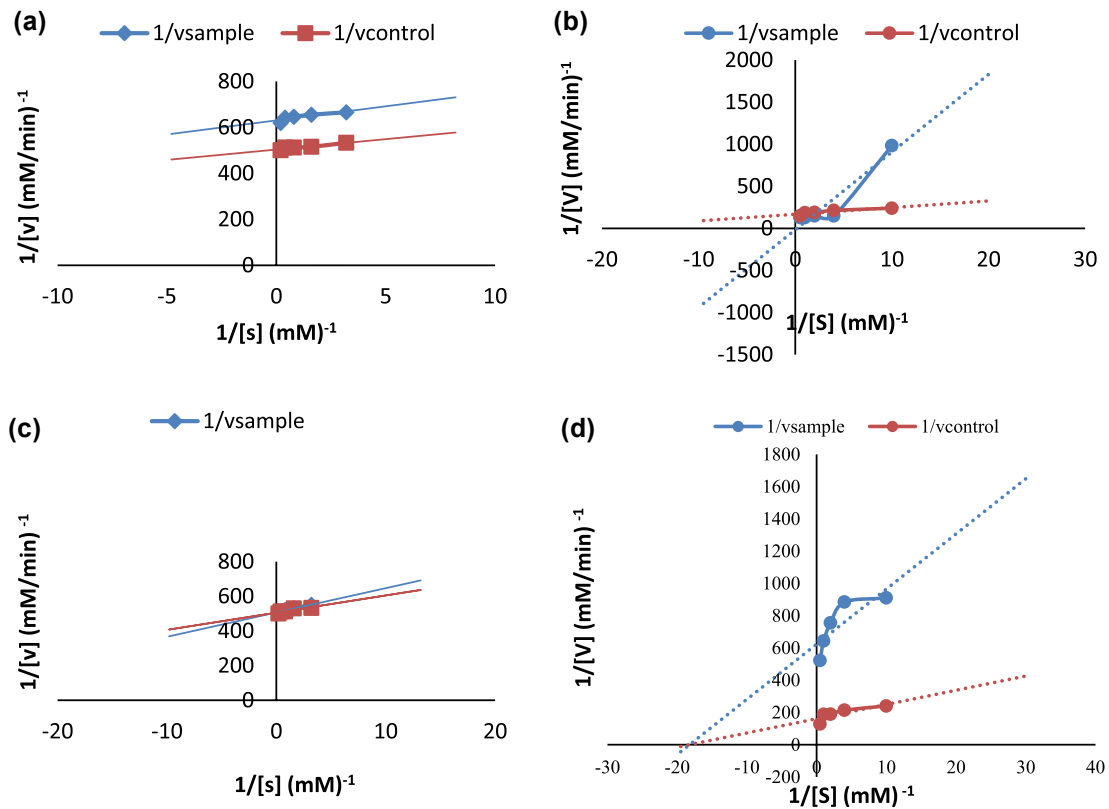


FIGURE 2 Lineweaver-Burk plot showing a noncompetitive mode of inhibition of α -amylase (a) and uncompetitive kinetics of inhibition of α -glucosidase (b) by methanol crude extract of the fruit *Musa acuminata*; Lineweaver-Burk plot showing competitive mode of inhibition of α -amylase (c) and uncompetitive kinetics of inhibition of α -glucosidase (d) by ethyl acetate fraction of the leaf of *Musa acuminata*

TABLE 2 Compounds in the H sub-fraction: means of total phenolic content (TPC), total flavonoid content (TFC), DPPH radical scavenging, α -glucosidase, and α -amylase inhibitory activities

Fraction H compounds	Yield (mg)	TPC (mg GAE/g)	TFC (mg QE/g)	DPPH [•] IC_{50} (μ g/ml)	α -Glucosidase inhibition IC_{50} (μ g/ml)	α -Amylase inhibition IC_{50} (μ g/ml)
HB ₂	3.7	24.6 \pm 3.0 ^c	2.9 \pm 0.6 ^b	355.6 \pm 32.3 ^b	174.8 \pm 13.1 ^c	135.5 \pm 2.2 ^d
HC ₁	36.4	34.9 \pm 0.9 ^a	3.2 \pm 0.2 ^b	389.5 \pm 26.1 ^b	129.3 \pm 11.3 ^b	84.3 \pm 4.1 ^b
HC ₂	30.9	27.7 \pm 1.5 ^b	2.8 \pm 0.1 ^b	277.1 \pm 9.7 ^a	127.6 \pm 14.7 ^b	16.1 \pm 1.9 ^a
HC ₅	33.0	27.7 \pm 0.6 ^b	0.7 \pm 0.3 ^c	259.6 \pm 6.8 ^a	138.5 \pm 9.5 ^b	126.5 \pm 0.2 ^d
HD ₁	484.0	31.7 \pm 0.9 ^a	6.9 \pm 0.0 ^a	236.5 \pm 7.2 ^a	85.3 \pm 2.9 ^a	102.5 \pm 1.0 ^c
HD ₂	55.3	22.3 \pm 0.5 ^c	2.9 \pm 0.7 ^b	466.0 \pm 21.3 ^c	224.5 \pm 21.1 ^d	97.8 \pm 1.7 ^{bc}

Note: Means ($n = 3$) bearing different superscript letters are significantly different ($p < .05$) from each other.

content (912 ± 2 mg GAE/g) and the strongest DPPH[•] radical scavenging activity as revealed by its low IC₅₀ value (9.0 ± 0.4 µg/ml), which is close to that of gallic acid (4.0 ± 1.2 µg/ml). However, for the fruit fractions, the DCM fraction had the highest DPPH[•] radical scavenging activity. Both leaf and fruit fractions showed hydroxyl and ABTS radical inhibitory ability, but the leaf crude extracts and fractions gave a higher radical scavenging activity than the fruit. Among the leaf fractions, the CME, NBF, and EAF depicted similar and better hydroxyl and ABTS radical scavenging activities when compared with other fractions and gallic acid (equivalent for ABTS at $p < .05$).

3.2 | 15-LOX (anti-inflammation) and acetylcholinesterase inhibitory activities of the leaf and fruit fractions

The polar leaf and fruit fractions exhibited a better 15-LOX inhibitory activity than the nonpolar fractions (Table 1). Overall, the NBF (IC₅₀ = 34.1 ± 2.6 µg/ml) and EAF (IC₅₀ = 43.1 ± 11.3 µg/ml) of the leaf had a better anti-inflammatory activity, than quercetin, the positive control (IC₅₀ = 54.8 ± 17.1 µg/ml) (Table 1).

Both leaf and fruit fractions showed AChE inhibitory activity. The EAF of the leaf gave the best activity (IC₅₀ = 404.4 ± 8.0 µg/ml), which was not significantly different from that of the NBF of the fruit (IC₅₀ = 419.0 ± 16.4 µg/ml). However, the positive control eserine inhibited the AChE (IC₅₀ = 26.5 ± 1.6 µg/ml) more than all the crude extracts and fractions.

3.3 | α-amylase and α-glucosidase inhibitory activities and mode of inhibition

For the antidiabetic activity, the AMF, NHF, and EAF of the leaf as well as EAF of the fruit had more efficient inhibition of α-amylase activity (Figure 1a,b), compared to other fractions ($p < .05$). These activities (if not better) were at par with the activity of the standard acarbose. However, for α-glucosidase inhibition, all the leaf fractions inhibited the enzyme better than the acarbose standard, while only AMF and CME fractions from the fruit samples had better α-glucosidase inhibition than the standard (Figure 1c,d). Above all, the EAF of the leaf showed strongest α-glucosidase inhibition with IC₅₀ of 4.9 ± 1.6 µg/ml which is largely better than that of acarbose (265.2 ± 6.0 µg/ml). Different modes of inhibition of the two carbohydrate hydrolyzing enzymes by the EAF of the leaf and CME of the fruit *M. acuminata* were observed (Figure 2). These two fractions were selected for the mode of inhibition study because they gave a strong α-glucosidase inhibition of and a mild α-amylase inhibition. The Michaelis–Menten equation, which explains the type of inhibition of a particular enzyme revealed that fruit fraction exhibited a noncompetitive and uncompetitive mode of α-amylase and α-glucosidase inhibition, respectively (Figure 2a,b), while the leaf fractions exhibited a competitive mode of α-amylase, but an uncompetitive mode of α-glucosidase inhibition (Figure 2c,d). The mode of inhibition as depicted by the Lineweaver–Burk plot revealed

a constant K_m (0.054 mM) for both the sample and control, while the V_{max} decreases from 0.0062 (control) to 0.0016 mM/min (sample), signifying a noncompetitive α-amylase inhibition for the fruit fractions. However, for α-glucosidase the V_{max} and K_m values changes or reduces for both the sample and the control signifying an uncompetitive mode of inhibition (Figure 2a). Moreover, for the leaf fractions, there was a constant V_{max} value (0.0019 mM/min) for both the extract and control with a decrease in K_m values from 0.028 (extract) to 0.020 mM (control, Figure 2c), suggesting a competitive α-amylase mode of inhibition. However, the α-glucosidase mode of inhibition of the leaf fractions is uncompetitive (Figure 2d), revealing a decrease in V_{max} values from 0.006 (control) to 0.002 mM/min (sample) and K_m values from 0.055 (control) to 0.0053 mM (sample).

3.4 | Identification and biological activities of HD₁ compounds using HPTLC-HRMS and NMR spectroscopy

Bioactivity guided fractionation of the ethyl acetate subfraction afforded H-subfractions. The results of the total phenolic and flavonoid contents as well as DPPH[•] radical scavenging, α-amylase, and α-glucosidase inhibitory activities of the subfraction H compounds are summarized (Table 2). The isolate, HD₁ had the highest total flavonoid content, DPPH[•] antioxidant, and antidiabetic activities. It was confirmed to contain flavonoids by HPTLC derivatization using the natural products reagent (Figure 3). Two compounds appeared as yellow and orange bands, confirming that they are flavonoids. These were characterized by HRMS after online elution via an elution head-based interface using electron spray ionization (ESI). The mass spectra of band 1 showed a base peak at m/z 593.1515 (Figure 4) and was assigned as $[M-H]^-$ with the molecular formula $C_{27}H_{29}O_{15}^-$. The actual molecular formula is $C_{27}H_{30}O_{15}$, which is kaempferol-3-O-rutinoside. The mass spectra of compound 2 showed a base peak at

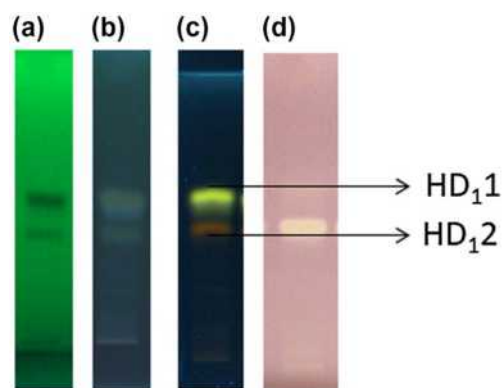


FIGURE 3 HD₁ on HPTLC plate silica gel 60 F₂₅₄ developed in ethyl acetate–toluene–formic acid–H₂O 6.8:1:1.4:1 and documented at (a) UV 254 nm and (b) UV 366 nm as well as after derivatization with (c) Neu's reagent at UV 366 nm, and (d) DPPH[•] reagent at white light illumination (transmittance mode) [Correction added on 11 January 2020, after first online publication: in Figure 3, the texts 'New Delhi India' has been deleted and the image was changed to color.]

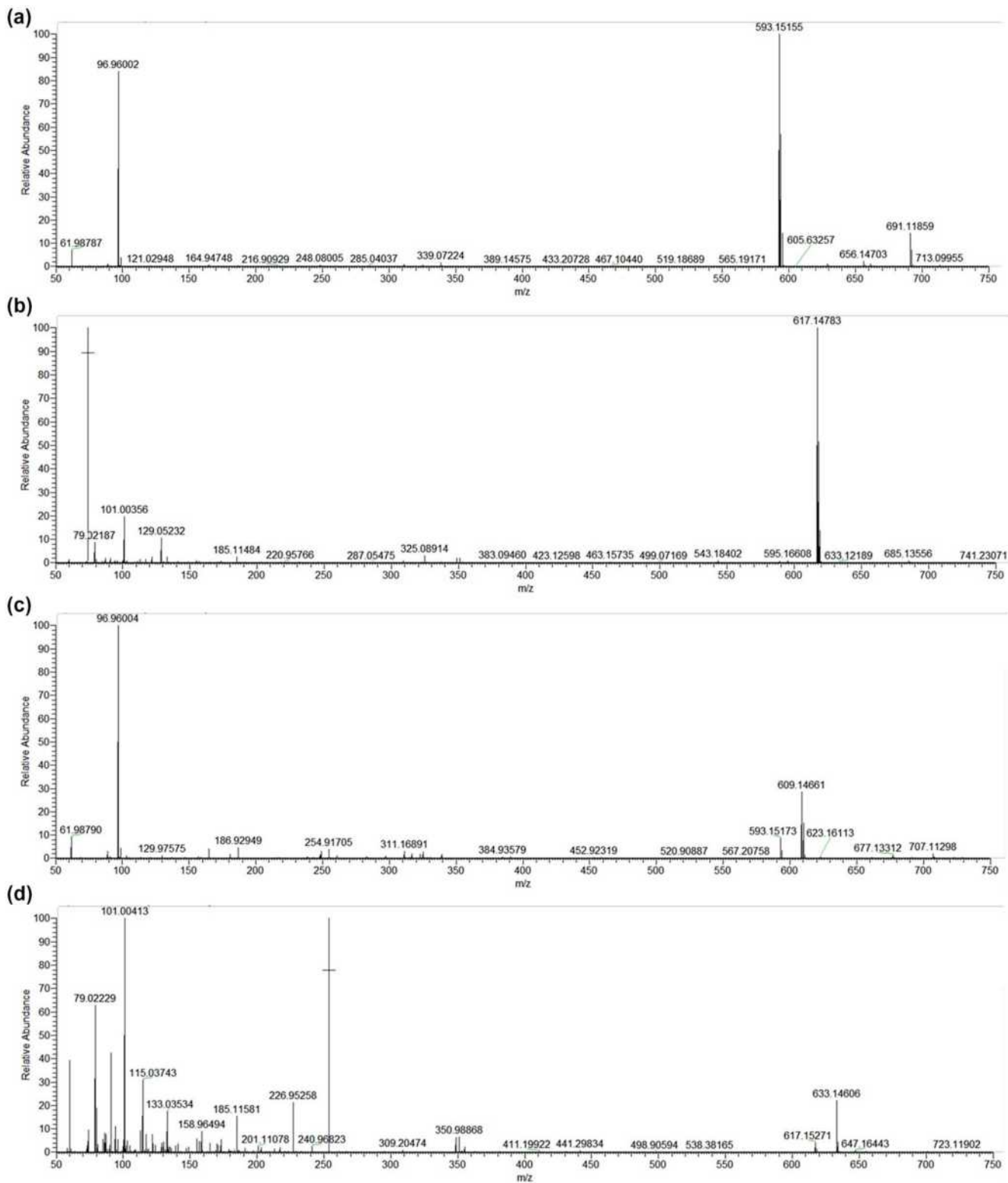


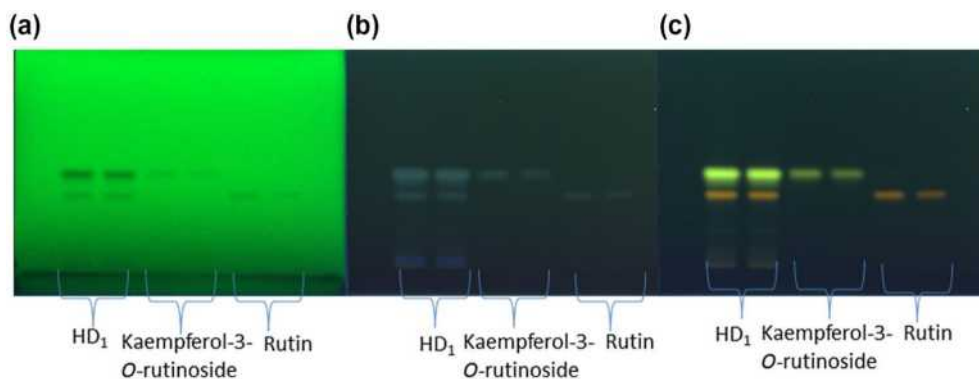
FIGURE 4 HPTLC-ESI-HRMS spectra of HD₁ compound 1 recorded in the (a) ESI⁻ mode (b) ESI⁺ mode; compound 2 recorded in the (c) ESI⁻ mode (d) ESI⁺ mode

m/z 609.1464 and was assigned as $[M-H]^-$ with the molecular formula $C_{27}H_{29}O_{16}^-$. The actual molecular formula is $C_{27}H_{30}O_{16}$, which is rutin. The mass spectra records show the base peak, calculated mass, and mass error of the two HD₁ compounds (Figure 4, Table 3).

The identification of these compounds was confirmed by comparing their hR_F with those of the purchased standards. Kaempferol-3-O-rutinoside is a yellow band, while rutin is an orange band when derivatized by natural products reagent. The two compounds

TABLE 3 HPTLC-HRMS data of compounds 1 and 2 in the HD₁ fraction

Sample	Compound	Observed mass	Assignment	Ion formula	Mass error	Intensity	Molecular formula	Identity
HD ₁	1	593.1515	[M-H] ⁻	C ₂₇ H ₂₉ O ₁₅	2.251	8E7	C ₂₇ H ₃₀ O ₁₅	Kaempferol-3-O-rutinoside
		691.1186	[M-HSO ₄] ⁻			1E7		
		617.1478	[M+Na] ⁺	C ₂₇ H ₃₀ O ₁₅ Na	2.299	2E8		
	2	609.1466	[M-H] ⁻	C ₂₇ H ₂₉ O ₁₆	0.5	5E6	C ₂₇ H ₃₀ O ₁₆	Rutin (quercetin-3-O-rutinoside)
		633.1461	[M+Na] ⁺			9E6		

**FIGURE 5** Confirmation of the two compounds in the subfraction HD₁ to be kaempferol-3-O-rutinoside and rutin, having the same hR_F values of 32 and 25, respectively, as the standard compounds on the HPTLC plate documented at (a) UV 254 nm, (b) UV 366 nm, and (c) after derivatization with Neu's reagent at UV 366 nm

kaempferol-3-O-rutinoside and rutin have close hR_F values of 32 and 25, respectively, which are the same as those of the standards (Figure 5). The proton (¹H), ¹³C NMR, and 2D NMR spectra of the two isolates were summarized for their identity proof (Tables 4 and 5). The flavonoids appear as white bands on a purple background showing that they have antioxidant activity and α -glucosidase inhibitory activity but no AChE inhibition (Figure 6). The rutin has higher antioxidant (DPPH[•] radical scavenging) and α -glucosidase inhibitory (435.96 and 3.61 mg/g) potential than the kaempferol-3-O-rutinoside (372.81 and 1.89 mg/g) resulting from the densitometry measurement (Table 6).

4 | DISCUSSION AND CONCLUSIONS

Leaf and fruit extracts of *Musa acuminata* (Simili radjah, ABB) have shown antioxidant, anti-inflammatory, anticholinesterase, and antidiabetic activities, which confirm their ethnomedicinal use for the treatment of neurodegenerative disorders and diabetes. It has been reported in the literature that *Musa* species have antioxidant and antidiabetic potential, especially the inflorescence part, fruit, and the flowers samples (Adedayo, Oboh, Oyeleye, & Olasehinde, 2016; Kalita et al., 2016). Vilhena et al. (2018) found 16 studies reporting the antidiabetic property of the inflorescence (flowers and bract) of *Musa* spp., which all supported the ethnomedicinal

claim that cooked flowers are able to treat *diabetes mellitus*. Some other extensive reviews have been compiled on the bioactive compounds from fruit, sap, and peel of banana (Pothavorn et al., 2010; Singh et al., 2016; Tsamo et al., 2015). This study, however, compared the antidiabetic activity of the fruit and leaves and showed that leaf fractions have higher antidiabetic activity than fruit samples. The noncompetitive mode of α -amylase inhibition by the fruit extract implies that some bioactive compounds in the fruit binds at other sites apart from the active site of the enzyme disrupting the enzyme-substrate complex and the enzyme activity. In addition, the competitive inhibition mode of the same α -amylase by the leaf fractions suggest the likelihood of a competition between the bioactive compounds and the substrate to bind at the active site of the enzyme, slowing down the breakdown of polysaccharides and oligosaccharides to disaccharides.

The results showed that the ethyl acetate and *n*-butanol fractions of the leaves had higher anti-inflammatory activity than quercetin, the positive control. The anti-inflammatory activity of the peels of some *Musa* species have been confirmed using nitric oxide inhibitory assay, formalin induced paw inflammation in rat and blood cell membrane stabilization method (Phuaklee, Ruangnoo, & Itharat, 2012; Ramya, Saraswathi, & Malathi, 2017; Yuei, Singaram, & Hassan, 2016). This study assessed the anti-inflammatory activity of *M. acuminata* fruits and leaves, which have been particularly used in traditional medicine for wound healing and ulcer. The putative

TABLE 4 ^1H , ^{13}C NMR and distortion-less enhancement by polarization of kaempferol-3-O-rutinoside

No.	^1H $\delta_{\text{H}}^{\text{O}}$	$\delta_{\text{H}}^{\text{L}}$	^{13}C ($\delta_{\text{C}}^{\text{O}}$)	$\delta_{\text{C}}^{\text{L}}$	Carbon type
2	-	-	159.4	159.4	C
3	-	-	135.5	135.5	C
4	-	-	179.3	179.4	C
5	-	-	161.5	163.0	C
6	6.21 (brs)	6.25 (d, $J = 2.1$)	100.1	100.1	CH
7	-	-	166.3	166.3	C
8	6.40 (brs)	6.45 (d, $J = 2.1$)	95.1	95.0	CH
9	-	-	158.5	158.6	C
10	-	-	105.6	105.6	C
1'	-	-	122.7	122.8	C
2'	8.06 (d, $J = 7.4$)	8.11 (d, $J = 8.9$)	132.4	132.4	CH
3'	6.90 (d, $J = 7.4$)	6.93 (d, $J = 8.9$)	116.2	116.1	CH
4'	-	-	161.5	161.5	C
5'	6.90 (d, $J = 7.4$)	6.93 (d, $J = 8.9$)	116.2	116.1	CH
6'	8.06 (d, $J = 7.4$)	8.11 (d, $J = 8.9$)	132.4	132.4	CH
1'' Glucose moiety	5.11 (d, $J = 7.4$)	5.17 (d, $J = 7.4$)	102.4	104.6	CH
2''	3.45 (m)	3.41–3.52 (m)	78.2	75.8	CH
3''	3.45 (m)	3.41–3.52 (m)	75.7	78.2	CH
4''	3.24 (m)	3.28–3.34 (m)	71.4	71.4	CH
5''	3.31 (m)	3.41–3.52 (m)	77.2	77.2	CH
6''	3.82 (d, $J = 10.8$) 3.31 (m)	3.85 (dd, $J = 11.0, 1.4$) 3.41–3.52 (m)	69.7	68.6	CH ₂
1''' Rhamnose moiety	4.52 (brs)	4.56 (d, $J = 1.4$)	104.7	102.4	CH
2'''	3.55 (m)	3.67 (dd, $J = 9.5, 3.5$)	72.3	72.1	CH
3'''	3.29 (m)	3.56 (dd, $J = 9.5, 3.5$)	73.9	72.3	CH
4'''	3.65 (m)	3.28–3.34 (m)	72.3	73.9	CH
5'''	3.29 (m)	3.41–3.52 (m)	72.1	69.7	CH
6'''	1.13 (d, $J = 6.1$)	1.16 (d, $J = 6.2$)	17.9	17.9	CH ₃

Note: Assignments were established from ^1H , ^{13}C , and 2D- NMR experiments; ^Oobserved spectrum; ^Lliterature value (Ganbaatar et al., 2015).

anti-inflammatory action, carried out in this study, is by the inhibition of the 15-LOX enzyme, considered as the key enzyme in the metabolism of arachidonic acid, responsible for leukotrienes formation involved in pathophysiology of chronic inflammatory and allergic diseases.

Anticholinesterase activity of *Musa* species is very scarce. In this study, the anticholinesterase activity observed from leaves samples was higher than the fruits. These observations are in line with the results of the previous study by Ayoola et al. (2017). Furthermore, comparing the activity of different fractions revealed that the nonpolar fractions (dichloromethane and *n*-hexane) had little or no anti-AChE activity, unlike for the polar fractions of both leaves and fruits where fractions with ethyl acetate displayed highest anti-AChE activity. All these results supports the ethnomedicinal claim of the use of *Musa* spp. in the management of neurodegenerative diseases. It was also discovered that the leaf had a better antioxidant, antidiabetic, and anti-inflammatory potentials than the fruit.

This confirms previous study revealing the better efficiency of leaf extracts in terms of antioxidant activity and total phenolic content, compared to fruit extracts, for all the *Musa* species tested (Ayoola et al., 2017). This suggests that *Musa* spp. leaf materials deserve more research focus, especially for phytochemicals isolation.

The polar fractions (methanol, *n*-butanol, and ethyl acetate) used in this study showed better antioxidant, anti-inflammatory, anticholinesterase, and antidiabetic activities. This suggests that many of the bioactive compounds, are polar in nature. Their presence in polar fractions could perhaps explain why polar solvents, such as water and alcohol, are used in indigenous medicine to macerate or prepare most herbal formulations. This finding is in congruent with the result of other studies (Faraone et al., 2018; Nakamura, Ra, Jee, & Kim, 2017). Phenolic compounds, which includes flavonoids, are known to exhibit antioxidant activities and are soluble in polar solvents such as alcohol and acetone (Luo, Basile, & Kennelly, 2002). The ethyl acetate fraction of the leaf was distinguished in this report as having

TABLE 5 ^1H , ^{13}C NMR, and distortion-less enhancement by polarization of rutin

No.	^1H $\delta_{\text{H}}^{\text{O}}$	$\delta_{\text{H}}^{\text{L}}$	^{13}C ($\delta_{\text{C}}^{\text{O}}$)	$\delta_{\text{C}}^{\text{L}}$	Carbon Type
2	–		159.4	159.5	C
3	–		135.5	135.7	C
4	–		179.3	179.5	C
5	–		162.9	163.2	C
6	6.21 (brs)	6.26 (d, $J = 2.1$)	100.1	100.0	CH
7	–		166.3	166.2	C
8	6.40 (brs)	6.45 (d, $J = 2.1$)	95.1	95.0	CH
9	–		159.4	158.5	C
10	–		105.6	105.7	C
1'	–		122.7	123.2	C
2'	7.69 (d, $J = 7.4$)	7.71 (d, $J = 2.2$)	117.7	117.8	CH
3'	–	–	146.0	146.0	C
4'	–	–	150.4	150.4	C
5'	6.90 (d, $J = 7.4$)	6.92 (d, $J = 8.4$)	116.2	116.2	CH
6'	7.65 (d, $J = 7.4$)	7.68 (dd, $J = 8.4, 2.2$)	123.6	123.7	CH
1'' Glucose moiety	5.11 (d, $J = 7.4$)	5.15 (d, $J = 7.8$)	104.8	104.8	CH
2''	3.45 (m)	3.38–3.53 (m)	75.7	75.9	CH
3''	3.45 (m)	3.38–3.53 (m)	77.2	77.4	CH
4''	3.27 (m)	3.29–3.33 (m)	71.4	71.5	CH
5''	3.31 (m)	3.38–3.53 (m)	78.1	78.3	CH
6''	3.82 (d, $J = 10.8$) 3.34 (m)	3.84 (dd, $J = 11.1, 1.5$) 3.38–3.53 (m)	68.6	68.7	CH ₂
1''' Rhamnose moiety	4.52 (brs)	4.56 (d, $J = 1.5$)	102.4	102.5	CH
2'''	3.52 (m)	3.67 (dd, $J = 3.4, 1.6$)	72.2	72.2	CH
3'''	3.25 (m)	3.58 (dd, $J = 9.5, 3.5$)	72.3	72.4	CH
4'''	3.65 (m)	3.29–3.33 (m)	73.9	74.1	CH
5'''	3.28 (m)	3.38–3.53 (m)	69.7	69.8	CH
6'''	1.13 (d, $J = 6.1$)	1.16 (d, $J = 6.2$)	17.9	18.0	CH ₃

Note: Assignments were established from ^1H , ^{13}C , and 2D NMR experiments; ^oobserved spectrum; ^lliterature value (Al-Majmaie et al., 2019).

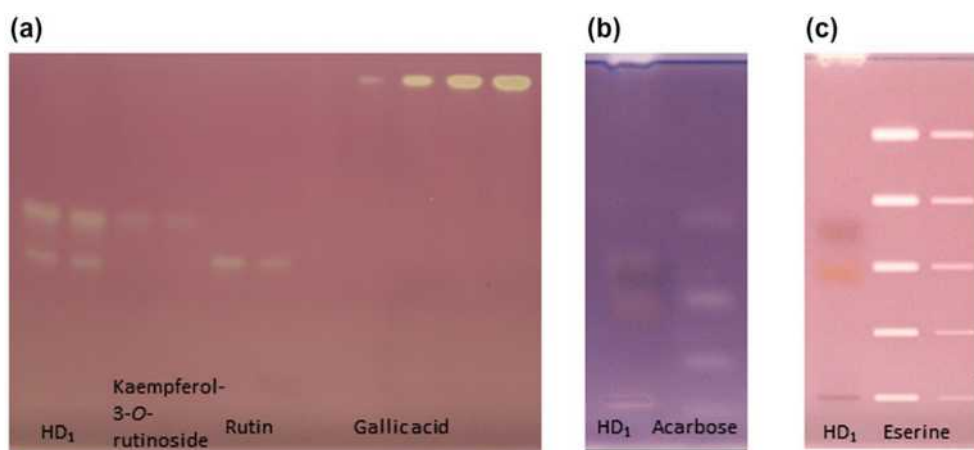


FIGURE 6 HPTLC-EDA autograms at white light illumination: Activities of the subfraction HD₁ detected by the (a) DPPH[•] radical scavenging, (b) α -glucosidase (c), and AChE assays (HD₁ compounds showed no AChE inhibition)

Samples		Antioxidant activity (mg/g)	Antidiabetic activity (mg/g)
HD1	Kaempferol-3-O-rutinoside	372.8 ± 3.1	1.9
	Quercetin-3-O-rutinoside	436.0 ± 5.4	3.6
Standards	Kaempferol-3-O-rutinoside	5,150.9 ± 114.9	ND
	Quercetin-3-O-rutinoside	5,556.1 ± 320.6	ND

TABLE 6 Mean antioxidant and antidiabetic activities ($n = 3$) of the compounds of subfraction HD₁ in comparison with the standards obtained by HPTLC densitometric measurement

the highest total phenolic content, antioxidant, antidiabetic, anti-inflammatory, and anticholinesterase activities. Similar results were reported by Mariem, Hanen, Inès, Mejdí, and Riadh (2014) where the ethyl acetate fraction of *Retama raetam* (Forssk.) Webb plant had the highest biological activity and was selected for the identification of the main compounds. Compounds were isolated from the leaf ethyl acetate fraction in this study.

Rutin and kaempferol-3-O-rutinoside were the two flavonoids isolated and identified. For rutin, the HRMS-ESI data in the negative ionization mode gave a base peak m/z at 609.15 assigned as $[M-H]^-$ with the formula $C_{27}H_{29}O_{16}^-$, while kaempferol-3-O-rutinoside gave a base peak positive ion m/z at 593.15 $[M-H]^+$ and 617.15 $[M + Na]^+$. Al-Majmaie, Nahar, Sharples, Wadi, and Sarker (2019) isolated rutin and rutin derivatives from *Ruta chalepensis* L. while Ganbaatar et al. (2015) isolated kaempferol-3-O-rutinoside as yellow powders from *Polygonum odoratum* (Mill.) Druce with the same approach and similar HRMS-ESI base peak. The structures of the two compounds were also assigned from the 1H and ^{13}C NMR spectra. This corresponds to data from other reports (Abdel-Raziq, Bar, & Gohar, 2016).

The ethyl acetate fraction of *Musa acuminata* leaves is rich in kaempferol-3-O-rutinoside and rutin, explaining its antioxidant, anti-inflammatory, and antidiabetic activities. Abdel-Raziq et al. (2016) also reported the isolation of flavonoids from the ethyl acetate fraction of *Musa cavendishii* leaf, having α -amylase inhibitory activity. Plants containing kaempferol and quercetin have already been reported to have antidiabetic properties (Tusevski, Krstikj, Stanoeva, Stefova, & Simic, 2018). Kappel et al. (2013) concluded that rutin is a major compound with antidiabetic property in the leaf of *Musa paradisiaca* L. Kaempferol and its glucoside have been reported to have many biological activities and they are found in many plant families including Musaceae (Calderon-Montano, Burgos-Morón, Pérez-Guerrero, & López-Lázaro, 2011). Kaempferol-3-O-rutinoside and rutin were shown to have antidiabetic and antioxidant activity from this study but rutin has a higher and very potent antioxidant activity as detected in the HPTLC-DPPH[•] assay. In this study, fractionation allowed the identification of the most active compounds and HPTLC-HRMS was used to characterize and confirm the identity of the isolated compounds.

This study shows that *Musa* spp. leaves contain important flavonoids with notable antioxidative, anti-inflammatory, and antidiabetic properties. Attention should therefore be drawn toward the leaf of *Musa* spp. for the isolation of important bioactive compounds by the pharmaceutical industries for the drug development and also for the production of supplements and or nutraceuticals in the management of Alzheimer's, diabetes and other inflammatory diseases.

ACKNOWLEDGMENTS

The authors thank Nele Hockamp for assistance during the HPTLC experiments as well as the African-German Network of Excellence in Science and the German Academic Exchange Programme for the short-term research grant (57378443) for 5 months stay at JLU Giessen.

CONFLICT OF INTEREST

The authors declare no conflict of interest.

ORCID

Ibukun Oluwabukola Oresanya  <https://orcid.org/0000-0001-5485-1132>

REFERENCES

- Abdel-Raziq, M. S., Bar, F. M. A., & Gohar, A. A. (2016). Alpha-amylase inhibitory compounds from *Musa cavendishii*. *British Journal of Pharmaceutical Research*, 13(4), 1–10. <https://doi.org/10.9734/BJPR/2016/29280>
- Adebayo, S. A., Dzoyem, J. P., Shai, L. J., & Eloff, J. N. (2015). The anti-inflammatory and antioxidant activity of 25 plant species used traditionally to treat pain in southern African. *BMC Complementary and Alternative Medicine*, 15(1), 159. <https://doi.org/10.1186/s12906-015-0669-5>
- Adedayo, B. C., Oboh, G., Oyeleye, S. I., & Olasehinde, T. A. (2016). Antioxidant and antihyperglycemic properties of three banana cultivars (*Musa* spp.). *Scientifica*, 2016. <https://doi.org/10.1155/2016/8391398>
- Adewoye, E. O., Ige, A. O., & Latona, C. T. (2011). Effect of methanolic extract of *Musa sapientum* leaves on gastrointestinal transit time in normal and alloxan induced diabetic rats: Possible mechanism of action. *Nigerian Journal of Physiological Sciences*, 26(1), 83–88.
- Ajayi, O. S., Aderogba, M. A., Obuotor, E. M., & Majinda, R. R. T. (2019). Acetylcholinesterase inhibitor from *Anthocleista vogelii* leaf extracts. *Journal of Ethnopharmacology*, 231, 503–506. <https://doi.org/10.1016/j.jep.2018.11.009>
- Ali, H., Houghton, P. J., & Soumyanath, A. (2006). α -Amylase inhibitory activity of some Malaysian plants used to treat diabetes; with particular reference to *Phyllanthus amarus*. *Journal of Ethnopharmacology*, 107(3), 449–455. <https://doi.org/10.1016/j.jep.2006.04.004>
- Alisi, C. S., Nwyanwu, C. E., Akujobi, C. O., & Ibegbulem, C. O. (2008). Inhibition of dehydrogenase activity in pathogenic bacteria isolates by aqueous extracts of *Musa paradisiaca* (Var Sapiantum). *African Journal of Biotechnology*, 7(12), 1821–1825. <https://doi.org/10.5897/AJB2008.000-5029>
- Al-Majmaie, S., Nahar, L., Sharples, G. P., Wadi, K., & Sarker, S. D. (2019). Isolation and antimicrobial activity of rutin and its derivatives from *Ruta chalepensis* (Rutaceae) growing in Iraq. *Records of Natural Products*, 13(1), 64–70. <https://doi.org/10.25135/rnp.74.18.03.250>
- Ayoola, I. O., Gueye, B., Sonibare, M. A., & Abberton, M. T. (2017). Antioxidant activity and acetylcholinesterase inhibition of field

- and in vitro grown *Musa L.* species. *Journal of Food Measurement and Characterization*, 11(2), 488–499. <https://doi.org/10.1007/s11694-016-9416-y>
- Azadnia, E., & Morlock, G. E. (2018). Bioprofiling of *Salvia miltiorrhiza* via planar chromatography linked to (bio) assays, high resolution mass spectrometry and nuclear magnetic resonance spectroscopy. *Journal of Chromatography A*, 1533, 180–192. <https://doi.org/10.1016/j.chroma.2017.12.014>
- Azadnia, E., & Morlock, G. E. (2019). Automated piezoelectric spraying of biological and enzymatic assays for effect-directed analysis of planar chromatograms. *Journal of Chromatography A*, 1602, 458–466. <https://doi.org/10.1016/j.chroma.2019.05.043>
- Bhaskar, J. J., Shobha, M. S., Sambaiah, K., & Salimath, P. V. (2011). Beneficial effects of banana (*Musa sp.* var. elakki bale) flower and pseudostem on hyperglycemia and advanced glycation end-products (AGEs) in streptozotocin-induced diabetic rats. *Journal of Physiology and Biochemistry*, 67(3), 415–425. <https://doi.org/10.1007/s13105-011-0091-5>
- Borovikova, L. V., Ivanova, S., Nardi, D., Zhang, M., Yang, H., Ombrellino, M., & Tracey, K. J. (2000). Role of vagus nerve signaling in CNI-1493-mediated suppression of acute inflammation. *Autonomic Neuroscience*, 85(1–3), 141–147. [https://doi.org/10.1016/S1566-0702\(00\)00233-2](https://doi.org/10.1016/S1566-0702(00)00233-2)
- Brooks, A. A. (2008). Ethanol production potential of local yeast strains isolated from ripe banana peels. *African Journal of Biotechnology*, 7(20). Retrieved from <http://www.academicjournals.org/AJB>
- Calderon-Montano, J. M., Burgos-Morón, E., Pérez-Guerrero, C., & López-Lázaro, M. (2011). A review on the dietary flavonoid kaempferol. *Mini Reviews in Medicinal Chemistry*, 11(4), 298–344. <https://doi.org/10.2174/138955711795305335>
- Diamond, J. (2003). The double puzzle of diabetes. *Nature*, 423(6940), 599–602. <https://doi.org/10.1038/423599a>
- Ekor, M. (2014). The growing use of herbal medicines: Issues relating to adverse reactions and challenges in monitoring safety. *Frontiers in Pharmacology*, 4, 177. <https://doi.org/10.3389/fphar.2013.00177>
- Ellman, G. L., Courtney, K. D., Andres, V. Jr., & Featherstone, R. M. (1961). A new and rapid colorimetric determination of acetylcholinesterase activity. *Biochemical Pharmacology*, 7(2), 88–95. [https://doi.org/10.1016/0006-2952\(61\)90145-9](https://doi.org/10.1016/0006-2952(61)90145-9)
- Essa, R., El Sadek, A. M., Baset, M. E., Rawash, M. A., Sami, D. G., Badawy, M. T., ... Abdellatif, A. (2019). Effects of turmeric (*Curcuma longa*) extract in streptozotocin-induced diabetic model. *Journal of Food Biochemistry*, 43(9), e12988. <https://doi.org/10.1111/jfbc.12988>
- Faraone, I., Rai, D., Chiummiento, L., Fernandez, E., Choudhary, A., Prinzo, F., & Milella, L. (2018). Antioxidant activity and phytochemical characterization of *Senecio clivicolus* Wedd. *Molecules*, 23(10), 2497. <https://doi.org/10.3390/molecules23102497>
- Ganbaatar, C., Gruner, M., Mishig, D., Duger, R., Schmidt, A. W., & Knölker, H. J. (2015). Flavonoid glycosides from the aerial parts of *Polygonatum odoratum* (Mill.) Druce growing in Mongolia. *Open Natural Products Journal*, 8(1), 1–7. <https://doi.org/10.2174/1874848101508010001>
- Giacco, F., & Brownlee, M. (2010). Oxidative stress and diabetic complications. *Circulation Research*, 107(9), 1058–1070. <https://doi.org/10.1161/CIRCRESAHA.110.223545>
- Houghton, P. J., Howes, M. J., Lee, C. C., & Steventon, G. (2007). Uses and abuses of in vitro tests in ethnopharmacology: Visualizing an elephant. *Journal of Ethnopharmacology*, 110(3), 391–400. <https://doi.org/10.1016/j.jep.2007.01.032>
- Imam, M. Z., & Akter, S. (2011). *Musa paradisiaca* L. and *Musa sapientum* L.: A phytochemical and pharmacological review. *Journal of Applied Pharmaceutical Science*, 1(5), 14–20.
- Jamshidi-Aidji, M., Macho, J., Mueller, M. B., & Morlock, G. E. (2019). Effect-directed profiling of aqueous, fermented plant preparations via high-performance thin-layer chromatography combined with in situ assays and high-resolution mass spectrometry. *Journal of Liquid Chromatography & Related Technologies*, 42(9–10), 226–272. <https://doi.org/10.1080/10826076.2019.1585631>
- Jamshidi-Aidji, M., & Morlock, G. E. (2018). Fast equivalency estimation of unknown enzyme inhibitors in situ the effect-directed fingerprint, shown for *Bacillus* lipopeptide extracts. *Analytical Chemistry*, 90(24), 14260–14268. <https://doi.org/10.1021/acs.analchem.8b03407>
- Joshi, S. G. (2000). *Medicinal plants*. New Delhi, India: Oxford and IBH Publishing.
- Kalita, H., Boruah, D. C., Deori, M., Hazarika, A., Sarma, R., Kumari, S., ... Devi, R. (2016). Antidiabetic and antilipidemic effect of *Musa balbisiana* root extract: A potent agent for glucose homeostasis in streptozotocin-induced diabetic rat. *Frontiers in Pharmacology*, 7, 102. <https://doi.org/10.3389/fphar.2016.00102>
- Kanazawa, K., & Sakakibara, H. (2000). High content of dopamine, a strong antioxidant, in Cavendish banana. *Journal of Agricultural and Food Chemistry*, 48(3), 844–848. <https://doi.org/10.1021/jf9909860>
- Kappel, V. D., Cazarolli, L. H., Pereira, D. F., Postal, B. G., Madoglio, F. A., Buss, Z. D. S., ... Silva, F. R. M. B. (2013). Beneficial effects of banana leaves (*Musa x paradisiaca*) on glucose homeostasis: Multiple sites of action. *Revista Brasileira de Farmacognosia*, 23(4), 706–715. <https://doi.org/10.1590/S0102-695X2013005000062>
- Kaushik, G., Satya, S., Khandelwal, R. K., & Naik, S. N. (2010). Commonly consumed Indian plant food materials in the management of diabetes mellitus. *Diabetes & Metabolic Syndrome: Clinical Research & Reviews*, 4(1), 21–40. <https://doi.org/10.1016/j.dsx.2008.02.006>
- Khatoon, M., Islam, E., Islam, R., Rahman, A. A., Alam, A. H. M. K., Khondkar, P., ... Parvin, S. (2013). Estimation of total phenol and in vitro antioxidant activity of *Albizia procera* leaves. *BMC Research Notes*, 6(1), 121. Retrieved from <http://www.biomedcentral.com/1756-0500/6/121>
- Kim, Y. M., Jeong, Y. K., Wang, M. H., Lee, W. Y., & Rhee, H. I. (2005). Inhibitory effect of pine extract on α -glucosidase activity and postprandial hyperglycemia. *Nutrition*, 21(6), 756–761. <https://doi.org/10.1016/j.nut.2004.10.014>
- Luo, X. D., Basile, M. J., & Kennelly, E. J. (2002). Polyphenolic antioxidants from the fruits of *Chrysophyllum cainito* L. (star apple). *Journal of Agricultural and Food Chemistry*, 50(6), 1379–1382. <https://doi.org/10.1021/jf011178n>
- Mariem, S., Hanen, F., Inès, J., Mejdji, S., & Riadh, K. (2014). Phenolic profile, biological activities and fraction analysis of the medicinal halophyte *Retama raetam*. *South African Journal of Botany*, 94, 114–121. <https://doi.org/10.1016/j.sajb.2014.06.010>
- Mathew, N. S., & Negi, P. S. (2017). Traditional uses, phytochemistry and pharmacology of wild banana (*Musa acuminata* Colla): A review. *Journal of Ethnopharmacology*, 196, 124–140. <https://doi.org/10.1016/j.jep.2016.12.009>
- McCue, P. P., & Shetty, K. (2004). Inhibitory effects of rosmarinic acid extracts on porcine pancreatic amylase in vitro. *Asia Pacific Journal of Clinical Nutrition*, 13(1), 101–106.
- Nakamura, M., Ra, J. H., Jee, Y., & Kim, J. S. (2017). Impact of different partitioned solvents on chemical composition and bioavailability of *Sasa quelpaertensis* Nakai leaf extract. *Journal of Food and Drug Analysis*, 25(2), 316–326. <https://doi.org/10.1016/j.jfda.2016.08.006>
- Oboh, G., Puntel, R. L., & Rocha, J. B. T. (2007). Hot pepper (*Capsicum annum*, Tepin and *Capsicum chinese*, Habanero) prevents Fe²⁺-induced lipid peroxidation in brain—In vitro. *Food Chemistry*, 102(1), 178–185. <https://doi.org/10.1016/j.foodchem.2006.05.048>
- Passo Tsamo, C. V., Herent, M.-F., Tomekpe, K., Happi Emaga, T., Quetin-Leclercq, J., Rogez, H., ... Andre, C. (2015). Phenolic profiling in the pulp and peel of nine plantain cultivars (*Musa sp.*). *Food Chemistry*, 167, 197–204. <https://doi.org/10.1016/j.foodchem.2014.06.095>
- Phuaklee, P., Ruangnoo, S., & Itharat, A. (2012). Anti-inflammatory and antioxidant activities of extracts from *Musa sapientum* peel. *Journal of the Medical Association of Thailand= Chotmaihet thangphaet*, 95, S142–S146. (PMID:23964457).

- Pothavorn, P., Kitdamrongsont, K., Swangpol, S., Wongniam, S., Atawongsa, K., Svasti, J., & Somana, J. (2010). Sap phytochemical compositions of some bananas in Thailand. *Journal of Agricultural and Food Chemistry*, 58, 8782–8787. <https://doi.org/10.1021/jf101220k>.
- Rabasa-Lhoret, R., & Chiasson, J. L. (2004). Alpha-glucosidase inhibitors. In R. A. De Fronzo, E. Ferrannini, H. Keen, & P. Zimmet (Eds.), *International textbook of diabetes mellitus* (Wyd. 3). New Jersey: John Wiley and Sons Ltd.
- Ramya, S., Saraswathi, U., & Malathi, M. (2017). In vitro anti-inflammatory activity of different varieties of *Musa sapientum* (banana) peel extract. *International Journal of Current Research*, 9, 47300–47302.
- Re, R., Pellegrini, N., Proteggente, A., Pannala, A., Yang, M., & Rice-Evans, C. (1999). Antioxidant activity applying an improved ABTS radical cation decolorization assay. *Free Radical Biology and Medicine*, 26(9–10), 1231–1237. [https://doi.org/10.1016/S0891-5849\(98\)00315-3](https://doi.org/10.1016/S0891-5849(98)00315-3)
- Rebello, L. P. G., Ramos, A. M., Pertuzatti, P. B., Barcia, M. T., Castillo-Muñoz, N., & Hermosín-Gutiérrez, I. (2014). Flour of banana (*Musa AAA*) peel as a source of antioxidant phenolic compounds. *Food Research International*, 55, 397–403. <https://doi.org/10.1016/j.foodres.2013.11.039>
- Singh, B., Bhat, T. K., & Singh, B. (2003). Potential therapeutic applications of some antinutritional plant secondary metabolites. *Journal of Agricultural and Food Chemistry*, 51(19), 5579–5597. <https://doi.org/10.1021/jf021150r>
- Singh, B., Singh, J. P., Kaur, A., & Singh, N. (2016). Bioactive compounds in banana and their associated health benefits—A review. *Food Chemistry*, 206, 1–11. <https://doi.org/10.1016/j.foodchem.2016.03.033>
- Sonibare, M. A., & Ayoola, I. O. (2015). Medicinal plants used in the treatment of neurodegenerative disorders in some parts of Southwest Nigeria. *African Journal of Pharmacy and Pharmacology*, 9(38), 956–965. <https://doi.org/10.5897/AJPP2014.4164>
- Susanti, D., Sirat, H. M., Ahmad, F., Ali, R. M., Aimi, N., & Kitajima, M. (2007). Antioxidant and cytotoxic flavonoids from the flowers of *Melastoma malabathricum* L. *Food Chemistry*, 103(3), 710–716. <https://doi.org/10.1016/j.foodchem.2006.09.011>
- Tabet, N. (2006). Acetylcholinesterase inhibitors for Alzheimer's disease: Anti-inflammatories in acetylcholine clothing! *Age and Ageing*, 35(4), 336–338. <https://doi.org/10.1093/ageing/af1027>
- Tusevski, O., Krstikj, M., Stanoeva, J. P., Stefova, M., & Simic, S. G. (2018). Phenolic profile and biological activity of *Hypericum perforatum* L.: Can roots be considered as a new source of natural compounds? *South African Journal of Botany*, 117, 301–310. <https://doi.org/10.1016/j.sajb.2018.05.030>
- Vilhena, R. O., Fachi, M. M., Marson, B. M., Dias, B. L., Pontes, F. L., Tonin, F. S., & Pontarolo, R. (2018). Antidiabetic potential of *Musa* spp. inflorescence: A systematic review. *Journal of Pharmacy and Pharmacology*, 70(12), 1583–1595. <https://doi.org/10.1111/jphp.13020>
- Vu, H. T., Scarlett, C. J., & Vuong, Q. V. (2018). Phenolic compounds within banana peel and their potential uses: A review. *Journal of Functional Foods*, 40, 238–248. <https://doi.org/10.1016/j.jff.2017.11.006>
- Yuei, L. P., Singaram, N., & Hassan, H. (2016). Study of anti-inflammatory and analgesic activity of *Musa* spp. peel. <https://doi.org/10.13140/RG.2.2.33612.10884>

How to cite this article: Oresanya IO, Sonibare MA, Gueye B, et al. Isolation of flavonoids from *Musa acuminata* Colla (Simili radjah, ABB) and the in vitro inhibitory effects of its leaf and fruit fractions on free radicals, acetylcholinesterase, 15-lipoxygenase, and carbohydrate hydrolyzing enzymes. *J Food Biochem*. 2020;00:e13137. <https://doi.org/10.1111/jfbc.13137>